OCULAR BIOMATERIALS AND THE ANTERIOR EYE

KATHRYN RUTH EVANS

Doctor of Philosophy

THE UNIVERSITY OF ASTON IN BIRMINGHAM

September 1997

THE UNIVERSITY OF ASTON IN BIRMINGHAM

OCULAR BIOMATERIALS AND THE ANTERIOR EYE

KATHRYN RUTH EVANS

Submitted for the Degree
of Doctor of Philosophy

September 1997

SUMMARY

Hydrogels, water swollen polymer matrices, have been utilised in many biomedical applications, as there is the potential to manipulate the properties for a given application by changing the chemical structure of the constituent monomers. The eye provides an excellent site to examine the interaction between a synthetic material and a complex biological fluid without invasive surgery. There is a need for the development of new synthetic hydrogels for use in the anterior eye. Three applications of hydrogels in the eye were considered in this thesis.

For some patients, the only hope of any visual improvement lies in the use of an artificial cornea, or keratoprosthesis. Preliminary investigations of a series of simple homogeneous hydrogel copolymers revealed that the mechanical properties required to withstand surgery and in eye stresses, were not achieved. This lead to work on the development of semi-interpenetrating polymer networks based on the aforementioned copolymers. Manufacture of the device and cell response were also studied.

Lasers have been employed in ocular surgery to correct refractive defects. If an irregular surface is ablated, an irregular surface is obtained. A hydrogel system was investigated that could be applied to the eye prior to ablation to create a smooth surface. Factors that may influence ablation rate were explored.

Soft contact lenses can be used as a probe to study the interaction between synthetic materials and the biological constituents of tears. This has lead to the development of many sensitive analytical techniques for protein and lipid deposition, one of which is fluorescence spectrophotometry. Various commercially available soft contact lenses were worn for different periods of time and then analysed for protein and lipid deposition using fluorescence spectrophotometry. The influence of water content, degree of ionicity and the lens material on the level and type of deposition was investigated.

Keywords: **Hydrogel, Fluorescence spectrophotometry, Laser ablation, Keratoprosthesis, Contact lenses**

For my family

ACKNOWLEDGEMENTS

I would like to take this opportunity to express my thanks to the following:

Firstly, to my supervisor Professor Brian Tighe for his advice, guidance and encouragement throughout the course of this work.

To Mr Christopher Liu of the Sussex Eye Hospital, for all the surgical discussions, his help and Dr Chris Stevenson of St. Thomas' Hospital for carrying out the laser ablation work.

To Lyndon Jones FBCO for carrying out all the clinical studies and so supplying me with tonnes of contact lenses, and for all of his help.

To Dr. Fiona Lydon, for her support and assistance, and many useful discussions!.

To Dr. Val. Franklin for completing the in vitro spoilation studies, and her help.

To Chris Graham for completing the cytotoxicity tests. Also to John Hunt and Patrick Doherty at Liverpool University for carring out the implantation work.

To everyone in the Biomaterials Research Unit, who have made my time at Aston so enjoyable, and make great drinking companions.

To EPSRC and Vista Optics for their financial support

And finally special thanks go to my family and friends for their support, patience and encouragement.

LIST OF CONTENTS

LIST OF TABLES

LIST OF FIGURES

LIST OF ABBREVIATIONS

ACLM	American Contact Lens Manufacturers	AMO	Acryloyl morpholine
Ar-F	Argon-fluoride	AZBN	Azo-bis-isobutyronitrile
CAB	Cellulose acetate butyrate	DSC	Differential Scanning Calorimetry
E_{mod}	Elastic modulus	ε_b	Elongation at break
EGDM	Ethylene glycol dimethacrylate	EWC	Equilibrium water content
FDA	Food and Drug Administration	γ_s^d	Dispersive component of surface free energy
γ_s^p	Polar component of surface energy	γ_s^t	Total surface free energy
GMA	Glycidyl methacrylate	HEMA	2-hydroxyethyl methacrylate
HPMC	Hydroxypropyl methylcellulose	IPN	Interpenetrating polymer network
KPro	Keratoprosthesis	MAA	Methacrylic acid
MMA	Methyl methacrylate	NVP	N-vinyl pyrrolidone
OOKP	Osteo-odonto keratoprosthesis	PEG1000DMA	Polyethylene glycol 1000 dimethacrylate
PEG200 MA	Polyethylene glycol 200 monomethacrylate	Phe	Phenylalanine
PMMA	Polymethyl methacrylate	PMT	Photomultiplier tube
PRK	Photorefractive keratectomy	PTK	Phototherapeutic keratectomy
PU	Ester polyurethane	PVA	Polyvinyl alcohol

SEM	Scanning electron microscopy	σ_b	Tensile strength
THFMA	Tetrahydrofurfuryl methacrylate	THPMA	Tetrahydropyranyl methacrylate
Trp	Tryptophan	Tyr	Tyrosine
USAN	United States Adopted Name	UV	Ultra violet

CHAPTER 1

INTRODUCTION

1.1 Introduction

The aim of this thesis is to investigate the use of synthetic hydrogels in three applications concerned with the ocular environment, contact lenses, artificial corneas and temporary prostheses. Hydrogels have been utilised in this area for many years, as contact lens materials[1] and intraocular lenses[2]. The knowledge gained from these applications will enable new materials for use in the eye to be developed.

The interaction of tears with a contact lens provides an insight into the processes that occur between a complex biological fluid and a synthetic material. By having an understanding of the factors and processes involved in this interaction, materials can be developed with specific characteristics for a range of purposes.

For many years now, there has been a lot of interest in the use of polymers in ocular surgery[3]. Over the last thirty years there has been an increasing interest in the development of an artificial cornea[4]. Many designs and materials have been investigated, meeting with a varying degree of success. The majority of research workers involved in this area are surgically based, so it is felt that by approaching the problem by considering the material requirements a more successful material can be developed.

Laser treatment for the correction of refractive defects of the eye, especially myopia, has been employed clinically since the 1980's[5]. However if an irregular corneal surface is ablated, the defects are merely mirrored on the treated cornea. To overcome this, it is proposed to cover the corneal surface with a viscous polymer gel which can be polymerised into a smooth surface prior to ablation and therefore produce a smooth cornea.

This thesis is concerned with two interconnecting aspects of material development. Firstly, investigating the interaction of commercially available contact lenses with the tear film, and how the material properties affect these interactions. Secondly, hydrogel

materials have been developed for use as an artificial cornea, and as a masking polymer for laser ablation. Chapter one gives an introduction to hydrogels, before considering the cornea in more detail in chapter two.

1.2. Hydrogels

Hydrogels can best be described as polymer networks that swell in, but do not dissolve in water, and can be either synthetic or natural in origin. They can contain between 20-98% water, and it is the water that has a major influence on the transport, mechanical and surface properties of the hydrogel.

Hydrogels were first proposed for biomedical applications in 1960 by Wichterle and Lim[6], when poly(2-hydroxyethyl methacrylate), poly(HEMA), was proposed as a contact lens material. Since then, hydrogels have been utilised in many sites in the body, fulfilling many roles, including heart valves[7], joint replacements[8,9], membrane oxygenators[10], haemodialysis membranes[11], intraocular lenses[12] and contact lenses[13,14].

1.3 Characterisation Techniques

1.3.1. Equilibrium Water Content

When a hydrogel is placed in water, it swells absorbing water until an equilibrium is reached. The equilibrium water content, EWC, of the hydrogel is probably the most significant single property of the gel, as it has a profound effect on permeability, mechanical, surface and biocompatibility properties of that gel. It can be defined as:

$$EWC = \frac{\text{Weight of water in the gel}}{\text{Total weight of the gel}} \times 100\ \% \qquad (1.1)$$

The EWC is influenced by the nature of the monomers used, the crosslink density and the temperature, pH and tonicity of the hydrating media. The EWC does not give a full indication of the many states in which water can exist within the hydrogel. Water acts as a plasticiser, being a 'bridge' between the synthetic polymer and the body fluids.

1.3.2 Water in Polymers

Previous work[15] carried out indicates that water exists in a continuum of states between two extremes in a hydrogel, ranging from freezing, or 'free' water, that is water that is unaffected by the polymeric environment, to non-freezing, or 'bound' water, that is water that is strongly bound to the polymeric network through hydrogen bonding[16]. The relative amounts of freezing and non-freezing water can be investigated using calorimetric techniques[17,18].

The properties of a hydrogel can therefore be influenced by both the amount of water present in the gel and the nature of that water.

1.3.2.1 Differential Scanning Calorimetry

Differential scanning calorimetry, commonly abbreviated to DSC, was developed in 1964 by Perkin-Elmer and works on the principle that a measured energy is required to keep the reference holder and sample holder at the same temperature. If the temperature is varied and a transition occurs, energy will have to be supplied to either the reference or sample to keep them at the same temperature. If energy needs to be inputted into the sample holder, the transition is endothermic, and if energy needs to be inputted into the reference, the transition is exothermic. The energy input is the transition energy and is measured directly as the area under a peak. The peak shape allows further information regarding the nature of the water binding states to be obtained[16].

A variety of techniques, for example nuclear magnetic resonance, NMR[19], dilatometry and specific conductivity, are available to study the water binding characteristics of polymers, with each one having some influence on the water structuring, the dynamic and thermodynamic properties of the water present and hence the ratio of freezing to non-freezing water obtained will depend upon the technique chosen[18]. Differential scanning calorimetry was used as it was a relatively quick method of determining the ratio of states present in the hydrogel. This is obtained as even at very low

temperatures only part of the water in the polymer will freeze, allowing a quantitative determination of the relative amounts of freezing and non-freezing water to be obtained. Further information about the structuring of water in the gel can be obtained from the fine structure of the thermogram[16]. In general, water bound to the backbone by hydrogen bonding will not freeze, whilst the more mobile water which is unaffected by the polymeric environment will freeze.

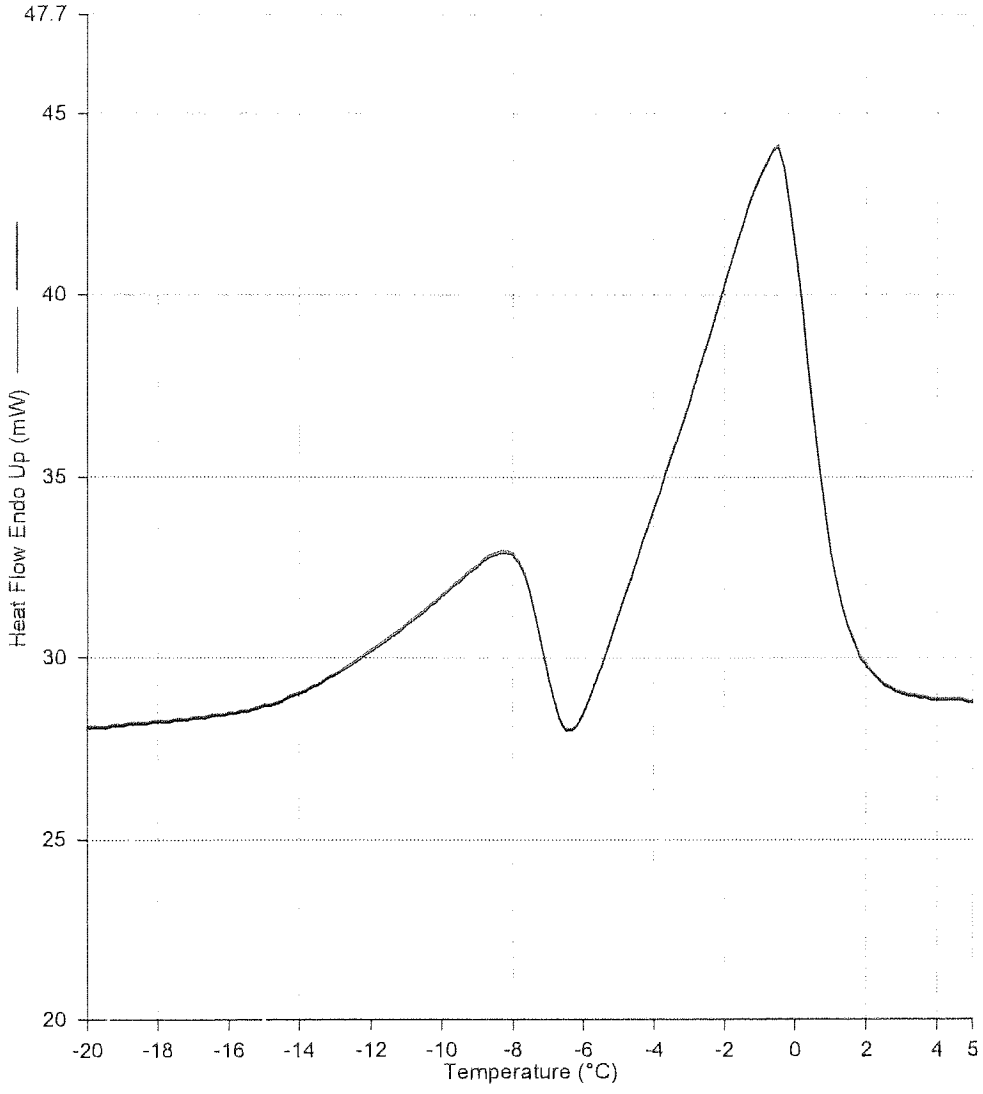

Figure 1.1 Typical melting endotherm

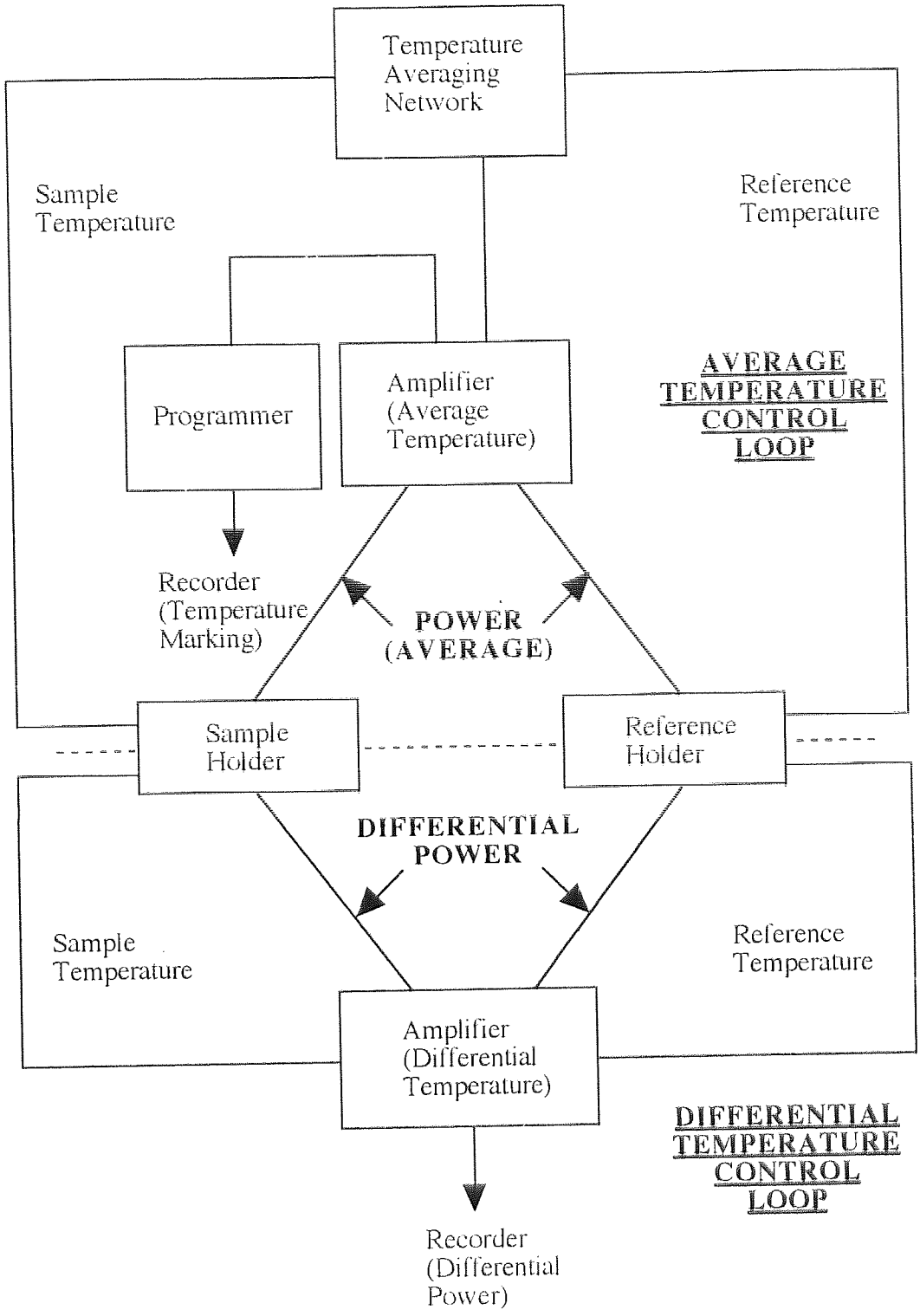

Figure 1.2 Block Diagram of a Differential Scanning Calorimeter

The chemical constituents, chain flexibility, water binding properties, and pore size and distribution all influence the properties of a hydrogel. Therefore, for any application, a balance must be obtained to produce the best possible combination of properties.

1.3.3 Mechanical Testing

PolyHEMA in its dehydrated state is hard and brittle, which is very similar to poly (methyl methacrylate). Upon immersion in water polyHEMA swells, making it soft and compliant, and has found many applications in the biological environment. Unfortunately, in this state polyHEMA, and many other hydrogels, have very low mechanical strength, thus limiting the range and life-span of the biomaterials they can be applied to. This is due to the absorbed water acting as an internal plasticiser.

Tensile testing is used to investigate the mechanical properties of the hydrogels. The standard testing conditions were determined by Trevett and Tighe[20] to overcome the difficulties encountered in testing a hydrogel in a non-aqueous environment, and allow for comparative (but not absolute) data to be obtained.

1.3.4 Contact Angles[15,17]

The wetting of a contact lens is an important factor in determining its physiological compatibility as the pre-corneal tear film needs to be maintained in the form of a thin capillary layer. The main factor in determining the wettability of a material is the chemical structure of the polymer at the air-solid-liquid interface. Polymer surfaces are mobile and the molecular orientation can be modified in response to the environment. When a liquid comes into contact with a solid surface, the liquid may wet the surface well, that is it will spread spontaneously over the surface, or not wet, i.e. not spread.

When the sample is in air, the hydrophobic groups are orientated towards the hydrophobic solid-air interface. As the liquid wets the sample, the hydrophilic groups reorientate themselves towards the liquid-solid interface. The wettability of solid can be

measured in terms of contact angles, θ, which is can be determined by several methods *in-vitro*. The greater the degree of wettability of the surface, the lower the value of θ.

Hydrogels used for biomedical applications come into contact with biological fluid, so an important consideration in determining biotolerance is the surface free energy of the material. This is investigated using goniometry. Contact angles were measured in the dehydrated state using the sessile drop technique, in the hydrated state using Hamilton's method and captive bubble technique, and in a dynamic situation using a Cahn wetting balance. Contact angle measurements involve resolving the forces at a three phase interface of a drop of wetting liquid on a solid surface either immersed in liquid or in air, i e. the sessile drop or captive bubble methods respectively. Dynamic contact angles can also be recorded.

The solid-vapour interfacial free energy, γ_{sv}, calculated from contact angle measurements, can, in most cases, be approximated to γ_s, the surface free energy of the solid in a vacuum. The total surface energy can be split into polar and dispersive components γ_s^p and γ_s^d. It is difficult to measure surface energies, especially in the dehydrated state where hydrophilic samples absorb water rapidly, changing the true readings. Results can also be inaccurate due to surface rugosity, heterogeneity, contamination of the liquid, the extent to which the drop is vibrated and reorientation of the polymer chains at the surface, which is known as contact angle hysteresis, all of which will change the value obtained for surface free energy.

1.3.4.1 Dehydrated Surfaces[15,17,18]

In 1805 Young resolved the forces at a point between a sessile drop and a solid surface deriving the equation 1.2:

$$\gamma_{sv} = \gamma_{sl} + \gamma_{lv} \cos\theta \qquad (1.2)$$

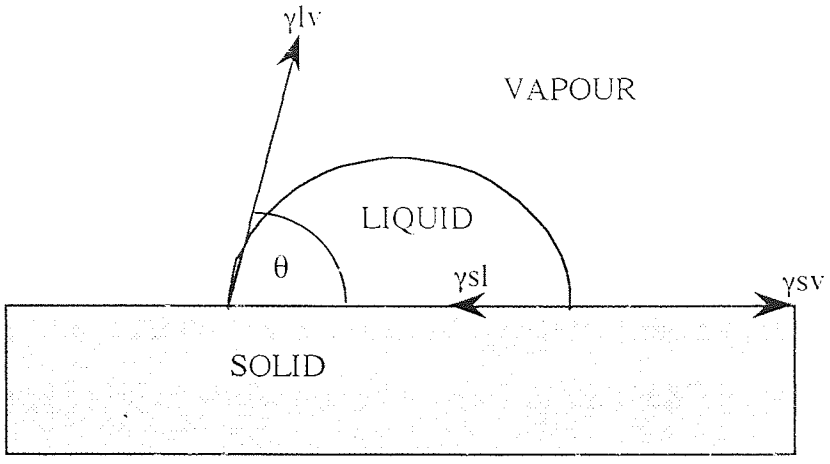

where:-

γ_{sv} = solid - vapour interfacial free energy $\approx \gamma_s$ = solid surface free energy

γ_{sl} = solid - liquid interfacial free energy

γ_{lv} = liquid - vapour interfacial free energy

Figure 1.3 Components of solid surface free energy

Sixty years after Young, Dupre demonstrated that the reversible work of adhesion of a liquid to a solid (W_a), could be expressed as

$$W_a = \gamma_s + \gamma_{lv} - \gamma_{sl} \qquad (1.3)$$

Combining equations 1.2 and 1.3 leads to the Young - Dupre equation (1.4)

$$W_a = (\gamma_s - \gamma_{sv}) + \gamma_{lv}(1 + \cos\theta) \qquad (1.4)$$

For a liquid-solid interface the work of adhesion will have a polar and dispersive component:

$$W_a = \gamma_s + \gamma_{lv} - \gamma_{sl} = 2[(\gamma_{lv}^{d}\gamma_s^{d})^{0.5} + (\gamma_{lv}^{p}\gamma_s^{p})^{0.5}] \qquad (1.5)$$

For many years the Dupre equation was used to express the reversible work of adhesion, but this was found to be inadequate when polar forces acted across a surface. Owens and Wendt resolved the polar and dispersive components, giving the expression:

$$1 + \cos\theta = (2/\gamma_{lv}) [(\gamma_{lv}^{d} \gamma_{s}^{d})^{0.5} + (\gamma_{lv}^{p} \gamma_{s}^{p})^{0.5}] \quad (1.6)$$

This equation, know as the Owens and Wendt equation, is the one most frequently used to determine the surface energy of polymers in the dehydrated state. The total surface free energy γ^{t}, can be determined once the individual components for the solid have been calculated.

$$\gamma_{s}^{t} = \gamma_{s}^{p} + \gamma_{s}^{d} \quad (1.7)$$

Two wetting agents whose polar and dispersive components are known are used. The contact angle of each liquid on the polymer surface is measured, and by solving the simultaneous equations, γ_{s}^{d} and γ_{s}^{p}, the polar and dispersive components of the surface free energy of the polymer can be determined.

The wetting solutions generally used are distilled water and diiodomethane, due to their high surface free energies and their balance of polar and dispersive components as seen in table 1.1.

Liquid	γ^{d} (mN/m)	γ^{p} (mN/m)	γ^{t} (mN/m)
Water	21.8	51.0	72.8
Diiodomethane	48.5	2.3	50.8
N-octane	21.8	0	21.8

Table 1.1 Polar and dispersive components of wetting liquids commonly used for contact angle studies

1.3.4.2 Hydrated Surfaces[15,17,18]

There are two major problems connected with measuring contact angles of hydrated polymers in air. The first is the lack of any efficient or reproducible method of removing the surface water, and the second is the dehydration of the polymer surface. Hamilton's method and the captive bubble technique have been developed to overcome these problems, by allowing the surface free energy to be measured in a fully hydrated state.

1.3.4.2.1 Hamilton's Method

Hamilton[21] resolved the forces at a three phase interface, measuring the contact angles of a small n-octane droplet on a solid surface under water. Assuming that the effects of gravity are negligible, the polar component of the surface free energy can be calculated.

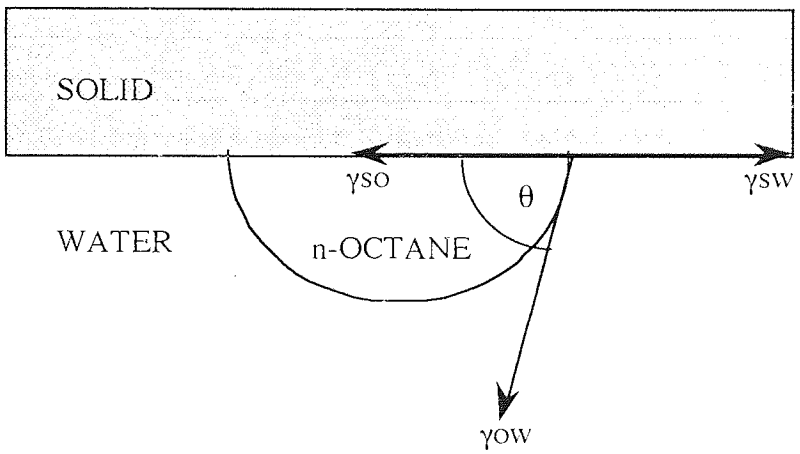

where γ_{sw} = solid-water interfacial free energy

γ_{so} = solid-octane interfacial free energy

γ_{ow} = octane-water interfacial free energy

Figure 1.4 Components of surface free energy for Hamilton's method

Fowkes developed an equation for the work of adhesion at the solid - liquid interface, assuming that there were no polar interactions across the interface.

$$\gamma_{sl} = \gamma_s + \gamma_{lv} - 2(\gamma_{lv}^{d}\,\gamma_s^{d})^{0.5} \qquad (1.8)$$

Tamai modified this equation, taking into account the stabilisation of a solid surface by the non-dispersive (polar) forces.

$$\gamma_{sl} = \gamma_s + \gamma_{lv} - 2(\gamma_{lv}^{d}\,\gamma_s^{d})^{0.5} - I_{sl} \qquad (1.9)$$

$$\text{where } I_{sl} = 2(\gamma_{lv}^{d}\,\gamma_s^{d})^{0.5} \qquad (1.10)$$

N-octane has no polar components, and the dispersive components for n-octane and water (γ_{lv}^{d}) are identical, (both 21.8 mN/m), by combining equations 1.2 and 1.9 gives the polar stabilisation energy between water and the solid.

$$I_{sw} = \gamma_{w'v} - \gamma_{ov} - \gamma_{ow}\cos\theta \qquad (1.11)$$

where $\gamma_{w'v}$ is the surface tension of n-octane saturated water and γ_{ov} and γ_{ow} are found experimentally. Solving the equation enables I_{sw} to be calculated and therefore from equation 1.10, the polar component of the surface free energy γ_s can be determined. From a calibration curve of Hamilton contact angle versus the polar component, it has been shown that as the contact angle becomes larger, i.e. moves towards 180°, γ_s^{p} also increases.

1.3.4.2.2 Captive Air Bubble Technique

The captive air bubble technique works using the same experimental set-up as Hamilton's method, except that an air bubble is placed in contact with the solid surface instead of a drop of n-octane, as shown in figure 1.5 .

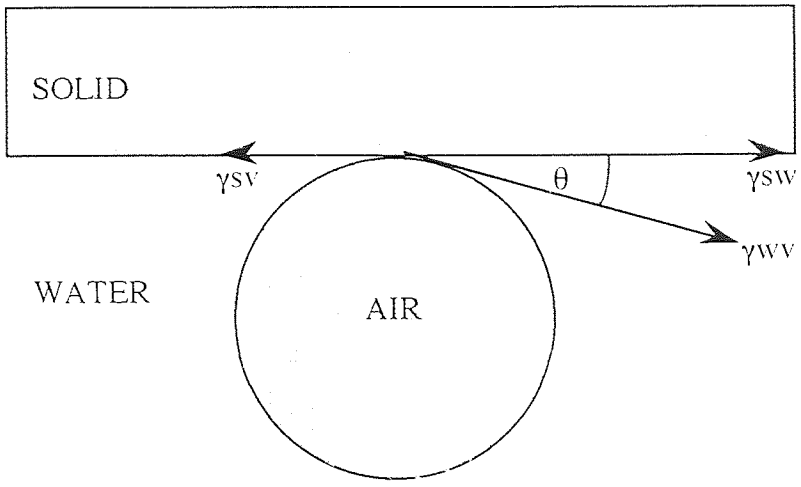

where γ_{sw} = solid-water interfacial free energy

γ_{wv} = water-vapour interfacial free energy (surface tension of the water)

γ_{sv} = solid-vapour interfacial free energy or approximately γ_s the solid surface free energy

Figure 1.5 Components of surface free energy for the captive air bubble technique

Andrade *et. al.*[15] showed that by using the data from Hamilton's method and the captive bubble technique, it was possible to obtain values for γ_{sv} γ_{sv}^{p}, γ_{sv}^{d}, and γ_{sw} for the hydrogel water interface. Applying Young's equation, (1.2) with water as the liquid phase gives:

$$\gamma_{sv} - \gamma_{sw} = \gamma_{wv}.\cos\theta' \qquad (1.12)$$

γ_{wv} is known to be 72.8 mN/m and θ' is the captive air bubble contact angle, the adhesion tension ($\gamma_{sv} - \gamma_{sw}$) can be calculated.

From equation 1.2, the polar stabilisation parameter is given by:

$$I_{sw} = \gamma_{wv} - \gamma_{ov} - \gamma_{ow} \cos\theta' \qquad (1.11)$$

As γ_{wv} = 72.8 mN/m, γ_{ov} = 21.8 mN/m and γ_{ow} = 51.0 mN/m this equation can be rewritten:

$$I_{sw} = 51.0\,(1 - \cos\theta') \qquad (1.13)$$

I_{sw} can now be calculated. Combining equations 1.9 and 1.12 gives:

$$(\gamma_{sv} - \gamma_{sw}) = 2(\gamma_{wv}^{d}\,\gamma_{sv}^{d})^{0.5} + I_{sw} - \gamma_{wv} \qquad (1.14)$$

This equation can be rearranged to give an equation for the dispersive component, (γ_{sv}^{d}), of the hydrogel:

$$\gamma_{sv}^{d} = [\{(\gamma_{sv} - \gamma_{sw}) - I_{sw} + \gamma_{wv}\} / 2(\gamma_{wv}^{d})^{0.5}]^{2} \qquad (1.15)$$

γ_{sv}^{p}, can also be derived by rearranging equation 1.10 to give:

$$\gamma_{sv}^{p} = I_{sw}^{2} / (4\gamma_{wv}^{p}) \qquad (1.16)$$

$(\gamma_{sv} - \gamma_{sw})$, I_{sw}, γ_{sv}^{p}, γ_{sv}^{d}, γ_{sv}, and γ_{sw}, were calculated using Macintosh Works™ software.

The dispersive component can also be found using the Owens Wendt equation (equation 1.6) for hydrated gels. The value of the polar component of the free surface energy, determined by the Hamilton method, and the experimentally determined water / air contract angles are substituted into the Owens Wendt equation and the dispersive component calculated. Corkhill[15] has shown that dispersive components obtained by this method correlate well (to within 0.2 mN/m).

1.3.4.3 Dynamic Contact Angles

Dynamic contact angles are measured by the Wilhelmy plate technique[22-24]. The wetting force at the solid/liquid/vapour interface is automatically recorded by a Cahn electrobalance as a function of time and immersion depth. The solid sample is held in a

fixed position whilst the wetting solution is moved along the sample at a constant speed by a computer-controlled stage.

Contact angles are measured in two directions. The advancing contact angle is recorded as the stage moves up, advancing the liquid across the solid surface, and then as the stage moves down the receding contact angle is measured across the previously wetted surface. The difference in these two contact angles is termed the contact angle hysteresis.

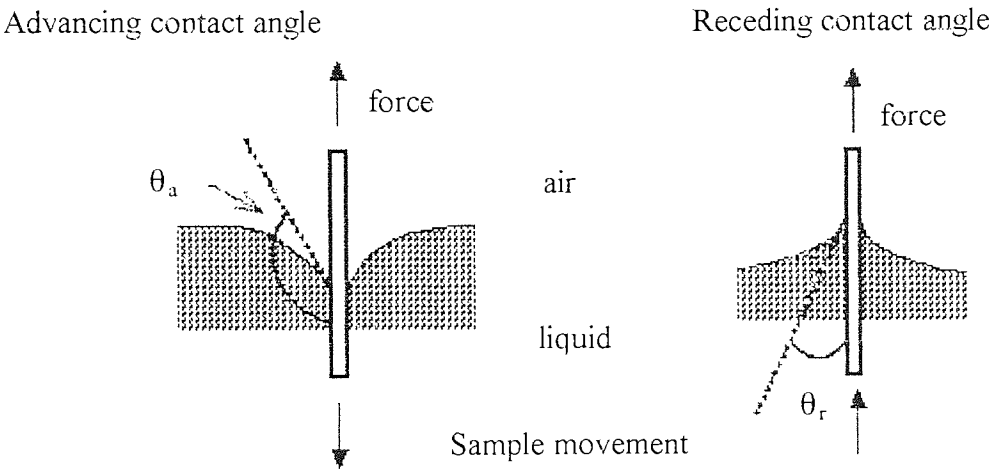

Figure 1.6 Schematic diagram of advancing and receding contact angles

The wetting force can be equated to the contact angle by the equation:

$$\cos\theta = \frac{F}{p\gamma} \qquad (1.17)$$

where F = force of meniscus at the solid / liquid / vapour interface, measured directly by the Cahn balance

p = perimeter of the sample in contact with the probe liquid

γ = surface tension of the probe liquid

Dynamic contact angles are a useful technique for investigating the orientation of functional groups at the surface and how this is altered due to the nature of the

environment[22]. As a liquid advances over a dry surface, hydrophobic groups are more likely to be expressed at the surface, but as the solid is immersed, the hydrophilic moieties reorientate themselves towards the surface to minimise the interfacial free energy.

1.3.5 *In vitro* spoilation

It is important to know how a synthetic material will behave in a biological fluid, as this will give an indication of the biocompatibility of the material. The Aston tear model was specifically designed, and developed[25], to mimic the ocular environment, by replicating the tear - contact lens interaction, so as to give an indication of performance[26]. Protein absorption is influenced by EWC and the nature of the water structuring in polymers, so protein studies will give an indication of the surface structure of the material at a molecular level[27,28].

1.4 Interpenetrating Polymer Networks

Mechanical properties can be greatly enhanced by the formation of interpenetrating polymer networks, IPN's[15,29]. IPN's have been defined as a combination of two polymers, each in network form, at least one of which was synthesised and/or crosslinked in the presence of the other[30]. Both networks will have an effect on the mechanical and physical properties of the system. Several routes can be used to synthesise IPN's which in turn determines the type of IPN produced[31]. A semi-IPN is formed when only one of the polymers is crosslinked, the other being linear.

Millar was the first to synthesise and name interpenetrating polymer networks, in the early 1960's, though it was not until the late 1960's and early 1970's that major research was carried out in this area[29].

There are several types of IPN's depending upon the method of formation. Thermoset IPN's can be divided into four types; simultaneous, semi-IPN's, homo-IPN's and

sequential IPN's. Simultaneous interpenetrating networks, SIN's, are formed when both polymerisation processes are carried out at the same time. The two networks are formed by different, non-interfering routes. Semi-IPN's are produced when one of the components is linear and one is crosslinked. Homo-IPN's consist of polymers that are chemically identical but retain their specific properties. Sequential IPN's are created when one polymer network is formed first, then swelled with the second monomer and its crosslinker and initiator, then polymerised.

Interpenetrating polymer networks and semi-IPN's are been utilised in many functions, including biomedical applications. Corkhill *et. al*[32]. have used this technology to produce a synthetic articular cartilage. Conventional synthetic hydrogels could be produced with a similar water content to that of natural cartilage, but the mechanical properties were poor. IPN's were produced that had similar water contents and much improved mechanical properties, as they were stronger and stiffer, and so mimicking more closely the natural hydrogel.

1.5 Water Soluble Polymers

Many macromolecules exhibit a degree of solubility in aqueous solution. Such materials have found commercial applications in several areas including pharmaceutical, food and coating industries[33]. The solution properties are dominated by the structural characteristics of the solvated polymer chain[34]. A large number of functional groups are able to contribute to the water solubility. The degree of solubility is dependent upon the number, position and frequency of these moieties.

Polymers dissolved in water can take several forms, ranging from random coils to vesicles[35]. Cellulose derivatives have an extended rod structure in aqueous solution. Water plays an important role in determining the properties of the polymer in solution. Solvation of the polymer chains may involve simple interactions of the ionic, polar or

hydrogen-bonded hydrophilic segments with water or more complex solvation of amphiphilic structures.

Rheological characteristics of an aqueous solution are dictated by molecular structure, solvation and inter- and intrachain associations. Viscosity gives information about the order and arrangement of the polymer chains in solution[36]. Dilute solution measurements can yield the intrinsic viscosity, [η], which is related to the molecular weight of the polymer. In semi-dilute or concentrated solutions, the polymer molecules are no longer isolated. This can lead to an increase in the apparent viscosity, η, which is then related to both the concentration and the molecular weight.

Several naturally occurring water soluble polymers have been utilised in ophthalmic preparations, such as artificial tear solutions[37]. Amongst these are hydroxypropyl methylcellulose and polyvinyl alcohol. These preparations are designed so that their physico-chemical properties are similar to those of natural tears, and are used to treat tear deficiencies, for example dry eye symptoms.

1.6 Biocompatibility.

When a synthetic material is placed into a biological fluid, a complex set of interactions occur, regardless of the material or fluid into which it has been placed[38]. If a material is to be biocompatible or biotolerant, it is imperative that the material causes no adverse effect on the environment it is placed in which would lead to the rejection or failure of the application it was designed for. Materials in use at present are prone to protein and lipid deposition with numerous factors affecting the speed and degree by which it occurs, including the chemical nature and surface properties of the synthetic material. The same fundamental process is involved at different interfaces, blood clotting, tear deposition and plaque formation can all be regarded as occurring in the same way. This process is referred to as biological interface conversion[39]. The process begins with the

adsorption of biochemicals at an interface followed rapidly by competitive adsorption of other biochemicals.

Biocompatibility is primarily concerned with the interactions between the material and the body fluid it is in contact with, and the physiological response to that material. These reactions are governed by the initial events at the molecular level at the interface. Therefore, it is the surface that determine the degree of biocompatibility.

1.6.1 Blood Contact Devices

Several theories have been proposed that would predict whether a material would be non-thrombogenic (blood compatible) or not[15,17].

Baier suggested that a material with a critical surface tension in the range 20-30 mN/m would exhibit some degree of biocompatiblity. The minimum interfacial energy hypothesis was suggested by Andrade et. al.. This stated that a low interfacial tension between the implant material and the host environment would improve biocompatibility. Ratner proposed that a balance between polar and apolar sites might lead to enhanced biotolerance. Various workers have looked at the relationship between microdomains of hydrophilic and hydrophobic regions and blood compatibility.

The factors that govern blood compatibility of hydrogel devices are very complex. Polymer structure, chain mobility and the balance of hydrophilic and hydrophobic groups on the surface of the polymer all make a contribution.

1.6.2 Hydrogels in the ocular environment

It is in the contact lens field that a great variety of different hydrogel materials have been employed[40]. The first widely used hydrogel was polyHEMA, which is flexible, transparent and relatively biocompatible, though has poor mechanical properties.

Various monomers and copolymers have been investigated in an attempt to improve the properties of the hydrogel lenses[13,41].

The major problem associated with the hydrogel contact lenses is ocular compatibility or spoilation as it is referred to in contact lens literature.

1.7 Naturally Occurring Hydrogels

The water in the hydrogel network allows for the transport of water soluble metabolites and gases to pass through the polymer network. Examples of naturally occurring hydrogels include articular cartilage and the cornea.

1.7.1 Articular Cartilage

Articular cartilage is a natural hydrogel, 1 - 2 mm thick, that covers the opposite bony faces[29]. It aids in force adsorption and provides a low friction bearing surface of the joint. When it is fully saturated, cartilage contains 70 - 85 % water. It is an insoluble gel suspended in a pool of liquid, acting as a porous sponge to absorb force and lubricate the joint.

Cartilage is comprised mainly of collagen and chondroitin sulphate. The collagen is present as a woven fibrous network in a polysaccharide matrix containing hyaluronic acid, chondroitin sulphate, keratin sulphate and stabilising proteins. Chondroitin and keratin sulphates are anionic mucosaccharides with many hydrophilic groups that bind water and cations helping to stabilise and strengthen the system. Hyaluronic acid is thought to act as a lubricant and contribute to the low coefficient of friction.

Cartilage is anisotropic in both composition and orientation of the collagen fibres. The fibres are arranged parallel to the articulating surface, randomly orientated in the middle zone, and present in oriented bundles near the bone. The water content is 85% at the surface and drops to 70% near the bone. The percentage of proteoglycans is low at the

surface, increasing towards the bone. The anisotropy leads to a wide variation in the measured mechanical properties, depending upon the section examined.

A synthetic equivalent of articular cartilage must exhibit a high tensile and compressive strength, and a low coefficient of friction. Several attempts have been made to mimic this natural hydrogel. Bray and Merrill[42] investigated the use of a polyvinyl alcohol hydrogel, and Corkhill and Tighe[32] have used semi-IPN technology to fabricate potential hydrogel materials.

Hydrogel	EWC (%)	E_{mod} (MPa)	σ_b (MPa)	ε_b (%)
cartilage	75-80	10-100	10-30	80
cornea	81	5		

Table 1.2 Properties of the cornea and articular cartilage[43,44]

1.7.2 Cornea

The cornea is a composite material, with a chemical composition defined by Haurice and Riley in 1968[29], shown in table 1.3:

Substance	%
water	78
collagen	15
other proteins	5
keratin sulphates	0.7
chondroitin sulphates	0.3
salts	1

Table 1.3 Composition of the cornea

The structure and function of the cornea will be discussed in detail in chapter 2.

1.8 The Eye

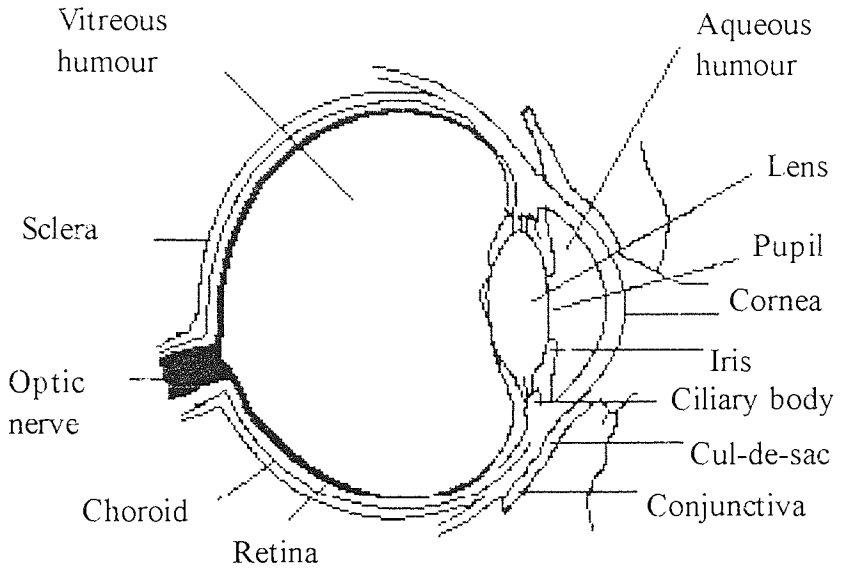

Figure 1.7 Simplified anatomy of the eye[45]

The eye makes an ideal site in which to study the interactions of a synthetic material with a complex biological fluid. A contact lens is easily placed in the eye, monitored, and removed after a given period of time, without the need for complex surgery. It is hard to envisage any comparable surgical procedure that would permit materials in contact with blood to give as much information. Blood and tears though not identical in composition can be regarded as having more similarities than differences[46].

There are three important aspects of the ocular environment which need to be considered in terms of material design: eyelid, tears and the cornea[3]. Considerable force is applied to the cornea during the blink cycle and so the eyelid dictates the range of acceptable mechanical properties. Any material placed in the eye must be able to withstand the deforming force of the eyelid and thus setting the upper and lower limits of elasticity of the material. The tear film covers the cornea and has a lubricating and

nutritional role. The tear fluid must sufficiently wet any material placed in the eye to maintain the continuous tear film. The cornea is avascular so the oxygen requirement is met by the tear film and the atmosphere. Any synthetic material in the eye must be highly oxygen permeable to prevent corneal oxygen deprivation.

1.8.1 Tear Film

The interaction of a hydrogel contact lens with the tear film is an example of the processes that occur when a synthetic material is placed into a complex biological environment[47].

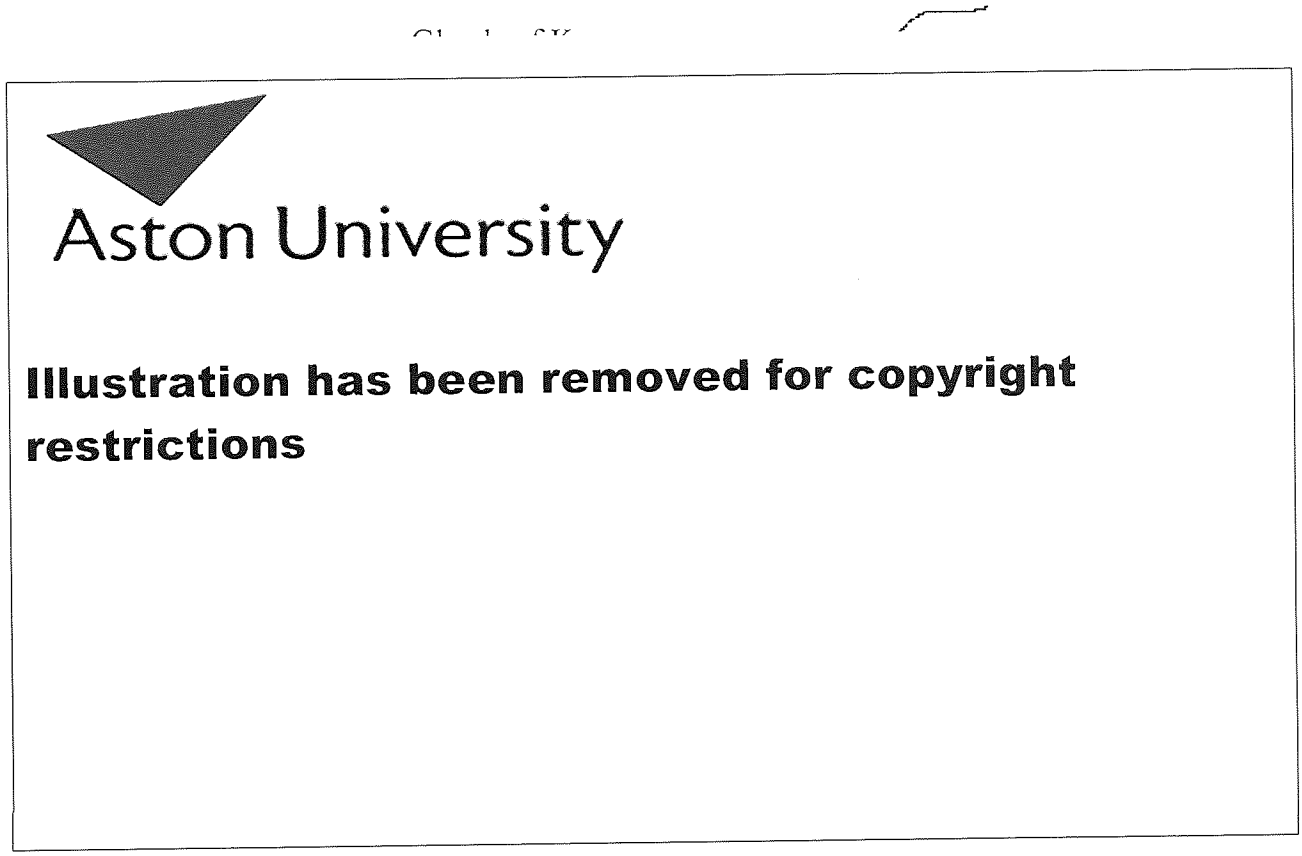

Figure 1.8 Cross-section through the anterior of the eye to show the location of the main tear forming glands[48]

Tears are formed by a group of glands collectively known as the lacrimal system[45]. The normal tear volume is approximately 7-10 ml in each eye. There is a continual secretion rate (referred to as nonreflex tears) of about 1 ml/min, with reflex tearing occurring in response to injury, irritation and emotions. The most widely accepted model of the tear film consists of three distinct layers: the lipid, aqueous and mucus layers. It is part of a dynamic system involving the eyelids and the epithelium surface. The lids play an important role in the formation and maintenance of the tear film. The tear film is thinner

between blinks, with a new blink restoring it. The surface of the cornea is covered in microvilli, providing an increased surface area of the eye and a much greater area for attachment of the tear film.

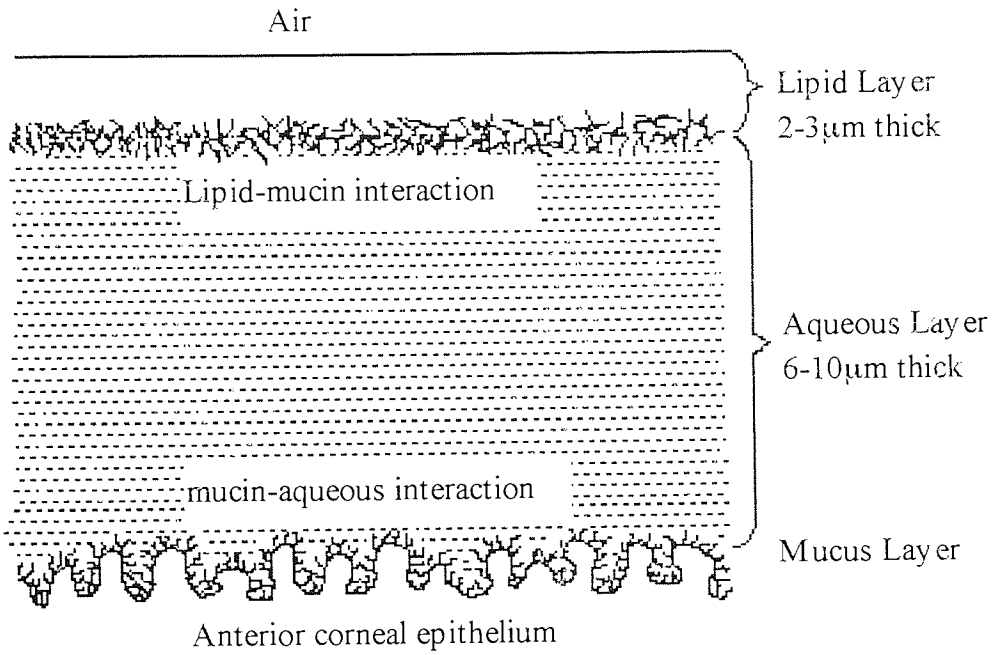

Figure 1.9 Cross-section of the tear film.

The lipid layer reduces evaporation of the tear film by forming a continuous barrier from lid margin to lid margin. It is extremely thin, and is secreted by the Meibomian glands and the glands of Zeis and Moll. It has a complex composition, containing a variety of lipids including waxes, cholesterol esters, fatty acids, fatty alcohol's and cholesterol phospholipids. However, the exact composition of human meibomian lipid varies considerably between individuals.

The aqueous phase forms the bulk of the tear film. It is produced by the lacrimal glands and the accessory glands of Krause and Wolfring. It is where the protein components of tears are normally found, along with immunoglobulins, enzymes, salts, urea, glucose, leucocytes and tissue debris.

The mucus glycoprotein or mucus layer forms a monolayer on the epithelial surface which substantially reduces the corneal hydrophobicity, allowing the surface to 'wet' the epithelium. It is produced by specialised goblet cells of the conjunctiva, in the crypts of Henle and glands of Manz. It consists of glycoproteins, carbohydrates, salts, free protein and water[49]. The electrolyte content resembles that of serum. It has an important role to play in corneal wettability and tear stability.

The tear film consists of over 98% water, in which is dissolved many components. The composition is shown table 1.4.

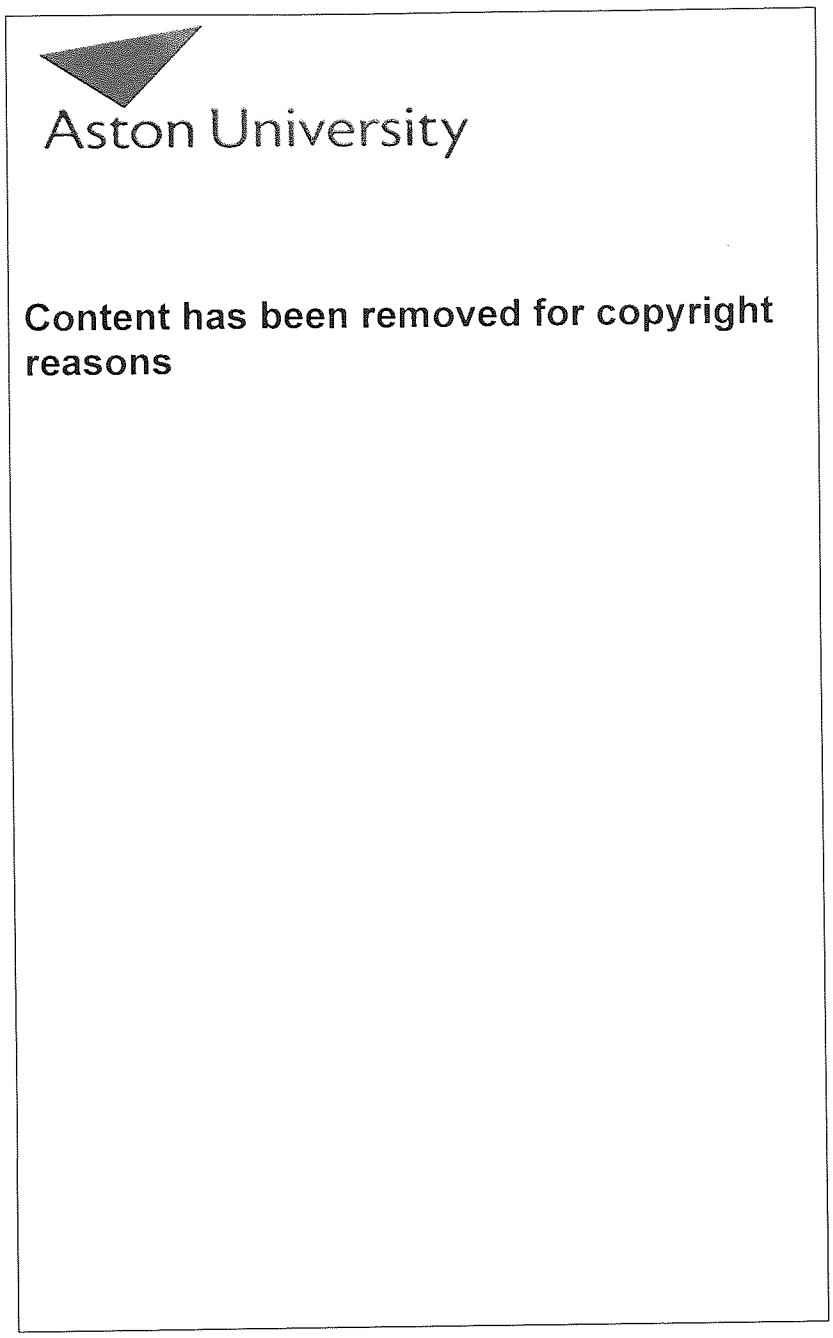

Table 1.4 Composition of the tear film[48]

The composition of the tear film is diverse due to the method and time of collection and the analytical technique used. Lipid components vary, especially from person to person.

1.8.2 Contact Lenses

Hydrogels are most widely used as soft contact lens materials[1] with over 100 patents being filed since the early sixties[14,50]. HEMA is still the major constituent of most of

the commercially available lenses although it is not necessarily the best material for this purpose.

Contact lenses have been classified in several ways depending on their chemical composition, ionicity and water content[51].

The American Food and Drug Administration, FDA, classifies the materials into four groups, depending upon their water content and ionicity.

Group 1	low water content	non-ionic
Group 2	high water content	non-ionic
Group 3	low water content	ionic
Group 4	high water content	ionic

Table 1.5 FDA classification of soft contact lenses

Low water content refers to less than 50% water, and to be classified as non-ionic the material must contain less than 0.5% methacrylic acid.

The American contact lens manufacturers (ACLM) classify the lenses by the polymers and relative amounts of each component from which the lens is made.

Group	Major Polymer(s)	% ionisable
Filcon 1a	pure HEMA	< 0.2% weight MAA
Filcon 1b	pure HEMA	> 0.2 % weight MAA
Filcon 2a	copolymer HEMA and/or other hydroxyalkyl methacrylates	< 0.2 % weight ionisable chemical
Filcon 2b	as 2a	> 0.2 % weight ionisable chemical
Filcon 3a	copolymer HEMA with an N-vinyl lactam and/or an alkyl acrylamide	< 0.2% weight ionisable chemical
Filcon 3b	as 3a	> 0.2% weight ionisable chemical
Filcon 4a	copolymer of alkyl methacrylate & N-vinyl lactam and/or alkyl acrylamide	> 0.2 % weight ionisable chemical
Filcon 4b	as 4a	< 0.2% weight ionisable chemical
Filcon 5	polysiloxanes	

Table 1.6 ACLM classification of soft contact lenses

The United States also introduced USAN (United States adopted names) classification that depended upon the chemical composition of the lens.

Lens	EWC	Monomers	FDA Group	USAN	Manufacturing method
Acuvue	58	HEMA + MAA	IV	Etafilcon A	moulded
Classic	43	HEMA + VP + MMA	I	Tetrafilcon A	lathed
Vistagel Plus	40	undisclosed	I	-	lathed
ES70	70	MMA + VP	II	-	lathed
Excelens	64	PVA + MMA	II	Atlafilcon	moulded
Focus	55	HEMA + PVP + MMA	IV	Vifilcon A	moulded
Medalist 66	66	HEMA + VP	II	Alphafilcon A	moulded
NewVues	55	HEMA + PVP + MMA	IV	Vifilcon A	moulded
Permaflex	74	MMA + VP	II	-	moulded
Dailies	69	functionalised PVA	II	Nelfilcon A	moulded
Precision UV	74	MMA + VP	II	Vasurfilcon A	moulded
Rythmic	73	VP + MMA	II	-	moulded
SeeQuence	38	HEMA	I	Polymacon	lathed
Surevue	58	HEMA + MMA	IV	Etafilcon A	moulded
Z6	38	HEMA	I	Polymacon	lathed

Table 1.7 Composition and classification of some commercially available soft contact lenses

There are three main methods for contact lens manufacture, and that chosen will be determined by the properties of the lens material involved[51].

Lathe-cutting: Monomers are polymerised in rod form with free radical initiation, and the dehydrated lenses lathe-cut prior to hydration. The back curve is cut and polished,

the button is reversed and the front surface and edge are cut and polished. It is the most commonly used process. However, demands are placed on the mechanical properties of the lens due to the generation of heat during the high speed cutting and polishing This in turn places a limit on the glass transition temperature of the polymer which can be used. Lathe cut lenses are expensive in comparison to lenses produced by alternative methods.

Spin casting: Polymerisation of a monomer or monomer mix and solvent takes place in an open concave mould which is spun around its central axis during polymerisation. The mould is made of glass or polypropylene, the quality of the mould surface having a direct influence on the front surface of the lens. Polymerisation is via UV initiation. This technique is economic, with minimal labour involvement, the process time is rapid, producing highly reproducible lenses with smooth surfaces.

Cast moulding: Moulding takes place in a disposable, two component closed mould, with polymerisation initiated by heat. The two part mould is filled with monomer and polymerised, and once opened the finished lens is ready for hydration. A lot of skill is required to fill, make, and close the mould. Problems have been encountered in forming a reproducible edge.

1.8.3 Contact Lens Spoilation

Contact lens spoilation is not a recent phenomenon, but it is only since the introduction of prolonged periods of soft contact lens wear that the problem has manifested itself[3]. There are many factors that contribute to the level and type of deposition on a lens, including the chemical constituents of the lens material and tear film[40].

Deposition, or spoilation, of chemical components onto hydrogel contact lenses is not a unique phenomenon. This example of an interaction of a synthetic material with a complex biological environment can also be observed at other body sites, for example, plaque formation, blood clotting on foreign surfaces, marine fouling, and the fouling of

membranes used in biochemical separations, and is a function of the surface properties of the hydrogel. The initiating process in all these interactions is fundamentally the same, and is referred to as 'biological interface conversion'[3].

The term 'spoilation' covers chemical and physical changes in the nature of the hydrogel lens and the many extraneous deposits which may impair the optical properties of the lens or produce symptoms of discomfort and often intolerance to the wearer[40]. The observed types of spoilation have been divided into various classes, though there is considerable overlap, as clinical and biochemical analysis is rarely undertaken systematically.

A complete review of contact lens spoilation which is given elsewhere[52] is beyond the scope of this thesis, though a brief overview is given below.

1.8.3.1 Protein Deposits

This appears as a thin semi-opaque white film consisting of denatured protein, the major constituent being lysozyme[53]. Accumulation of protein layers on soft contact lenses can lead to an increase in surface rugosity and affect the clarity of the lens. Protein adsorption is extremely rapid and generally adsorbs from solution as a monolayer, though the presence of lipids within the ocular environment can disrupt this. Following adsorption, the protein molecules reorientate in response to the new surface environment. The protein usually remains on the surface, though for some high water content lenses, lysozyme may penetrate into the matrix. This can result in a decrease in visual acuity, and may cause irritation to the wearer leading to red eye or conjunctivitis. Cleaning systems are only capable of removing a limited amount of protein with enzyme tablets often being necessary to cleave bonds formed between the lens and proteins.

1.8.3.2 Lipid Deposits

Pure lipoidal deposits arise from the meibomian glands, and are greasy and shiny in appearance[54,55]. They are removed by surfactant cleaning and render the surface of the lens hydrophobic, which may reduce visual acuity. High performance liquid chromatography (HPLC) has been used to identify the different lipids involved. These naturally occurring lipids include phospholipids, neutral fats, triglycerides, cholesterol, cholesterol esters and fatty acids. Some deposits may be caused by extraneous sources such as cosmetics. Lipids attach through polymerisation and produce areas of non-wettability, which act as further sites for lipid attachment.

1.8.3.3 Calculi

Calculi are formed by the successive laying down of globular structures packed tightly together, creating discrete, elevated, round or oval deposits that are also termed 'jelly-bumps', 'calcium deposits', mucoprotein lipid deposits and calculi[56]. They can occur singly or in clusters on the anterior surface of the lens and continue to grow until the lens is replaced. As they grow into the lens surface, removal leaves an indentation on the surface which acts as a site for further deposition[57].

They have a complex chemical composition, with several constituents being proposed including calcium, protein and lipid. The most widely accepted theory is that they consist of a combination of all the major components of the tear film, of which 90% is lipoidal in nature.

1.8.3.4 Mucin

Mucin is produced by the conjunctival goblet cells, which may then attach to the lens where they are often found associated with proteins and lipids[40]. Mucin coats the anterior surface of the contact lens soon after insertion acting to decrease the surface tension of the tear fluid in order to promote the binding of the aqueous layer of the tear film onto the lens surface.

1.8.3.5 Inorganic Deposits

There is significant amount of calcium present in the tear film[56]. Calcium salt deposition can occur which results in the formation of a whitish film or discrete, localised deposits which are chalky-white. This layer is often overlaid by a lipid-rich organic layer.

Iron containing metallic components can become embedded in the hydrogel matrix where they oxidise to form iron oxide, which is seen as an orange coloured 'rust spot'. They are very difficult to remove so lens replacement is required.

1.8.3.6 Discolouration

Many colours have been reported for hydrogel lenses that discolour, which is particularly common for high water content lenses[58]. A yellow or brown pigmentation in worn soft contact lenses may be due to the direct absorption of nicotine from tobacco smoke. Other factors that have been found to produce discolouration include the disinfection system used, medication, and cosmetics.

1.8.3.7 Microbial Spoilation

Fungi and yeast's can use contaminants on the lens surface as nutrient sources[40]. They are caused by inadequate cleaning and require the lens to be replaced immediately. Colonies are formed which exhibit filamentary growth inside the lens matrix, and are more common in high water content lenses.

1.8.3.8 Extrinsic Factors

Several extrinsic factors can contribute to contact lens spoilation[59,60]. These include finger lipids, cosmetics and care solutions. Finger lipids are transferred upon insertion and removal of the lenses, in particular unsaturated fatty acids are transferred. A typical mascara will contain 15 or more components, including various surfactants and preservatives. Fortunately, the oils and waxes used as binding agents are almost always

based on saturated compounds, so do not possess reactive double bonds. Cosmetic debris can be deposited on the lens surface during blinking or as the make-up is removed.

1.9 Scope and Objectives of this Work

Hydrogel properties can be manipulated to fulfil the criteria required for specific applications. The aim of this thesis is to use this knowledge to investigate the use of hydrogels for three different areas related to the ocular environment.

Fluorescence spectrophotometry is developed as an analytical technique to investigate the interaction of synthetic materials with complex biological fluids. Contact lenses are analysed to consider the factors that contribute to the type and level of spoilation encountered following a known period of wear.

A keratoprosthesis is developed based on hydrogel materials. There have been many devices investigated to date, the components of which are often commercially available synthetic polymers. Hydrogels have not been studied to any great extent as potential materials for this application. Copolymers and IPN's are investigated as potential materials based on previous knowledge of soft contact lenses, synthetic articular cartilage and work carried out to mimic other naturally occurring hydrogels. The materials, morphology and fabrication of the device are considered.

A temporary prosthesis that is applied to the eye as a mask for laser ablation is also considered. This takes the form of a fluid that is applied to the ocular surface, polymerised and ablated to reprofile the corneal surface and so correct refractive errors. To date, hydrogels have not been utilised in this area. A series of hydrogels with water contents similar to that of the cornea were synthesised to analyse the factors that affect the ablation rate.

CHAPTER 2

The Cornea

2.1 Introduction

In this chapter, attention is focused on the cornea, which is an example of a naturally occurring hydrogel. Its structure is considered, along with the history of two different aspects of corneal surgery.

2.2 Anatomy of the Cornea

The cornea is the major refractive element in the eye[49]. As such, maintenance of transparency is essential. This is a function mainly of the epithelial cells on its surface. The living cells within the cornea are rich in glycogen, enzymes and acetylcholine. The human cornea is approximately 50% thicker at the periphery than at the centre[45]. The structure of the cornea is complex, consisting of five discrete layers.

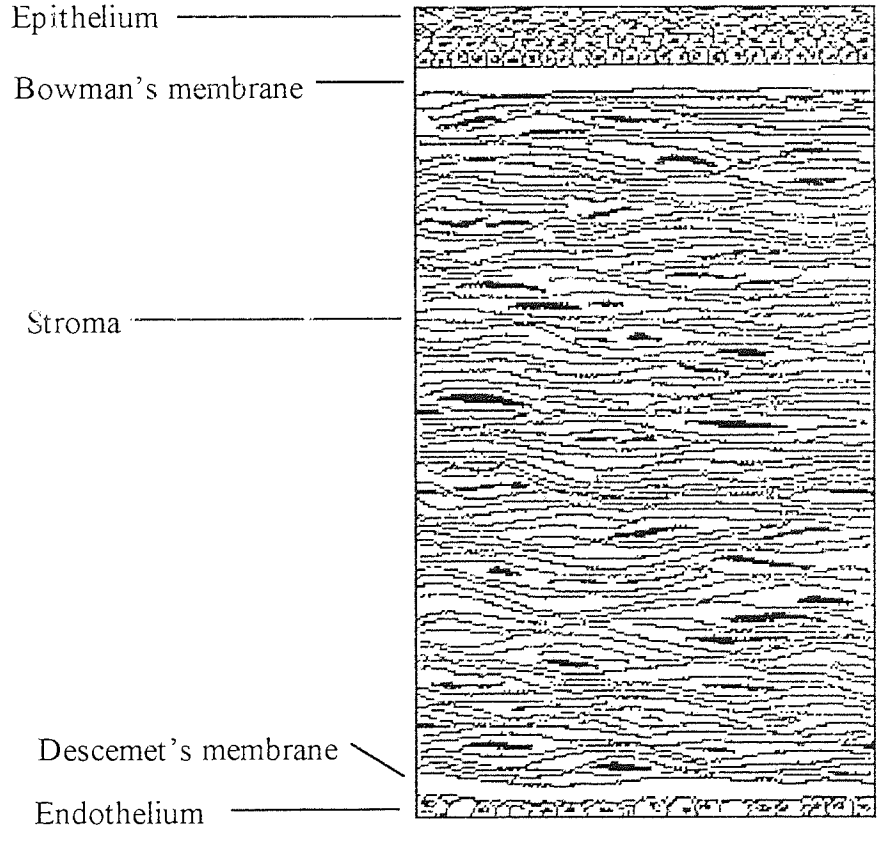

Figure 2.1 Simplified structure of the cornea

The layer of stratified squamous epithelium can be regarded as a continuation of the conjunctival epithelium. This layer is approximately 50μm thick and consists of five or six layers of cells. In humans, there are three to four layers of squamous cells, one to three layers of wing cells and a single layer of columnar basal cells[61]. The deepest of these, the basal cells, stand in perfect alignment on a basement membrane, and are continuous at the corneal periphery with the same layer in the conjunctiva. The epithelium is avascular, but does regenerate rapidly following abrasion. The epithelium is nonkeratinizing, complete turnover of adult corneal epithelium occurs approximately every five to seven days. The epithelium is compact with no gaps between cells, thus enhancing its strength. The corneal epithelium fulfils a number of vital functions[62]. For a healthy cornea and maintenance of normal vision, the epithelium must provide an effective barrier to injury. It must be strong enough to withstand rubbing of eyes and the presence of a contact lens or other foreign body within the eye. The epithelium must also resist micro-organism and fluid entry. For good vision, the epithelium must be transparent, and have a smooth surface to provide an ideal refractive surface. Covering the surface is a glycocalyx, which increases the surface area, provides a roughened surface to assist the adherence of the precorneal tear film.

The anterior limiting lamina, or Bowman's membrane, is a thin homogenous sheet, 8-14μm thick, between the basement membrane and the stroma. It is composed of randomly arranged collagen fibrils that are interwoven. The anterior surface is parallel with the corneal surface. It has a small degree of elasticity and does not regenerate once it has been destroyed, but it does show good resistance to injury and infection.

The substantia propria, or stroma, is about 0.5mm thick, forming approximately 90% of the corneal thickness, and composed of a modified connective tissue, consisting of alternating lamellae of collagenous tissue, the planes of which are parallel to the surface of the cornea. The collagen fibrils are embedded in a fluid consisting of proteins,

glycoproteins and mucopolysaccharides. Along the lamellae are many 'fixed' cells, the corneal fibroblasts or keratocytes.

The posterior limiting lamina, or Descemet's membrane, is a strong, homogenous and very resistant membrane. It is 10-12μm thick, being thinner centrally and thickest near the periphery. Unlike Bowman's membrane, Descemet's membrane will regenerate following injury. It is composed of very regular strata of fine collagenous fibres, and displays elastic characteristics.

The endothelium consists of a single layer of flattened cells, measuring 4-5μm thick. The cells exhibit a high degree of metabolic activity, it's pump mechanism maintains the cornea's fluid balance which in turn is responsible for the transparency.

2.2.1 Corneal Functions

The cornea performs many varied functions. It acts as a tough protective membrane between a potentially damaging environment and the internal sensory ocular elements. Due to its elasticity and thickness, the cornea can withstand and contain the intraocular pressure from within the eye. Approximately 75% of the total dioptic power of the human eye is due to the interface between the cornea and air, so serving as the major optical component in the eye by transmitting and refracting light. Transparency and refraction require a thin avascular tissue of uniform refractive index and a smooth surface. The containment of the intraocular pressure and good mechanical properties are required to deal with the deforming force of the eyelid during the blink cycle. This demands a thick elastic tissue, preferably with the capability for vascularisation which would allow it to regenerate easily. The human cornea appears to be an ideal compromise able to fulfil all functional requirements[49].

Water content	81 %

Deforming force of the eyelid	~ 2.6×10^3 N/m^2

Table 2.1 Table showing some properties of the cornea and its environment[3]

The maintenance of the strength and transparency of the cornea is essential for its good performance and normal vision. The cornea maintains its normal characteristics through a complex set of processes. If diseased or as a result of injury, these processes can be dramatically altered. The resulting degenerated, scarred or opacified cornea leads to problems with vision which may require surgery, of varying degrees of complexity and severity, to correct.

In the most extreme cases, the cornea may be damaged so much that the only hope of any visual improvement lies in a corneal transplant. Transplantation of human corneal grafts, an operation known as penetrating keratoplasty, which involves the replacement of the central zone of an opaque cornea by donor tissue, has a high success rate for certain categories of patients. However, there are not enough cadaver corneas available for transplantation, or in certain cultures, tissue donation is unacceptable. Some severely damaged eyes will not accept a transplant, such as those patients suffering

from ocular pemphigoid, chemical burns, Stevens-Johnson syndrome, severe dry eye syndrome, and recurrent graft failure, where the success rate will be nil. The only hope for these patients of any visual improvement lies in replacing the damaged cornea with an artificial cornea, keratoprosthesis, in a process referred to as prosthokeratoplasty, which means the replacement of the central zone of an opaque cornea by artificial materials. The history of the development of keratoprostheses, commonly abbreviated to KPro, will be discussed later in this chapter.

For some conditions, the cornea need not be replaced, merely altered. Surgical procedures for altering the refractive power of the cornea by changing the anterior radius curvature have been developed. The excimer laser has been utilised to remove precise amounts of tissue, in order to change the curvature of the cornea, correcting refractive errors, in a procedure termed photorefractive keratectomy PRK. The laser is used to remove corneal opacities and other superficial diseases in a process termed phototherapeutic keratectomy PTK. A potential use of lasers in corneal surgery is in anterior lamellar keratectomy, where an irregular corneal surface is smoothed. However, if an irregular surface is ablated without masking the irregularities, the contours of the irregular cornea are simply replicated. This will be discussed in more detail in section 2.3.

2.3 Lasers in Ophthalmic Applications

Lasers have been utilised in many varied surgical procedures, including use in the eye. Interest recently has been heightened, due to the introduction of lasers to correct refractive defects, as in the treatment of myopia.

2.3.1 History

Early work carried out by Barraquer in 1949, saw the start of surgical procedures for altering the refractive power of the cornea by selectively changing its profile or anterior

radius of curvature[62]. Trokel *et. al.*[64] were the first to suggest that an excimer laser could be used to remove a precise amount of corneal tissue following work that proved that the laser could be used to etch submicron patterns onto the surfaces of plastics[65]. They demonstrated that an excimer laser, emitting light at 193nm, could be used to remove corneal tissue, with the depth and lateral dimensions of the incision regulated with great accuracy by modulating the different parameters of the laser. Lasers have been used clinically for several types of procedures in the body, for example in surgery of the retina, to unblock coronary arteries and to remove certain types of birthmarks[5].

2.3.2 Tissue interactions

Two theories have been proposed as to the mechanism by which tissue is removed by radiation from excimer lasers[66]. The first[5] is that the laser-tissue interactions are predominantly the result of ultra-fast thermal reactions, or photon-photon interactions[67]. The discrete nature of the induced change occurs because of the short penetration or absorption depth of the ultraviolet light. The second theory suggests that the reaction is not thermal, but probably photon-induced molecular decompensation or photoablation[5]. The theory suggests that molecules in the target area are released as a direct consequence of the rupture of intermolecular bonds, whose breaking has been induced by the absorption of high energy photons. Several experiments have been undertaken in an attempt to determine the exact mechanism involved, though the exact procedure involved is not clear[68]. However, the majority of workers support the photoablation theory, as this fits with their observations. This procedure directly broke the organic molecular bonds in the tissues without creating heat. Advantages were immediately seen using this 'no-touch' technique[5] over conventional surgical procedures used to correct the corneal curvature as it removed the need for the surgeon to make an incision which was prone to several problems, for example sharpness of blade, hand pressure and speed.

2.3.3 Laser

The word laser is an acronym formed from light amplification by stimulated emission of radiation. Normally a beam of light loses intensity as it passes through an absorbing material. If molecules are present in an excited state, stimulated emission can occur, and the light beam can gain intensity. An intense monochromatic light source is used to produce a large population of atoms with their electrons in high energy levels.

Excimer is derived from the words excited dimers. In an argon-fluoride (Ar-F) excimer laser, argon and fluorine atoms are promoted into excited states by the application of electrical energy[66,69]. The atoms are held together in this excited state, forming a temporary but highly unstable bond. As these molecules decay, photons in the UV region are emitted. In the case of an Ar-F excimer laser, this occurs at 193 nm. Synder[66] reported that each photon from a Ar-F excimer laser had an energy of 6.4eV, and that the carbon-carbon bonds holding together biological tissue required a photon energy of about 6.4eV to be cleaved. This process has been termed ablative photodecomposition. The laser beam is homogenised and focused by a complex series of mirrors, prisms, convex lenses and pinhole or slit apertures[70].

2.3.4 Laser ablation of the cornea

Lasers have been utilised to alter the refractive power of the eye, in a process termed photorefractive keratectomy, PRK, and to treat certain disorders, phototherapeutic keratectomy, PTK, both of which make use of the laser ablating part of the surface of the cornea.

It is the wavelength of the laser that determines where the energy will be absorbed and thereby the tissues which are potential targets. Early studies[71] showed that the cornea was an excellent target for ultraviolet ablation. Many wavelengths have been investigated[5,64,66,72-74] with the best results of ablation being achieved for corneal tissue using a 193 nm argon-fluoride excimer laser.

Table 2.2 Table showing the excitation wavelengths of some excimer lasers[64]

The 193nm Ar-F laser showed further advantages in comparison to other wavelengths. It was found[71,73] that there was minimal thermal damage to the surrounding tissues using 193nm compared to 248nm. Krueger reported that at 193nm, the tissue had sharply defined boundaries where it had been irradiated with no evidence of heating in adjacent tissues[76]. Ablations made at longer excimer wavelengths produced incisions with ragged edges and the adjacent nonirradiated tissue showed signs of thermal damage[74]. The ablation depth and energy could be controlled by varying the fluence or number of pulses, with more precision when carried out at 193nm than 248nm[76]. In general, the higher the fluence, (where fluence is energy density per pulse, mJ/cm^2), the greater the amount of material ablated per pulse. Little or no mutagenic effects were observed[76]. At 193nm the cornea is virtually opaque and displays limited light penetration, therefore deeper structures are protected. 193nm photons have a reported penetration depth in biological tissues of a few microns[77]. Marshall[78] reported that the optical properties of the cornea were preserved following irradiation at 193nm.

The extent and depth of ablation are determined by several parameters including the shape and diameter of the laser beam, laser beam fluence, the duration of the radiation bursts (nanoseconds), the pulse rate and number of pulses. Ablation rate is determined by:

$$\text{ablation rate} = \frac{\text{number of pulses}}{\text{thickness removed by ablation}} \qquad (2.1)$$

The depth of ablation required to achieve a given refractive change is calculated by[79]

$$\text{depth } (\mu m) = [\text{diameter (mm)}]^2 \times 1/3 \text{ power (diopters)} \qquad (2.2)$$

It was reported[80] that with pig eyes, there was a near linear increase in ablation rate with increasing fluence, and that ablation rate increased with increasing ablation diameter from 2 to 4mm, then decreased as the diameter increased to 5 and 6mm. Several methods have been employed to determine the ablation rate of the human cornea, including perforation experiments, photoacoustic studies and histological evaluation of deep nonpenetrating keratectomies[81]. It was reported that using a laser beam with fluence of 180 mJ/cm^2, the ablation rate ranged between 0.4 and 0.5μm per pulse. However, using this ablation rate in the early clinical PRK studies resulted in significant undercorrection. A nominal ablation rate was obtained through optimising the refractive outcome by trial and error. This resulted in an ablation rate of 0.23 to 0.3μm per pulse which is the clinical rate used routinely today[81]. Early experiments had shown that the ablation rate of Bowman's layer was lower than the stromal ablation rate[82], and that corneal dehydration had an impact on the ablation rate[83] with the ablation rate decreasing as the cornea dries.

Complications associated with laser surgery include improper correction[84], decentration of the ablation, corneal haze, optical degradation, malfunctioning of the laser, excessive or inadequate wound healing, inconsistent corneal hydration, infectious keratitis and inflammatory infiltrates[85].

Marshall *et. al.*[73] reported a marked swelling of the stroma following ablation which was localised in the area of ablation, in response to disturbed water distributions. However, much of the early work was carried out on rabbits, who do not have Bowman's layer.

There are three stages associated with corneal epithelium healing[85]. The first, the latent phase, occurs within the first six hours postoperatively. This is followed by a healing phase and a resurfacing phase. The healing process must not result in the formation of

scar tissue, as the cornea must remain transparent. It was found[86] that the regrowth of epithelium over the wound was essential before the synthesis of new connective tissue could occur. Observations[73] of an ablated surface usually showed it to be smooth and regular, bounded by an electron dense deposit termed a pseudomembrane. Many workers proposed that reepithelialisation of the irradiated area may be aided by the formation of this pseudomembrane, as it forms a seal around the exposed area and acts as a template for reepithelialisation[87].

As a consequence of the healing process, subepithelial haze has been reported in most cases[88]. It does not develop until after reepithelialisation has occurred. The haze was attributed to increased fibroblastic activity associated with new collagen synthesis and its random deposition[89]. This was shown to be collagen type III and VI[70,89]. Results indicated that the degree of haze was dependant upon the depth of ablation Haze is not normally a problem for the patient, it has been observed at one month postoperatively and usually disappears after six months[85].

2.3.5 Reprofiling of the cornea

Reprofiling of the cornea has been reported by using varying ablation diameters and operating conditions. This required the accurate control of the laser and prevention of any eye movement during the surgery. Marshall *et. al.*[90] reported the design of an ablation algorithm that could be used to produce the desired recontoured surface, which involved removing a series of concentric tissue circles to produce a smooth surface. Several workers[75,91,92] have investigated the use of a mask to cover any corneal irregularities prior to exposure by the laser in order to obtain a smooth cornea, figure 2.2.

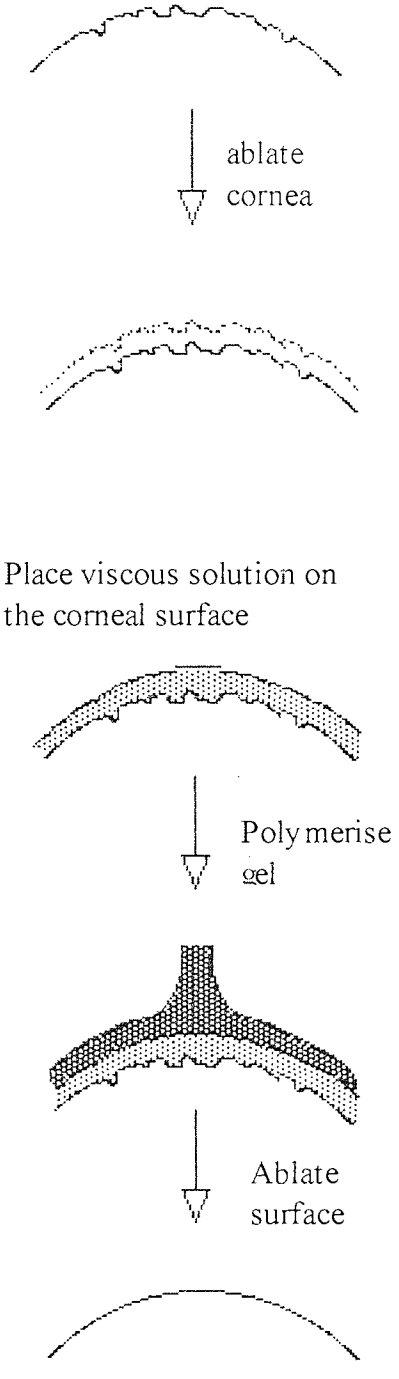

Figure 2.2 Figure showing effect a mask has on ablated cornea

DeVore[75] reported the use of collagen, though this took nearly one hour to form a gel when placed on the eye underneath a polymethyl methacrylate contact lens as the mould[93]. Kornmehl[94] suggested that a fluid which had a viscosity between saline and a

1% carboxymethyl cellulose solution would be the most desirable to fill the localised depressions on the corneal surface prior to preferential ablation of any remaining elevated tissue[95]. A hydroxypropyl methylcellulose 0.3% solution was used to investigate the different laser conditions required to give a reproducible smooth corneal surface[95,96].

Sodium hyaluronate has also been investigated as a potential masking agent[97]. *In vitro* studies claimed that this was an ideal masking agent.

Pallikaris[98] reported the use of a two component gel that could be placed on the eye then moulded beneath a PMMA contact lens. The gel was at 50°C and gelation occurred within 30 seconds.

A selection of masking agents have been investigated[98], with the one chosen dependent upon the nature of the surface to be ablated. Methylcellulose is commonly used, with a variety of viscosity's available, 0.5% Cellufresh and 1% Celluvisc (Allergan) and 2.5% Goniosol (IOLab). Methylcellulose turns white during ablation, allowing the surgeon to see when the mask has been eroded.

Experimentally, there are mixed opinions in several aspects concerning the surgery. It is debated whether or not the epithelium should be removed prior to ablation, and if it is removed, how, manually or laser. Some workers feel the need for nitrogen to be blown across the corneal surface during surgery with a vacuum to remove the debris. The eye must also be fixed during surgery.

2.4 Artificial Cornea

Corneal blindness can be caused by conditions such as severe Stevens-Johnson syndrome, chemical burns and leucomas. Repeated graft failure, and a world-wide

shortage of corneal donors mean that the only hope of any visual improvement for these patients lies with the use of an artificial cornea[49]. The development of the artificial cornea can be conveniently separated into three periods of time[100].

2.4.1 1789 - 1905

An artificial cornea was first suggested by Pellier de Quengsy in 1789, when he proposed the replacement of an opaque cornea with a glass plate which was held in place with a circle of silver which had been sewn onto the front of the cornea with cotton. The surgical procedure suggested that the operation should only be carried out on a "good" day and that the patient should lie down at all times to prevent the prosthesis falling out and embarrassing the surgeon. There is no evidence to suggest that the experiment was ever undertaken[101].

The first recorded implantation of a keratoprosthesis, KPro, was by Nussbaum in 1856, who placed a rock crystal glass plate in a rabbit cornea[102]. It was described as a 'cuff-link' prosthesis due to its shape, it consisted of two plates connected by an optical cylinder, and the method of fixation was extracorneal. This prosthesis was reputedly retained for three years. Heusser in 1859 was the first to report implanting a small glass disc into a human cornea, though it only lasted for a couple of months. Later that century, Von Hippel, in 1877, and Salzer, in 1898, used a glass disc in animal studies with the glass cylinder in a gold case[103]. Dimmer reported using celluloid plates to hold the glass in place on the cornea, but failure was rapid. Various modifications to the Nussbaum 'cuff-link' KPro, experimental tests and clinical tests were carried out, but as expected the early results were not encouraging with the prostheses all extruding and hence discouraged further work[104].

Significant improvements were being made in all forms of surgery by the turn of the century including the discovery of anaesthetics and the implementation of aseptic conditions resulting in the increased success of surgical procedures. Techniques for

corneal transplantation were developed and improved diverting, to some extent, attention from the keratoprosthesis development, where very little progress was made[105].

2.4.2 1905 - 1950

Due to the limited success of the early artificial corneas, work on KPro's was almost abandoned[49]. Failures in implanting the 'stud' model lead to the majority of leucomas being treated with keratoplasty, even though it had been proved that vision could be restored by using a keratoprosthesis, even if it was for a limited period of time. In 1937, Salzer claimed that glass plates had been successfully implanted in rabbits, and suggested the use of an egg membrane to cover the prosthesis to improve retention.

Some work continued in Russia, with Elsching (1920) and Filatov (1924)[100] who concentrated on methods of securing the prosthesis and new techniques for the operation. Filatov became the first to implant a penetrative KPro in 1935, into an eye with a burn leucoma. The prosthesis was made of glass, in the shape of a stud, extrusion occurred after six weeks.

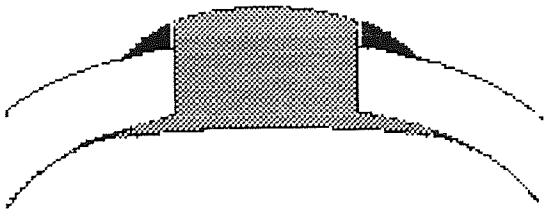

Figure 2.3 Gyorffy two piece KPro with posterior and anterior extracorneal securing devices

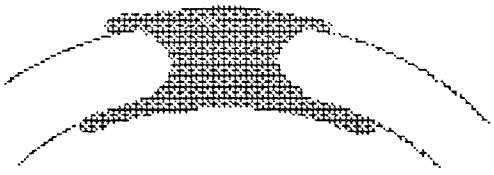

Figure 2.4 Baron single piece KPro with extracorneal securing devices

2.4.3 1950's to Present day

Little progress in the development of KPro's occurred, with glass being the preferred material until the second world war. Following this, it was noted how pieces of polymethyl methacrylate (PMMA) from shattered canopies were well tolerated in some pilots eyes. PMMA was adopted as a replacement for glass in many applications, often under the tradename Plexiglass™[106,107]. The introduction of synthetic polymers for use in the manufacture of KPro's lead to a significant increase in interest and the number of workers this area[104].

Stone from America is often credited with introducing PMMA into corneal surgery in 1953, but both Franeschetti in Switzerland, and Györffy in Hungary had reported its use some years earlier, though they had been unsuccessful[49,108,109]. Dorzee and Barraquer separately performed the first human KPro surgery using synthetic polymers in 1955[103]. Amazingly, at this early stage in development, the idea of using an interlamellar supporting PMMA plate (or flange) around the PMMA optical core was introduced. The initial prostheses were unsuccessful, but from this two ideas developed further leading to a whole range of devices that have been invented and tested since[110]. The two ideas were firstly, interlamellar plates should be perforated, fenestrated or made of meshwork, and secondly, the plates could be made of different materials to that used for the optical core[111].

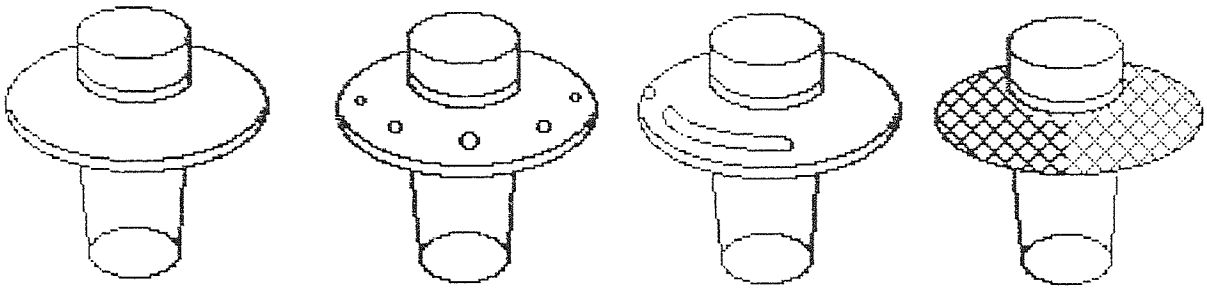

Figure 2.5 Diagram showing the variations in skirt design (Cardona 1967[112]), solid disc, holes, loops and mesh

The 'core-and-skirt' design[112] was introduced as an attempt to improve mechanical fixation with the host cornea, and improve the integration by use of a perforated skirt which would allow cell ingrowth into the periphery. Several workers (Fyodorov 1970, Puchkovovskaya 1970, Turss 1970 and Bagrov 1973)[100,102] later showed that a nonperforated plastic membrane inserted into the corneal layers caused the destruction of the corneal epithelium, and impeded the supply of nutrients from the aqueous humour of the anterior chamber. Reports of a modified 'stud' model being implanted were still made by a few workers (Gyorffy 1951, Sommer 1953, Vodovozov 1964)[100] but they all extruded within seven months. Subsequent work has centred on optimising the skirt material to gain the best possible fixation and retention of the skirt within the eye. Implantation can be carried out in one or two stages, involving complicated surgery.

Since the 1970's investigations have continued into the use of different materials and forms of devices as keratoprostheses. Implantation experiments have continued, though problems were still encountered[113-118]. Many patents for various devices have been granted[119-131]. Surgical procedures have been considered, with novel instruments and techniques being developed[132,133]. Several fabrication methods have also been explored[134].

2.4.4 Fixation

Early corneal implants consisted essentially of a cylindrical optical core penetrating either the anterior portion of the eye, the posterior portion, or a through-and-through design. The optical core was held in place by an intralamellar flange, with perforations to allow for the ingrowth of tissue[112]. These have been referred to as 'core-and-skirt' prosthesis and various methods of fixation in the eye have been investigated.

The first KPro with intracorneal fixation was introduced by MacPherson and Anderson in 1953[111]. It consisted of radial extensions to help retain the implant. Early surgical techniques for the implantation of a device involved embedding a flat disc of alloplastic material into the cornea with a hole anterior to the prosthesis[102]. Optical lenses were then placed in full-thickness holes in the cornea. Next, optical cores were held in place by plates on the anterior and posterior surfaces of the cornea. Following on from this, a two-piece nut-and-bolt device was designed by Cardona, in which either the anterior or posterior plate had to be placed on the mushroom-shaped part of the prosthesis after it had been inserted into the cornea[135]. This was a technically difficult operation involving the use of specifically designed instruments. At a similar time, Dohlman assembled his prostheses on cadaver eyes prior to implantation[136].

Choyce[137] and Cardona independently designed a two piece device involving an optical core held by a skirt, referred to as a 'core-and-skirt' KPro. Cardona used a nut-and-bolt design to allow for adjustment of the height of the optical core above the conjunctiva following implantation. Choyce's two piece device facilitated the adjustment of the core to allow for the removal of retroprosthetic membranes.

Figure 2.6 Diagram showing different types of penetrative prostheses[102]

In 1969, Cardona described a 'nut-and-bolt' KPro[111]. It was made from PMMA and consisted of an external cosmetic contact lens attached to a central optical cylinder which passed through the cornea and screwed into a supporting plate or nut which lay against the posterior surface of the cornea. The core height above the conjunctiva could be adjusted, which would prevent epithelial downgrowth, and the contact lens, it was claimed, would reduce excessive evaporation form the corneal surface. The extrusion rate was not improved, with retroprosthetic membrane formation and glaucoma still a problem.

Dohlman reported in 1974, a 'collar-button' PMMA KPro[100], which consisted of an optical core that passed through the entire corneal thickness, with an anterior plate and

a back plate that screwed into the stem to lie against the posterior corneal surface. The main complication was ulceration around the plastic stem, leading to leakage, extrusion retinal detachment and retroprosthetic membrane formation.

Cardona developed the 'through-and-through' prosthesis which was fixed to the anterior corneal surface and has a perforating optical cylinder that reaches the anterior chamber One of the latest models is very complex, consisting of a central PMMA core, surrounded by a perforated PTFE plate, which is reinforced with both a mesh of Dacron™, and autologous tissue, usually periosteum from the patients tibia[135].

The lack of a firm junction between the optical cylinder and the skirt, and between the skirt and the host corneal tissues has been the cause of most of the complications. It became apparent that the peripheral skirt must become incorporated into the host material through cell invasion and growth across the interface[113]. In most cases, a section of mucous tissue, either conjunctival or buccal mucosa, is placed over the anterior surface of the prosthesis to aid fixation. Surgery in all these cases is complicated and often involves the removal of the lens, iris and tarsus, the partial removal of the vitreous body and some of the ocular muscles. Specialised surgical instruments had to be developed to perform such complex procedures[132,133].

2.4.4.1 Keratoprostheses with extracorneal fixation

The prosthesis is implanted into the centre of the cornea, and an anterior plate is pressed against the corneal epithelium and the posterior plate against the endothelium[100]. In most cases, these prostheses stayed in place for approximately seven months. This type of prosthesis could not be tightly fixed to the tissue. The 'nut-and-bolt' prosthesis of Cardona's can also be characterised in this area. It has been classed as a retrocorneal prosthesis by its method of fixation and a 'nut-and-bolt' by its structure.

2.4.4.2 Keratoprostheses fixed between lamellae

The first prosthesis that had its supporting plate placed in an interlamellar pocket was designed by MacPherson and Anderson in 1953, followed by Legrand and Baron in 1954[102]. The length of the optical cylinder was less than or equal to the thickness of the cornea, which lead to anterior or posterior surface of the cylinder quickly being grown over by a retroprosthetic membrane. Cardona introduced a model in 1962[103] which had no perforations in the supporting plate which proved to be a considerable disadvantage and is no longer used.

Stone, in 1965, was the first to introduce a removable optical core. Choyce later designed a dismountable penetrating prosthesis consisting of two parts, which was implanted in two stages. Fyodorov, Zuev and Moroz further developed dismountable prostheses[100].

Cardona studied several devices in an attempt to determine the optimal size for the peripheral skirt and the implantation depth. He concluded that the deeper the supporting plate, the more likely that the prosthesis would be extruded. Choyce investigated how far into the anterior chamber the optical core should protrude, and reported that the further the optical part extended into the anterior chamber the less likely the rear surface would prevent retroprosthetic membrane formation. However this would mean that the lens would have to be removed[137].

2.4.5 Materials

2.4.5.1 Synthetic Materials

Early work centred on the use of PMMA as the material used for both the optical core and the skirt material. For most of the devices, PMMA is still used as the optical portion, though many materials have been investigated as potential skirt materials[104]. PMMA has good optical clarity and relatively good tissue tolerance, though the purity of the polymer is hard to control due to the toxicity of any unreacted methyl

methacrylate monomer. PMMA is also rigid and impermeable to fluids which can cause necrosis in the surrounding soft tissue.

Cardona reported a study on over 160 acrylic resins and found that the toxicity of the plastic was significant in the extrusion process[112-139]. Use was made of several materials that had been employed previously as implant materials, as the majority of work was being carried out by surgeons who had a limited knowledge of synthetic polymers. Teflon, Dacron, siliconised Teflon, Silastic, fibreglass, nylon and cellulose were all investigated.

Many commercially available synthetic materials have been investigated for use as the skirt material, as shown in table 2.3.

Material	Pioneer(s) and Major workers	Ref(s)
Aluminium oxide ceramic	Polack and Heimke	140-142
Proplast™	Lamberts and Grandon; Barber; Girard	143-144,113
Dacron™	Pintucci	145-147
Porous Teflon™ (EPTFE Impra™)	Legeais	148-154
Carbon fibre	Kain	153
Polyurethane	Caldwell and Py	154
Goretex™	Jacob-LaBarre and Caldwell	130
Teflon™	Cardona	112,135
Hydroxyapatite	Tu	155
polyHEMA	Mester; Chirila	49,156, 157
Polybutylene-polypropylene	Trinkaus-Randall	158,159
Titanium	Fyodorov, Zuev and Moroz	100,160
Silicon coated titanium	Linnola	161
tooth-bone	Strampelli; Falcinelli	162-167
tibia	Temprano	168
PMMA	Dohlman, Stone etc.	108,109
Nylon	Bertelsen	169
Medpor™	Miller	170
Tantalum	Bedilo	100
polypropylene	Knowles	100

Table 2.3 Table showing some of the materials used for the periphery of a keratoprosthesis and the workers who introduced them

2.4.5.2 Use of Biological Tissues

In an attempt to improve biocompatibilty and retention of the prosthesis, Strampelli and Marchi in 1963[162], considered using autologous body tissues as the skirt material. Many tissues were investigated, including nail, cartilage and skin but the best results were obtained with the use of a section of tooth and bone[163]. This technique is termed osteo-odonto keratoprosthesis, which is abbreviated to OOKP. The surgery involved in fitting this device is very complex, though promising results have been obtained[165]. The technique has been further developed by Falcinelli[167], and during 1997 the first successful operation was completed in Britain by Liu.

Fitting the OOKP is a two stage surgical procedure. In the first, a section of healthy tooth and jaw bone are removed from the patient, the tooth is a single root and usually a canine[171]. This section is ground into the correct shape, and a hole drilled through the centre where a PMMA optical core is glued in place. The prosthesis is placed into a subcutaneous pocket below the patients eye, where it is left for three months to allow for soft tissue ingrowth. A piece of buccal mucosa is removed from the patients cheek and placed over the diseased cornea. This will regenerate providing a blood supply to the cornea.

After three months, the prosthesis is removed from the subcutaneous pocket underneath the eye and the soft tissue removed from the optical core. The buccal mucosa graft is pulled back from the surface of the eye, and the prosthesis introduced. A hole is cut into the graft to accommodate the protruding optical cylinder, and replaced over the prosthesis. A cosmetic contact lens is used to cover the graft, leaving the eye looking normal.

The extrusion rates associated with this surgery are low, and visual improvement is reported in 90% of patients. However, the field of vision is restricted to 40^0 due to the

size of the biological support, which restricts the diameter of the PMMA core that can be used[172].

2.4.5.3 Hydrogels

Hydrogels have a long history of use in the eye as soft contact lenses, with a variety of materials being investigated for this application, but their use as keratoprosthetic materials was not utilised until the late 1970's. Mester, in 1976[49], found that a polyHEMA prosthesis was well tolerated in rabbits, with no extrusion noticed during the observation period of three years[173] The design of these prostheses moves away from the previous devices, taking the form of a full-thickness contact lens.

Trinkaus-Randall *et. al.* proposed a polyvinyl alcohol copolymer hydrogel[174] as the optimal material for the central transparent portion of a perforating keratoprosthesis[177,178]. They claimed that the advantages of this hydrogel were strength, elasticity, optical clarity and a high water content. It was shown that ions and glucose could diffuse across the hydrogel. The periphery was made using a fibrous web of polybutylene-polypropylene 80:20% copolymer. The polyvinyl alcohol hydrogel was preseeded with epithelial cells, protein impregnated or surface modified prior to implantation in rabbits, and the skirt treated with fibrin adhesives to retard epithelial downgrowth. As the materials were chemically different in their nature and properties, problems arose in joining them together. It was demonstrated that stromal keratocytes could penetrate the material, proliferate and synthesise collagen[158].

Chirila *et. al.* in 1990[49], proposed a prosthesis that consisted of a polyHEMA optical core with a porous polyHEMA skirt. The junction between the skirt and periphery is formed by a sequential interpenetrating polymer network, providing a permanent connection between the two chemically identical polymer systems[177]. By varying the amount of water in the initial monomer mixture, the porosity of the skirt could be controlled. The polymerisation is a two stage procedure carried out sequentially in a

special mould. The skirt is formed by phase separation polymerisation in an aqueous solution, followed by polymerisation of the central core *in situ*. They showed that the polyHEMA porous sponge displaying pores larger than 10μm could support cellular invasion when implanted intrastomally in the rabbit cornea when preimpregnated with collagen type I, claimed that extrusion did not occur in the short term, and that stromal fibroblasts trapped within the sponge were synthetically active and deposited neocollagen, mainly type III, a 'healing' collagen[178]. The fixation of the device through fibrovascular invasion into the skirt is proposed as the reason why extrusion is not observed, though the mechanical properties are weak, and need to be improved. Stromal necrosis, inflammatory reactions and epithelial downgrowth have been observed, and epithelialisation of the core is poor[157].

To date, neither of these hydrogel prostheses have been implanted into human eyes. Due to the widespread application of hydrogels as soft contact lens materials, it is understandable that this class of materials is investigated for use as a KPro. The devices have the appearance of a contact lens, so less invasive surgery is potentially required. The design of hydrogels for biomedical applications has been investigated for many years, as the properties can be manipulated for each application. The interaction of hydrogels in the eye has been studied for many years, with hydrogels being designed for extended wear contact lenses, and synthetic analogues of other natural hydrogels, i.e. cartilage, have been synthesised, use of this knowledge is utilised in order to produce a hydrogel keratoprosthesis.

CHAPTER 3

Materials and Methods

3.1 Introduction

This chapter deals with the identification and source of raw materials, the preparation and characterisation techniques of the hydrogel samples derived for use as an artificial cornea or a temporary prosthesis for laser ablation.

3.2 Reagents

The reagents used in this work are listed in Table 3.1, and the principle structures shown in Figure 3.1. All liquid monomers were distilled under reduced vacuum prior to use to remove the inhibitor, as described in the literature[179]. These were then refrigerated prior to use. All other chemicals were used without further purification.

Reagent	Abbreviation	Molecular weight	Supplier
2-hydroxyethyl methacrylate	HEMA	130	Vista Optics
Methyl methacrylate	MMA	100	BDH
Acryloyl morpholine	AMO	141	Vista Optics
N-vinyl pyrrolidone	NVP	111	Vista Optics
Tetrahydrofurfuryl methacrylate	THFMA	170	Polysciences
Methacrylic acid	MAA	86	BDH
ester polyurethane	PU		Goodrich
Ethylene glycol dimethacrylate	EGDMA	198	BDH
Azo-bis-isobutyronitrile	AZBN	164	Aldrich
Riboflavin		376	Aldrich
Irgacure 184		236	Ciba Geigy
Polyethylene glycol x dimethacrylate, where x = 200, 400, 600, 1000	PEGxDMA	398, 498, 698, 1098	Polysciences

Table 3.1 Suppliers, molecular weights and abbreviations of reagents used

Reagent	Abbreviation	Molecular weight	Supplier
Hydroxypropyl methylcellulose	HPMC	various	Aldrich
Polyvinyl alcohol	PVA	various	Aldrich, BDH
Polyethylene glycol 200 monomethacrylate	PEG200MA	360	Aldrich
Glycidyl methacrylate	GMA	142	Aldrich
Tetrahydropyranyl methacrylate	THPMA	184	Aldrich

Table 3.1 continued. Suppliers, molecular weights and abbreviations of reagents used

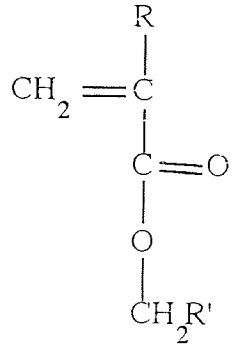

$R = CH_3$ $R' = CH_2OH$ 2 - Hydroxyethyl methacrylate

$R = CH_3$ $R' = H$ Methyl methacrylate

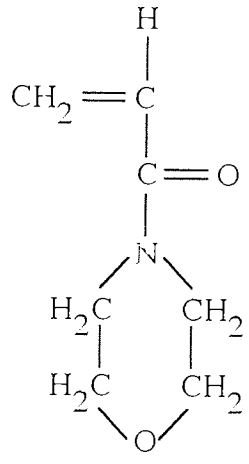

Acryloylmorpholine

Figure 3.1 Structures of principle chemicals used

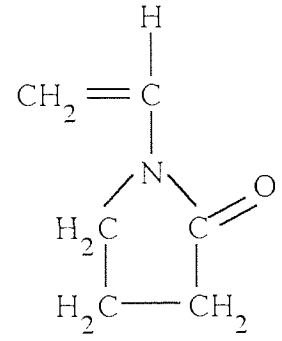

N - vinyl pyrrolidone

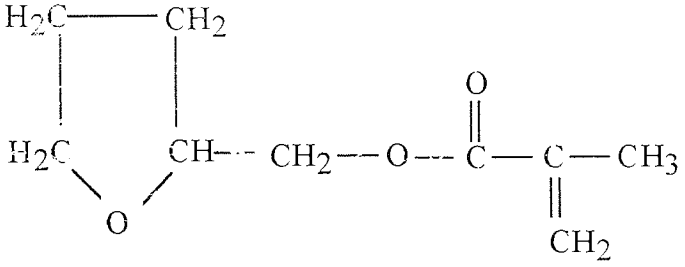

Tetrahydrofurfuryl methacrylate

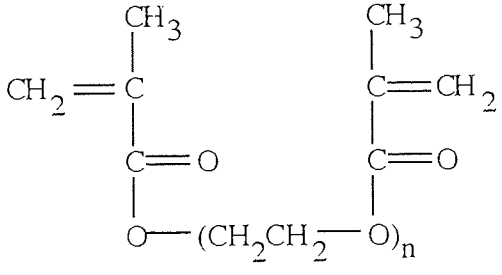

n = 1 Ethylene glycol dimethacrylate

n = 4 to 5 Polyethylene glycol 200 dimethacrylate

n = 9 to 10 Polyethylene glycol 400 dimethacrylate

n = 15 to 16 Polyethylene glycol 600 dimethacrylate

n = 22 to 23 Polyethylene glycol 1000 dimethacrylate

Figure 3.1 continued. Structures of principle chemicals used

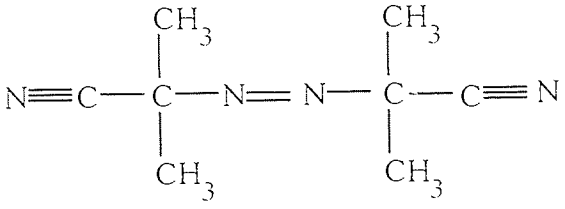

Azo -bis - isobutyronitrile

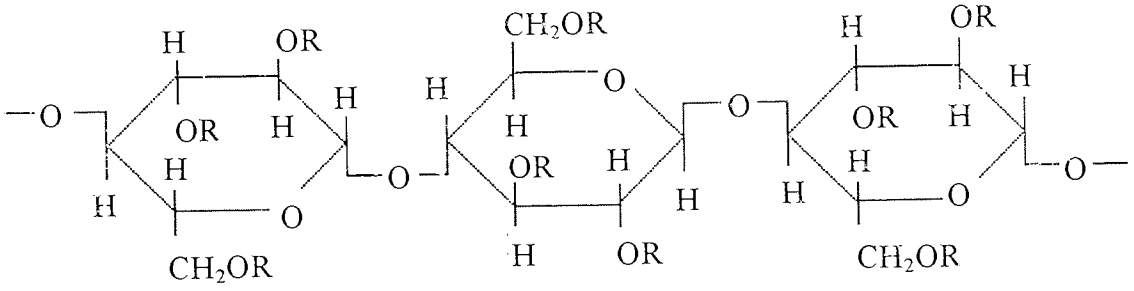

R = H, CH_3, or $CH_2CH(OH)CH_3$

Hydroxypropyl methylcellulose

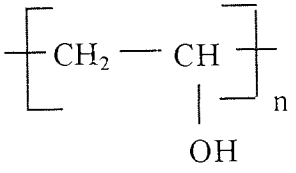

Poly vinyl alcohol

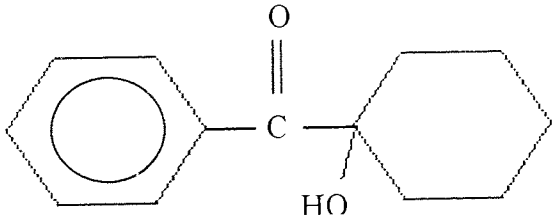

Irgacure 184

Figure 3.1 continued Structures of principle chemicals used

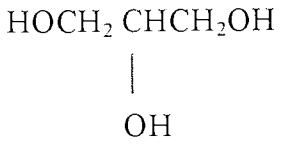

Glycerol

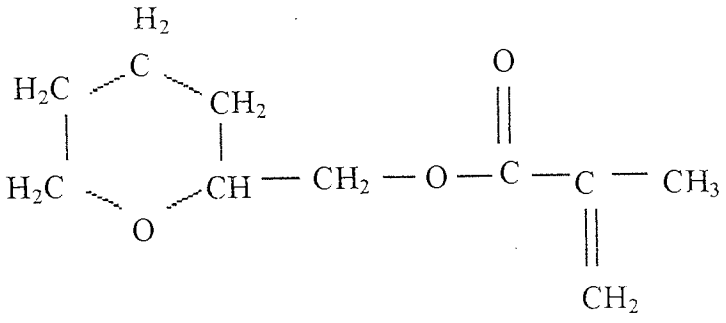

Tetrahydropyranyl methacrylate

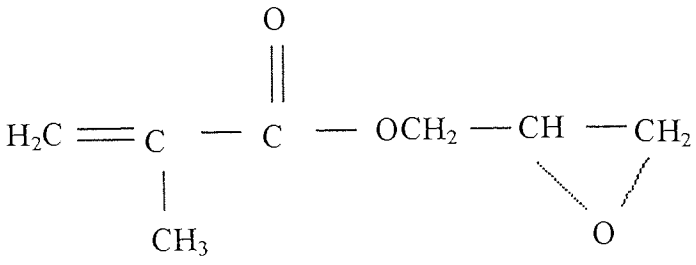

Glycidyl methacrylate

Figure 3.1 continued Structures of principle chemicals used

3.3 Polymer Synthesis

3.3.1 Preparation of Hydrogel Membranes.

Hydrogels were produced in the form of a membrane sheet, using the mould shown in Figure 3.2.

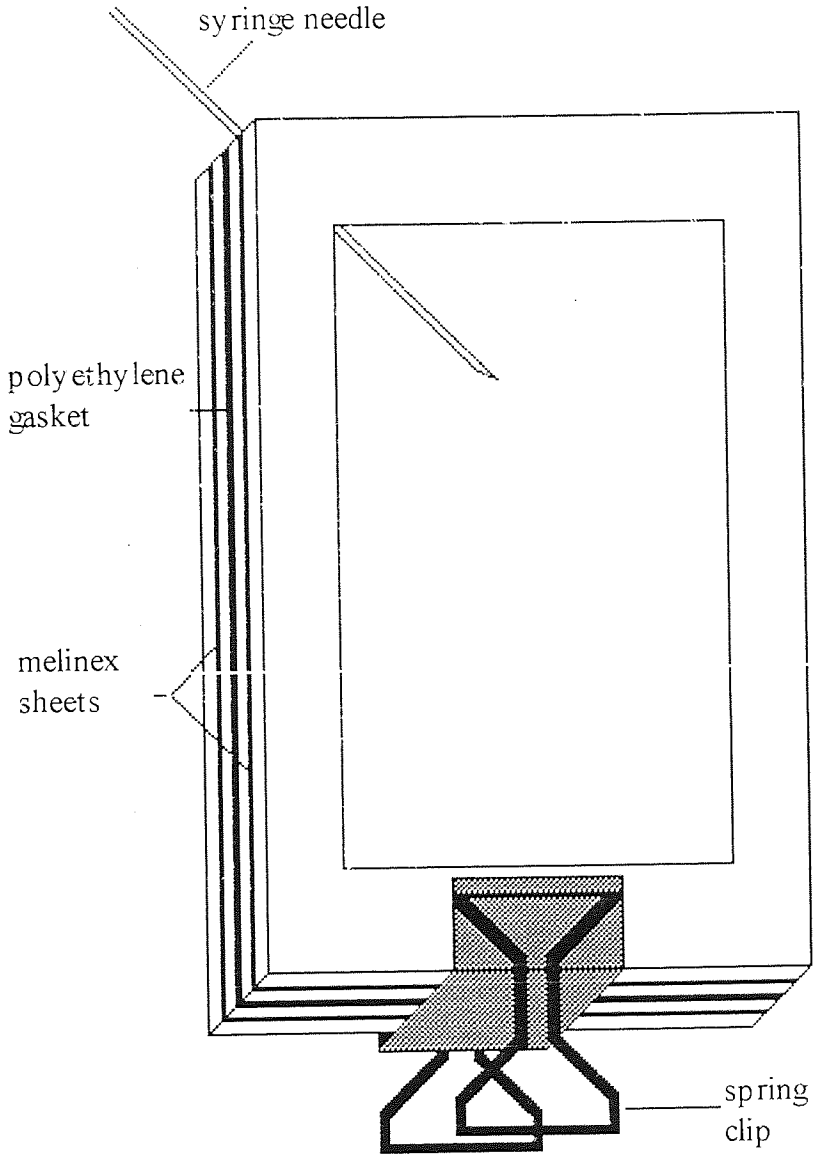

Figure 3.2 Diagram of a hydrogel membrane mould

Two glass plates (15cm x 10cm) were each covered with a sheet of Melinex (polyethylene terephthalate) secured by spraymount, and the surfaces wiped with acetone. The glass plates were covered to prevent adhesion of the polymer to the plates and allow for easy separation of the plates, as well as providing a clean, smooth surface.

The plates were placed together with two polyethylene gaskets, each 0.2mm thick, separating the Melinex sheets (cavity 5 x 9 cm). The whole mould was held together by sprung clips and the monomer mixture inserted via a G22 syringe needle and syringe.

A standard comonomer mixture was made up containing the required amounts of monomers mixed together, with 1% w/w crosslinker (ethylene glycol dimethacrylate), and 0.5% initiator (for thermal polymerisation this was Azo-bis-isobutyronitrile) to a total of 5 grams. Once a homogeneous mixture of the monomers was obtained, the initiator and crosslinker were added and the mixture was degassed with nitrogen for ten minutes to ensure that all the oxygen is removed from the sample. The mixture was then introduced to the mould via the syringe and needle, the needle was removed so that the monomer mixture filled the mould cavity, and the mould tapped gently to remove any air bubbles that may have been introduced.

The mould was then placed into a 60°C oven for three days to effect polymerisation, followed by two to three hours post-cure in a 90°C oven. The mould was then removed, and whilst it was still warm, the spring clips were removed, and following the careful opening of the mould, the membrane was placed in distilled water to hydrate. The membrane was hydrated for at least a week, changing the water daily to remove any unreacted monomer or crosslinker. Following the required soaking period, the membrane had reached equilibrium.

3.3.2 Interpenetrating Polymer Networks

For semi-interpentrating polymer networks (semi-IPN's), a slight modification to the method outlined above was needed. The linear or interpenetrating polymer was dissolved in the monomer or comonomers, with up to 15% of the solvent tetrahydrofuran, THF, if necessary. Once a homogeneous mixture was obtained, the initiator and crosslinker were added, and the mixture degassed. This was then poured

directly into one half of the mould cavity and the second plate placed onto it as the mixture was too viscous to be injected into the mould.

3.3.3 Porous Membranes

A porous membrane was synthesised in the same way as above, with an added porosigen, usually dextrin (pore size 38-63 μm). The required amount of porosigen was added to the monomer mixture prior to the addition of the crosslinker and initiator once a homogeneous mixture had been obtained. Porous materials can be made using either the thermal or UV polymerisation techniques described here.

3.3.4 UV Polymerisation

For UV initiated polymer sheets, a UV initiator, which was Irgacure 184, 0.5% w/w, was used as an alternative to AZBN. The preparation of the monomer mixture was identical to that above for thermal polymerisation, with the exception that the mould was placed under a UV source for up to thirty minutes and not placed in an oven. The membrane was hydrated in the same way.

3.4 Determination of Equilibrium Water Content

Once a sample had hydrated with appropriate water changes, as seen in section 3.3.1, for at least one week, the equilibrium water content, EWC, was determined. This was measured by weight differences. Samples of the hydrated membrane sheet were cut with a size seven cork borer, and the surface water carefully removed with filter paper. Care is needed not to squeeze the membrane thus removing water from within the sample. The discs were then weighed on a five place balance. Five discs were used from each sheet, and the results obtained were an average of all the samples from that membrane.

The weighed hydrated samples were then dehydrated in the microwave, reweighed and dehydrated further if necessary to constant weight. Usually ten minutes was adequate.

The EWC was calculated using equation 3.1, and the final value quoted is the average of at least three values obtained for that membrane.

$$EWC = \frac{\text{Weight of water in the gel}}{\text{Total weight of the hydrated gel}} \times 100\% \qquad (3.1)$$

3.5 Measurement of Mechanical Properties

The mechanical properties of the hydrogel samples were investigated using a Hounsfield Hti tensometer which was interfaced to an IBM 55SX computer. The tensometer was fitted with a 10N or 100N load cell, and the relative positions of the crossheads resulted in the sample being held vertically. Standard testing parameters were entered into the computer, along with the dimensions of the sample allowing the computer program to calculate Young's modulus (E_{mod}), tensile strength at break (σ_b), and elongation at break (ε_b). These were calculated using the following equations:

$$\text{Elastic modulus } (E_{mod}) = \frac{\text{stress}}{\text{strain}} \qquad (3.2)$$

$$\text{where stress } (\varepsilon) = \frac{\text{load}}{\text{cross-sectional area}} \qquad (3.3)$$

$$\text{and strain (e)} = \frac{\text{extension of gauge length}}{\text{original gauge length}} \qquad (3.4)$$

$$\text{Tensile strength } (\sigma_b) = \frac{\text{load at break}}{\text{cross-sectional area}} \qquad (3.5)$$

$$\text{Elongation at break } (\varepsilon_b) = \frac{\text{extension of gauge length}}{\text{original gauge length}} \times 100\ \% \qquad (3.6)$$

The mechanical testing of hydrated samples presents many difficulties which are discussed elsewhere[20].

The samples to be tested are cut from hydrated membrane sheets using a purpose designed, dumbbell shaped, cutter of 8mm gauge length and 3.3mm width. The thickness was measured with a micrometer.

The sample was clamped vertically between jaws of the tensometer. A test speed of 20mm.min^{-1} was selected under conditions of room temperature and pressure. Test conditions and the sample dimensions were entered into the computer. Complete hydration (100% humidity) was maintained throughout by spraying the sample with an atomised stream of distilled water before and during the test. Upon completion, the computer program calculated Young's modulus (E_{mod}), tensile strength at break (σ_b), and elongation at break (ε_b).

The results presented are an average of at least five samples.

3.6 Differential Scanning Calorimetry

Differential Scanning Calorimetry (DSC) was used to determine the percentage of freezing water present in a hydrated hydrogel sample.

Previous work has shown that the heat of fusion in polymers is identical to that of pure water[17], this allows a quantitative determination of the amounts of freezing and non-freezing water in the polymer to be calculated.

Thermograms were obtained using a Perkin-Elmer differential scanning calorimeter, DSC-7, in conjunction with a 7500 professional computer and liquid nitrogen cooling accessory. 1-4mg of material was cut from a hydrated hydrogel membrane using a size one cork borer and the surface water removed using filter paper. The hydrogels were weighed, sealed in aluminium pans and placed in the sample holder of the thermal analyser unit.

Samples were cooled to 223K, ensuring that any supercooled water was frozen, and then allowed to reach equilibrium. They were then heated to 253K and subsequently heated to ambient temperature at a rate of $5Kmin^{-1}$.

From the resulting thermogram the proportion of freezing to non-freezing water was calculated by the computer software. The area under the melting peaks of the hydrogel sample was measured which enabled ΔH to be calculated. ΔH for the samples was obtained using equations 3.7-3.9.

$$\text{Freezing water (\%)} = \frac{\Delta H \text{ calculated}}{\Delta H \text{ for pure water}} \times 100\ \% \qquad (3.7)$$

$$\text{where:-} \quad \Delta H = \frac{\text{area under the peak}}{\text{weight of the sample}} \qquad (3.8)$$

$$\text{and} \quad \Delta H \text{ for pure water} = 333.77\ Jg^{-1} \qquad (3.9)$$

The process was repeated three times for each sample, and at least three separate samples from each hydrogel sheet were tested.

3.7 Surface Properties.

The experimental techniques used to measure contact angles are described here. Techniques for the measurement of surface properties have been extensively investigated in these laboratories[28] which has lead to acceptable working practices being

determined. The theory, with diagrammatic representations, used to calculate surface energy from contact angles is presented in chapter 1.

Samples were cut from a hydrated hydrogel sheet using a size seven cork borer, cleaned using Tepol 'L' and rinsed thoroughly in distilled water. They were then left to soak in distilled water for several days, typically for two weeks, before testing, ensuring that any remaining detergent was removed.

A Rame Hart goniometer with a calibrated eye piece was used to measure the contact angle at the three phase interface, with the contact angle quoted being an average of that measured at each side of the bubble or drop. The polar, dispersive and total surface free energies could then be calculated using Macintosh Works™ which was programmed with the relevant equations as seen above.

3.7.1 Hamilton's Method

Surface water was removed from the sample using filter paper, which was then glued to an electron microscope stub using super glue. The sample was inverted and suspended in an optical cell which was filled with distilled water. A small drop of n-octane was placed on the surface of the sample using a curved G25 syringe needle. This was repeated at least three times on three samples so as to reduce any errors arising from surface topology irregularities and experimental error.

3.7.2 Captive Air Bubble Technique

Samples were mounted as described above for Hamilton's method, however, air bubbles were released onto the surface using a specially curved G25 needle. This allowed for accurate control of the bubble volume onto the surface of the sample. At least nine readings were taken to reduce errors.

3.7.3 Sessile Drop Technique

Samples were dehydrated to constant weight in a microwave oven for approximately ten minutes and placed on a microscope slide which was placed on the support of the goniometer. The wetting liquids used were distilled water and diiodomethane. A drop of liquid was placed onto the surface of the sample using a straight G25 needle. Using the calibrated eye piece, contact angles were recorded. Several samples were tested to reduce errors.

3.7.4 Dynamic Contact Angles

Dynamic contact angles were obtained using a Cahn DCA-300 series analyser interfaced to an IBM computer, and a dynamic surface tensiometer, Nima Technology Coventry, Model DST 9025, utilising a modified Wilhelmy Plate method. The advancing and receding contact angles were recorded.

Hydrated hydrogel membranes were cut into strips, 10mm x 3.3mm, with a rectangular cutter, the thickness measured using a micrometer and recorded. This was then suspended from the Cahn balance by a connecting wire and a small crocodile clip with the lower edge 3mm above the probe liquid. The sample was prevented from curling by attaching a small weight at the bottom of the sample. The depth of immersion and number of immersion cycles were programmed into the computer. The sample was then lowered into the probe liquid at a rate of 0.1 $mm.s^{-1}$ to a depth of 7mm. The sample is then raised at the same rate until it returned to its starting point, making sure that at this point no contact is made with the meniscus of the probe liquid. The immersion cycle is repeated at least three times for each sample. The computer plotted the results obtained as force versus immersion depth.

The surface tension of the probe liquid is calculated using a dynamic surface tensiometer, by dipping a circular probe into the liquid, drawing it out and recording the value. An average of five readings was taken for each sample run. This enabled the

dimensions of the sample and surface tension values to be input into the computer program, which then automatically calculated the advancing and receding contact angles.

3.8 *In-Vitro* Ocular Spoilation Model

The *in-vitro* ocular spoilation model has been developed over several years in these laboratories[180], and is used routinely in order to show the effects of lipid and protein deposition on a hydrogel sample. Spoilation studies were carried out by Dr. Val. Franklin. This model depends upon having a suitable and stable tear substitute. The tear substitute is based upon a 1:2 (v/v) solution of foetal calf serum (FCS) diluted with phosphate buffered saline (PBS) as a base. This was then 'spiked' with additional components such as mucin, lactoferrin and lysozyme in order to mimic the natural tear composition.

The tear model enables controlled spoilation to be carried out using two forms[25]:

1. The 'shaker' model
2. The 'drop and dry' model

In this work the 'shaker' model has been used.

A small number of glass beads were placed into a glass vial, providing an uneven surface on which the samples could rest and allowing contact with the air and the tear solution. The tear solution was pipetted into the vial to a level just below the top surface of the beads. Samples were cut from the hydrated hydrogel membrane using a size seven cork borer and placed in the vial. These were then placed on a flatbed vibrating shaker, set at 200 cycles per minute, which enhanced the air and tear solution contact with the samples. The tear solution was replaced every twenty-four hours to maintain a fresh supply of protein and lipid components. The experiment was run over 28 days, which gave an accelerated spoilation profile equivalent to several times this period of normal contact lens wear and being representative of an extended wear regime. *In-vitro* spoilation carried out in this was has been found to give spoilation equivalent to six

months wear, and removes the patient-to-patient variability that occurs *in-vivo*[25]. Spoilation is patient, material and wear regime dependent so no single spoilation correlation factor can be obtained. The spoilation model does not aim to mimic the tears but to mimic the proportional spoilation chemistry encountered from an array of proteins and lipids.

The deposition of both proteins and lipids was monitored at regular intervals over the period of 28 days using fluorescence spectroscopy. Lipids were monitored using an excitation wavelength of 360nm and proteins at 280nm.

3.9 Scanning Electron Microscopy

The surface of a sample is viewed under very high magnification, using this well established technique. The samples are dehydrated, either in a microwave oven or vacuum oven, prior to being mounted onto an aluminium stub. This is then coated with gold in a sputter coater, placed in the Cambridge Instruments Stereoscan 5150 microscope and evacuated. A beam of electrons is shot at the sample and the reflected electrons are collected and an image formed on a cathode ray tube.

3.10 Fluorescence Spectrophotometry

A modified Hitachi F100 Spectrophotofluorimeter was used to monitor the fluorescence of unworn and spoilt contact lenses, the theory and experimental technique will be discussed in chapter 6. An excitation wavelength of 280nm was used to record protein fluorescence, with 360nm being the excitation wavelength to monitor lipid fluorescence.

3.11 Laser Ablation

Laser ablation studies were carried out externally at St Thomas' Hospital London, by Dr Chris Stevenson, on hydrogel samples using a Summit SVS 50Hz Laser at a fluence of 180 $mJ.cm^{-1}$. The ablation diameter was 6mm and the excimer laser wavelength was 193nm.

3.12 Cytotoxicity Testing

Cytotoxicity tests[11] were carried out by Chris Graham. A cell suspension containing 3T3 Swiss mouse embryo cells in DMEM complete medium, foetal bovine serum (FBS) and L-glu was prepared by trypsinisation, centrifugation and counted to a total of 1 x 10^5 cells/ml under the optical microscope with the aid of a haemocytometer slide. 1ml of the cell suspension was added to each well which contained the polymer samples that were under investigation. The polymer samples were cut with a size six cork borer to give an approximate diameter of 14mm. Control cells with no polymer sample were also prepared so that a background cell death could be obtained. The background cell death is the number of cell deaths incurred during the running of the assay. The cells and polymer in the well plates were incubated at 37^0C for 18 hours. On completion of the required incubation period, one drop of the cell suspension from each well was taken and mixed with one drop of trypan blue, and then transferred to the haemocytometer slide. A cover slip was fixed firmly to the slide, with Newton's rings evident, allowing it to run into the counting chamber. The cells and stain mixture was left to sit for approximately one minute, and was then placed under the microscope on a 10x magnification. The number of stained cells, and total number of cells were counted. The slide is removed and washed, repeating the procedure for each of the wells in the same manner. The average number of the control wells non-viable cells were used as the background death to be subtracted from the experimental well counts.

$$\frac{\text{stained cells}}{\text{total cells}} \times 100 = x\,\% \tag{3.10}$$

$$100 - x\,\% = \%\ \text{viable} \tag{3.11}$$

The percentage viability of the cells indicates the effect the polymer exerts on the cells.

CHAPTER 4

DEVELOPMENT OF A NOVEL KERATOPROSTHETIC DEVICE

4.1 Introduction

This chapter investigates the use of novel hydrogels as potential materials for keratoprostheses. For many years now hydrogels have been utilised in many varied biomedical applications[3]. One major use has been as soft contact lenses. The eye provides an excellent site for studying interactions between a complex biological environment and a synthetic material. Lenses can easily be inserted, their wear time monitored and care regime controlled without the need for any invasive surgical procedure. The cornea is a naturally occurring hydrogel, so synthetic hydrogels are an obvious choice to investigate in an attempt to produce an artificial cornea, or keratoprosthesis (KPro).

Keratoprostheses have been around for many years, though the surgery required is often complicated, and the device is prone to extrusion[49]. The first suggestion of an artificial cornea was in the eighteenth century, though it was not until the 1950's and the introduction of the use of synthetic materials, that any significant progress was made. One of the more successful procedures to date is based on the technique devised by Strampelli, known as osteo-odonto keratoprosthesis, or OOKP. The technique was described in chapter two, and involves complicated, painful surgery. Hydrogels have been inserted into the eye in the form of contact lenses for numerous years with their behaviour and tolerance well documented. However, it has not been until fairly recently that hydrogels have been investigated for use as an artificial cornea. Most of the polymers used have been available commercially and not specifically designed for this application.

In order to develop ophthalmic biomaterials, the interaction between a material and the ocular environment must be considered. Contact lenses form an interface with tears, the eyelid and the cornea, so knowledge gained from studying this area can be utilised. Keratoprostheses must also integrate with the surrounding tissue to prevent extrusion, as the major cause of failure of KPro devices has been the lack of healing between the

periphery of the device and the host cornea. As a result, wound leakage, tissue necrosis, epithelial downgrowth and intraocular infections have occurred. Work has previously been carried out by Corkhill *et. al.* to mimic articular cartilage[32], another naturally occurring hydrogel, using synthetic analogues, with a certain amount of success. Studies of this type require the knowledge of how such materials interact with body fluids and their subsequent cellular responses[181].

4.2 Requirements of a keratoprosthesis

The development of KPro's has shown that a porous periphery is required into which stromal keratocytes can penetrate, proliferate and synthesise connective tissue proteins in order to form a tight junction between the device and the host tissue. Therefore, it is thought that an ideal KPro will need to consist of an optically transparent centre, with an anterior surface that will support adhesion of the host epithelium, and support the tear film[72]. It will also require a porous periphery which encourages fibrous tissue ingrowth from the host cornea so that the device heals securely in place. The posterior surface should, preferably, discourage adhesion of the epithelium, so decreasing the potential for extrusion and provide an effective barrier against micro-organisms. The device must have suitable mechanical properties to withstand the stresses of the surgical procedure and forces applied to it once it is in the eye (i.e. blink deformation). The materials must be chemically stable, being non-toxic and not acting as an immunological or inflammatory stimulus so exhibiting an allergic response. Therefore, the device must be biotolerant. The junction between the optical core and the porous periphery needs to be coherent. Once in place, it must not be susceptible to enzymatic degradation or fibrous overgrowth, but still allow for drug permeation. The chemicals used in the devices production should be reproducibly pure, and the finished device needs to be sterilised prior to implantation.

By using knowledge gained through hydrogel synthesis and contact lens production, a contact lens like, or 'full thickness' prosthesis was developed. It can be seen that

producing an 'ideal' full thickness KPro device is a complex problem, requiring knowledge in several areas.

4.3 HEMA Based Copolymer Hydrogels

HEMA is the principle component of the majority of commercially available soft contact lenses. This was used as the basis for the initial membranes synthesised as the behaviour of these materials in the eye are well documented. PolyHEMA is also being studied by one research group as a potential material for a keratoprosthesis[49]. As such it was used as a starting point to find a suitable selection of monomers for investigation for use in a keratoprosthesis. The comonomers chosen were N-vinyl pyrrolidone (NVP), methyl methacrylate (MMA) and methacrylic acid (MAA) which are used in soft contact lenses, and so had known toxicology, and acryloyl morpholine (AMO) which in work previously carried out[18] had displayed properties similar to that of NVP. The structures of the monomers are shown in figure 3.1. NVP and MMA copolymers had also previously been investigated for use in synthetic cartilage[32] A series of copolymers were produced which contained a range of relative amounts of each monomer, as described in chapter 3. The water contents obtained are reported in figure 4.1. Full details of all the membranes discussed in this chapter are given in appendix 1.

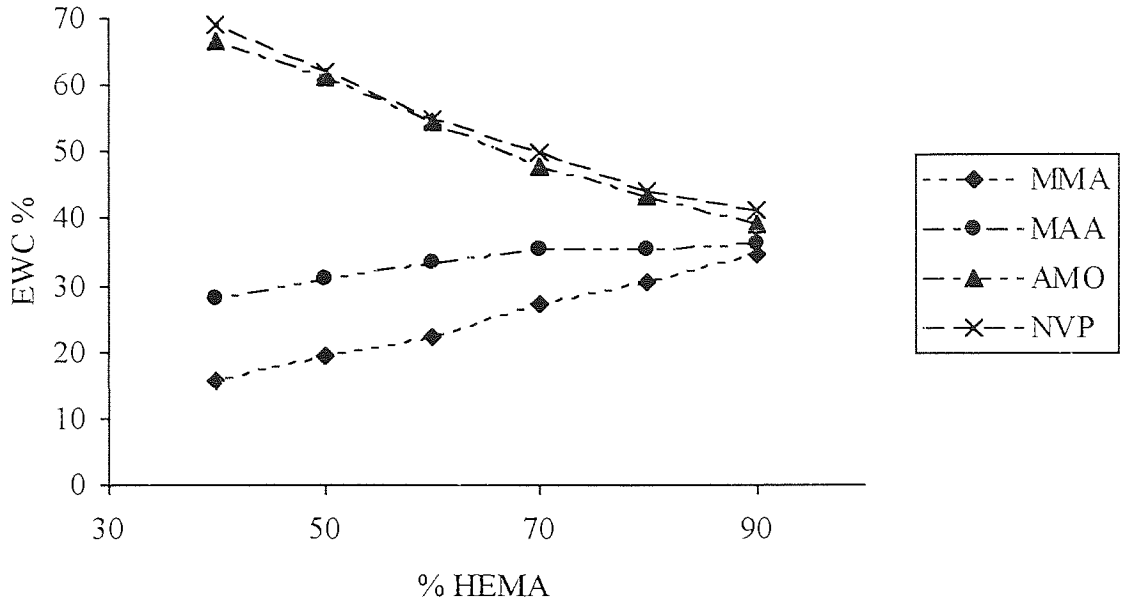

Figure 4.1 Equilibrium water contents for a series of HEMA copolymers

It can be seen from figure 4.1, that water contents increase as the amount of hydrophilic comonomer increases. The structure of the comonomer influences the degree of hydrophilicity of the resulting polymer. Values obtained for NVP are comparable to those gained with AMO, indicating that both monomers are of a similar hydrophilicity, which is greater than that of HEMA. MMA is a hydrophobic monomer, and so the water content decreases with increasing amounts of MMA. MAA also acts as a hydrophobic monomer in this case due to the pH of the hydrating media. The dissociation constant for MAA occurs at around that of the pH of physiological solutions, which leads to it being unstable in ocular environment. Previous work indicated the leaching effect and poor polymerisation associated with NVP would lead to problems with long term wear in the eye due to the toxicity effects of the NVP[26] and the degree of spoilation caused by the 'blocky' nature of the resulting copolymers. Studies have shown the potential for replacing NVP with AMO in hydrogels which would overcome these problems[18].

For a successful KPro device, a degree of cell adhesion is required on the surface. Previous work carried out by this research group[188] investigated the cell response of hydrogels of different water contents and monomer compositions. PolyHEMA was found to display very little cell adhesion. The mechanical properties are also fairly weak, so would be incapable of withstanding the stresses placed on the device prior to surgery and following implantation. A high water content is also preferable. As was seen with the cartilage work, a NVP-MMA hydrogel was used as the basis for subsequent work, as the membranes formed were strong and had a high water content. AMO was utilised here as a replacement for NVP, as an important consideration for the KPro is the level of deposition on the material once it is placed in the eye. The mechanical properties of a hydrogel can be enhanced by the incorporation of monomers with bulky side chains. A series of AMO copolymers were synthesised to consider alternative comonomers, as this gave high water content hydrogels without the toxicity and leaching problems associated with NVP copolymers.

4.4 Acryloyl Morpholine Based Copolymer Hydrogels

Heterocyclic monomers have been used in dental applications for many years[181-185]. Tetrahydrofurfuryl methacrylate, THFMA, has been investigated as an alternative to PMMA in dental applications, and used in drug delivery systems that have been implanted in the cartilage's of rabbits[182]. As such its biotolerance has been studied and was found to be relatively non-irritant in dental applications[183]. PMMA has been used as the optical core material in the vast majority of KPro devices.

4.4.1 Water Content

A range of AMO copolymers were synthesised with several heterocyclic monomers, namely, tetrahydrofurfuryl methacrylate (THFMA), tetrahydropyranyl methacrylate (THPMA) and glycidyl methacrylate (GMA). The structures of these monomers are shown in figure 3.1. The water contents of the membranes synthesised are displayed in figure 4.2.

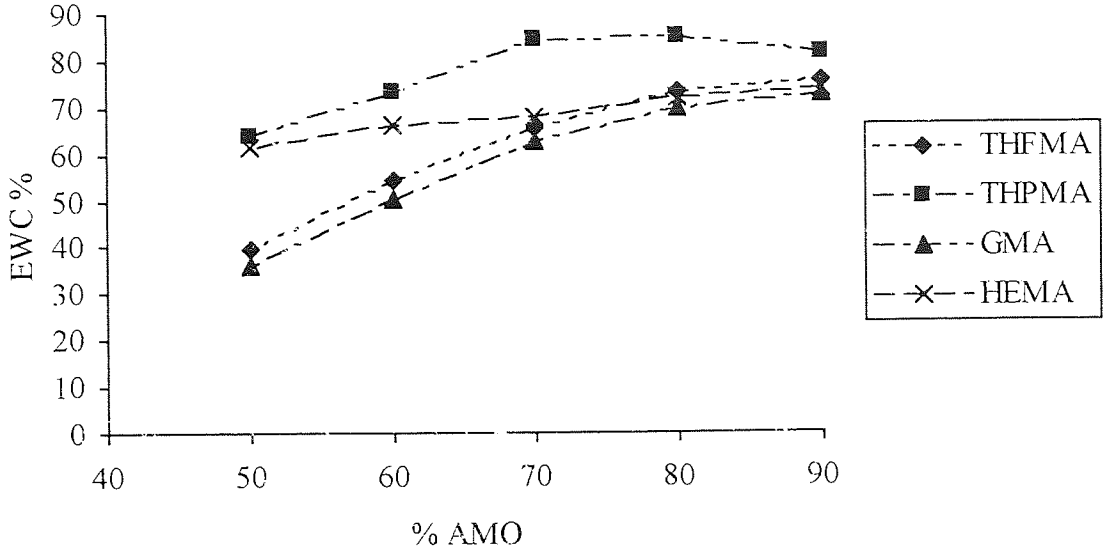

Figure 4.2 Equilibrium water contents for a series of AMO copolymers

It can be seen in figure 4.2 that an increase in the percentage of the hydrophilic acryloyl morpholine results in an increase in water content. However, the chemical structure of the comonomer also influences the water content. HEMA is used as a comparison to previous work, and the other copolymers are examples of heterocyclic methacrylates. The size of the heterocyclic ring increases from three carbons through to five, in the order, glycidyl methacrylate, tetrahydrofurfuryl methacrylate and tetrahydropyranyl methacrylate, respectively. As the size of the ring increases, the oxygen atom in the heterocyclic ring becomes more accessible and available for hydrogen bonding to water molecules, thus increasing the water content, as the increased ring size prevents rotation about the polymer backbone.

Equilibrium water content is a major factor in governing the mechanical, surface and transport properties of a hydrogel[3]. Factors that can influence the EWC of a given hydrogel composition include crosslink density and the crosslinking agent used, and the temperature and tonicity of the hydrating media. All of the hydrogels in this study are

made using the same crosslinker, ethylene glycol dimethacrylate, at the same concentration, in order to examine the effect of the monomer concentration and structure on the properties of the resulting polymers.

4.4.2 Mechanical Properties

The mechanical properties of the AMO copolymer compositions that were discussed in the previous section were measured using the techniques described in chapter 3, and the results are shown in figures 4.3 to 4.5.

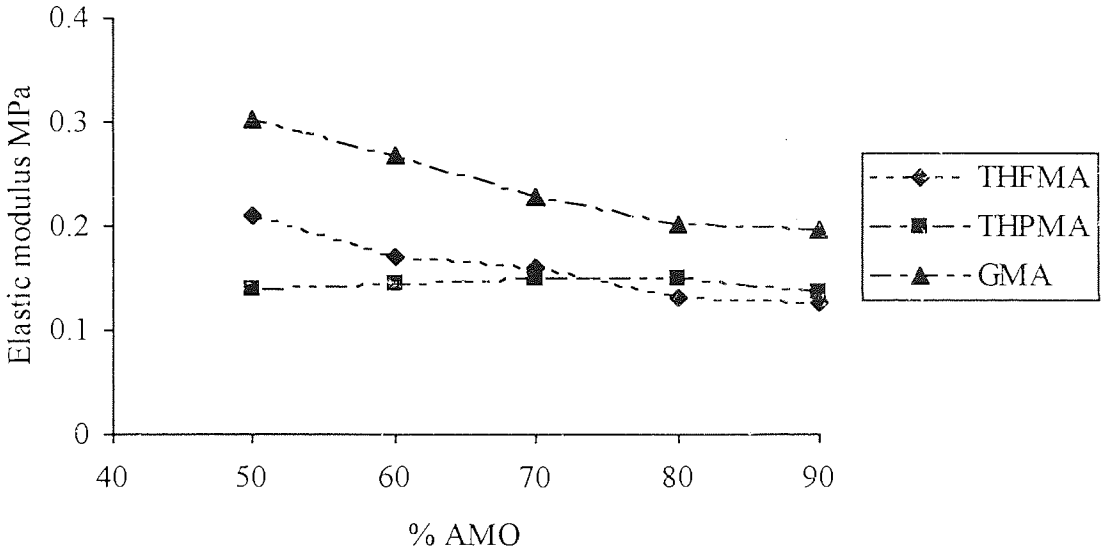

Figure 4.3 Elastic modulus results for a series of AMO copolymers

It should be noted that all the values of elastic modulus quoted throughout this work are the initial Young's modulus.

As the size of the heterocyclic ring increases, the elastic modulus increases. The elastic modulus is a measure of the stiffness of the polymer, which can be related to the chain mobility of the network. As the size of the heterocyclic ring increases, there will be less

rotation about the carbon backbone due to the increase in steric interactions because of the larger ring, this is seen in an increase in the glass transition temperatures of these materials[29.182-185].

The increase in elastic modulus also corresponds to a decrease in equilibrium water content. This is due to the reduction of the imbibed water which acts as an internal plasticiser.

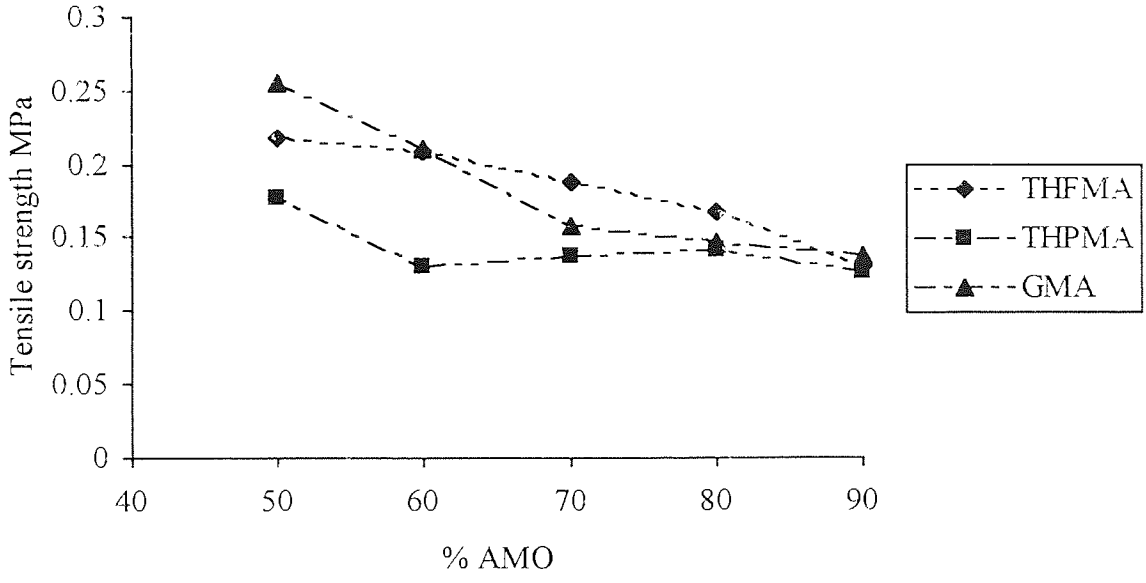

Figure 4.4 Tensile strength results for a series of AMO copolymers

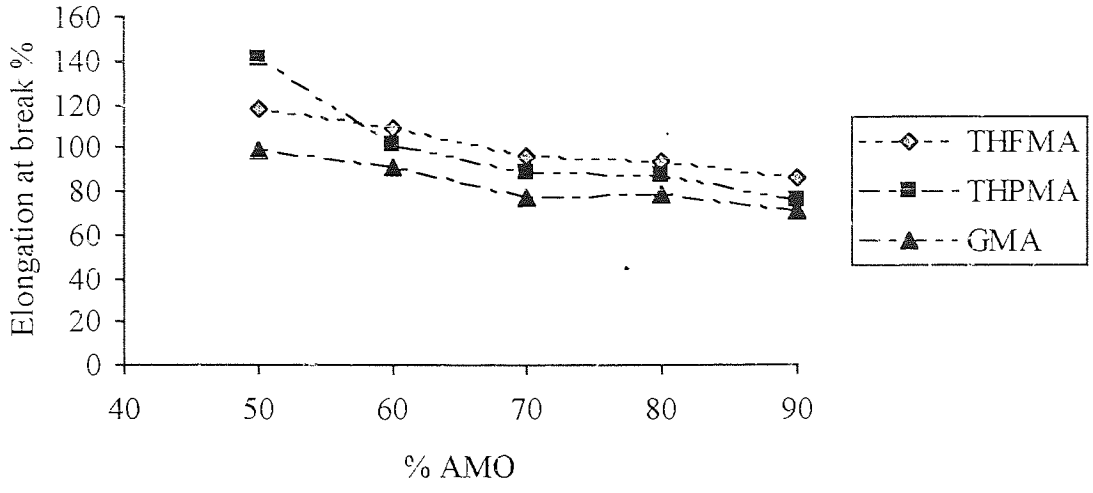

Figure 4.5 Elongation at break for a series of AMO copolymers

Figure 4.4 indicates that there is very little difference in the recorded values for tensile strength, as both the monomer is changed, and the amount of hydrophilic monomer is increased. The strength of the polymers decrease slightly as the percentage of the AMO is increased.

Elongation at break measurements display the greatest standard deviations of the three mechanical properties described. Figure 4.5 indicates that elongation at break decreases as the content of the hydrophilic monomer increases. Increasing the AMO concentration in the systems increases the EWC, which in turn produces a more flexible, but weaker polymer. This is reflected in figures 4.3 to 4.5.

The results presented above indicate that the mechanical properties of the AMO-heterocyclic comonomers are not as high as those obtained for MMA-NVP comonomers[32]. However, for this application, several other properties must also be considered in the choice of monomers. It is important that there is a balanced reactivity of the monomers to reduce spoilation, that is associated with blocky sections of polymers formed when one of the monomers has a low reactivity ratio. Cytotoxicity

and cell response need also to be considered, as the materials should not cause any immunological or inflammatory response once they are placed in the eye.

4.4.3 Cytotoxicity tests

Cytotoxicity tests were carried out, by Chris Graham, on the 70:30 AMO-heterocyclic copolymers described in the section above, using the method described in chapter 3. The results indicated the materials were non-toxic in both short and long term studies that were undertaken. A high cell viability was obtained which indicates that the samples were sufficiently inert with relation to the reaction media, and did not release any cytotoxic materials during the course of the study. The AMO:THFMA membrane showed a slight increase in cell viability, to around 90%.

4.4.4 *In vitro* Spoilation Studies

A series of membranes were subjected to the in vitro tear model to assess how the materials would react in the eye. The materials were all in a 50:50% ratio, and the results are shown in figures 4.6 to 4.8.

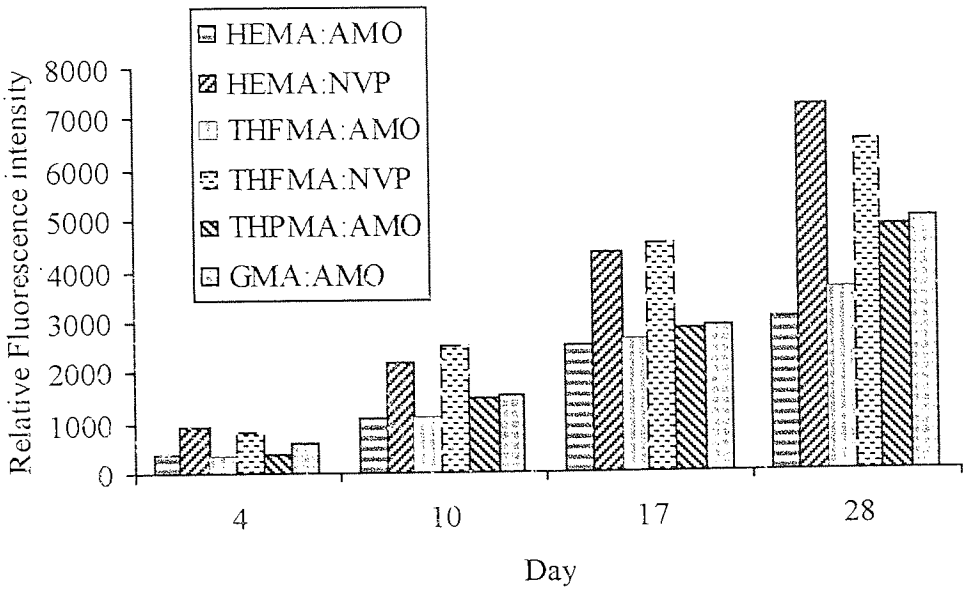

Figure 4.6 Progressive build up of protein spoilation measured using fluorescence spectroscopy at an excitation wavelength of 280nm for a series of 50:50 copolymer membranes

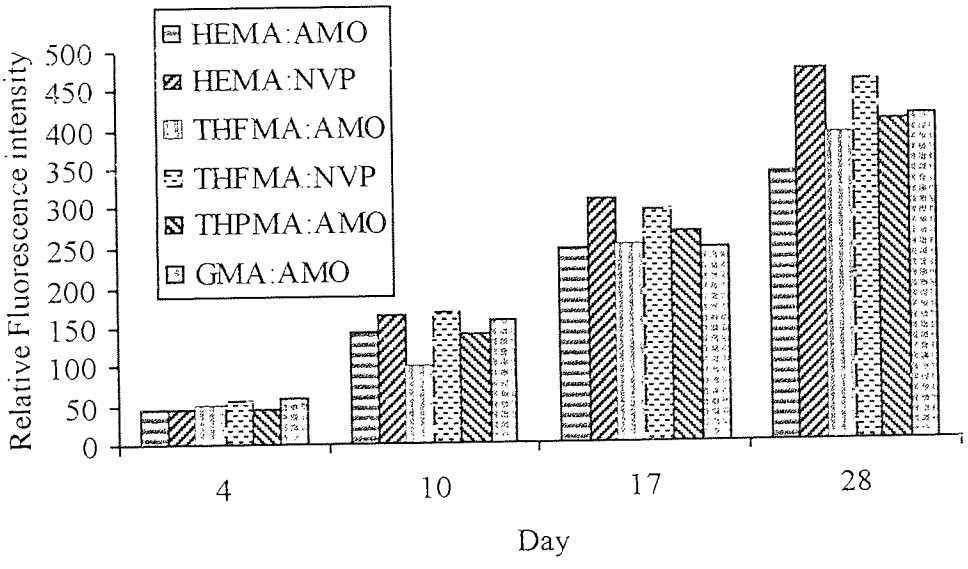

Figure 4.7 Progressive build up of lipid spoilation measured using fluorescence spectroscopy at an excitation wavelength of 280nm for a series of 50:50 copolymer membranes

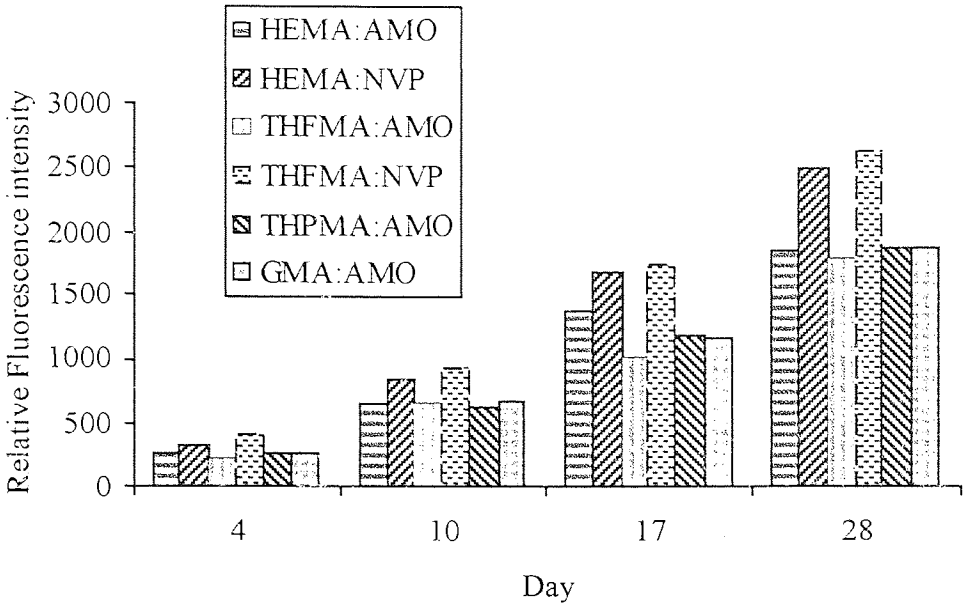

Figure 4.8 Progressive build up of lipid spoilation measured using fluorescence spectroscopy at an excitation wavelength of 360nm for a series of 50:50 copolymer membranes

Spoilation studies are carried out using the *in vitro* spoilation model, which is described in chapter 3. The materials are examined every three days over a total of twenty eight days, though only a few such days are represented in the figures above. The spoilation is assessed using fluorescence spectroscopy, which is described in more detail in chapters six and seven.

HEMA copolymers were included above as a comparison to previous work carried out in the research group, and as it is the base material for the majority of commercially available soft contact lenses. The results indicate the enhanced spoilation that is associated with NVP copolymers in relation to AMO copolymers, which can be seen for both HEMA and THFMA. The low reactivity ratio of NVP leads to 'blocky' copolymers, which leads to enhanced levels of spoilation. AMO is more polar, and its copolymers have a controlled sequence distribution, with short, regular repeat units mimicking those found in nature, due to its higher reactivity ratio. This results in

decreased levels of spoilation in comparison to copolymers containing the same amount of NVP. There are many factors that contribute to the levels of spoilation observed. These include the monomer structure and the water content of the hydrogel.

The spoilation observed on the heterocyclic copolymers is within the limits obtained for currently available soft contact lenses. The levels obtained for THFMA:AMO show an improvement on those obtained for both the other heterocyclics, and for HEMA.

4.4.5 Discussion

The monomers used in contact lens production have been analysed for their toxicity, as have those methacrylates used in dentistry[181-185]. Rigid contact lenses are based on polymethyl methacrylate, PMMA, which to date is the material of choice for the optical core in the majority of KPro devices.

HEMA is the principle component of the majority of soft contact lenses, so initially a series of copolymers were synthesised, based on monomers that have been used in commercially available contact lenses. The water content of these hydrogels can be controlled by the amount and type of comonomer used. However, HEMA is not an ideal material for a KPro device[186,187] as it is mechanically weak and displays poor cell adhesion.

N-vinyl pyrrolidone is a hydrophilic monomer and is one of the components used in Etafilcon A, which is copolymerised with HEMA to give high water content, ionic lenses. However, NVP has a poor reactivity to free radical polymerisation which leads to the formation of a 'blocky' copolymer. Hydrogels which have a sequence distribution that results in large irregular molecular domains where components of the same chemical type become aggregated (or 'blocky') tend to show much greater levels of spoilation than hydrogels that have a sequence distribution that tends to mimic the natural cell structures that have short, regular repeat units. Hydrophobic clusters on the

surface and monomers with methyl side groups also increase the potential spoilation levels by providing an area capable of docking proteins and adsorbing lipids. In the design of the KPro, it is important to keep spoilation to a minimum. The prosthesis is permanent, unlike a contact lens which can easily be removed for cleaning. Recent work in the group[18] has shown the potential of acryloyl morpholine, AMO, for use in hydrogel systems for biomedical applications. It is a hydrophilic monomer which shows a good alternating sequence distribution, water content and mechanical properties, along with promising *in vitro* spoilation studies[18].

A series of AMO hydrogels were synthesised together with a range of heterocyclic methacrylate monomers that had previously been utilised in dental applications. A range of water contents and mechanical properties were obtained, dependent upon the size of the heterocyclic ring and percentage used.

An important consideration for material selection for use as a keratoprosthesis is the mechanical strength of the polymer. The hydrogel for use in this application must be able to withstand the stresses involved in the surgical procedure involved with the KPro, and the *in situ* stresses such as the deforming force of the eyelid during the blink cycle. The copolymers investigated in the preceeding sections do not display significant strength to tolerate the strain that it would exposed to for this application. The initial cytotoxicity tests carried out on the AMO based copolymers revealed that the material had no adverse effect on the cells. As both the cytotoxicity and spoilation results proved promising for the AMO:THFMA polymer, the mechanical properties were an aspect that needed to be enhanced to ascertain whether they may be suitable candidates for KPro devices. Mechanical properties can be increased in several ways, such as fibre reinforcement, copolymerisation and the formation of IPN's and semi-IPN's[29]. This work has concentrated on the use of semi-IPN's.

4.5 Interpenetrating Polymer Networks

As described in chapter 1, both articular cartilage and the cornea are examples of naturally occurring hydrogels. Corkhill *et. al.*[32] studied the use of semi-interpenetrating polymer networks to enhance the mechanical properties of hydrogels for use as a synthetic articular cartilage. It was this approach that was employed in an attempt to improve the mechanical properties of the aforementioned hydrogel copolymers. The studies are restricted here to hydrogels based on AMO:THFMA, as it can be seen from the previous section, these materials gave slightly enhanced cytotoxicity results, and mechanical properties and the spoilation studies indicated that the build up of protein and lipid was within the range that is observed for many commercially available soft contact lenses, and in comparison to some was greatly enhanced.

Corkhill[32] based the formulation for synthetic articular cartilage on a copolymer of 45% NVP and 23% MMA with 12% CAB being used as the interpenetrant in that system. In addition 20% (w/w) of dextrin was added. The dextrin, when polymerised in a thick sheet, increased in concentration at the underside of the membrane, forming a smooth low friction upper surface, and a porous underside. It is this porous area that has been shown to enhance cell integration. This composition was quoted to have a EWC of 54.4% and an elastic modulus of 23.6 MPa, which is significantly higher than simple copolymers at this EWC.

The formation of semi-IPN's involved polymerising a mixture of monomers, crosslinker and initiator, similar to those examined above, around a reinforcing linear polymer, termed the interpenetrant. Two interpenetrants were investigated initially, CAB and an ester polyurethane. However, cellulose acetate butyrate gave opaque hydrogels and would therefore be of no use as the central optical core in a KPro. Therefore, these results are confined to those obtained when an ester polyurethane interpenetrant was used.

4.5.1 Equilibrium water content

A series of tetrahydrofurfuryl methacrylate, polyurethane semi-IPN's were synthesised, as described in chapter 3. The compositions and corresponding equilibrium water contents are reported in table 4.1

Monomers	composition	EWC %
NVP:MMA:CAB:DEX	45: 23: 12: 20	54.9
THFMA:NVP:PU	41.6: 41.6: 16.8	20.2
THFMA:AMO:PU	41.6: 41.6: 16.8	29.9
THFMA:NVP:PU	36.6: 41.6: 21.8	45.4
THFMA:AMO:PU	36.6: 41.6: 21.8	47.9

Table 4.1 Equilibrium water contents for a series of THFMA:PU semi-IPN hydrogels

A decrease in the amount of THFMA coupled with an increase in the amount of PU causes the water content increases. By changing the hydrophilic monomer from NVP to AMO the water content increases slightly. As it has previously been shown in figure 4.1 that NVP and AMO have a similar hydrophilicity, this may be due to the better sequence distribution which arises by substituting NVP with AMO.

Monomers	composition	EWC %
THFMA:AMO:PU	41.6: 41.6: 16.8	29.9
THFMA:AMO:PU	36.6: 41.6: 21.8	47.9
THFMA:AMO:PU	30: 50: 20	41.4
THFMA:AMO:PU	25: 60: 15	53.7

Table 4.2 Equilibrium water contents for a series of THFMA:AMO:PU semi-IPN hydrogels

The hydrogels formed comprise of three components, so it is not as easy to determine trends associated with changes in composition, as more than one variable is altered. An

increase in PU content and a corresponding decrease in THFMA results in an increase in water content, indicating that PU is more hydrophilic than THFMA. The water content is dependent upon the relative proportions of each of the components, though an increase in the hydrophilic monomer AMO leads to an increase in water content.

4.5.2 Mechanical properties

The mechanical properties of the materials from the previous section were investigated and the results are reported in tables 4.3 to 4.5.

Monomers	Composition	EWC %	Elastic modulus MPa
THFMA:AMO:PU	41.6: 41.6: 16.8	29.9	12.6
THFMA:AMO:PU	36.6: 41.6: 21.8	47.9	24.4
THFMA:AMO:PU	30: 50: 20	41.4	8.4
THFMA:AMO:PU	25: 60: 15	53.7	7.3

Table 4.3 Elastic modulus results for a series of THFMA:AMO:PU semi-IPN hydrogels

Monomers	Composition	EWC %	Tensile strength MPa
THFMA:AMO:PU	41.6: 41.6: 16.8	29.9	4.2
THFMA:AMO:PU	36.6: 41.6: 21.8	47.9	5.6
THFMA:AMO:PU	30: 50: 20	41.4	1.4
THFMA:AMO:PU	25: 60: 15	53.7	1.6

Table 4.4 Tensile strength data for a series of THFMA:AMO:PU semi-IPN hydrogels

Monomers	Composition	EWC %	Elongation at break %
THFMA:AMO:PU	41.6: 41.6: 16.8	29.9	168
THFMA:AMO:PU	36.6: 41.6: 21.8	47.9	106
THFMA:AMO:PU	30: 50: 20	41.4	139
THFMA:AMO:PU	25: 60: 15	53.7	121

Table 4.5 Elongation at break data for a series of THFMA:AMO:PU semi-IPN hydrogels

By comparing tables 4.3 to 4.5 with figures 4.3 to 4.5, it is immediately evident that the mechanical properties of the hydrogels are vastly increased through the addition of an interpenetrant. It is clear that the mechanical properties are not governed only by water content, but that the composition of the hydrogel also plays an important part. Comparing the AMO:THFMA hydrogels at approximately 50% EWC, in figure 4.1 the initial Young's modulus is about 0.2 MPa, whereas with a reinforced polymer this increases to about 24 MPa. The massive differences in the mechanical properties such as this, show how great the potential is for producing tough hydrogels not too dissimilar to those produced by nature.

4.5.3 Surface properties

The surface properties of the AMO:THFMA:PU polymers were analysed, using the method described in chapter 3. The results showed only a slight variation as the composition of the material was altered. The results for the preferred material, which was AMO:THFMA:PU in the ratio 50:30:20, are displayed in table 4.6.

	Polar component mN/m	Dispersive component mN/m	Total surface free energy mN/m
Dehydrated state	9	34	43
Hydrated state	42	21	63

Table 4.6 Surface free energy values in the hydrated and dehydrated states for a AMO:THFMA:PU 50:30:20% hydrogel

4.5.4 Cell response

Cytotoxicity tests, as described in chapter 3, were carried out by Chris Graham, on the semi-IPN hydrogels described in table 4.3. Initial experiments studied the viability and cell growth rate of 3T3 Swiss mouse embryo cells. The results indicated that there was no significant adverse response to the cells as a result of exposure to the polymers, with very little difference being observed for the variation in material composition, with cell viability levels of above 90% being obtained in each case.

4.5.5 Spoilation studies

The materials shown in table 4.2 were subjected to the *in vitro* spoilation model, as described in chapter 3. This was carried out in order to gain an insight into how the materials would behave in the eye. The results are displayed in figures 4.9 to 4.11.

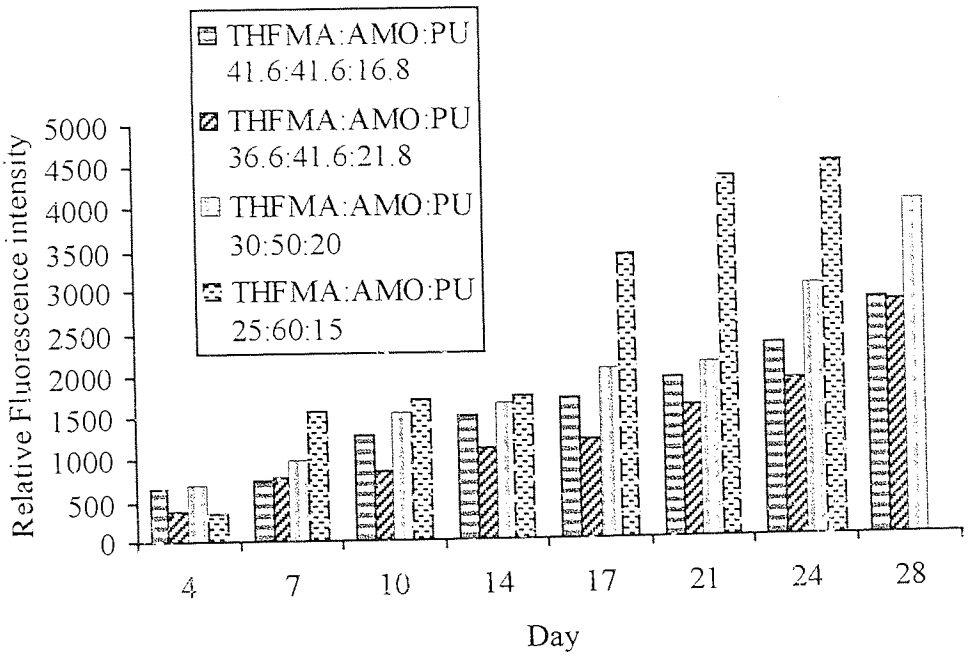

Figure 4.9 Progressive build up of protein spoilation measured using fluorescence spectroscopy at an excitation wavelength of 280nm for a series of AMO:THFMA:PU membranes

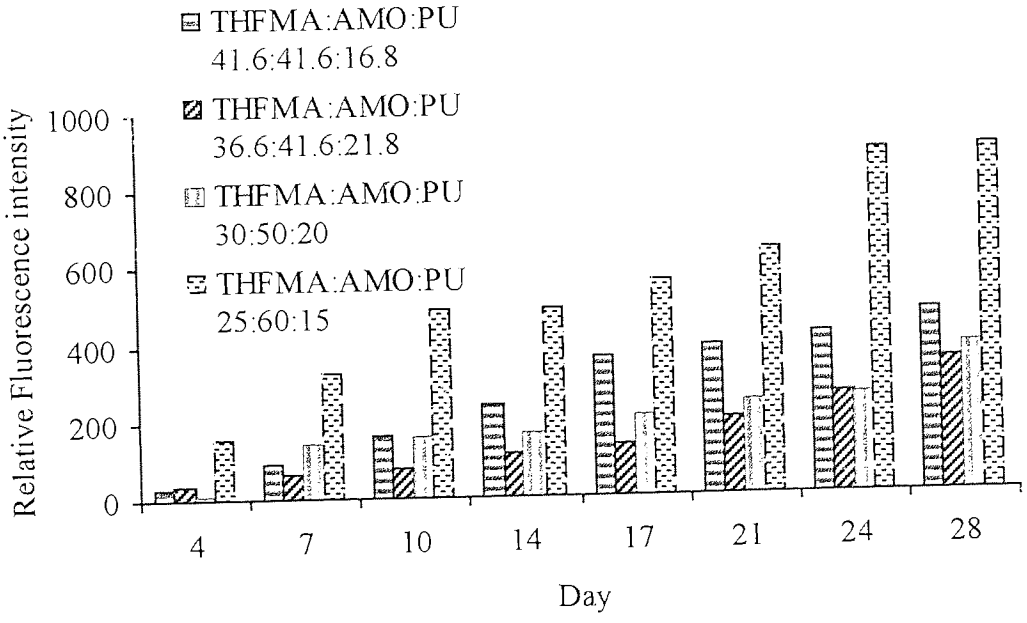

Figure 4.10 Progressive build up of lipid spoilation measured using fluorescence spectroscopy at an excitation wavelength of 280nm for a series of AMO:THFMA:PU membranes

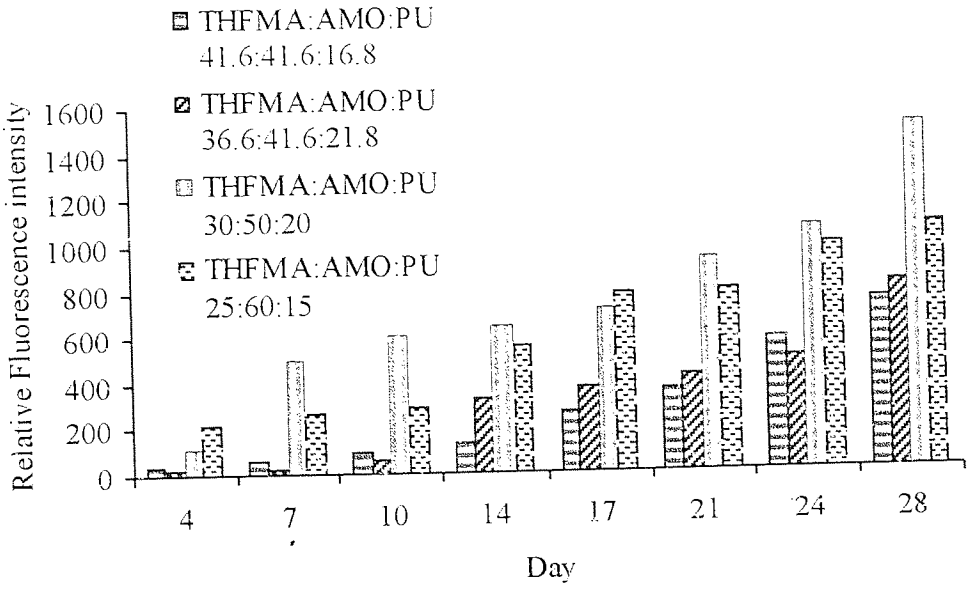

Figure 4.11 Progressive build up of lipid spoilation measured using fluorescence spectroscopy at an excitation wavelength of 360nm for a series of AMO:THFMA:PU membranes

Figures 4.9 to 4.11 show the progressive build up of both protein and lipid on the materials tested. The *in vitro* spoilation model has been shown to produce an accelerated spoilation equivalent to approximately six months extended wear *in vivo*. Spoilation is dependent on the patient, the wear regime and the material so there is no single correlation factor between *in vivo* wear and the *in vitro* model. In the studies presented here, the materials are exposed to the model for 28 days, using the procedure described in chapter 3. The materials are analysed every three days using fluorescence spectroscopy. This technique is discussed further in chapters six and seven.

It can be seen that although the levels of protein and lipid on the materials are not too high, in comparison to the levels obtained for commercially available contact lenses exposed to the same model, it does vary between materials. There is no single factor that governs the level of deposition on a material. The structure of the monomers, the polarity of the surface and the water content of the hydrogel all have an influence on the

spoilation observed. The values obtained for the AMO:THFMA:PU semi-IPN's are well within the limits obtained for currently available contact lenses.

4.6 Porous periphery

The design of the KPro consists of an optically clear central core, surrounded by a porous periphery. A sound junction between the two components is easier to achieve if the materials for each portion is of the same basic material. A more precise description of the technique used to form this junction is given in section 4.7.

Pores were formed using the method outlined in chapter 3. With knowledge gained from chondrocyte responses in porous hydrogels[11] developed for synthetic articular cartilage[32], findings from this study were used as a starting point for this work. A series of different porosities were introduced into the periphery of the device and each assessed using 3T3 cells for cytotoxicity testing.

4.6.1 Equilibrium water contents of porous hydrogels

A series of porous materials were synthesised with comparable compositions to those reported in table 4.2. Dextrin was used to produce the pores, and dextran to produce channels. The water content of these hydrogels are shown in table 4.6. Dextrin and dextran were added on top of the 100% basic monomer composition, as the porosigen is dissolved out of the final composition, the final material is chemically identical to those in table 4.2. The dextrin used initially created pores in the range 40-60μm.

Monomers	Composition	EWC %
THFMA:AMO:PU:DEX	43.75:43.75:12.5:20	34.8
THFMA:AMO:PU:DEX	37.5:43.75:18.75:20	33
THFMA:AMO:PU:DEX	30:50:20:20	41.6
THFMA:AMO:PU:DEX	25:60:15:15	50
THFMA:AMO:PU:DEX:dextran	37:42:21:10:4	50
THFMA:AMO:PU:DEX:dextran	30:50:20:10	43

Table 4.7 Equilibrium water contents or a series of porous THFMA:AMO:PU semi-IPN hydrogels

Mechanical properties of the porous membranes were not tested, due to the increased errors that would be encountered in their testing[11]. The randomly porous nature of the hydrogels would cause inconsistencies in the results. However, a previous study had revealed that the introduction of pores into a hydrogel will not greatly alter the mechanical properties in comparison to the equivalent non-porous hydrogel[32]. The initial Young's modulus, as expected was very close, being a function of the material. The elongation at break and consequently the tensile strength were slightly lower. This was due to the higher stress concentrations that occurred in the irregular pores where the porosigen had clustered.

To improve the integration of the two components of the prosthetic device, the core and skirt materials were made from the same basic composition. Hydrogels with very different EWC, and consequently different swelling ratios[15], would cause high stress at a join which would usually be formed in the dehydrated state. Therefore, it is important to check that the EWC of the optical core and periphery are not too dissimilar.

Monomers	Composition	EWC %
THFMA:AMO:PU	41.6:41.6:16.8	29.9
THFMA:AMO:PU:DEX	43.75:43.75:12.5:20	34.8
THFMA:AMO:PU	25:60:15	53.7
THFMA:AMO:PU:DEX	25:60:15:15	50
THFMA:AMO:PU	36.6:41.6:21.8	47.9
THFMA:AMO:PU:DEX	37.5:43.75:18.75:20	33
THFMA:AMO:PU:DEX:dextran	37:42:21:10:4	50
THFMA:AMO:PU	30:50:20	41.4
THFMA:AMO:PU:DEX	30:50:20:20	41.6
THFMA:AMO:PU:DEX:dextran	30:50:20:10:4	43

Table 4.8 Table comparing the equilibrium water contents for a series of porous and non-porous semi-IPN hydrogels

During hydration of the membranes, care must be taken to ensure that all of the porosigen is removed. In the final membranes, this was found not to be a problem. However, with the thicker samples that were required for the implantation work, residual porosigen was first detected when the samples were cleaned with iodine and later observed in some of the sections under SEM. The pores and channels are sites for water to be held within the matrix, which would lead to a slight increase in water content.

It can be seen from table 4.7 that the water content for the preferred composition for the optical core and periphery are slightly different. The swelling of the two components will therefore be different, which will have an effect on the junction between them. However, the difference is small and should have only a marginal effect.

Different combinations of pores and channels were investigated to chose the optimum morphology of the periphery material, which will enable cells to penetrate and proliferate. Although results from keratocyte cell studies are not yet available, work previously carried out with chondrocytes[32], have shown that a pore size of 40-60μm was preferred. Therefore, results quoted throughout this work, unless otherwise stated, relate to peripheries formed with pores in this range.

The preliminary cytotoxicity results, carried out using 3T3 Swiss mouse embryo cells, indicate that the materials are non-toxic, and that the cell viability and cell growth rate are not affected by the morphology of the hydrogel. The cell viability was 96.1% for the AMO:THFMA:PU 50:30:20% membrane.

Initial subcutaneous implantation studies have been carried out by Dr John Hunt at Liverpool University, to assess the effect that the differing morphologies has on cell infiltration. The samples used were the same base material, with membranes containing various pore sizes and others with both pores and channels. The materials were the placed in subcutaneous pockets in rats for up to one month. The samples used were of a thickness which meant that not all of the dextran and dextrin had been removed from the material during the hydration stage of the hydrogel preparation. This led to reduced cell infiltration. The results did however indicate that there was no adverse inflammatory response exhibited, and that the materials which contained both pores and channels, provided the best pathway for cells to infiltrate the material, with the larger pores being more effective in promoting integration. An inflammatory response was observed at the square cut edges of the implant, but there was no degradation of the material or fibrous encapsulation.

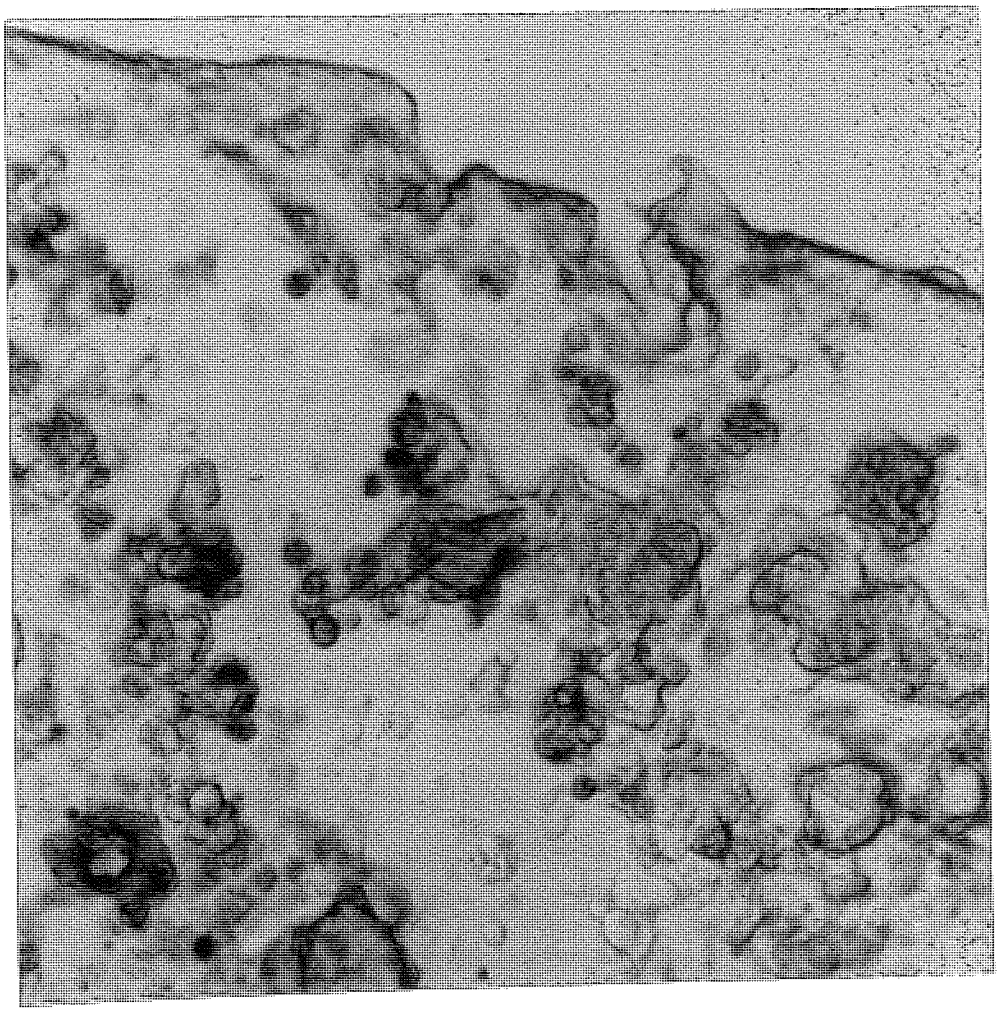

Figure 4.12 Porous periphery following subcutaneous implantation for two weeks showing cellular ingrowth

Implantation was carried out, in rats, for differing periods of time, between 1 and 28 days. Like the Strampelli implant, it is thought that the polymeric device must be implanted subcutaneously prior to implantation in the eye, in order to encourage initial cell growth into the material before placing the prosthesis into the eye.

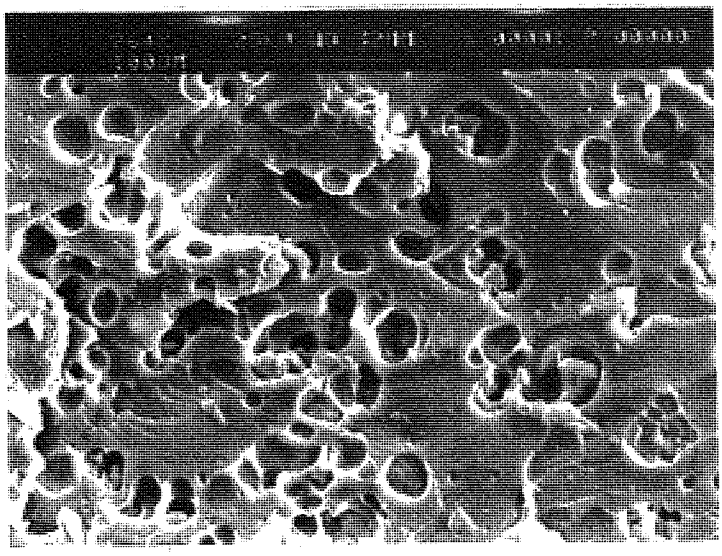

Figure 4.13 Scanning electron micrograph of a porous semi-IPN hydrogel

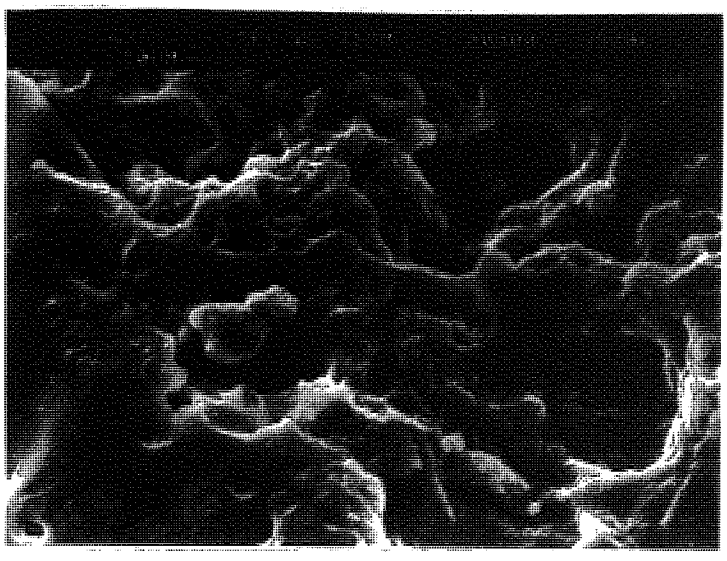

Figure 4.14 Scanning electron micrograph of a semi-IPN hydrogel containing pores and channels

4.6.2 *In Vitro* Spoilation studies

The porous materials were also tested using the *in vitro* spoilation model. The results are shown in figures 4.14 to 4.16. It has previously been shown[26] that an irregular or rough surface will result in an increase in spoilation. This is illustrated by comparing the increase in spoilation caused by the increase in surface rugosity, from smooth, porous and hydrogels containing pores and channels. Spoilation is not only a function of the material, but also the surface morphology.

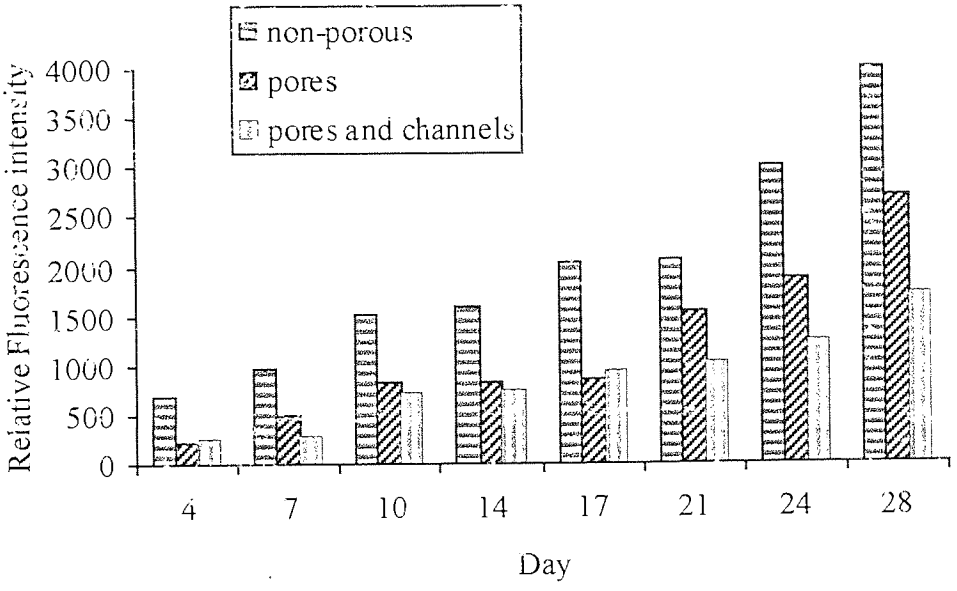

Figure 4.15 Progressive build up of protein spoilation measured using fluorescence spectroscopy at an excitation wavelength of 280nm for a series of AMO:THFMA:PU 50:30:20 membranes with differing morphologies

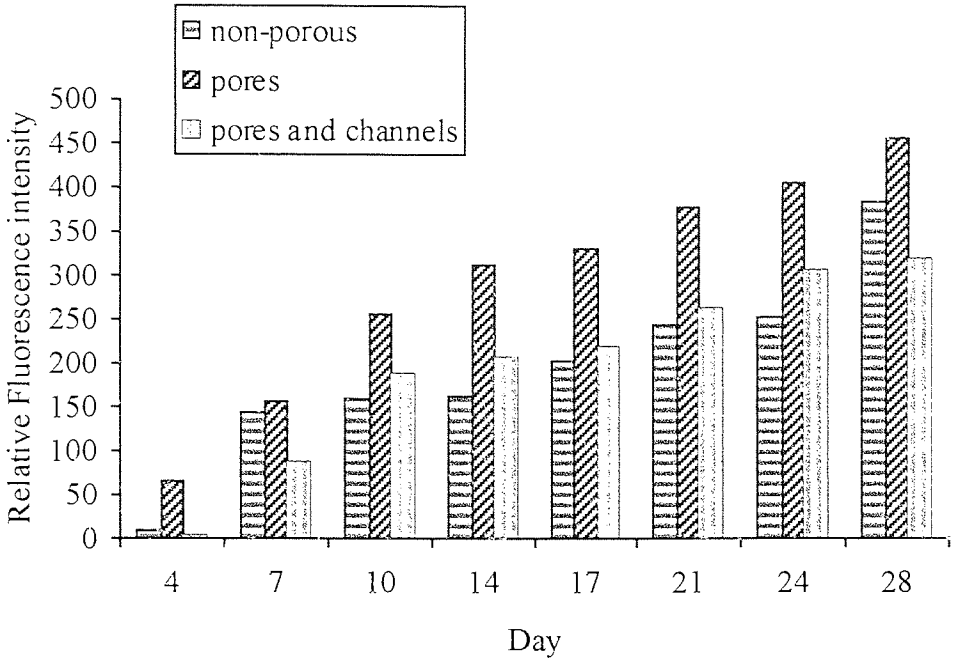

Figure 4.16 Progressive build up of lipid spoilation measured using fluorescence spectroscopy at an excitation wavelength of 280nm for a series of AMO:THFMA:PU 50:30:20 membranes with differing morphologies

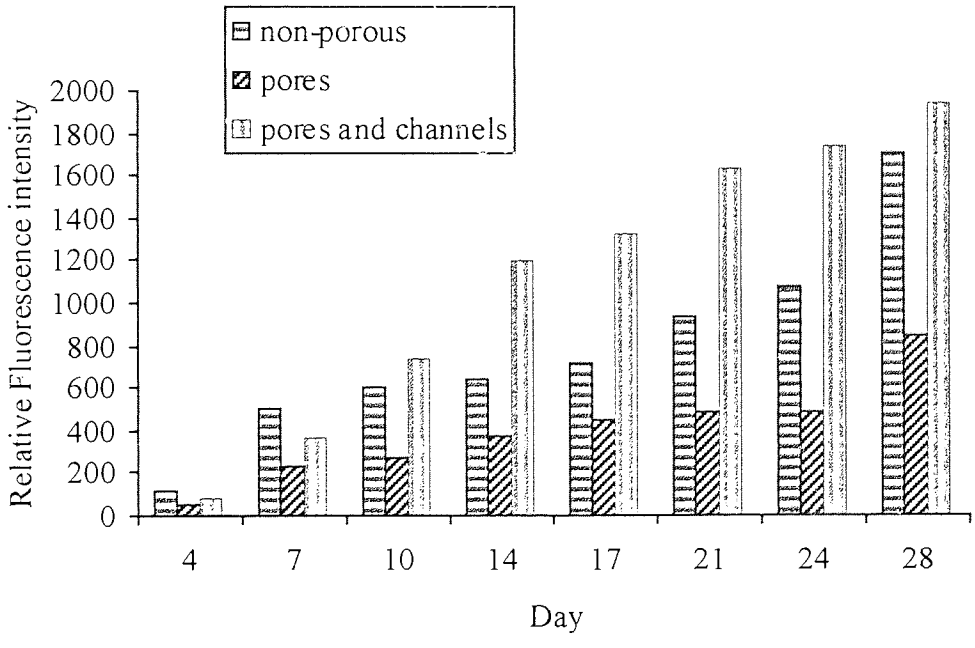

Figure 4.17 Progressive build up of lipid spoilation measured using fluorescence spectroscopy at an excitation wavelength of 360nm for a series of AMO:THFMA:PU 50:30:20 membranes with differing morphologies

Figures 4.14 to 4.16 show the progressive build up of proteins and lipids on materials displaying different morphologies. It would be expected that a rough surface would lead to an increase in the level of spoilation. Fluorescence spectroscopy is a surface technique so an increase in surface rugosity can lead to an increase in the level of scattered light that is observed, which in turn can give misleading results about the level of deposition on an irregular surface. It must also be taken into account that a background measurement for an unspoilt section of the material being tested is subtracted from the reading obtained following exposure to the spoilation model. As deposition proceeds, the surface may to a certain degree become smoother, but the initial reading was high due to the pores and channels. This will lead to a large background reading being subtracted from the relatively low reading obtained for the spoilt material.

4.7 Fabrication of a Keratoprosthestic Device

The aim was synthesise a hydrogel which had an optically clear central core, surrounded by a porous periphery. A major reasons for the failure of other keratoprostheses is the lack of a firm junction between the core and periphery, which results in the extrusion of the device. By using the same material for both the components it is hoped that this problem will be overcome.

Several procedures are employed to produce contact lenses[51]. Two of the most common methods are the formation of buttons or rods. As the final prosthesis will be in the form of a contact lens, these methods, along with the use of centrifugal force, were investigated as possible routes to the manufacture of a keratoprosthesis. During the early stages, the dimensions used were larger than those required for the final device. This is simply due to it being easier to work on a larger scale. There was also interest in the interface between the periphery and the core, which would be expected to have the same interface characteristics, irrespective of the size used.

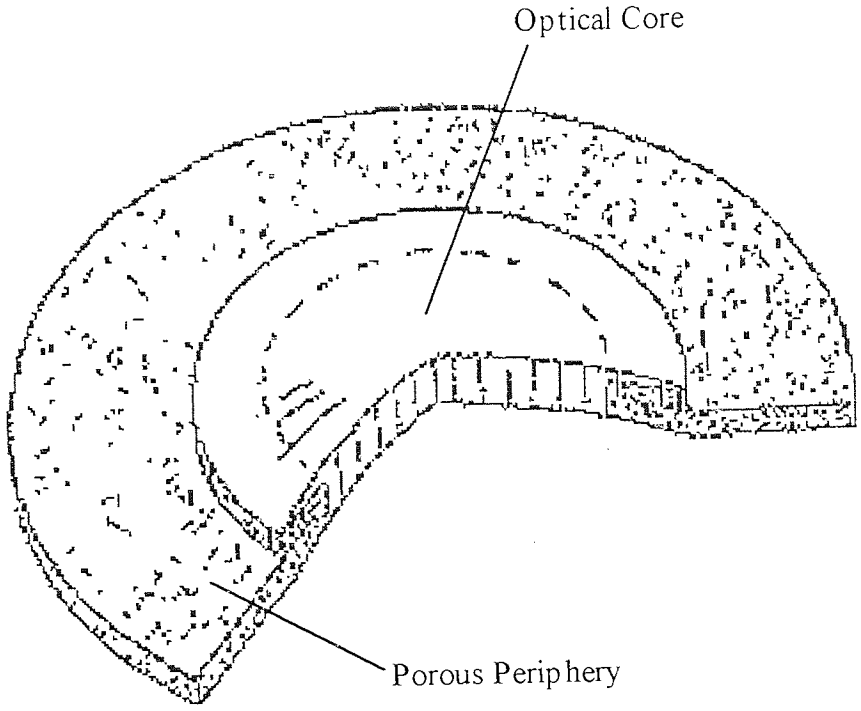

Figure 4.18 Schematic diagram of full thickness keratoprosthesis

4.7.1 Rotational method

As the base material for both components of the device are to be the same, a centrifugal force was investigated to produce this porous periphery. The liquid monomers and porosigen, based on the IPN mixtures in the previous section, were placed in a polypropylene tube. This was attached to an overhead stirrer, with the axis of the stirrer passing through the central axis of the tube. This allowed for the centrifugal force to be exerted towards the walls of the tube. The heat generated by stirring would allow polymerisation to take place as the tube spun, so that the porosigen would be forced to the periphery leaving an optically clear core.

Initially the mould was rotated at a speed of rotation ranging from 0 to 6000 revolutions per minute with polymerisation occurring when a temperature of 50°C was reached.

The resultant rods had porosigen distributed throughout the material. A higher speed of rotation resulted in a rod with the porosigen predominately at the base of the rod. Further attempts were made varying the speed of rotation and also rotating the mixture prior to polymerisation, in an attempt to achieve the required distribution of the porosigen. However, the necessary control was not possible using the overhead stirrer, though the method showed potential.

Factors, other than speed of rotation, that will influence the outcome of rods formed by this method are the viscosity of the monomer mixture, polymerisation temperature, the composition and diameter of the tube, the percentage of porosigen used and the depth of porosigen required at the periphery.

4.7.2 Rod Polymerisation

The most common method of making contact lenses is to form a rod and then to lathe cut the polymer into the required curvature and thickness. This method was modified to produce a prosthetic device. The core and periphery need to be polymerised in sequential steps, with integration between the two components to form a water tight junction. This could be achieved either by polymerisation of the core followed by polymerisation of the periphery, or vice versa.

Polymerisation takes place in tubes of different diameters, but as there are two components, the polymerised rod has to transferred between the two tubes to produce the final device. A degree of integration is required between the core and periphery, so complete polymerisation of the component formed first was not desired. However, partial polymerisation needs to occur prior to removal from the mould, so that the rod is formed and can be transferred without loss of shape.

4.7.2.1 Methodology

Monomers, crosslinker and initiator were weighed and degassed with nitrogen for 10 minutes. The mixture was then poured into the polypropylene rod mould, which was then sealed. The rod was then placed in a water bath at ambient temperature, and heated to the polymerisation temperature of 40°C at a rate of 5°C per minute. On completion of the desired degree of polymerisation the mould was removed from the water bath, and the partially polymerised rod removed from the mould.

For the polymerisation of the core followed by the periphery, a mould was made up consisting of the polypropylene mould with silicon tubing inside to give the desired diameter for the core. The monomer mixture was poured in, and polymerised in the water bath for approximately four hours. The rod formed was handleable, though complete polymerisation had not occurred. The core was carefully removed from the silicon tubing, and fixed centrally in the polypropylene tube by the use of a small ring of tubing at each end of the core to anchor it in place. The monomer mixture for the periphery was the same composition as that for the core, with the addition of dextrin to make it porous. This mixture was poured around the core, left for several hours to diffuse into the edge of the core, and then polymerised.

The polymerisation of the periphery followed by polymerisation of the core was also investigated. A solid polypropylene rod was placed centrally through the rod mould, and the monomer mixture for the periphery poured round it. Polymerisation of the periphery was carried out as described above. The central rod was then removed from the mould, and the monomer mixture for the core added and polymerised.

The completed rods were then removed from the moulds, and lathed into small discs which were then hydrated in distilled water. The best results were obtained when the core was polymerised first, as there was some difficulty in removing the solid polypropylene rod from the periphery without damaging the periphery. The dextrin

remained at the periphery, unlike in the centrifugal method, though it appeared to show a slight variation in distribution due to gravity.

The interface between the two components appeared to be integrated as the device remained intact following hydration, dehydration and subsequent examination by SEM.

4.7.3 Button Polymerisation

Monomer mixtures were produced by the same method as described above, but a photoinitiator was used instead of a thermal initiator. Small pieces of silicon tubing were cut which had the required diameter for a core. The monomer mixture was poured into the mould and polymerised using UV light. A polymerisation time of 30 minutes was sufficient to produce a partially polymerised core. The silicon tubing was carefully removed and replaced with a piece that was the required diameter of final device, with the core central. The monomer mixture for the periphery was carefully added, taking care not to place any over the core. The whole device was then exposed to UV light for 15 minutes to complete the polymerisation.

4.8 Discussion

The aim of this chapter is to develop novel hydrogels for use as synthetic artificial corneas. The materials for use in a keratoprosthesis need to fulfil certain criteria. The need for a porous periphery that will allow for cell integration to form a watertight junction between the device and the host cornea is well known. The device needs to be mechanically strong enough to withstand the stresses involved in both the surgical procedure and the deforming force of the eyelid during the blink cycle. The optical centre must by transparent, with good integration with the periphery of the device. The device must also be non-toxic and not evoke an inflammatory response once it is placed in the eye, and not show a considerable level of spoilation over a long period of time.

Materials that were initially investigated had previously been used as components of soft contact lenses, and use was made of the work carried out to synthesise a hydrogel that could be used to replace the articular cartilage. The comonomer hydrogels had a range of EWC's and mechanical properties, though these were not strong enough for this particular application. This is important in a KPro device as the prosthesis will need to withstand both the surgical procedure involving placing sutures through the periphery, and the deforming force of the eyelid once it is in place. The materials investigated had previously been used in other forms in the body, as components of soft contact lenses or in dental products, so the toxicology had been assessed. Semi-interpenetrating polymer network technology was employed to enhance to mechanical strength of the hydrogels. The initial results had indicated that the materials were non-toxic and the spoilation properties were within the limits observed for many commercially available soft contact lenses. HEMA was not considered for a base monomer as it not cell adhesive. NVP was not used as it forms 'blocky' polymers due to its low reactivity ratio. A series of heterocyclic monomers were investigated, as the incorporation of bulky side chains can increase the mechanical strength. From these, a series of THFMA:AMO hydrogels were chosen for further investigation as semi-interpenetrating polymer networks, as these gave good cell response and spoilation profiles in the comonomer form. These properties were maintained upon the addition of a polyester urethane interpenetrant, along with greatly enhanced elastic modulus.

The semi-IPN's were also synthesised in a range of morphologies so that the behaviour of cells could be monitored. Pores and channels were created by the addition of dextran and dextrin, respectively, to the monomer mixture prior to polymerisation. The initial subcutaneous implant studies suggested that the cells favoured the pore and channel structure as this gave a pathway for the cells to integrate into the material. The best results were obtained for the larger pore sizes, and the materials showed no degradation throughout the course of the 28 days implantation. The hydrogels also displayed no adverse immunological response when implanted.

Manufacture of a device was also considered. Partial polymerisation of one component is required to enable integration of the second part, to form a tight junction between the components, which has previously been a major contributing factor for the failure of many devices. The time required to achieve this needs to be assessed for each monomer mixture for each method. Removal of the partially polymerised sections has to achieved carefully so that no damage takes place. The dimensions that have been used to date are not those that are actually required for the final device, but are on a larger scale. The correct dimensions need to be ascertained and used to produce potential devices. It is important that a method of reproducibly manufacturing the device is identified. The interface between the two components, needs to be tested fully, with both the water swelling and the mechanical strength investigated. The best results were obtained using the rod method of manufacture, with the core being polymerised prior to the core. The final rod can then be lathe-cut into the required curvature.

Further approaches to the periphery include using hydroxy apatite which is found in teeth, and would copy the copy the Strampelli approach, and polymerising around calcium alginate.

The initial cytotoxicity tests revealed that the materials did not have an adverse effect on the cells. However, the cells used were not keratocytes, so this interaction needs to be studied to gain an understanding of what will happen once the device is placed in the eye. Further work is currently being undertaken to assess the materials response to foetal and adult keratocytes. It is important to know how the cells will react to the material, and the optimum periphery morphology can be determined, as it may be different for keratocytes than chondrocytes.

The spoliation studies indicate that the materials considered above, do not show any increased levels of deposition in comparison to some commercially available contact lenses. The surface of the keratoprosthesis may need to be treated in some form to limit

deposition as the device will not be able to be removed from the eye as conventional contact lenses are for cleaning.

CHAPTER 5

Development of a Hydrogel Mask for Laser Ablation

5.1 Introduction

Lasers are being used increasingly in surgical procedures to alter the refractive power of the eye[5]. Argon-fluoride excimer lasers have been found to remove precise amounts of corneal tissue with submicron accuracy, without causing too much localised damage. This laser has been utilised clinically in the treatment of myopia.

If an irregular corneal surface is ablated, the contours will be reproduced deeper in the cornea. This could be overcome by masking the surface so that a smooth corneal surface is produced following ablation. For this to be achieved, several criteria must be met, it must be photopolymerisable with a very quick polymerisation time, have a suitable viscosity to enable the solution to fill all the irregularities, adhere to the corneal surface without causing an immune response, and display ablation characteristics similar to that of the cornea.

Collagen and methylcellulose are among various materials that have been investigated for this application, as described in chapter 2. A temporary prosthesis based on a hydrogel is investigated in this chapter.

5.1.1 Temporary Prosthesis Requirements

The temporary corneal prosthesis is applied to the corneal surface as a fluid and polymerised *in situ* underneath a mould of the curvature required. There must be no adverse ocular response brought about by the procedure. The prosthesis must exhibit similar ablation characteristics to those of the host cornea.

Initial ablation studies indicate that ablation rate is dependent upon water content. Results obtained from ablation of a series of hydrogels with different water contents are shown in figure 5.1.

Ablation rate is defined as:

$$\text{ablation rate} = \frac{\text{number of pulses}}{\text{thickness removed by ablation}} \qquad (5.1)$$

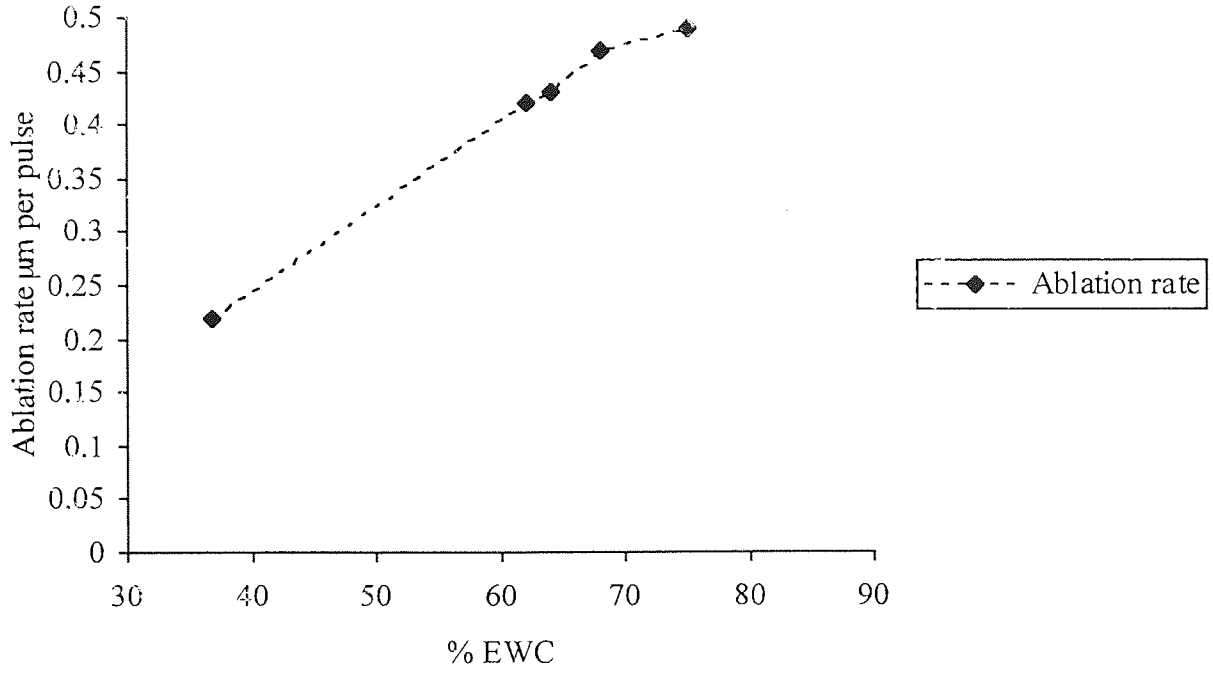

Figure 5.1 Ablation rate of a group of hydrogels with different water contents

The corneal stroma has a water content of about 75%, though the water content of the whole cornea varies with depth[83]. The ablation rate for the stroma has been reported as 0.49 µm per pulse. As water content has been shown to influence the ablation rate, a series of hydrogels of different chemical compositions having water contents similar to that of the cornea were investigated. Other properties of the hydrogels were also considered to see the effect these played in determining the ablation characteristics.

5.2 Materials

Initially, work was carried out to modify the backbone of these polymers to introduce UV polymerisable groups. However, the degree and position of modification could not

be controlled, which may lead to problems with reproducibility of the hydrogels and toxicity. Therefore, the polymers were used without any prior modification along with a crosslinkable polymer which contained double bonds.

If a hydrogel is to be used for this application, water must be present in the system prior to polymerisation, as it is not feasible to hydrate the gel once it has been formed on the ocular surface[189]. Water soluble polymers have been used in many ophthalmic solutions as viscosity agents[37]. These were utilised as the base polymers in the temporary prostheses systems.

In order to produce a temporary prosthesis that could be polymerised on the corneal surface, a number of components are required. A water soluble polymer, a photopolymerisable functionalised polymer, a crosslinking agent, a diluent and a photoinitiator make up the basic components of the system. The fluid applied to the eye needs to be of a viscosity that will allow it to fill in the crevices between the irregularities on the corneal surface, and then be moulded to the correct curvature underneath a template. It must be handleable and compatible with the ocular surface.

Two water soluble polymers were investigated as the preformed polymer component of the system, namely polyvinyl alcohol, PVA, and hydroxypropyl methylcellulose, HPMC. Both are available in a variety of molecular weights enabling a range of viscous solutions to be made up. They are used in commercially available ophthalmic solutions.

The second component of the system was a crosslinkable polymer. The functionalised polyethylene glycol's, PEG's[190], provide a photopolymerisable polyethylene glycol network around the preformed polymer solution. Glycol's are often used as the crosslinking agent so an additional crosslinker, similar to that used for the hydrogels in chapter 4, may not be required

The photoinitiator used in each case was Irgacure 184. Polymerisation was carried out using a Gallenkamp UV mercury discharge lamp, which has a wavelength of 365nm, and occurred within a maximum of thirty minutes. The polymerisation is bought about using a water soluble photoinitiator[191]. Riboflavin[192] was used initially, but it was found that it was not effective. An alternative initiator, Irgacure 184, was used.

The hydrogels were made in membrane form, through UV initiation and polymerisation, as described in chapter 3, to enable full characterisation to take place. The results are presented graphically in this chapter, and are tabulated in appendices 2 and 3.

5.3 Effect of Molecular Weight and Percentage Solution

5.3.1 Water binding studies

PVA and HPMC were obtained in three different molecular weights. 1%, 2% and 5% (w/w) solutions of each were made up and hydrogels synthesised with 25% (w/w) polyethylene glycol 1000 dimethacrylate, PEG1000DMA, and 0.5 % Irgacure 184. The equilibrium water contents of the resulting hydrogels are shown graphically in figure 5.2.

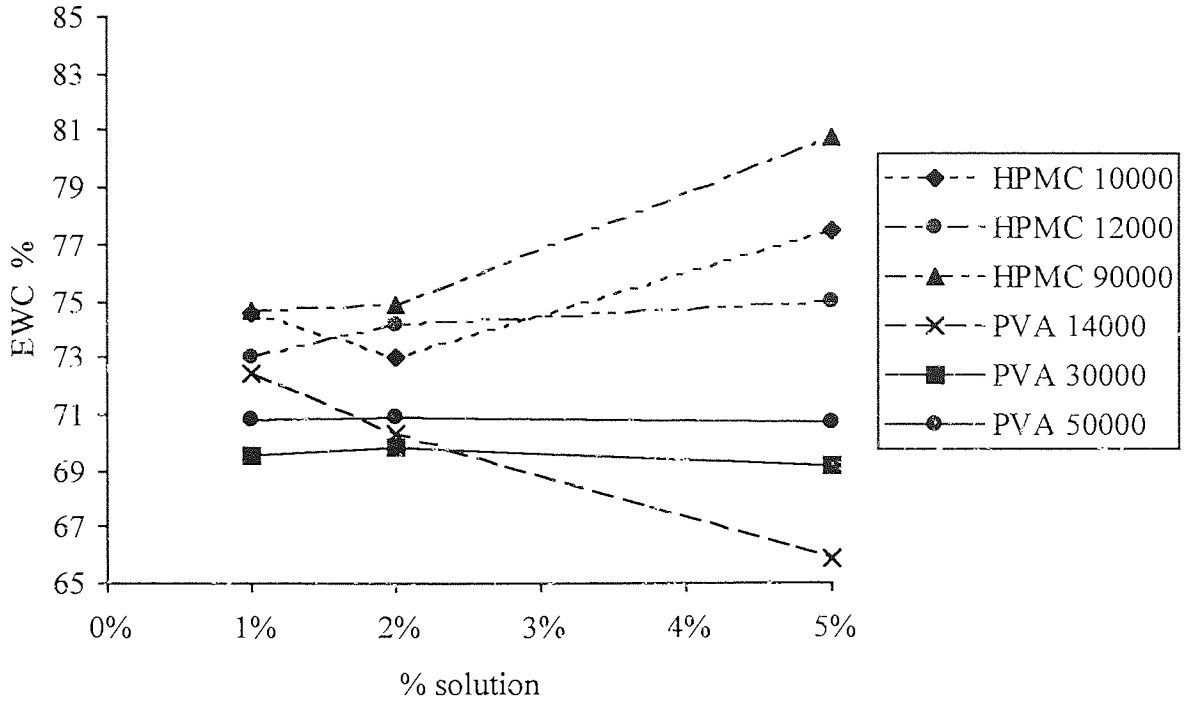

Figure 5.2 Graph to show the effect molecular weight and the percentage solution used has on equilibrium water content

The starting solutions for these hydrogels have different viscosity's, due to the various molecular weights and percentage solutions used. The 5% solution of the highest molecular weight for HPMC was very viscous, and there was poor miscibility will the PEG. The viscosity of the solution needs to be such that it will fill any surface crevices. Sufficient mixing will occur between the components, and there will be no air bubbles introduced during mixing.

PVA hydrogels showed very little difference in water content as the percentage solution increased, though if anything actually decreased slightly 1 - 5 %, on whole as molecular weight increased, water content decreased. HPMC hydrogels water content generally increased as the percentage solution increased, as there were more sites for bonding to

the water molecules. There is a considerable amount of water present in the system prior to polymerisation, some of which is lost during the process.

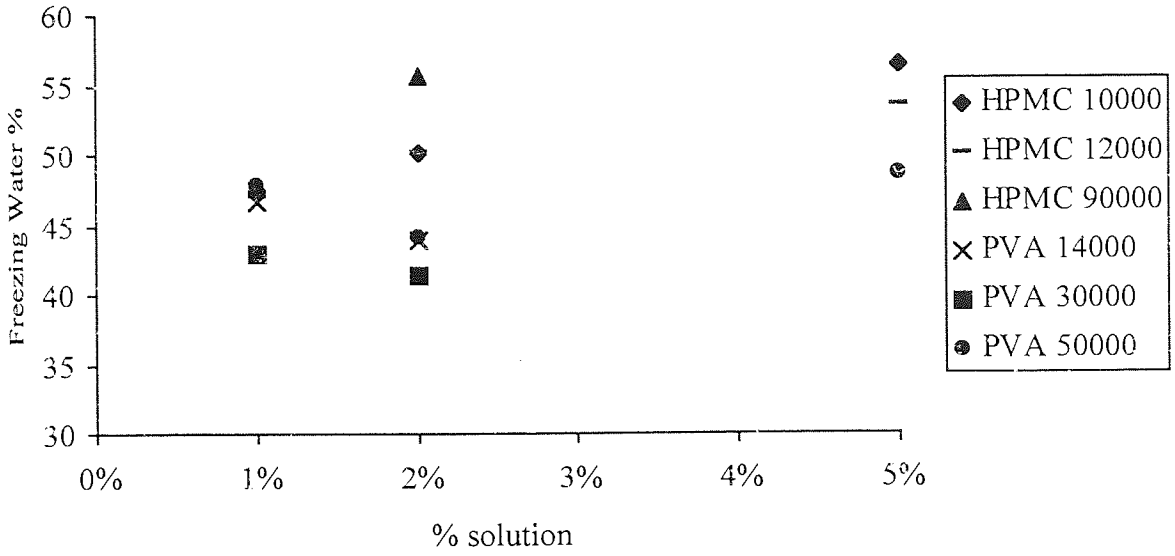

Figure 5.3 Graph to show the effect molecular weight and the percentage solution used has on freezing water content

Ablation rate has been related to the water content of the system. The state in which the water is present within the polymer network may therefore play an important role in determining the ablation rate of the hydrogel. Freezing water is free within the polymer network, and so is a lot more mobile than non-freezing water. This could affect the ablation rate as the free water may be pulled to the site of ablation, affecting the overall distribution of water within the polymer.

5.3.2 Mechanical Properties

Initial studies suggest that ablation rate is related to water content. Mechanical properties were also tested so that any factors contributing to the ablation rate could be determined.

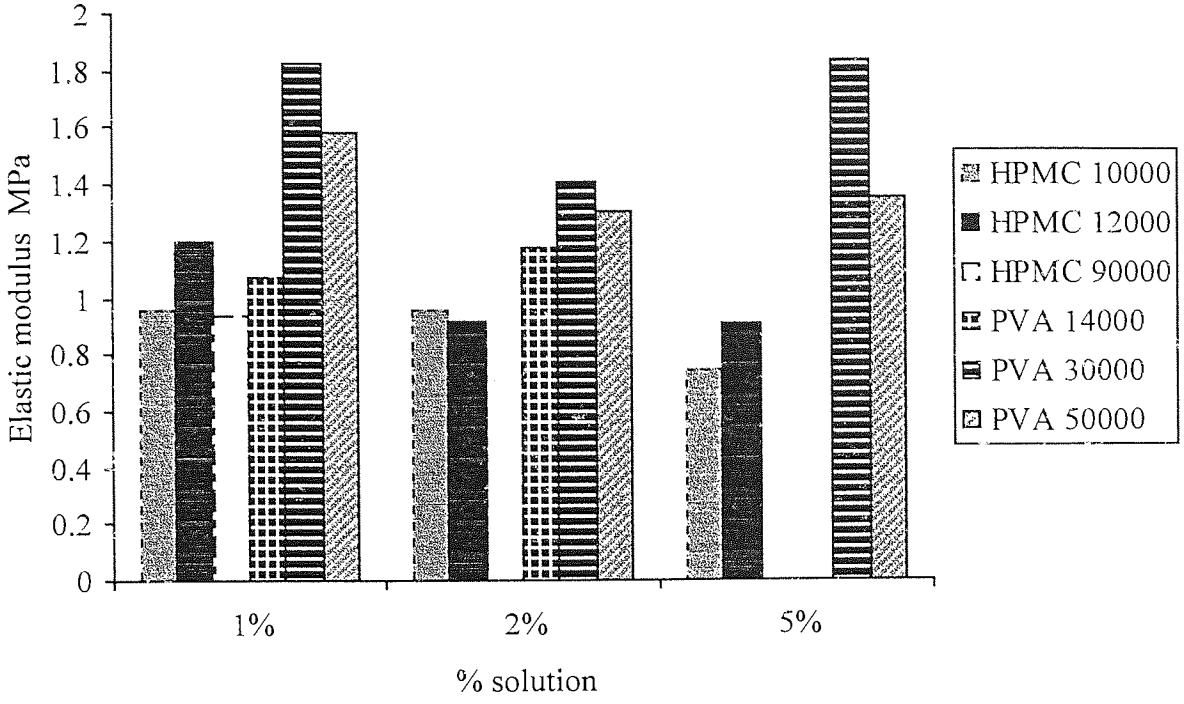

Figure 5.4 Graph to show the effect molecular weight and the percentage solution used has on elastic modulus

Figure 5.4 indicates that there is very little difference in the elastic modulus, as the percentage of preformed polymer is increased in the system, though it does vary with molecular weight. This could be due to the differences in water content. The general trend observed is from a 1% solution to a 5% solution, the elastic modulus decreases.

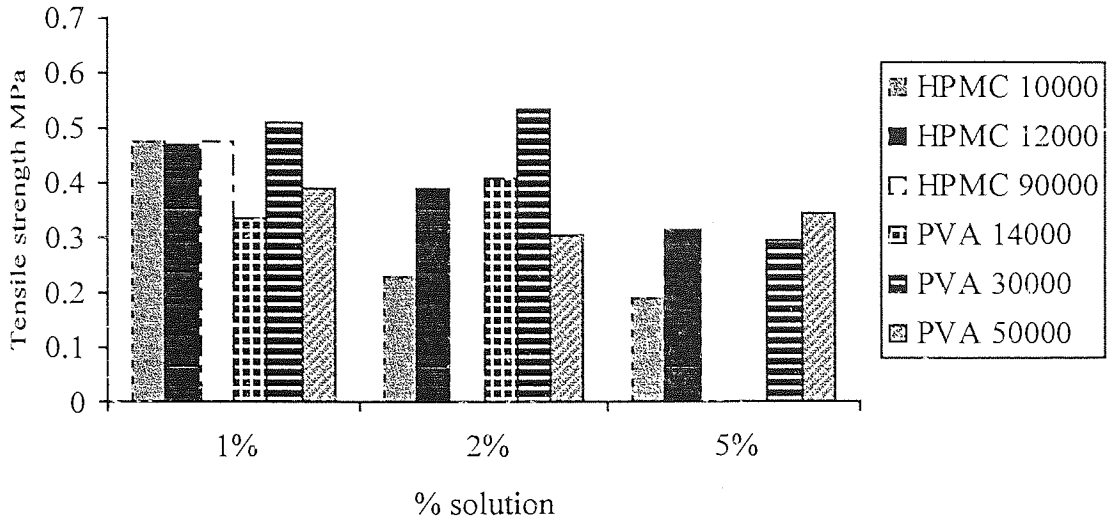

Figure 5.5 Graph to show the effect molecular weight and the percentage solution used has on tensile strength

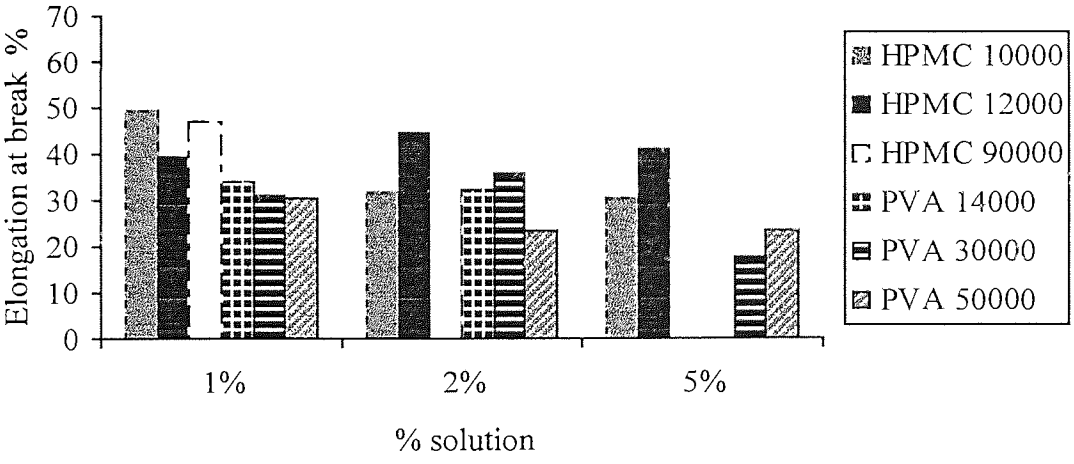

Figure 5.6 Graph to show the effect molecular weight and the percentage solution used has on elongation at break

From figure 5.3 it can be seen that the elastic modulus was greatest for 1% solutions, though not all of the materials were strong enough to test, as they were breaking as they were put in the jaws of the tensiometer.

An increase in water content resulted in a decrease in the tensile strength and elastic modulus. A large amount of freezing water increases the polymer flexibility, as the freezing water is regarded as plasticising water.

The viscosity of the solutions can be altered by varying the molecular weight and the percentage of polymer in the system. The ideal viscosity for this application will depend upon the depth and type of the irregularities on the corneal surface. The viscosity will increase with an increase in molecular weight and percentage solution. There are various factors that affect the viscosity of the polymer. In the case if PVA, the number of residual acetate groups and the degree of hydrolysis both contribute to the intrinsic viscosity of the system.

5.4 Effect of the length of the PEG chain

1% (w/w) solutions of PVA (molecular weight 14,000) and HPMC (molecular weight 10,000) were used to produce hydrogels with a range of different PEG dimethacrylates. 25% (w/w) of the PEG's were used in each case. The effect the length of chain had on water content and mechanical properties were investigated.

5.4.1 Water binding

The EWC of the hydrogels produced using different PEG lengths is shown graphically in figure 5.7, and tabulated in appendix 2.

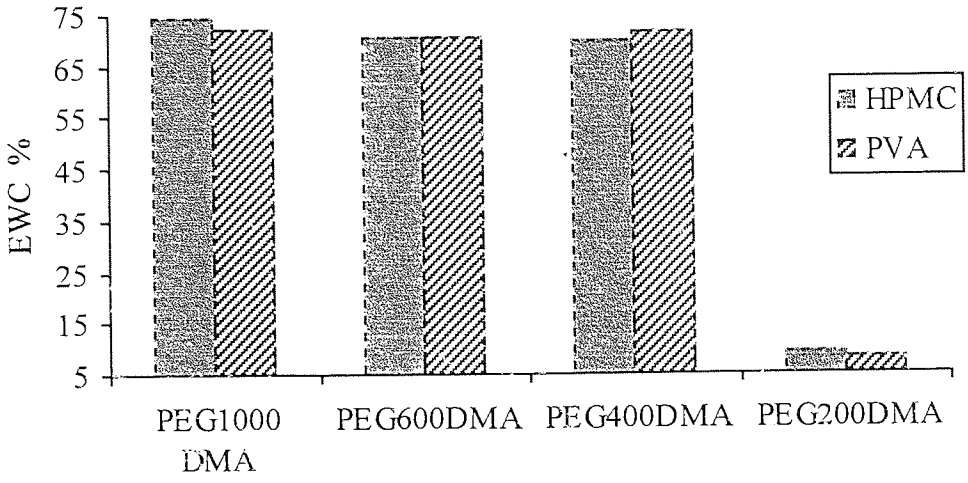

Figure 5.7 Graph to show the effect the length of PEG chain used has on the EWC

Figure 5.7 shows that as the number of polyethylene glycol units increases, the water content increases. The retractive forces between the polymer chains will increase as the PEG chain increases, resulting in larger areas for the water to be held within the matrix. There is a considerable difference in the water content as the length of PEG chain is increased from 200 to 400, and then there is very little variation as the chain length is increased up to 1000. This could be due to impurities in the samples used, and the difficulty involved in controlling the length of the PEG chain and ensuring that both ends of the chain are functionalised.

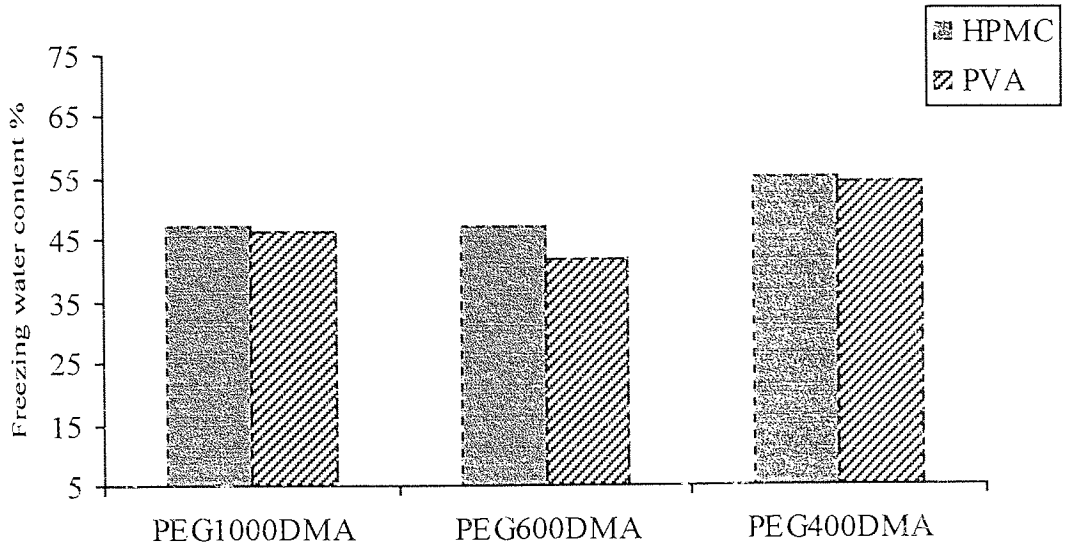

Figure 5.8 Graph to show the effect the length of PEG chain used has on the freezing water contents

The amount of freezing water increases as the PEG chain length decreases, corresponding to a decrease in EWC. As the freezing water content increases, the amount of bound water decreases. This leads to a more flexible polymer.

5.4.2 Mechanical properties

The membranes formed with PEG200DMA were very brittle and could not be cut without breaking to enable mechanical testing to take place. The mechanical properties of the other membranes were tested, and the results shown below.

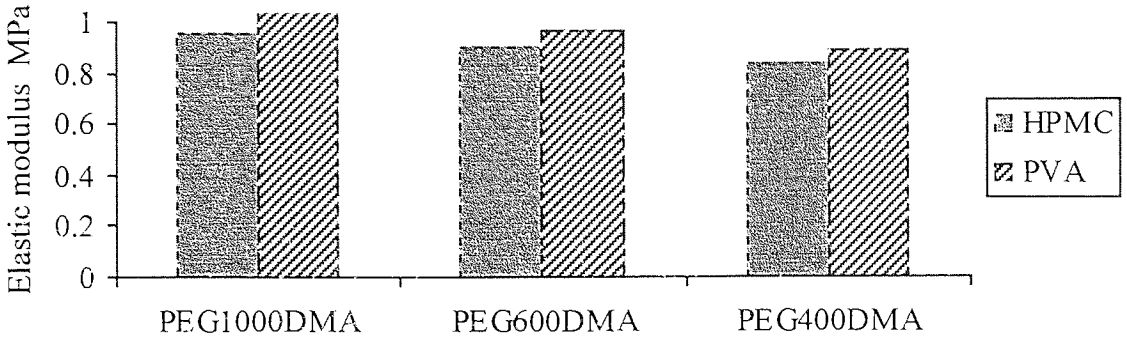

Figure 5.9 Graph to show the effect the length of PEG chain used has on the elastic modulus

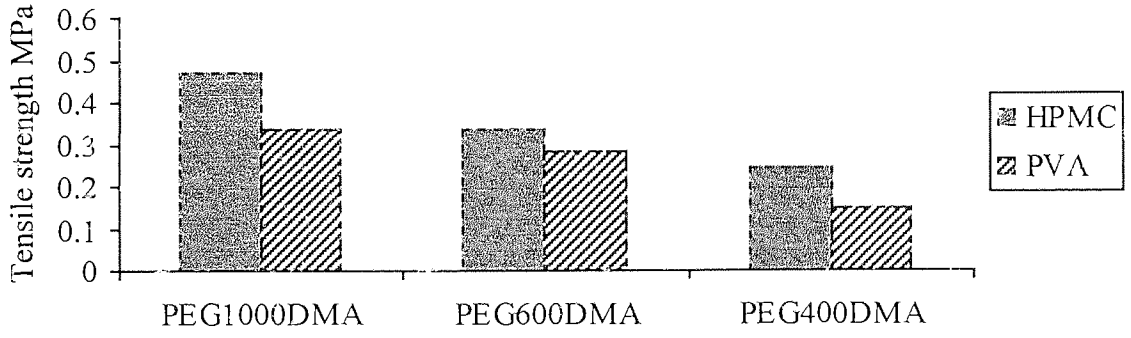

Figure 5.10 Graph to show the effect the length of PEG chain used has on the tensile strength

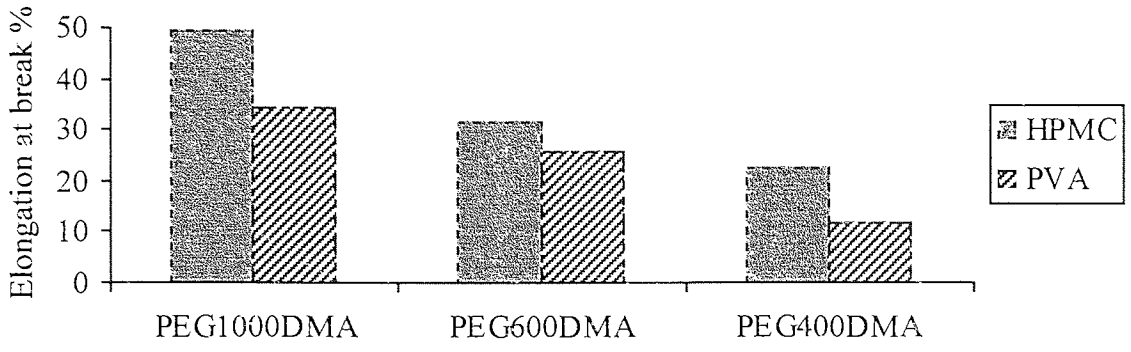

Figure 5.11 Graph to show the effect the length of PEG chain used has on the elongation at break

As the length of the PEG chain is increased, an increase in the elastic modulus, tensile strength and elongation at break are observed, though the change in elastic modulus is small. The space between crosslinks increases with the increase in PEG chain length, which results in more flexibility in the polymer.

5.5 Effect of mixed PEG methacrylate systems

A monomethacrylate, dimethacrylate mixture was investigated to study the effect on both the water binding and mechanical properties.

5.5.1 Water binding

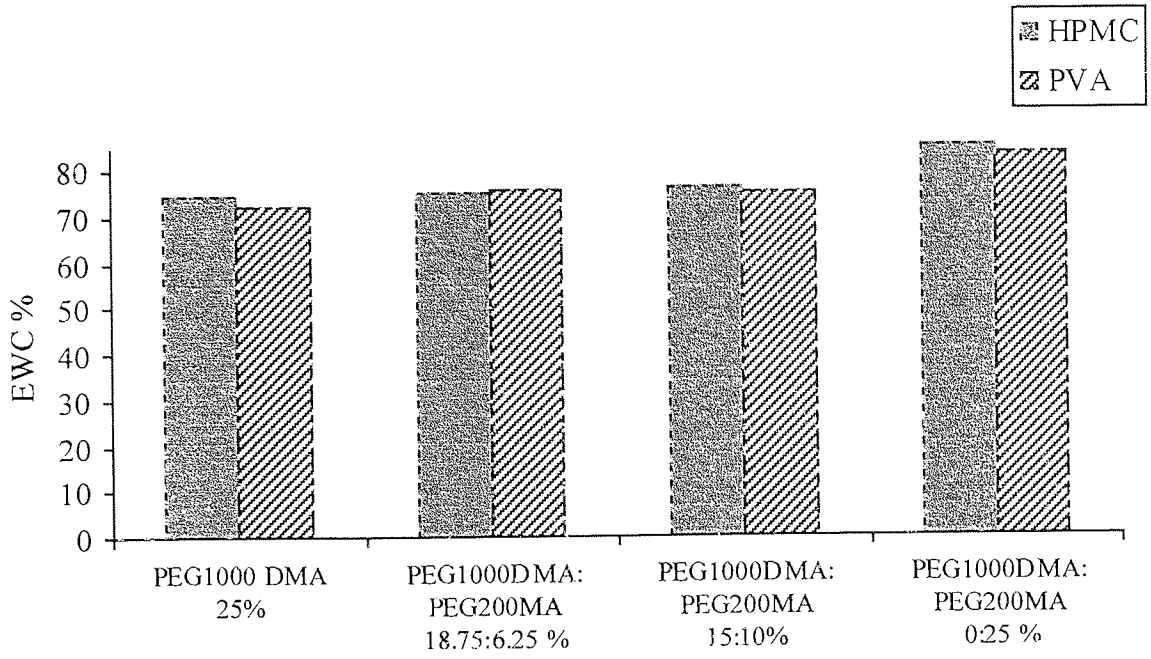

Figure 5.12 Graph to show the effect a mixed PEG methacrylate system has on the equilibrium water content

As the amount of PEG200MA is increased, there is a slight increase observed in the water content.

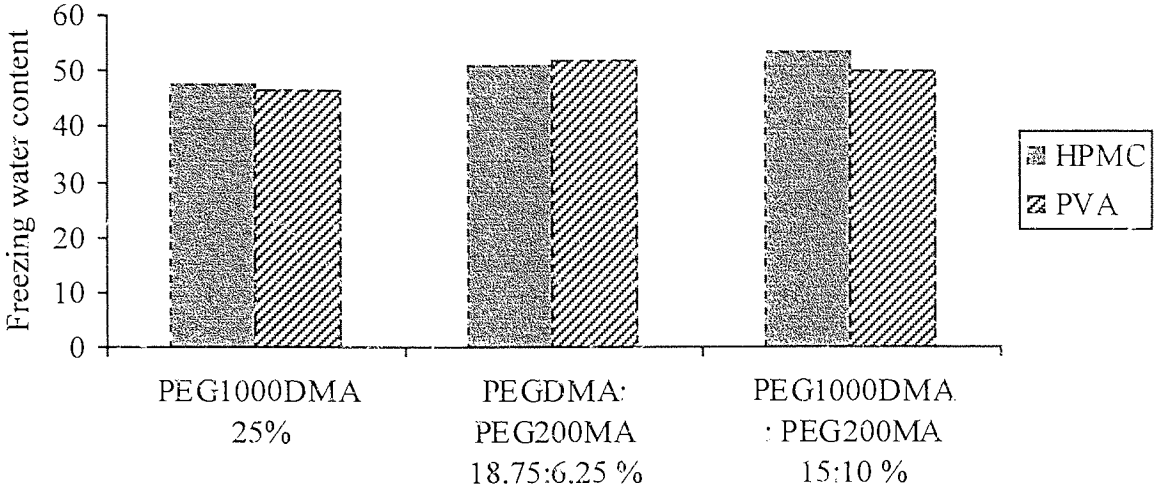

Figure 5.13 Graph to show the effect a mixed PEG methacrylate system has on the freezing water content

The freezing water content held within the matrix increases as the amount of PEG 200MA increase, corresponding to the slight increase in EWC.

5.5.2 Mechanical properties

The mechanical properties of the materials discussed above were tested. The results are shown in figures 5.14 to 5.16.

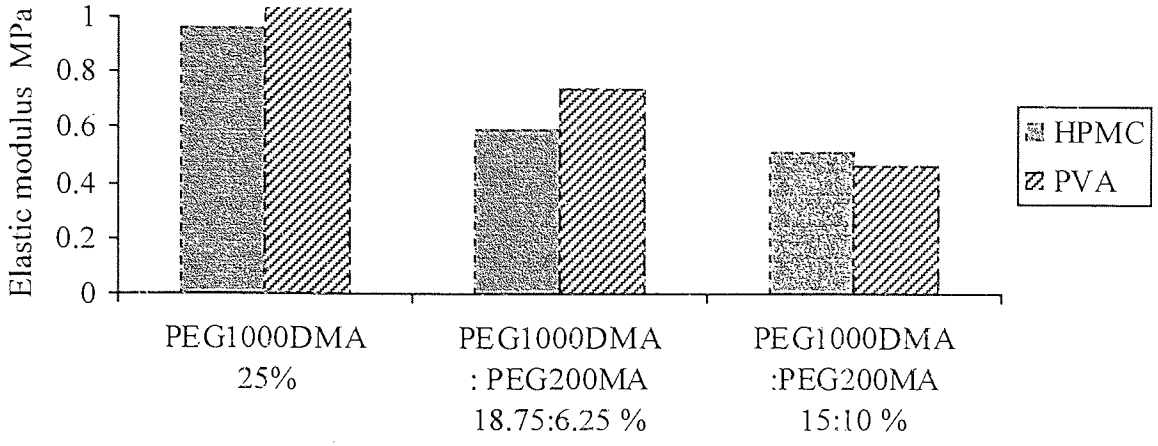

Figure 5.14 Graph to show the effect a mixed PEG methacrylate system has on the elastic modulus

As the amount of PEG200MA in the system increases, the elastic modulus decreases. The effective crosslink density decreases with the introduction of a monomethacrylate, which leads to the formation of more flexible, weaker polymers as the number of crosslinks is reduced.

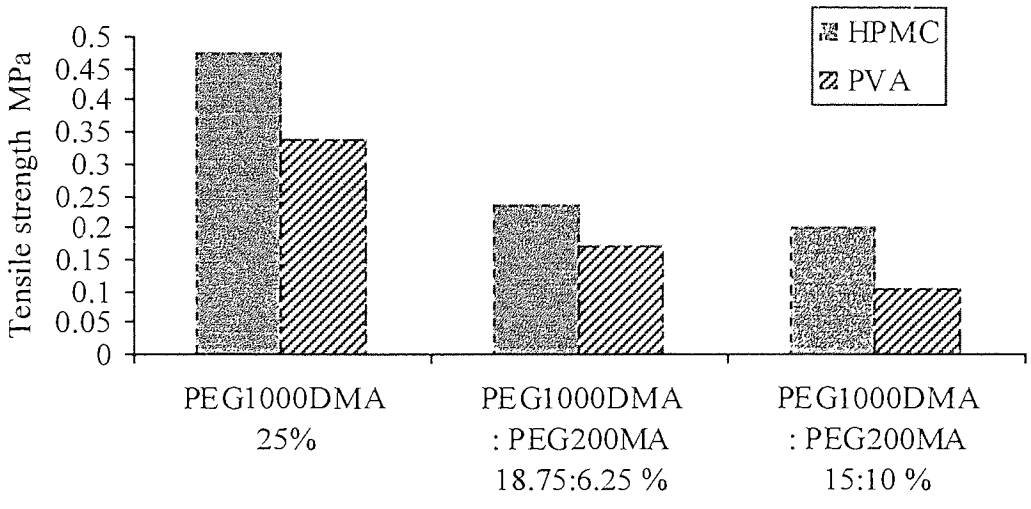

Figure 5.15 Graph to show the effect a mixed PEG methacrylate system has on the tensile strength

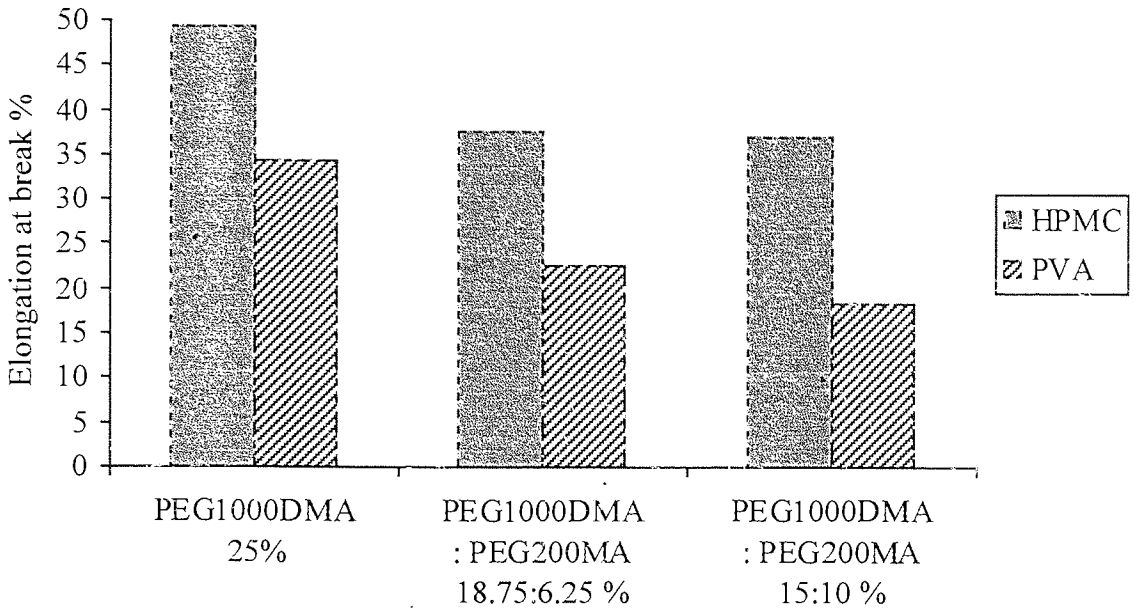

Figure 5.16 Graph to show the effect a mixed PEG methacrylate system has on the elongation at break

Tensile strength and elongation at break decrease as the amount of PEG200MA in the system increases. The inclusion of the monomethacrylate results is a more flexible polymer due to the reduction in the effective crosslink density.

5.6 Effect of amount of PEG used and the addition of a different crosslinker

The previous set of results demonstrated that the properties of the hydrogels could be altered by addition of different amounts of PEG200MA. However, by increasing the amount of PEG200MA, the amount of PEG1000DMA in the system was decreased. The effect that the amount of PEG dimethacrylate used had on the system was then investigated.

A series of hydrogels were made up with differing amounts of PEG1000DMA, and additional crosslinker (EGDMA).

5.6.1 Water binding

Equilibrium water contents and the type of water binding experienced in the system were investigated.

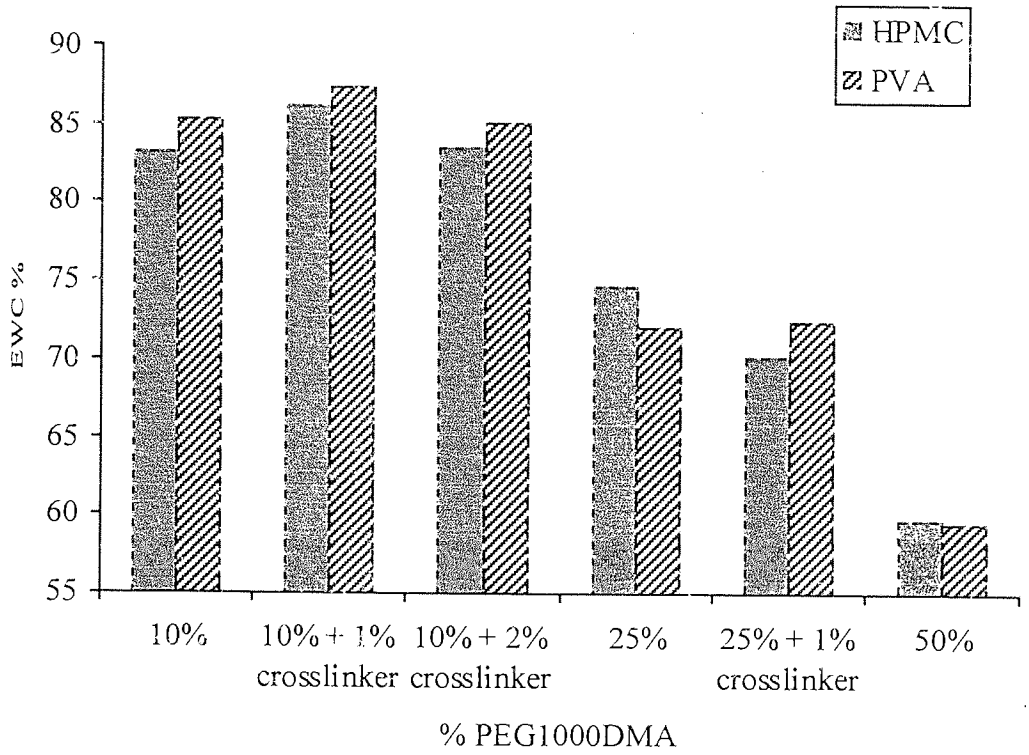

Figure 5.17 Graph to show the effect the amount of PEG1000DMA used has on the equilibrium water content

As the percentage of PEG1000DMA increases, the water content decreases. The effective crosslink density will increase as the amount of PEG1000DMA increases. This will lead to a decrease in the water content, as the polymer matrix will be more tightly packed allowing less space for the water.

The crosslink density will be lowest in 10% PEG1000DMA membrane so has highest EWC and more bulk water. Addition of the extra crosslinker will increase the amount of crosslinking, but the effect is much more noticeable with extra PEG1000DMA.

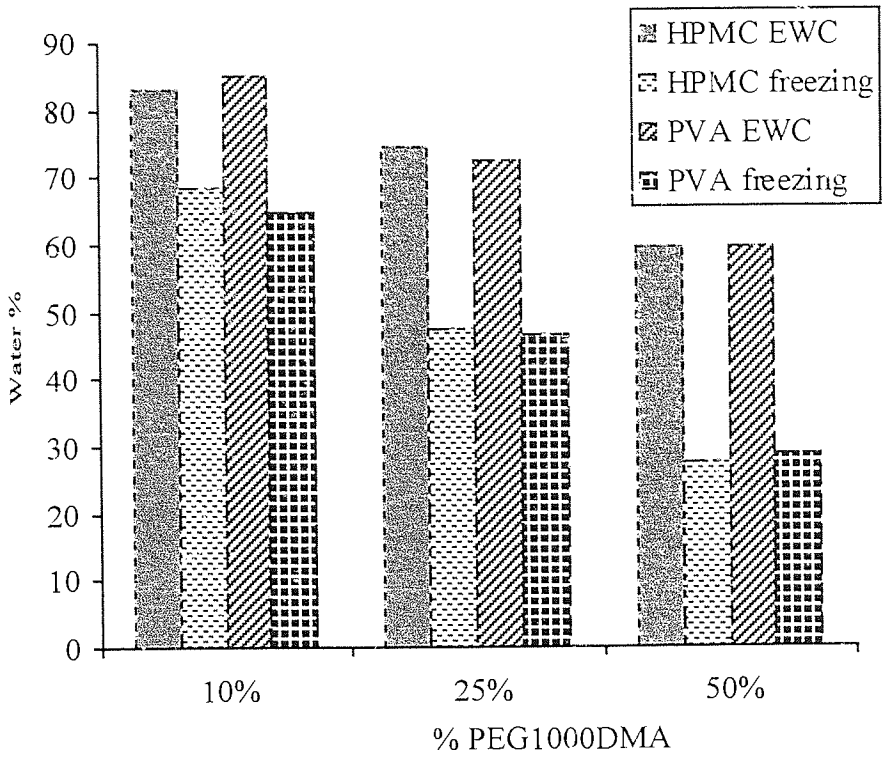

Figure 5.18 Graph to show the effect the amount of PEG1000DMA used has on the freezing water content

Figure 5.18 shows the effect the increase in PEG has on the water binding in the hydrogels. An increase of PEG1000DMA leads to a decrease in both EWC and freezing water. As the crosslink density increases, the amount of bulk water will decrease.

5.6.2 Mechanical properties

The mechanical properties of the hydrogels discussed above were also investigated.

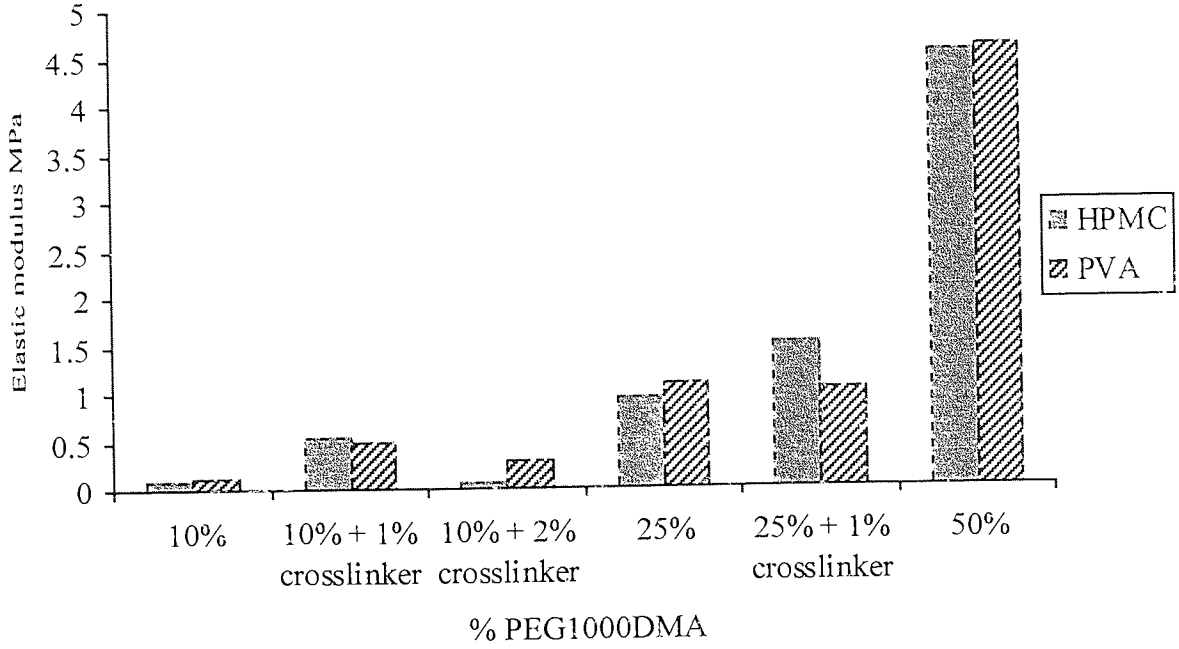

Figure 5.19 Graph to show the effect the amount of PEG1000DMA used has on the elastic modulus

The 10% PEG1000DMA copolymers with PVA, and to a lesser degree the HPMC copolymers, were breaking up as they were placed in the jaws of the tensiometer to test. The errors obtained for these results will therefore be higher as the number of samples tested is lower.

An increase in the freezing water content is associated with a higher EWC, as the pore structure within the polymer network is enhanced. The elastic modulus is decreased as extra crosslinker is added, as the polymer matrix becomes more brittle.

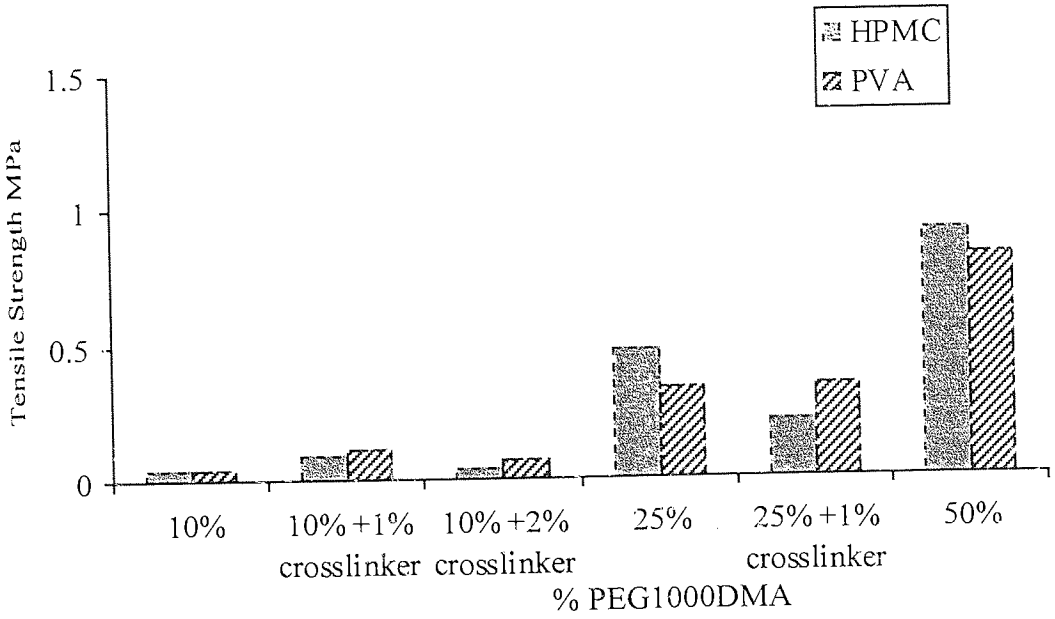

Figure 5.20 Graph to show the effect the amount of PEG1000DMA used has on the tensile strength

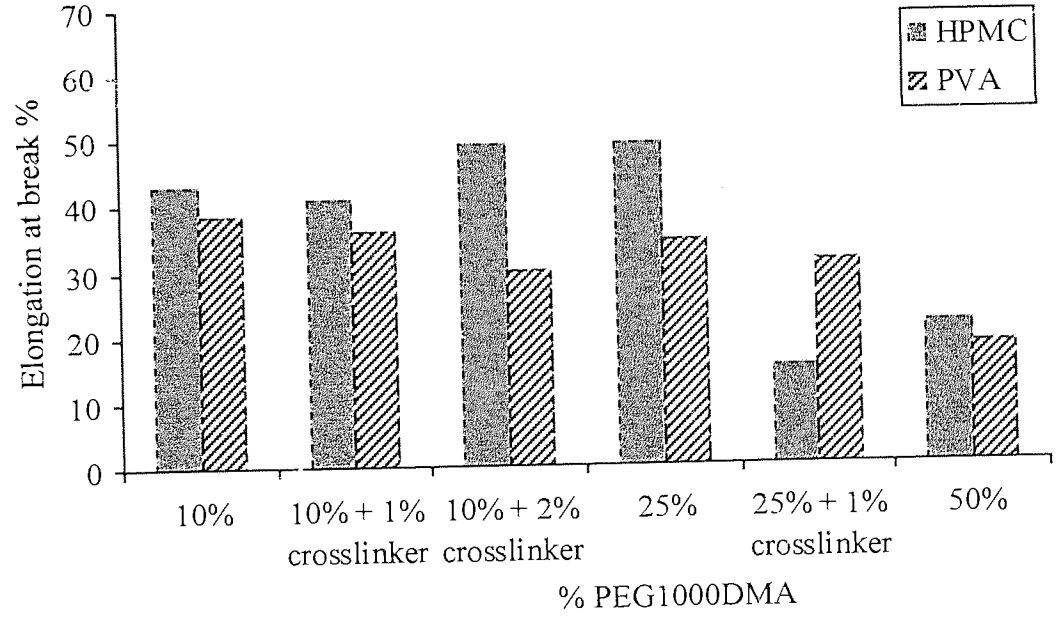

Figure 5.21 Graph to show the effect the amount of PEG1000DMA used has on the elongation at break

Figures 5.19 to 5.21 indicate that as the water content and freezing water decreases, and elastic modulus increases, the tensile strength increases with increasing percentage of PEG1000DMA, and also with the addition of crosslinker. As the amount of freezing water decreases, the elongation at break decreases. The addition of a separate crosslinker has some affect on the hydrogel properties, though the major governing factor is the percentage of PEG1000DMA in the system.

As the percentage of PEG1000DMA increases, the polymers become stiffer and stronger, due to the increase in the crosslink density.

5.7 Effect of Adding a Diluent

As the solutions will be polymerised *in situ* on the ocular surface, water is an essential part of the initial system, which is why attention has centred on the use of concentrated aqueous solutions. Water content has been shown to be related to the ablation rate, so any factors that have an impact on the water content during ablation must be considered. There may be surface evaporation, or the ideal viscosity solution may not give quite high enough water content, so a diluent, glycerol, was investigated which may reduce surface evaporation.

A series of hydrogels were synthesised using 25% (w/w) PEG1000DMA, and 1% (w/w) solutions of PVA (molecular weight 14000) and HPMC (molecular weight 10000). Water in the 1% solutions was gradually replaced with glycerol.

5.7.1 Water binding

The equilibrium and freezing water contents of the hydrogels were investigated. The results are shown in figures 5.22 and 5.23.

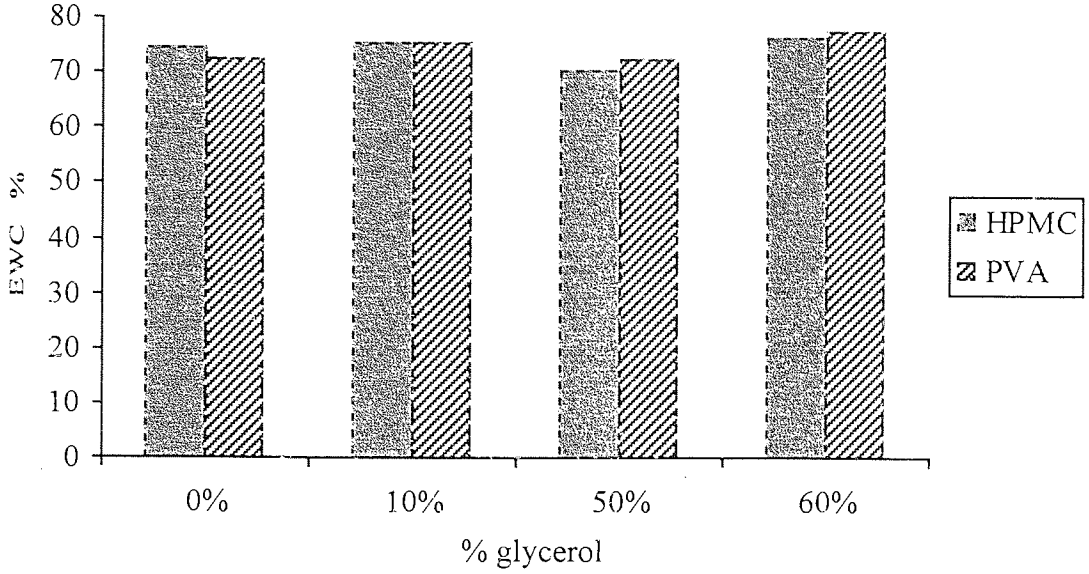

Figure 5.22 Graph to show the effect that using a diluent has on the equilibrium water content

Glycerol is a larger molecule than water, so an increase in the amount of glycerol will result in an increase in water content due to the increase in the pore structure of the polymer matrix. The equilibrium water content is measured by the weight difference between the hydrated and dehydrated states of the membrane following soaking in distilled water. Glycerol has a higher molecular weight than water, so the weight difference will be higher if there is any still left in the system. However, it can be seen that there is only a small change in the water content with the addition of glycerol.

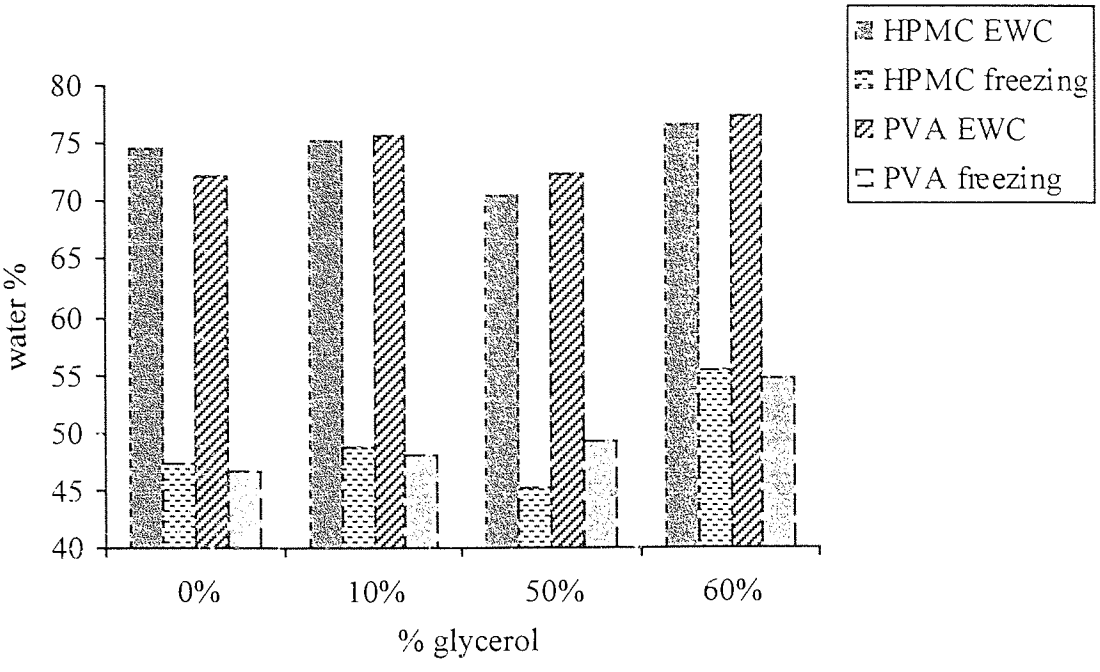

Figure 5.23 Graph to show the effect that using a diluent has on the states of water present in the hydrogel

The amount of free water increases with an increase in equilibrium water content. Glycerol is a trihydric alcohol, so water will be attracted to form hydrogen bonds, though not to the polymer backbone.

5.7.2 Mechanical properties

The mechanical properties were investigated, to study the effect of the diluent. The results are shown in figures 5.24 to 5.26.

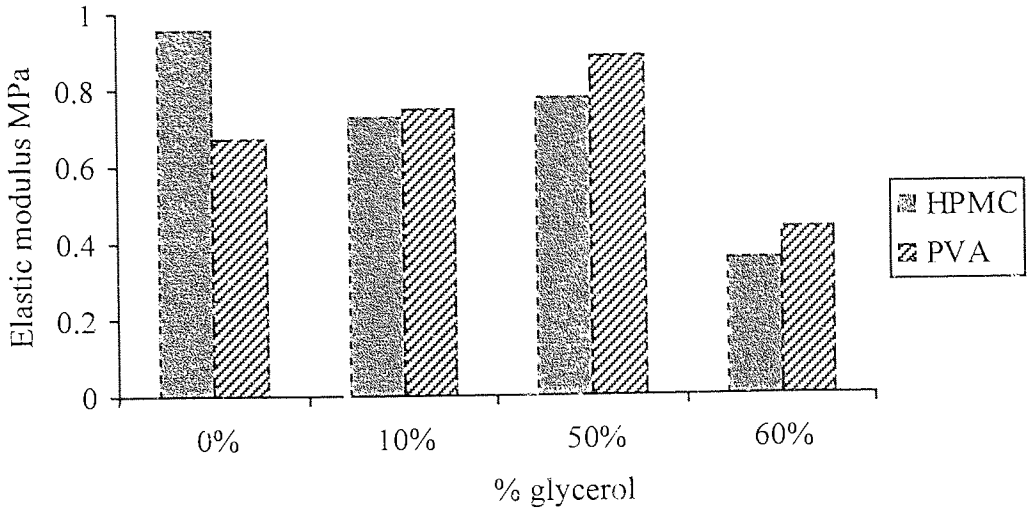

Figure 5.24 Graph to show the effect that using a diluent has on the elastic modulus

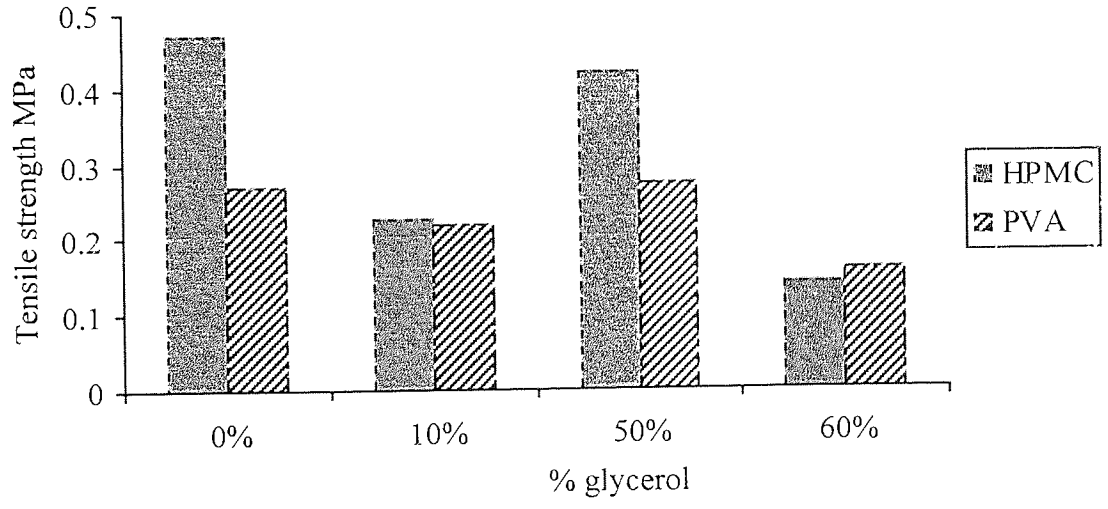

Figure 5.25 Graph to show the effect that using a diluent has on the tensile strength

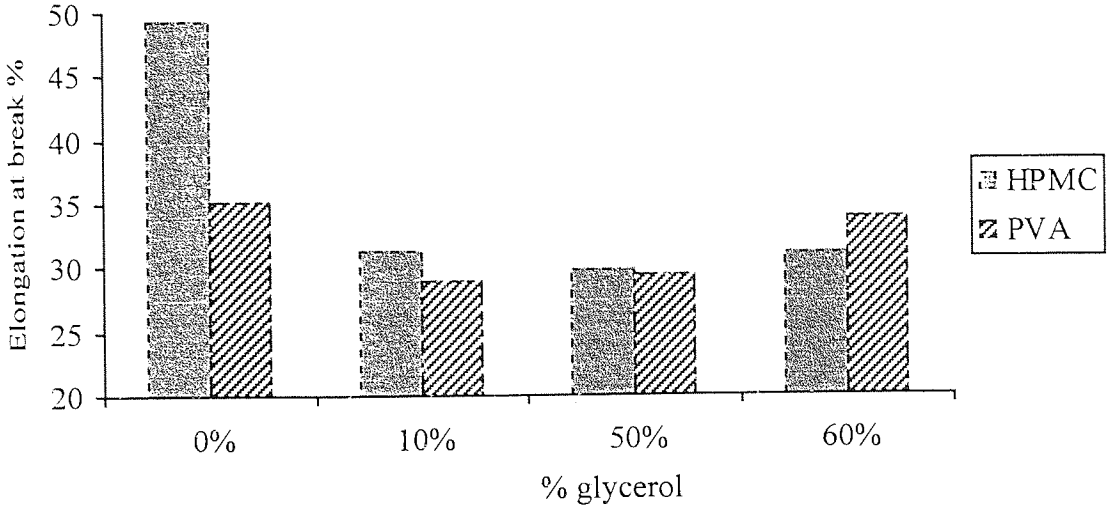

Figure 5.26 Graph to show the effect that using a diluent has on the elongation at break

The general trend for the results shown above shows that as the water content increases, the elastic modulus, tensile strength and elongation at break all decrease, though the changes are small. Glycerol is a larger molecule than water, so as the percentage of glycerol increases, the spaces between the polymer chains will increase resulting in a more elastic, flexible hydrogel. The incorporation of glycerol within the polymer network may lead to irregularities in the distribution of glycerol and water in the matrix, with some regions of high water and others of high glycerol. This may account for the mechanical properties not showing a smooth trend as the glycerol content is increased.

5.8 Discussion

This chapter is concerned with developing a hydrogel system that can be placed on the eye and polymerised prior to laser ablation. The results have demonstrated that hydrogel properties can be manipulated to give a variety of water contents and mechanical properties. Several considerations must be taken into account when selecting the most suitable material for use as a temporary prosthesis prior to laser ablation. The gel must be of a suitable viscosity to fill any irregularities on the corneal surface. This

can be altered by varying the molecular weight of the preformed polymer, or using different percentages of the polymer in the aqueous solution. It can also be changed by the addition of a diluent. There must also be no allergic response from the eye as the solution is placed on the surface, and no adverse affects as the material is polymerised.

One important characteristic that the materials must display are that the ablation rates should be similar to that of the cornea. Ablation rate has been found to be related to the equilibrium water content of the system. In hydrogels, the EWC plays an important role in governing the other properties associated with that hydrogel. Initial laser ablation studies will give an indication of other factors that may influence the ablative characteristics of the hydrogel. This in turn will help identify the water content, freezing water content and mechanical requirements of the hydrogel that gives the best correlation to that of the cornea in terms of the rate of ablation. The crosslink density required will give an indication of the number of photopolymerisable groups that are needed in the system. If the level of PEG required to give the ideal crosslink density is high, modification of the preformed polymer backbone could be used to introduce vinyl groups for polymerisation. This would also be beneficial in an attempt to reduce polymerisation time once the system is placed on the ocular surface. Work must be undertaken to reduce the polymerisation time to the minimum possible, to seconds rather than minutes.

A suitable mould and UV source needs to be used so that the hydrogel can be investigated using a similar set-up to that which would be used during the surgical procedure. This would allow for the volume and viscosity requirements of the starting system to be investigated, along with analysing the suitability of the initiator used. Temperature control and evaporation during the surgical procedure also need to be considered, as does the generation of debris during ablation.

The UV source is held at an angle to the cornea so that there is minimal damage to the cornea. A Tearscope is being investigated as the source of UV radiation. This has been employed in optometry to examine the retina, so the effects the light has on the eye has been studied. Initial ablation studies have involved Focus Dailies, which are a functionalised PVA based soft contact lenses, with a water content of 69%, with the aim that these would give similar ablation rates as both the synthetic temporary prostheses and the cornea, and so could be used as the mould. This would then give a smooth surface of a known curvature, which could then be ablated quickly. The ablation rate achieved for the Dailies was 61μm per pulse.

CHAPTER 6

Development of Fluorescence Spectrophotometry as a Technique for the Analysis of Contact Lenses

Several analytical techniques have been utilised to study the interaction of biological species with synthetic materials[53,54,57-59]. This chapter addresses the development of one technique, namely fluorescence spectroscopy, considering both the theory and the instrumentation required to analyse the levels of protein and lipid deposition on contact lenses. Fluorescence spectroscopy enables the surface of contact lenses to be analysed, and is a sensitive and non-destructive technique. When used in conjunction with other analytical techniques, an overall picture of the processes involved in spoilation can be studied.

6.1 Introduction

The initial adsorption of a photon by a molecule takes that molecule into an electronically excited state which will not be its most stable state. In order to return to its stable state the excitation energy must be released. This can be achieved by several methods. Luminescence is the process by which a molecule returns to its ground state by the emission of photons from an excited electronic state. This can be further divided into phosphorescence and fluorescence, depending upon the nature of the ground and excited states[193-199].

Phosphorescence is the emission resulting from a transition between states of different multiplicity, normally a triplet excited state to a singlet ground state, due to intersystem crossing. This transition is quantum mechanically 'forbidden', as it requires a change in spin orientation. Hence, the return to the ground state is slow, resulting in long decay times (msec to sec).

In comparison, fluorescence is the emission resulting from the transition involving the return of a paired electron to its ground state. These transitions are 'allowed', so the rates of emission are high with fluorescent lifetimes around 10^{-8} sec (or 10 nsec). The lifetime of the fluorophore is defined as the average time the fluorophore remains in its excited state. The emitted photon is at a longer wavelength, lower frequency, to the

adsorbed photon i.e. can adsorb in UV and emit in visible as observed by Stokes in 1852 (Stokes shift).

Fluorescence and phosphorescence are competitive pathways.

The adsorption and emission on photons can be described schematically using the Jablonski diagram (figure 6.1).

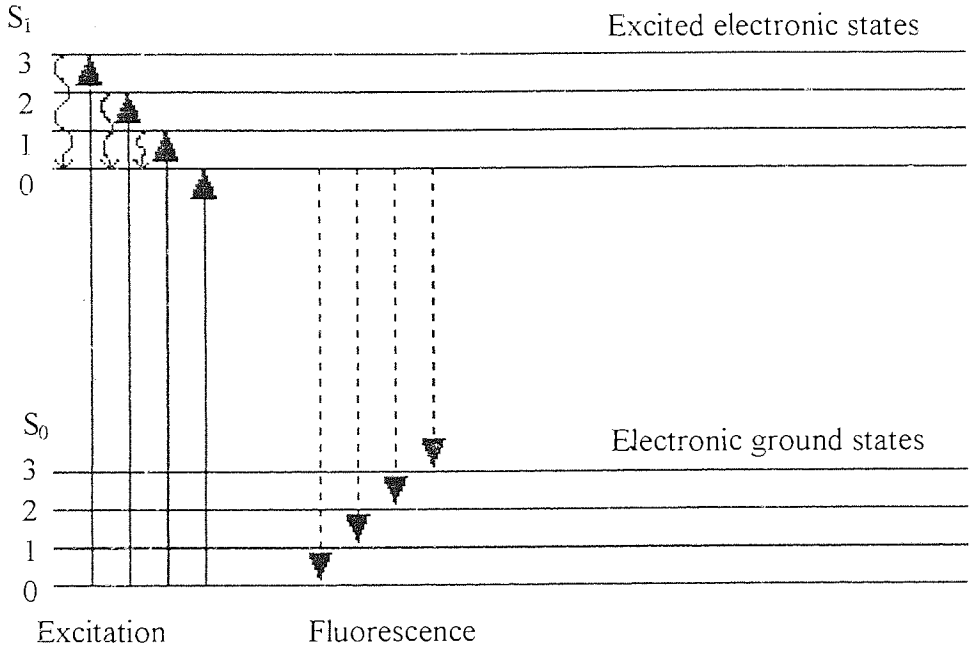

Figure 6.1 Jablonski Diagram

The ground and first excited electronic states are shown as S_0 and S_1 respectively. At each of these electronic levels, the fluorophore can exist in a number of vibrational energy levels, depicted as 0,1,2,3. Transitions between the various electronic levels are vertical, illustrating the instantaneous nature of light adsorption. The whole process takes approximately 10^{-15} seconds, which is too short a time for any significant displacement of the nuclei, in accordance with the Franck-Condon principle[196].

The initial adsorption of energy takes the molecule to an excited electronic state, which is often coupled with an excited vibrational state. The excited molecule is then subjected to collisions with surrounding molecules which can remove vibrational energy from the excited molecule by a process termed vibrational relaxation. This leads to the excited molecule being reduced to its lowest vibrational state. The excited molecule returns to S_0, usually within 10^{-8} seconds, by emitting light (fluorescence) or by a non-radiative transition. Fluorescence occurs at a lower frequency than the absorbed light, as the radiation is emitted after some vibrational energy has been lost to the surroundings.

6.2 Absorbance

When light comes into contact with a material, two things can happen. The light can either pass straight through with no absorption taking place, or be partly or wholly absorbed by the material[195]. The absorbance of light is related to the amount of light transmitted by the sample. The energy, E, of the photon absorbed or emitted, and therefore the frequency, ν, of the radiation emitted or absorbed are shown by the equation:

$$E = h\nu \qquad (6.1)$$

This is related to the wavelength λ as

$$c = \lambda\nu \qquad (6.2)$$

where c is the speed of light. Therefore

$$E = h\, c/\lambda \qquad (6.3)$$

where h is the Planck's constant = 6.63×10^{-34} J s

$$\Delta E = E_{excited} - E_{initial} = h\, c/\lambda = h\nu \qquad (6.4)$$

$$A = \log_{10} (I_o/I_t) \qquad (6.5)$$

where A is absorbance, I_o intensity of light arriving at the detector in the absence of the sample, and I_t the intensity of light reaching the detector in the presence of the sample. This can be written as

$$A = \log_{10} (T) \qquad (6.6)$$

where T is transmittance.

6.3 Fluorescent Intensity

The relationship between fluorescent intensity of a dilute solution and its concentration can be derived from the Beer-Lambert Law of absorption[199]. This considers the reduction in intensity, dI, that occurs when light passes through a layer of thickness, dx, containing an absorbing species, J, at a molar concentration, [J], is proportional to the thickness of the layer, the concentration, and the incident intensity because the rate of stimulated absorption is proportional to the intensity. Therefore:

$$dI = -\kappa[J]I\,dx \qquad (6.7)$$

where κ is the proportionality coefficient. Similarly

$$d \ln I = -\kappa[J]I\,dx \qquad (6.8)$$

Therefore for a sample of thickness l, the intensity I' that emerges from the sample where the incident intensity is I is given in the Beer-Lambert law:

$$I' = Ie^{-\kappa[J]l} \qquad (6.9)$$

and is often expressed as

$$I' = I\,10^{-\kappa[J]l} \qquad (6.10)$$

where $\kappa = \varepsilon \ln 10 = 2.303\varepsilon$, so

$$\lg (I' / I) = - \varepsilon[J]l \qquad (6.11)$$

ε is the molar absorption coefficient and optical density A is given by

$$A = \varepsilon[J]l \qquad (6.12)$$

That is, the absorbance is proportional to the concentration of the absorbing compound in solution.

Theoretically, the more intense the source is, the higher the observed fluorescent intensity will be. However, a very intense source can cause photodecomposition in the sample. To overcome this, either a more moderate source needs to be used, or the sample should only be exposed to the incident light for a very short time. The π-π^* transitions in aromatic compounds display relatively high intensities.

6.4 Quenching

Quenching of fluorescence is any process that decreases the fluorescent intensity[195]. Several processes can lead to quenching[201] including excited state reactions, energy transfer, complex formation and collisions, and they can be described as static or dynamic quenching. Collisional quenching occurs when a fluorescent molecule in an excited state collides with a quencher, transferring energy, with the result that intersystem crossing occurs[202,203]. Molecular oxygen is one of the most widely encountered quenchers. In its ground electronic state, O_2 is a triplet species. The excited fluorophore is a singlet, but when this collides with the oxygen, the fluorophore becomes a triplet, and the oxygen a singlet. The excited oxygen molecules quickly return to the ground triplet state upon further collisions or interaction with the solvent. Collisional quenching of fluorescence is described by the Stern-Volmer equation[193]:

$$F_o / F = 1 + k_q \tau_o [Q] = 1 + K_D [Q] \qquad (6.13)$$

where F_o and F are the fluorescence intensities in the absence and presence of a quencher, k_q is the bimolecular quenching constant, τ_o the lifetime of the fluorophore in the absence of a quencher, [Q] the concentration of quencher and $K_D = k_q \tau_o$ is the Stern-Volmer quenching constant.

A combination of collisional and static quenching can explain why the fluorescence observed for a macromolecule is often different from the sum of the emissions of the component fluorophores. Protein fluorescence is rarely the sum of the emissions from the relative amounts of the three fluorescent amino acid residues present in the macromolecule. Some residues may be subjected to static quenching, that is through interactions between the fluorophore, and other parts of the folded protein chain, or protected inside the folded macromolecule from any collisional quenching.

6.5 Characteristics of fluorescence spectra[193,195]

6.5.1 Secondary peaks

Second-order scatter peaks arise due to the fact that diffraction gratings pass harmonics of the wavelength of interest, so a grating monochromator selecting wavelength λ also passes λ/2, λ/4 etc. For a spectrum recorded using an excitation wavelength of 280nm, a smaller peak will be observed at 560nm, which is the second order peak from the 280nm excitation.

6.5.2 Stokes shift

Except for atoms in the vapour phase, there is a shift to a lower wavelength, that is a loss of energy, for the emission radiation relative to the absorption. This was first observed by Stokes and is referred to as the Stokes shift. One common cause of this is

the rapid decay to the lowest vibrational level. At high temperatures in dilute gases, an anti-Stokes shift may be observed, where the emitted wavelength is shorter than the absorption wavelength.

6.5.3 Light scattering

Rayleigh scattering is light scattering by fine dust or suspensions of particles. The scattering contribution can be calculated as it varies as λ^{-4}.

The scattering of light by molecules in which there is a change of frequency, due to the molecules gaining or losing vibrational energy as a result of transitions between vibrational or rotational levels is known as the Raman effect.

Fluorescence is emitted in all directions. Use is made of this by observing fluorescence at 90° to the incident light to eliminate the effects of stray light.

6.5.4 Extrinsic factors

Fluorescence spectra are influenced by external factors[193]. The time the sample is exposed to the radiation source will have an effect due to the lifetime of the fluorophore, quenching possibilities and may also increase the temperature at which the measurements are being carried out. The pH also will influence the spectra as ionicity will increase the delocalisation of the electron distribution in a molecule.

6.6 Types of Fluorophore

Substances that display significant fluorescence generally possess delocalised π electrons, usually in the form of conjugated double bonds, and are known as fluorophores[199]. There are two types of fluorophore, intrinsic and extrinsic. Intrinsic fluorophores are contained within the molecule, for example proteins and quinine. Extrinsic fluorophores are added to a system that does not possess a natural

fluorophore, for example fluorescent tagging of proteins can be achieved by the use of fluorescein.

Each fluorophore has a characteristic adsorption and emission wavelength, some of which are shown in table 6.1. FITC and TRITC are fluorescent tags, and are fluorescein isothiocyanate and tetramethyl rhodamine isothiocyanate respectively.

Fluorophore	Excitation wavelength (nm)	Emission wavelength (nm)
Tryptophan	280	354
Tyrosine	280	308
Phenylalanine	280	282
Riboflavin	450	515
FITC	490 - 495	517
TRITC	550	580

Table 6.1 Characteristic excitation and emission wavelengths for several fluorophores

6.7 Protein and Lipid Fluorescence

Fluorescence spectrometry has been used in this work to study the deposition of proteins and lipids from the tear film onto soft contact lenses[204,205]. This can be carried out as both proteins and lipids contain intrinsic fluorophores. That is they posses conjugated double bonds and delocalised electrons.

There are three fluorescent amino acids present in proteins[202,206], each of which contains a structure based on the indole ring. Tryptophan is the most highly fluorescent residue and generally accounts for the vast majority of the fluorescence observed from proteins. This natural fluorophore is highly sensitive to the polarity of the surrounding environment. Fluorescent lifetimes of the tryptophan residue are in the range of 1 to 6 nanoseconds. Tyrosine is highly fluorescent in solution, though generally weaker in

proteins. Denaturation of proteins often results in increased tyrosine emission. The third amino acid fluorophore is phenylalanine, which exhibits weak fluorescence in comparison to both tryptophan and tyrosine. Proteins adsorb radiation at 280nm, and the fluorescence emission maxima occurs in the region 320 to 360 nm[204].

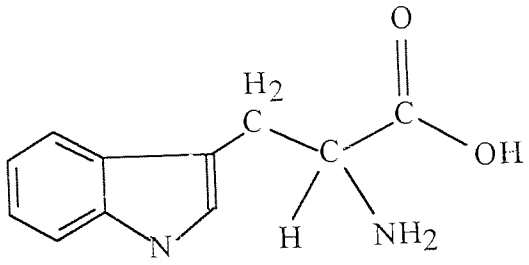

Tryptophan

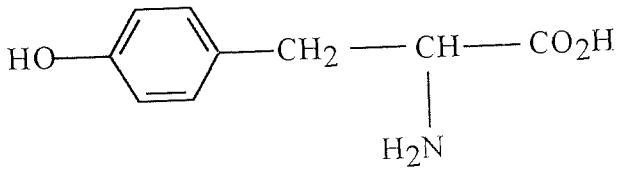

Tyrosine

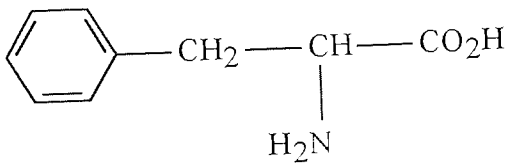

Phenylalanine

Figure 6.2 Structures of the three fluorescent amino acids present in proteins

Many of the fatty acids and lipids present in the tear film contain conjugated double bonds[204,207,208]. These would be expected to fluoresce, though at a very low level which

would require a sensitive instrument to observe the resulting spectra. Several workers detect lipid fluorescence through the use of extrinsic labels[209,210]. Fluorescence microscopy studies have previously been used to study white spots on the surface of contact lenses[25,204]. Distinctive autofluorescent patterns were observed using an excitation wavelength of 360nm. White spots are predominantly lipoidal in composition, so fluorescence spectroscopy was investigated as a technique for studying the deposition of lipids on contact lenses. Few other workers use the intrinsic fluorescence of lipids to study them[207].

Fluorescence spectroscopy is a technique enabling the surface of materials to be investigated. It is used as it is a quick and easy, highly sensitive, reproducible and non-destructive method for assessing the interaction of proteins and lipids with synthetic materials prior to further destructive analysis.

6.7.1 Protein Mobility

Small proteins, especially lysozyme, will not remain static in solution[211]. Proteins will move into solution and penetrate into the lens matrix altering the concentration and conformation at the surface given time. This mobility must be taken into account when the storage solution, length of time the lens is stored prior to testing, and the solution the spectra is run in, are considered. Proteins will also denature which will effect the structure of the protein.

There may be a degree of 'masking' of fluorescent species involved at the surface[204]. Fluorescence is observed from the surface of the contact lenses, as quenching prevents the light from entering the matrix of the polymer with sufficient energy to cause excitation of the molecules and so bring about fluorescence. Fluorescent material is being laid upon a fluorescent material having the effect that the initial layer is masked. Thus, if the protein concentration at the surface is high, the weakly fluorescent lipid may not be detected, as it will be masked to some extent.

6.8 Instrumentation

A modified Hitachi F-4500 fluorescence spectrophotometer was used to obtain the spectra. A schematic diagram (figure 6.3) shows the major components of the spectrophotometer.

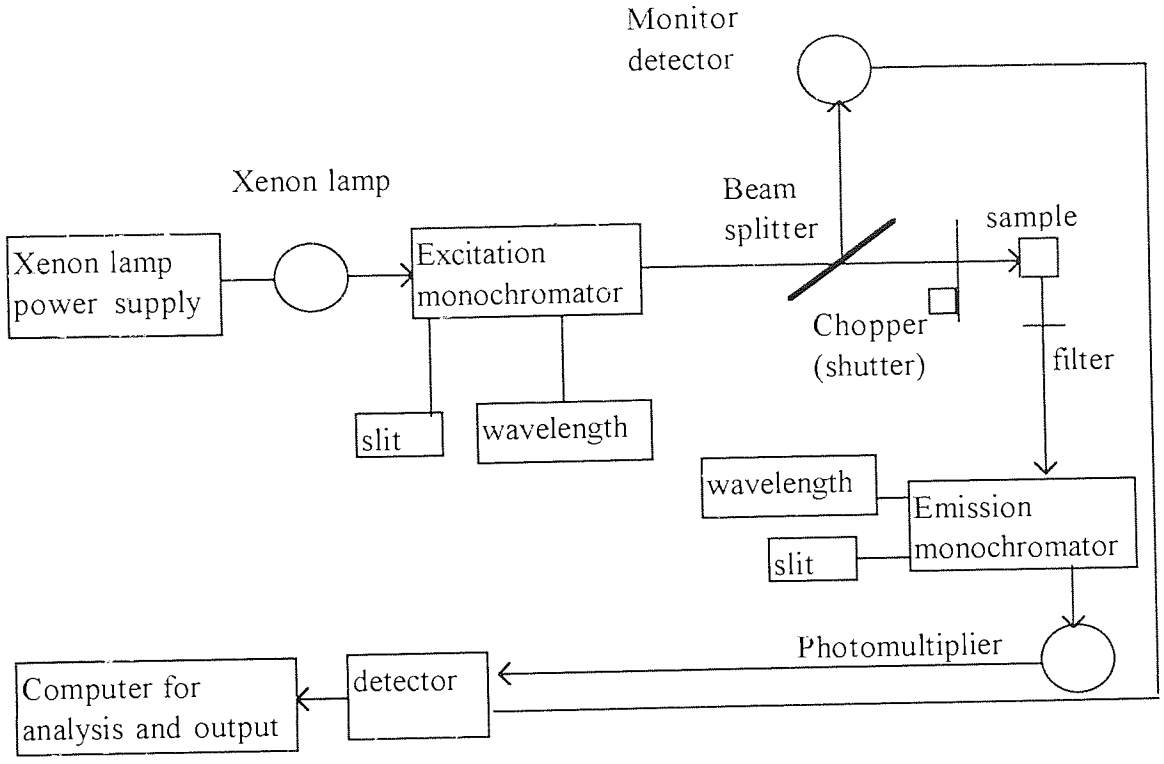

Figure 6.3 Schematic diagram of the major components of a fluorescence spectrophotometer

6.8.1 Components of A Spectrophotometer

A basic fluorescence spectrophotometer requires a light source, monochromators to select the excitation and emission wavelengths, a detector and an output.

The fluorescence spectrophotometer is interfaced to a computer which is programmed by Microsoft Windows™ software enabling the operating parameters to be carefully controlled.

The intense 150 watt xenon lamp provides light energy over the entire 200-900nm wavelength range covered by the spectrophotometer. The light passes through a monochromator for the selection of the excitation wavelength, giving a slit width in mm. Light passing through monochromator is proportional to the slit width squared. At larger slit widths, the signal levels are increased and so a higher signal to noise ratio is observed. The transmission efficiency is a function of the wavelength. The optical arrangement in the fluorescence spectrophotometer means that the light travels through a complex set of mirrors and diffraction gratings before passing through the sample. The Hitachi machine uses a horizontal excitation beam of light. This increases the sensitivity by illuminating more of the sample with the excitation beam and reduces the volume of sample required, which for a 10mm square cuvette is 0.6mL For other instruments it is usually greater than 2mL.

To avoid detecting the incident beam, and to minimise interference from scattered light, use is made of the fact that fluorescence is emitted in all directions. Thus, the fluorescence emission is detected at 90^0 to the excitation beam. The light then passes through another monochromator for analysis of the emission wavelength and finally falls onto a photosensitive device, the photomultiplier tube (PMT). A PMT is regarded as a source of current, which is proportional to the light intensity, and consists of a photocathode, which is a thin film of metal, and a series of dynodes which are the amplification stages. The incident photon ejects electrons from the photosensitive surface, the electrons are accelerated by a potential difference and ejects a shower of electrons where it strikes a screen. Each original photon is converted into a cascade of electrons, which is converted into a current in an external circuit, thus amplifying the fluorescent signal. The data is sent to the computer for display and analysis.

The shutter control mechanism reduces the amount of time the sample is exposed to the radiation, a factor which needs to be considered when photolabile species are under

examination. A filter is also present to remove any incident light at a wavelength below 280nm.

6.9 Analysis of Samples

Fluorescence spectrophotometry was used to study the emission spectra obtained from contact lenses and their storage and cleaning solutions. Previous work carried out in the group[25,204] had used an Aminco Bowman Spectrophotometer. Calibration of this machine had been carried out to establish that protein fluorescence could be monitored using an excitation wavelength of 280nm and lipid fluorescence at 360nm, and quantification of the levels of fluorescence that were obtained. Calibration had involved running spectra of lenses that had been spoilt with proteins and lipids, with the material then being extracted and the species identified using HPLC. Spectra were then run on both the Aminco Bowman and Hitachi machines, to ensure that the parameters used on the Hitachi spectrophotometer gave consistent results to those obtained previously, and that the data collected by both machines was comparable.

A specially designed quartz cylindrical cell was used. This allowed for the reproducible alignment of both the cuvette and the lens within the cuvette to be obtained. To eliminate the effects that differences in the quartz surface would have on the spectra obtained, initial experiments were carried out to determine the position of the cuvette that gave the minimum contribution to the final spectra. A notch was taken out of the top of the cuvette to mark it so that each time a spectrum was run, this notch was lined up to the same position in the sample holder. Care was always taken to ensure that the cuvette was clean and dry before any sample was examined.

When contact lenses were examined, care was taken to ensure that the relative position of the lens in the cuvette was kept constant. Again, initial experiments were carried out to determine the placement of the lens that gave a maximum signal from the spoilt

surface. This was achieved by pushing the lens to the bottom of the cuvette, making sure it was in contact with the side of the cuvette, noting which side of the lens would be examined, and aligning it in relation to the notch. Care was taken to ensure that the excitation beam only passed through the sample once, and this was not via the edge of the lens. The cuvette was kept clean throughout the work, with special care taken to remove any finger lipid from the outer surface of the cuvette and prevent the introduction of any air bubbles to the solution or attaching to the contact lens.

With the Hitachi spectrophotofluorimeter that was used in this work, single wavelength spectra and three dimensional spectra can be obtained. Standard operating parameters were used in each case, these included control of the excitation and emission slit widths and the scanning time. Examples of the spectra obtained are shown in figures 6.4 to 6.6.

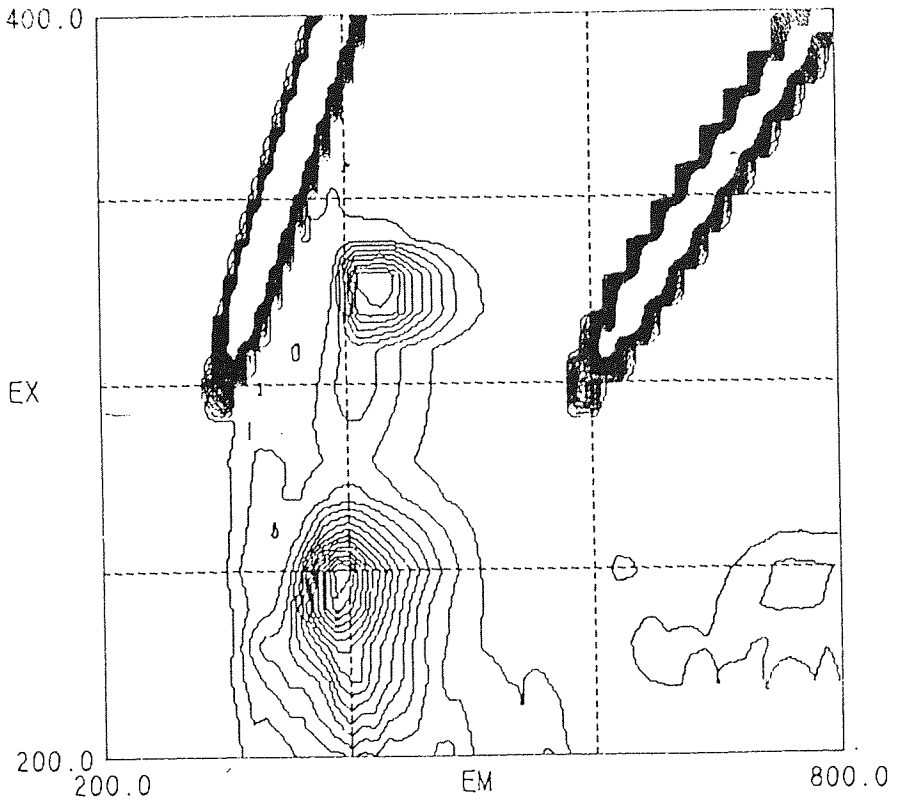

Figure 6.4 An example of a three dimensional fluorescence spectrum of an unworn Acuvue contact lens

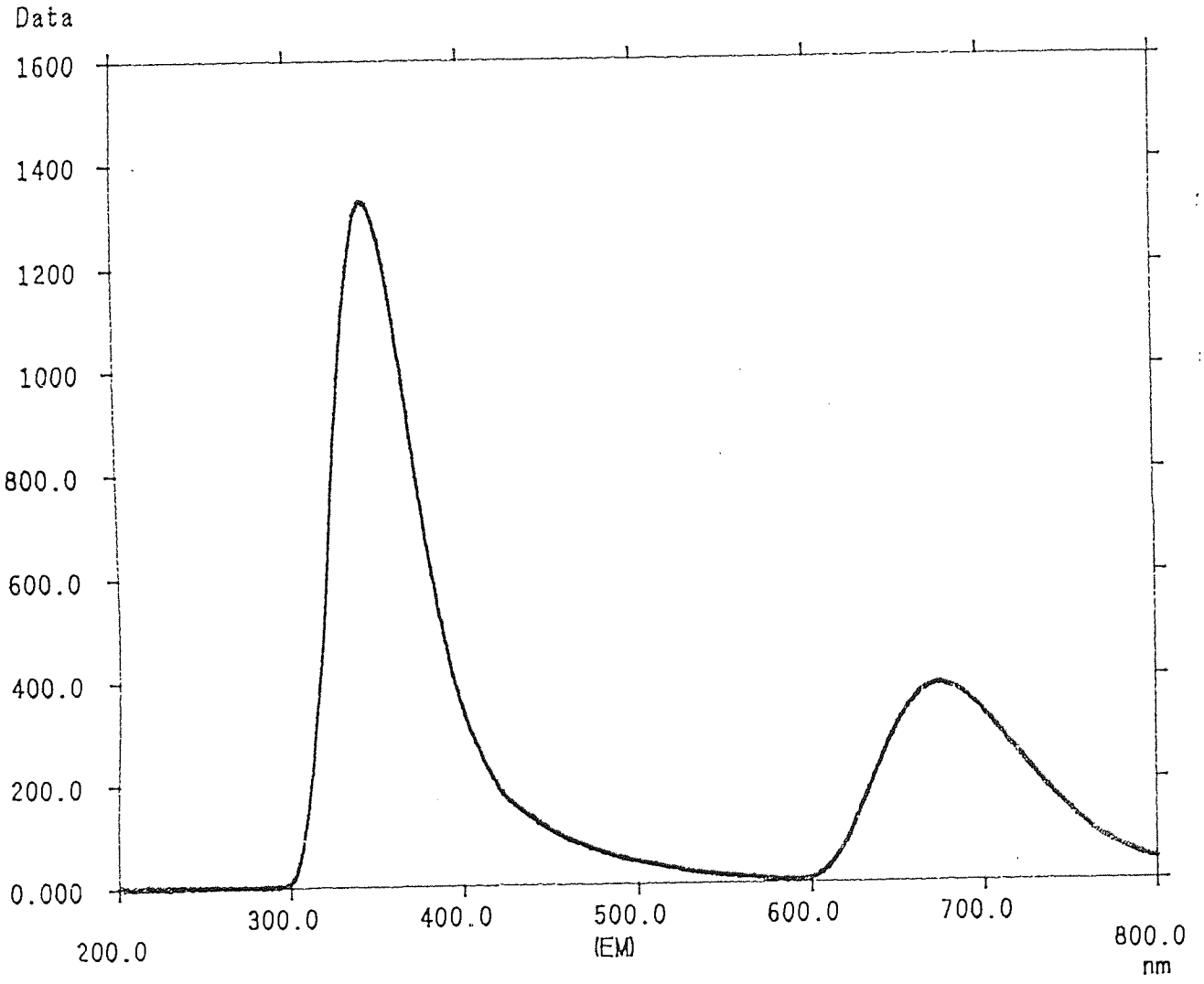

Figure 6.5 An example of a fluorescence spectrum of a worn Acuvue contact lens recorded at an excitation wavelength of 280nm

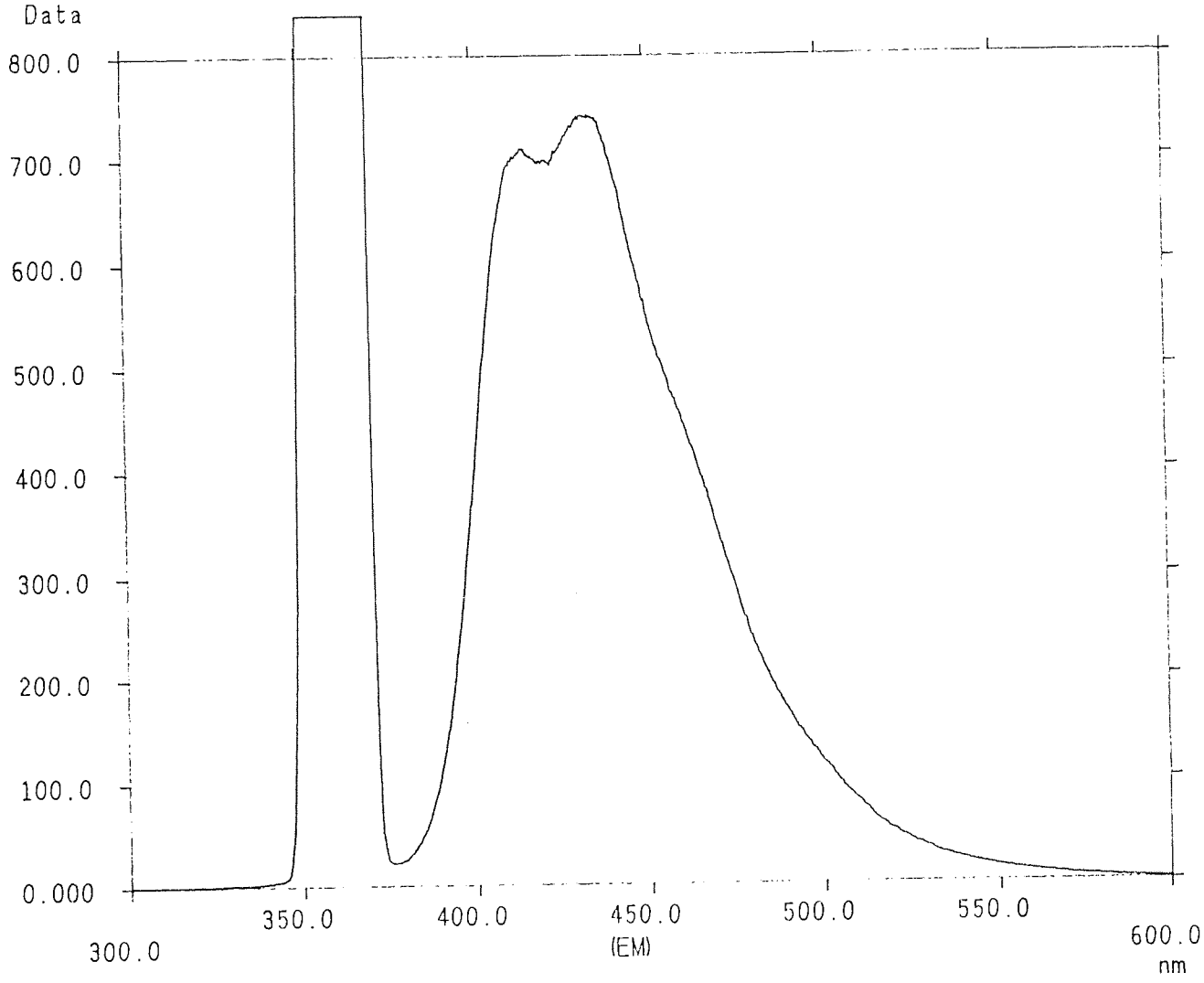

Figure 6.6 An example of a fluorescence spectrum of a worn Medalist 66 contact lens recorded at an excitation wavelength of 360nm

6.10 Recording spectra

An excitation wavelength of 280nm was used for protein analysis, and 360nm for lipids. The cuvette was cleaned thoroughly, and filled with enough distilled water to cover the

contact lens. The contact lens was then placed in the cuvette, ensuring that it was aligned correctly and that no air bubbles were present. Standard operating parameters were used, with the excitation wavelength the only parameter that needed to be altered during the analysis of the lenses. The cuvette was placed into the sample compartment of the fluorimeter, again ensuring that it was aligned correctly. The excitation wavelength was selected at 280nm, and the spectra collected. The excitation was then changed to 360nm, and the second spectra collected. Emission from 250 to 550nm was recorded in both cases. The spectra were then analysed, noting the maximum peak height, and the wavelength at which it occurred. The sample was removed, and the cuvette cleaned prior to further use. Storage solutions were tested using the same procedure.

The spectra obtained for all the contact lenses examined were collected using the same procedure, though many variables must be taken into account. In all cases the standard operating parameters were used, along with the same cuvette. The placement of the cuvette in the sample compartment was marked so that this could be kept as consistent as possible, though slight variations will occur. The major problem is quenching, from collisions and oxygen in the system The technique is very sensitive, so differences could be observed in the spectra if a contact lens had been in the cuvette for a longer period of time than it normally takes to run the spectra. This could be due both to quenching and protein mobility. The positioning of the contact lens in the cuvette could not always be kept constant. The lens was placed against the side of the cuvette, and needed to be in close contact with it to maintain a consistent pathlength for the sample cell. The lens may also move during the time in the cuvette. Contamination of the cuvette, through finger lipid on the cuvette or insufficient cleaning would lead to higher recorded values than expected.

The use of this sensitive technique as an analytical technique to study the deposition of proteins and lipids on the surfaces of contact lenses is demonstrated in the following

chapter. The results obtained from clinically controlled studies on the factors affecting spoilation are presented. The sensitivity, and unique characteristics of the technique are demonstrated in the results.

CHAPTER 7

Ex-vivo Clinical Studies of Contact Lenses

7.1 Introduction

Hydrogels have found widespread use as soft contact lens materials since their introduction in the 1960's, with well over 100 patents appearing in this area following Wichterle's original work[14]. This has lead to developments in both lens materials, care regimens and modality of wear. Clinical investigations were undertaken to consider the various factors that contribute to the type and degree of spoilation on different hydrogel lenses. The lenses were assessed using fluorescence spectrophotometry. The previous chapter described this technique.

In this work, fluorescence spectroscopy is used to analyse the protein and lipid deposition on the surfaces of contact lenses. It is a non-destructive, sensitive method, which when used in conjunction with other techniques enables a full picture of the processes involved in deposition to be assessed. Fluorescence spectroscopy allows the surface of the lenses to be examined. This would be extremely difficult to ascertain by any other technique. When used in conjunction with UV spectroscopy, the amount of protein on the surface and the total amount of protein within the lens matrix can be examined.

Spoilation is dependent on many factors, several of which are discussed in chapter 1. The sensitivity of fluorescence spectroscopy means that many variables can be considered in this chapter. These include patient to patient differences, right eye to left eye variations for the same patient, the water content, composition and ionicity of the lens material, the wear time for the lens and the effect of the cleaning regime. Extrinsic factors must also be taken into account.

7.2 Clinical Protocol

Clinical trials were set up to investigate various factors that contribute to protein and lipid deposition on soft contact lenses. This involved different lenses, length of time in

the eye and cleaning regimes. All of the clinical work was carried out by Lyndon Jones. Upon completion of the required wear schedule for each lens, the lenses were removed with plastic-tipped tweezers to prevent any transfer of finger lipid, stored in sterile saline and refrigerated prior to analysis.

7.3 *Ex-vivo* Analysis

Each lens was examined in the same way. Proteinaceous and lipoidal deposits were analysed by fluorescence spectrophotometry, as described in chapter 6. An excitation wavelength of 280nm was used for proteins and 360nm the excitation wavelength for lipids. The peak heights from the emission spectra were studied to indicate the relative amounts of fluorescence obtained from each lens. Fluorescence is a non-destructive technique, so this was carried out prior to any further non-destructive analysis, such as UV spectroscopy, and destructive techniques, for example, HPLC and electrophoresis, the results of which are beyond the scope of this thesis.

Several studies were carried out to investigate the effects of different lens materials, duration of wear and cleaning regimens. All of the worn lenses were examined using fluorescence spectrophotometry to ascertain the level of surface deposition of both lipoidal and proteinaceous species.

Contact lenses have been classified in several ways, depending upon their chemical composition, ionicity and water content. This was described in chapter 1, along with contact lens manufacture, factors affecting spoilation and the composition of the tear film. Several factors that affect the level and type of deposition on soft contact lenses were investigated.

7.4 Long term use of Group II lenses

Two high water content hydrogel lenses were tested using twelve patients in a study to investigate the effect the material has on the level of deposition. It is well known that increasing the water content and/or the ionicity of the lens material greatly enhances the protein deposition[212] but there is little information available on the effect of neutral hydrophilic groups on deposition. The two lenses examined in this study were high water content, non-ionic lenses, classified by the FDA as group II, as seen in table 7.1. The materials were carefully chosen to ensure that the equilibrium water contents were similar, and that one of the constituents remained constant.

Lens	Lunelle ES70	Excelens
EWC	70	64
Monomers	MMA + NVP	MMA + PVA
Manufacturer	Essilor	CIBA-Vision
FDA Group	II	II
USAN	-	Atlafilcon
Manufacture	Lathed	Moulded

Table 7.1 Characteristics of Lunelle ES70 and Excelens contact lenses

7.4.1 Methodology

The patients wore each lens type for six months, cleaning the lens each day with an isopropyl alcohol based surfactant cleaner (CIBA-Vision 'Miraflow'), rinsing in non-preserved saline and disinfecting overnight with a two-step 3% hydrogen peroxide system (CIBA-Vision '10:10'). The following morning the lenses were neutralised for at least twenty minutes with sodium pyruvate before insertion. No enzyme tablets or rewetting drops were used at any time during the study. The lenses were collected at the completion of the six month wear period and stored in saline prior to further laboratory based analysis.

7.4.2 Results

The results obtained by fluorescence spectroscopy for each patient are shown graphically in figures 7.1 and 7.2. The mean protein and lipid deposition for each lens type are shown in figures 7.3 and 7.4.

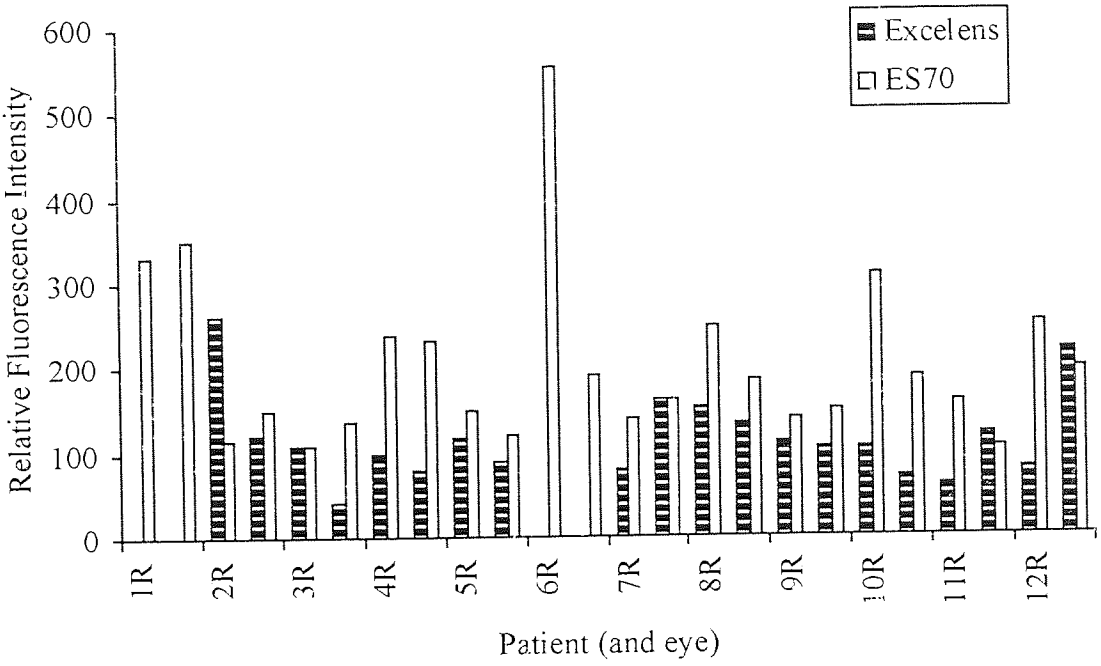

Figure 7.1 Protein deposition on two group II contact lenses by fluorescence spectrophotometry

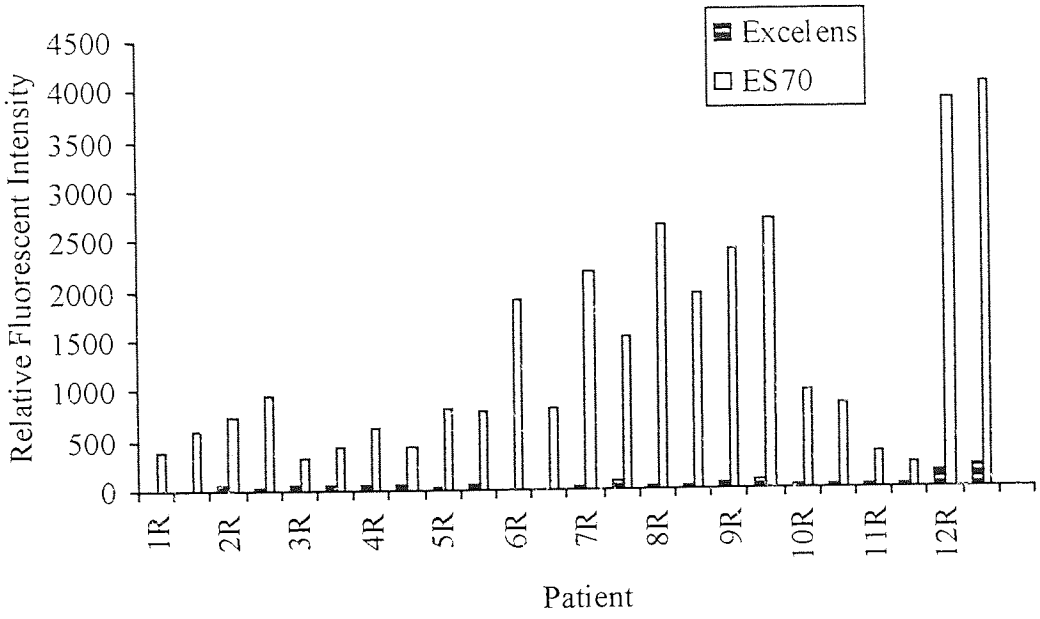

Figure 7.2 Lipid deposition on two group II contact lenses by fluorescence spectrophotometry

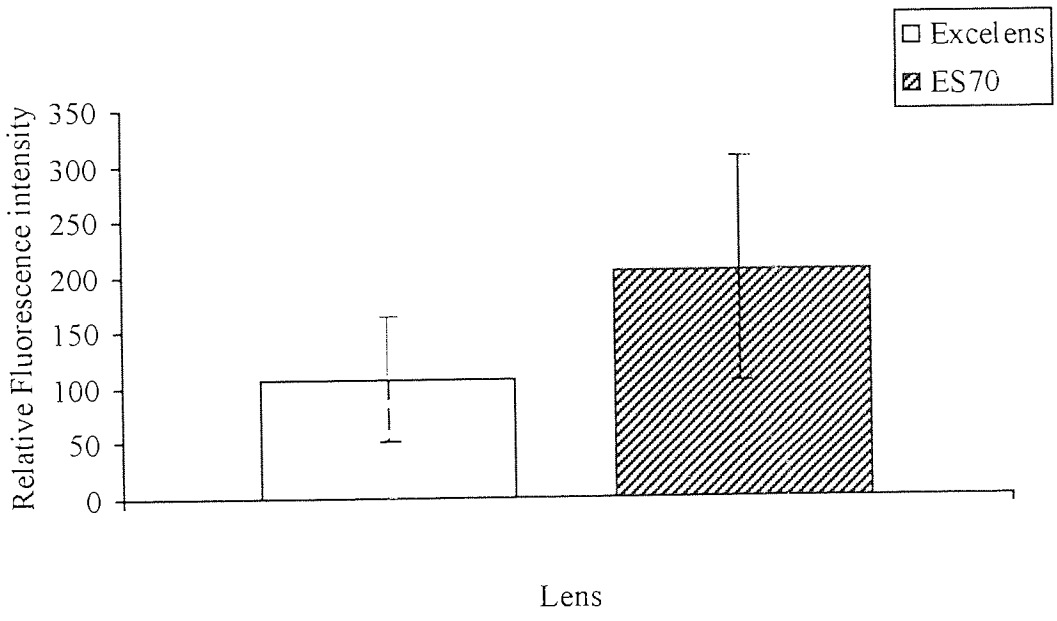

Figure 7.3 Graph to show the average protein deposition on two group II contact lenses

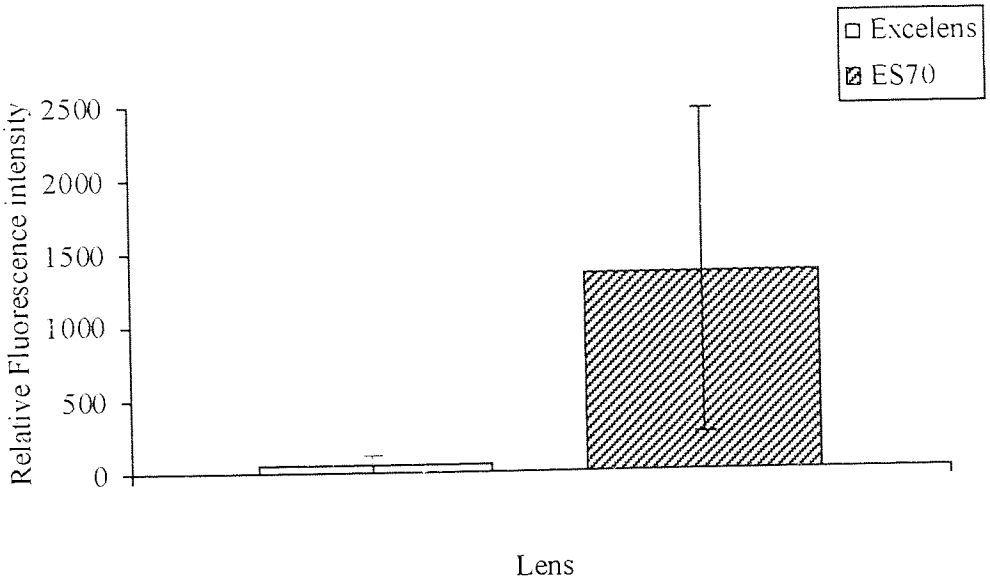

Figure 7.4 Graph to show the average lipid deposition on two group II contact lenses

The error bars in figures 7.3 and 7.4 indicate the standard deviation of the results obtained.

7.4.3 The effect of long term use of Group II lenses

It is immediately evident from the results obtained that fluorescence spectroscopy is a very sensitive technique. Differences can be observed not only between the two materials, but also between individual patients. It is also possible to detect differences between a patients right and left eye in the levels of deposition. The results above show how deposition can vary both between patient and material, with more protein and lipid deposition on the VP based material (ES70). Clinical performance between the lenses showed that comfort, visual quality, visual acuity and physiological performance were virtually identical[212].

The lenses were worn in both eyes, and it is clear that there are contralateral eye differences in spoilation. There are also significant variations between patients, due to the diverse nature of individuals tear compositions. The differences are more

pronounced for lipid than protein. There was very little correlation between the relative levels of protein and lipid deposited per patient, that is if the patient was a high protein depositor, they were not necessarily a high lipid depositor.

The two materials studied are classified in the same FDA group, so the water content and degree of ionicity are similar. This study showed that other factors must be considered to gain a full understanding of the levels of deposition that may be found on different lens materials. FDA group II lenses deposit more lipid than any other FDA group, but as both these lenses belong to the same group, it can be seen that differences occur within the same classification, due to the chemical composition of the lenses.

The principle component of the majority of commercially available contact lenses is polyHEMA. Optical grades of HEMA monomer are used, though the major problem in its manufacture is obtaining the monomer completely free of methacrylic acid, MAA[213]. The residual MAA leads to an increase in the anionicity of the surface of the lenses, which in turn leads to the accumulation of the positively charged protein lysozyme. Excelens is based on a polyvinyl alcohol and methyl methacrylate polymer, which contains a hydroxyl hydrophile and avoids the presence of the anionic impurity present in HEMA.

The N-vinyl pyrrolidone monomer, present in the ES70 lens, can be prepared in a pure state, though it polymerises ineffectively with several monomers including HEMA, due to its low reactivity ratio. This results in 'blocky' polymers, with these sites leading to increased spoilation. It is neutral at physiological pH though the pendant pyrrolidone ring presents a relatively hydrophobic external surface which leads to an increase in albumin (negatively charged) deposition. The amphiphilic nature of the pyrrolidone ring is the underlying reason for its susceptibility to lipid accumulation. There is a need to remove any unreacted NVP monomer prior to insertion in the eye due to its toxicity[213].

The results show that the NVP based lenses deposited 42 times more lipid and 9 times more protein than the PVA based lens. PVA is a neutral hydroxyl hydrophile that interacts only weakly with the range of proteins in the eye. Previous work has shown that FDA group II lenses attract more lipid than other FDA groups and deposit a higher level of lens calculi[212].

One theory proposed to account for lipid deposition on hydrogels is the 'push-pull' theory[214]. The 'pull' is the attraction the polymer matrix has for the lipid material, which shows greater selective solubility in the lens matrix than in the polar aqueous medium. It is more pronounced with non-ionic matrices. The less ionic a matrix, the more likely it is to attract lipid molecules. The 'push' is the water in the lens, forcing the lipid molecules into the polymer matrix. The water molecules have a relatively strong attraction for each other and will repel non-polar lipid molecules. Therefore the higher the water content, the more likely it is to deposit lipid.

The method of manufacture of the two lenses is different. As fluorescence is a surface technique, any factors that may influence the surface must be considered. Any surface rugosity will lead to an increase in deposition. This is more likely with the lathed lens.

The lenses were cleaned throughout the study. Patient compliance with the cleaning instructions can play a part in the level of deposition at the end of the study. Repeated surfactant cleaning and disinfection of the lenses can produce chemical and conformational changes to the deposits. A selection of the lenses were cleaned and refluoresced. It was not possible to remove all of the protein or lipid deposition, with the cleaning not being as effective with the NVP based lens. Surfactant cleaning is more effective at removing proteinaceous deposits than lipoidal species.

7.5 Material Dependency

The previous study demonstrated that spoilation is related to the material. This study was undertaken to evaluate three lens types, one of which was designed to reduce spoilation, to investigate further the role played by the material in the level of deposition encountered.

7.5.1 Methodology

Three materials were studied to investigate the effect that water content and material ionicity had on the degree of deposition, the details of which are shown in table 7.2.

Lens	Vistagel Plus	Classic	Excelens
EWC	40 %	42.5 %	64 %
Monomers	undisclosed	MMA + VP + HEMA	MMA + PVA
Manufacturer	Vista Optics	PBH	CIBA-Vision
FDA Group	I	I	II
USAN	-	Tetrafilcon A	Atlafilcon A
Manufacture	lathed	lathed	lathed
ACLM	Filcon 1a	Filcon 3a	Filcon 4a

Table 7.2 Characteristics of Vistagel Plus, Classic and Excelens contact lenses

Twelve patients wore each of the three lens types for one month on a daily wear basis, with the same lens type used in both eyes. The lenses were cleaned using LC65 surfactant cleaner and Oxysept II-Step as the disinfection solution. No enzyme tablets were used at any time during the study.

The lenses were collected at the end of the months wear, stored in saline and refrigerated prior to analysis.

As described before, fluorescence spectroscopy was used to evaluated the levels of protein and lipid deposition.

7.5.2 Results

The protein deposition for three patients is given in figure 7.5, with the lipid deposition for the same patients in figure 7.6.

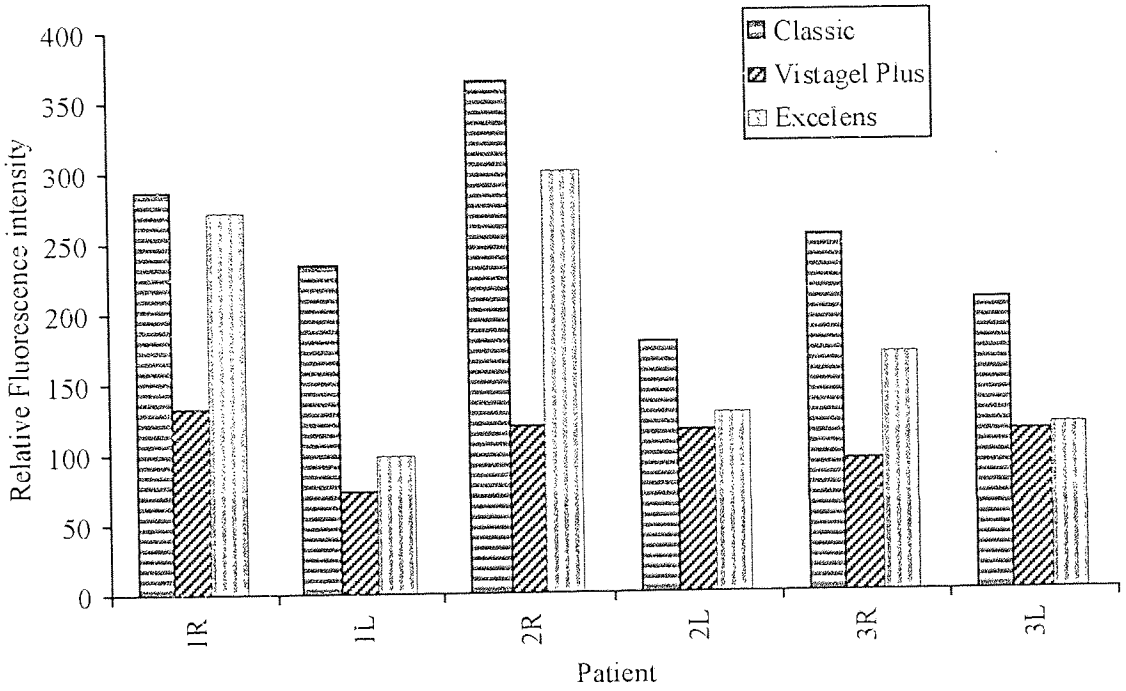

Figure 7.5 Protein deposition for three patients wearing three different lens types

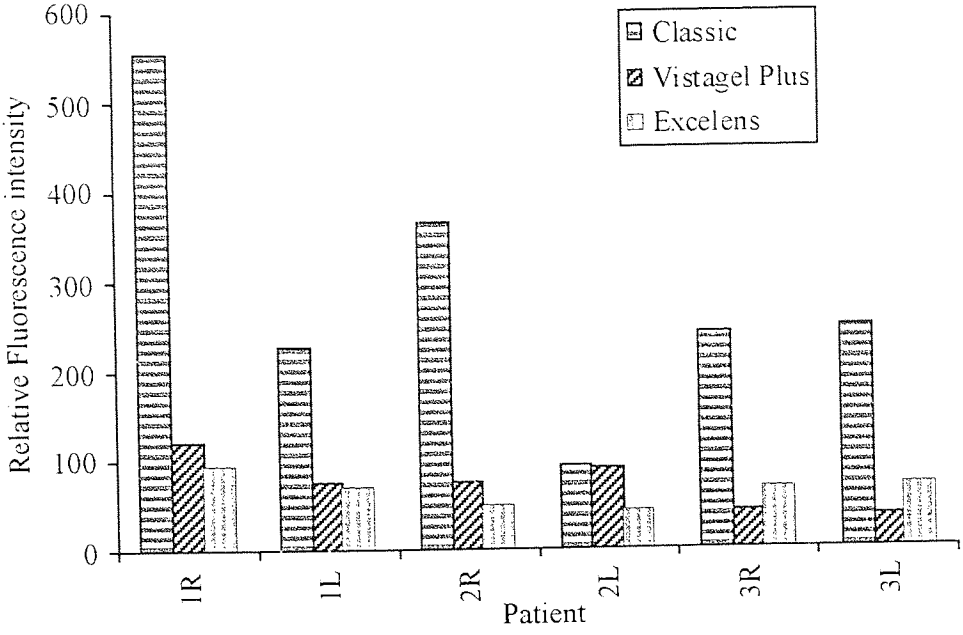

Figure 7.6 Lipid deposition for three patients wearing three different lens types

The average protein deposition for all of the patients is given for each lens in figure 7.7, and the lipid deposition is given in figure 7.8. The error bars indicate the standard deviation of the fluorescence values obtained.

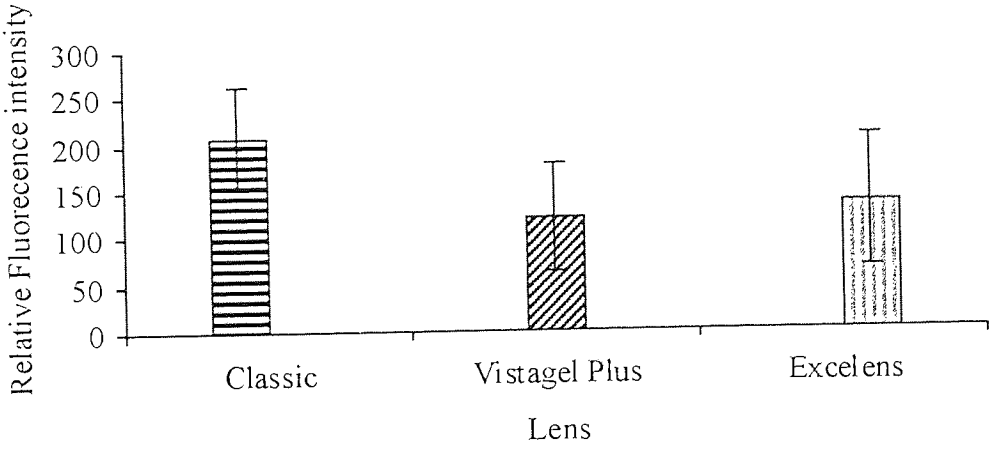

Figure 7.7 Graph to show the average protein deposition for twelve patients wearing three different lens types

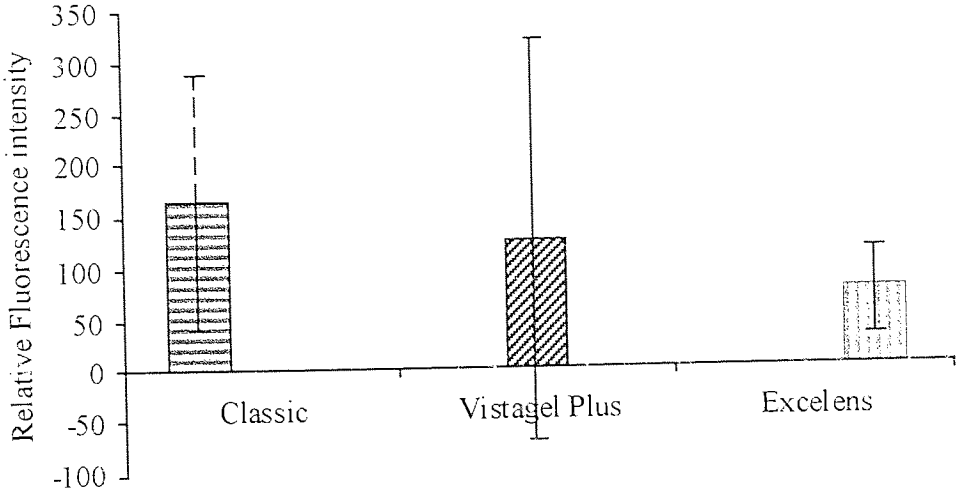

Figure 7.8 Graph to show the average lipid deposition for twelve patients wearing three different lens types

Lipid and protein deposition for individual patients are plotted in figure 7.9. It can be seen that Vistagel Plus lenses are in a small cluster, indicating that protein and lipid deposition are relatively low, and that a patient depositing a small amount of lipid on the lens, also tends to deposit a low amount of protein. The other lenses show a much wider spread of results, with Classic lenses showing more protein and lipid variation and Excelens low lipid deposition, but a much greater variation in protein spoilation.

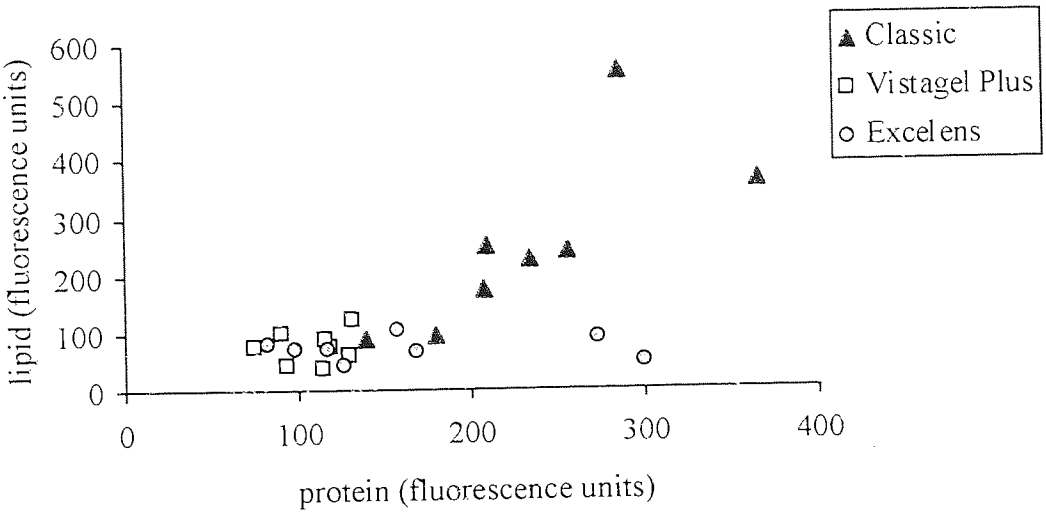

Figure 7.9 Graph to show the protein and lipid deposition for several patients for three different lens types

7.5.3 The effect of the lens material on deposition

Figures 7.5 and 7.6 indicate that spoilation is patient dependent, with differences between patients eyes. There are also considerable material variations.

Protein deposition is greatest on the Classic lens, which is a group I lens. It has a very similar water content to the Vistagel Plus lens. They are both classified in the same FDA group, but they vary in chemical composition. The Vistagel Plus lens was designed with a controlled sequence distribution and the principle of water structuring in an attempt to reduce spoilation[18,215]. The controlled sequence distribution of the polymer prevents the 'blockiness' that occurs with NVP polymers. This can lead to an increase in spoilation. Water structuring groups act to shield the polymer surface from depositing species preventing them from adhering firmly[216].

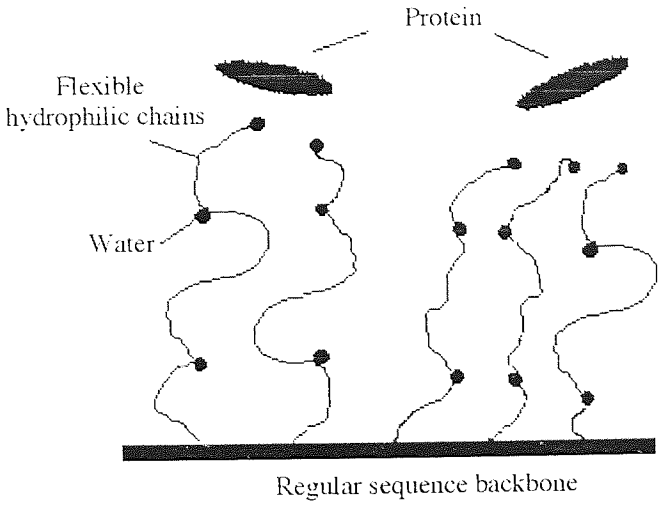

Figure 7.10 Diagrammatic representation of the biomimetic surface principle

The biomimetic principle on which the Vistagel Plus lens is based, is effective in reducing the amount of protein deposition on a lens.

Lipid deposition is greatest on the Classic lens, though Vistagel Plus showed the largest variation. The Classic lens is based on much older technology than Excelens and Vistagel Plus. As seen in the previous study, the polyvinyl alcohol based Excelens deposits little lipid.

Ideally, a biomimetic surface should exhibit a low contact angle with biological fluids and minimal contact angle hysteresis[216]. The dynamic contact angles of the three lenses considered in this study, were investigated in saline and ReNu. The procedure is described in chapter 3. ReNu is a surface active cleaning solution which becomes associated with the polymeric surface. The contact angle hysteresis provides an indication of the mobility of the functional groups at the surface between the wet and dry states. A low hysteresis indicates that the material has less movement of the functional groups. Table 7.3 gives the results of the advancing and receding contact angles along with the contact angle hysteresis.

	Advancing		Receding		Hysteresis	
	Saline	ReNu	Saline	ReNu	Saline	ReNu
Classic	51.1	77.4	31.4	55.6	19.7	21.8
Excelens	58.7	56.3	44.3	51.3	14.4	5
Vistagel Plus	40.8	41.2	24.4	29.5	16.4	11.7

Table 7.3 Dynamic contact angle measurements in saline and ReNu for three lens types

The results indicate that Vistagel Plus and Excelens exhibit minimal hysteresis in comparison to the Classic lens. Excelens is a polyvinyl alcohol based polymer and shows a minimal hysteresis when exposed to the alternating hydrophobic-hydrophilic environments. In a hydrophilic environment, the hydroxyl groups will be expressed at the surface and in a hydrophobic environment the hydrogen atoms are exposed. Both of these surfaces have a degree of hydrophilicity resulting in a minimal change in wettability when moving from one environment to the other. The Classic lens is a terpolymer, comprising of HEMA, MMA and NVP. In a hydrophilic environment the hydroxyl and pyrrolidone groups are exposed at the surface, and hydrophobic methyl and methacrylate groups are exposed in air. This change in the nature of the surface leads to an increased hysteresis. The water structuring groups present on the surface of the Vistagel Plus are expressed at the surface in the hydrophilic environment. They are still at the surface in the hydrophobic environment though in a different state, resulting in a minimal hysteresis. This indicates an advantage of the contact lens based on the biomimetic approach.

7.6 Longer wear of Group I lenses

Two group I lenses, of similar water content, were studied to investigate their long term performance in the eye. This was done to investigate the effect the length of wear time had on the levels of deposition on the lenses. One of the lenses is based upon the

biomimetic principle, and the other is made from HEMA. The details about the lenses are given in table 7.4.

Lens	Vistagel Plus	Z6
EWC	40 %	38 %
Monomers	undisclosed	HEMA
Manufacturer	Vista Optics	Hydron
FDA Group	I	I
USAN	-	Polymacron
Manufacture	Lathed	Lathed

Table 7.4 Lens characteristics for Z6 and Vistagel Plus contact lenses

7.6.1 Methodology

Twelve patients wore each of the lens types for three months on a daily wear basis. The same lens type was worn in both eyes. LC65 was used as the surfactant cleaner and Oxysept II-Step as the disinfectant.

7.6.2 Results

The protein and lipid deposition results for each patient are shown in figures 7.11 and 7.12 respectively.

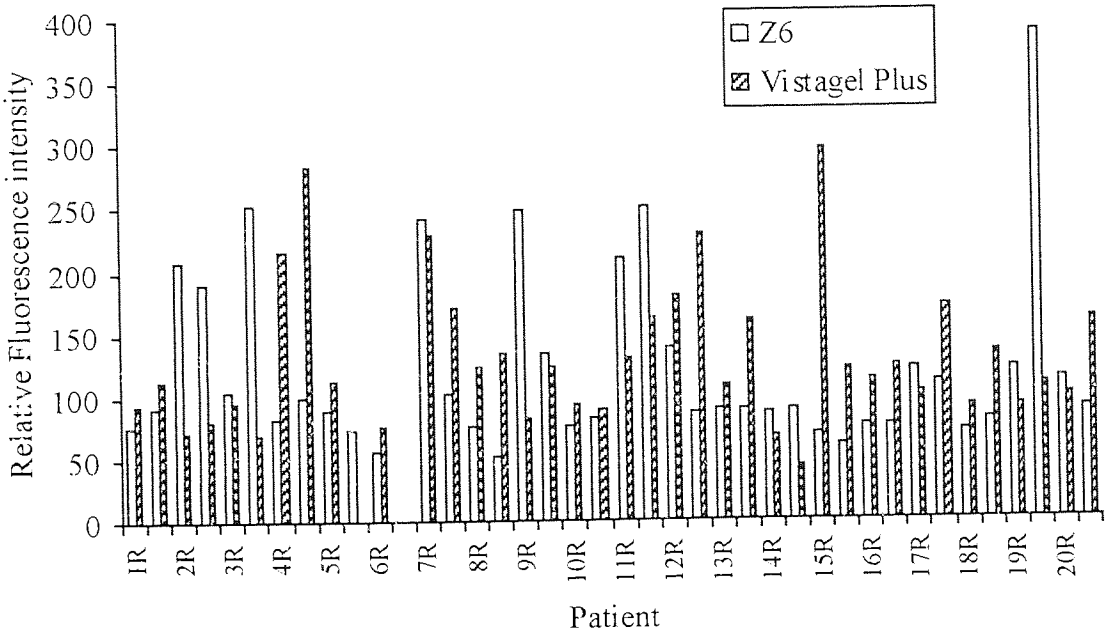

Figure 7.11 Protein deposition on Z6 and Vistagel Plus contact lenses by fluorescence spectrophotometry

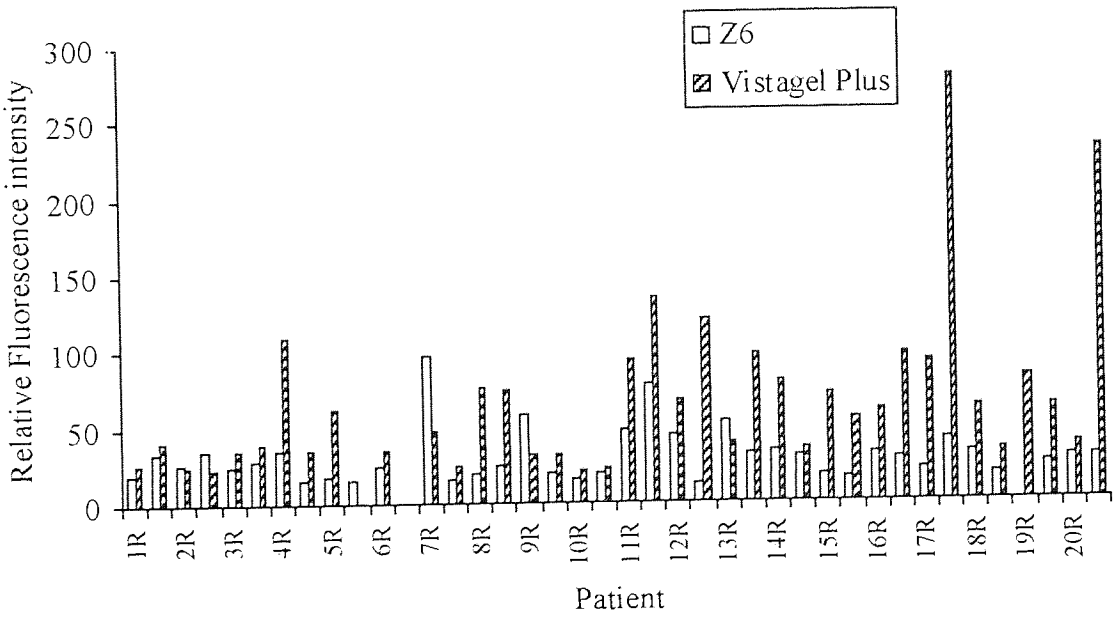

Figure 7.12 Lipid deposition on Z6 and Vistagel Plus contact lenses by fluorescence spectrophotometry

The differences can be seen more clearly if a few patients are considered. Figures 7.13 and 7.14 show the levels of protein and lipid deposition recorded for four patients.

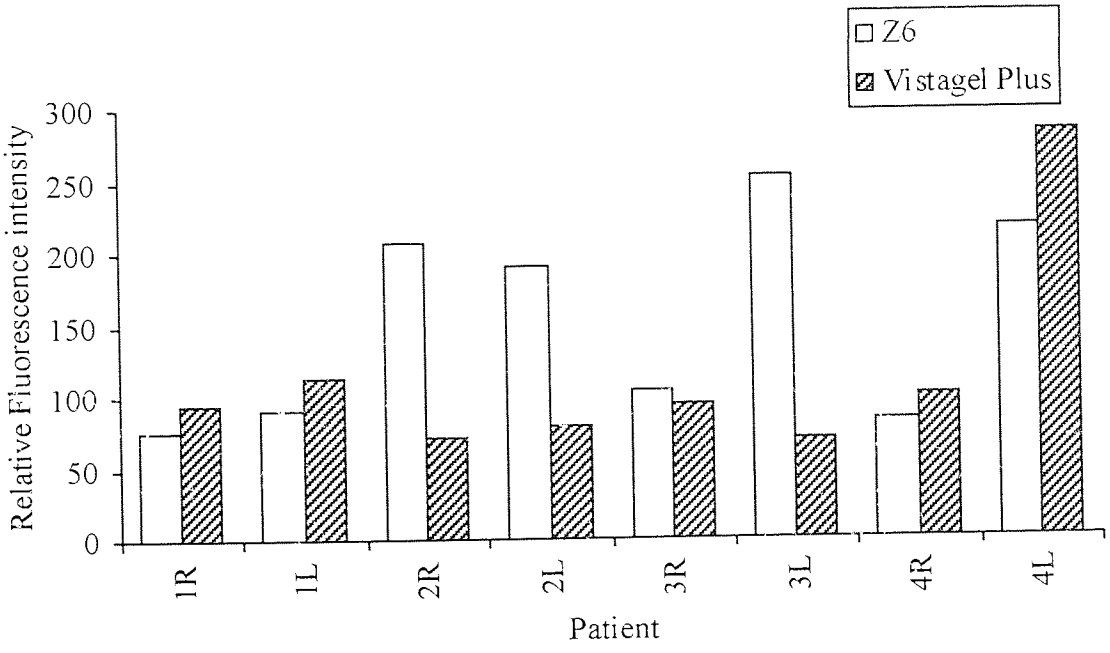

Figure 7.13 Protein deposition for four patients wearing Z6 and Vistagel Plus contact lenses

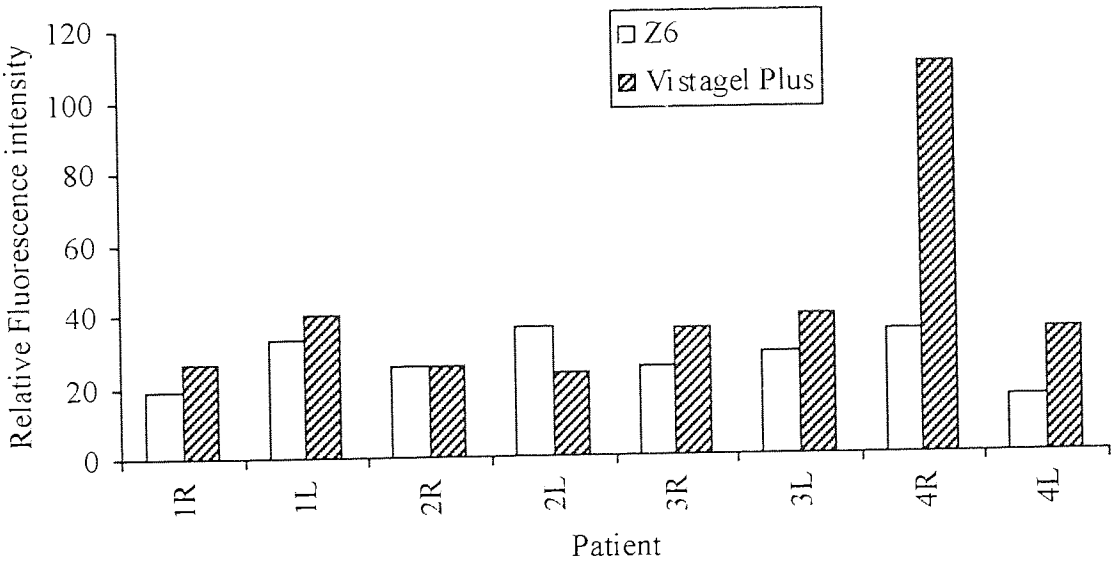

Figure 7.14 Lipid deposition for four patients wearing Z6 and Vistagel Plus contact lenses

It can be seen that there are general trends connected with each material, though some patients, notably patients 2 and 3 in figure 7.13, and patient 2 in figure 7.14, who do not follow the general pattern.

Figures 7.15 and 7.16 show the mean protein and lipid deposition for each lens type respectively. The error bars indicate the standard deviation for the fluorescence results.

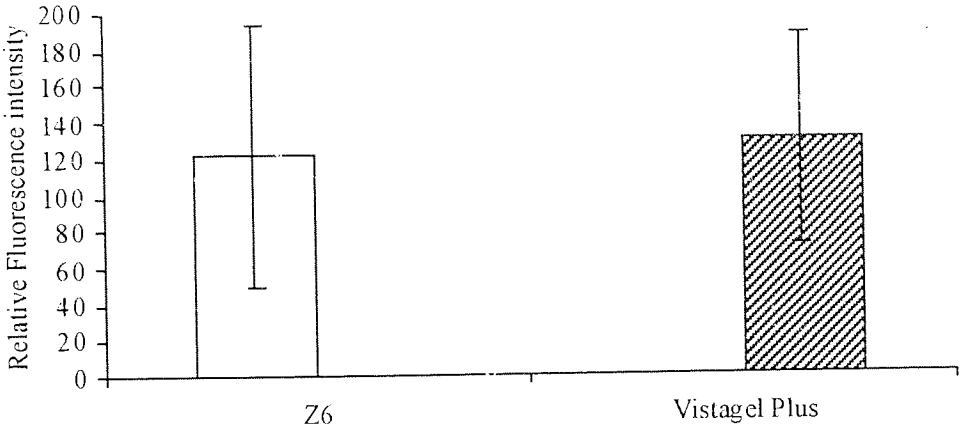

Figure 7.15 Graph showing the average protein deposition on Z6 and Vistagel Plus contact lenses by fluorescence spectrophotometry

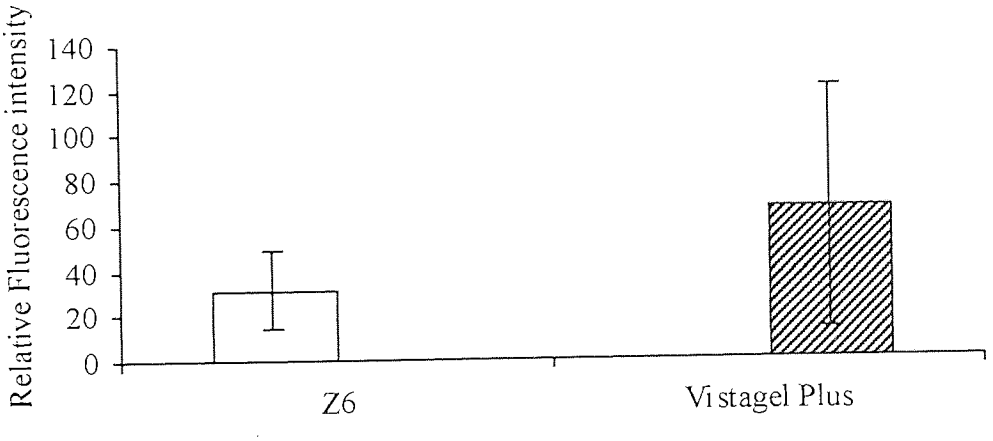

Figure 7.16 Graph showing the average lipid deposition on Z6 and Vistagel Plus contact lenses by fluorescence spectrophotometry

7.6.3 The effect of long term wear of Group I lenses

The results in figures 7.11 and 7.12 indicate the patient variability observed with both protein and lipoidal deposition. They also show that deposition varies between the lens types which must be as a consequence of the different chemical composition, as the wear time was the same for both lenses, and the water content was similar.

The amounts of protein deposition were generally higher for Vistagel Plus than Z6. The results for Vistagel Plus were worse than expected based on the short-term wear study of this lens. The lenses are of similar water content and are classified in the same FDA group, so the differences must be attributable to the chemical structure of the material. Investigations were carried out on the batch of HEMA used in the production of the Vistagel Plus lens[213]. These indicated that there was contamination by MAA. This could account for the increase in spoilation, as it has been shown that residual MAA can increase the anionicity of the material and thus increase its susceptibility to protein deposition.

Lipid deposition was, on average, higher for Vistagel Plus than Z6. One of the components of Vistagel Plus is NVP. Lipid absorption has been seen to be increased in materials that contain this monomer, as seen in the previous section. It is due to this that vinyl pyrrolidone has been used as a transdermal penetration enhancers[217].

7.7 Repeatability of Deposition

This study was performed to investigate the reproducibility of deposition. The previous studies had shown how spoilation can vary between patients and wear time, so it is important to know whether an individual patient exhibits different spoilation profiles for the lenses of the same make that are worn for the same length of time. One lens type was worn for a year, replacing it every month.

7.7.1 Methodology

Ten patients wore Medalist 66 lenses on a daily wear basis for a month. This was repeated for twelve months. The lenses were cleaned using ReNu. The lenses were collected at the end of each month and stored in ReNu prior to analysis. Information regarding the Medalist 66 lens is given in table 7.5.

Lens	Medalist 66
EWC	66 %
Monomers	HEMA + VP
Manufacturer	Bausch and Lomb
FDA Group	II
USAN	Alphafilcon A
Manufacture	Moulded
ACLM	Filcon 4a
Centre thickness	0.11 mm

Table 7.5 Lens characteristics of Medalist 66 contact lenses

7.7.2 Results

Protein and lipid results for twelve months wear for two patients are given in figures 7.17 and 7.18.

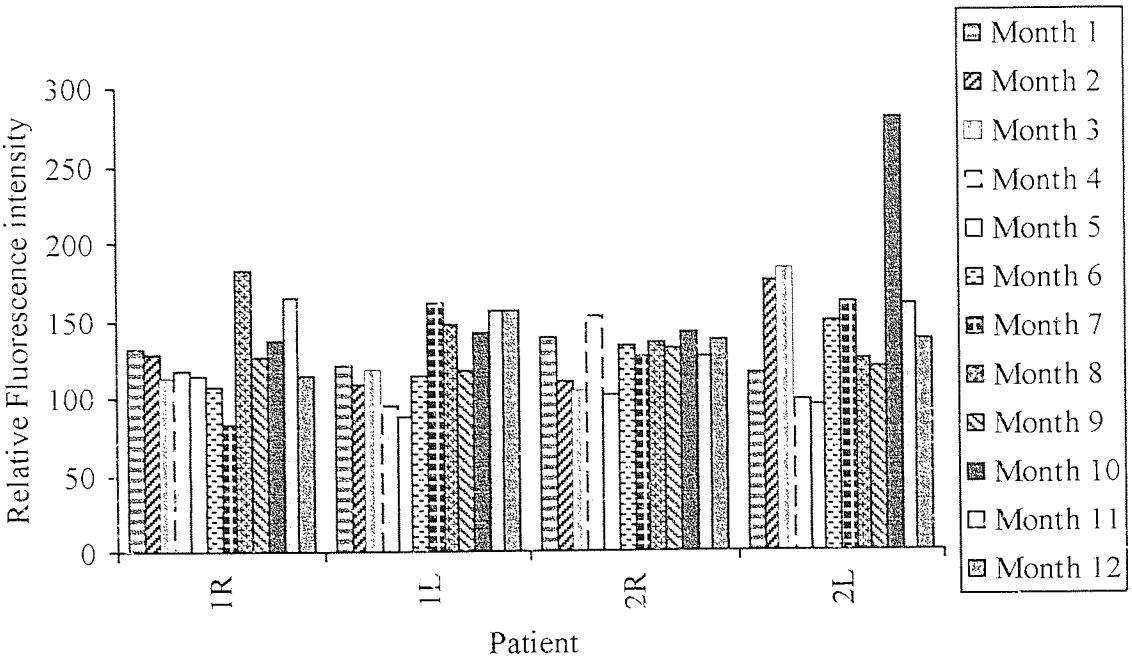

Figure 7.17 Protein deposition for two patients wearing Medalist 66 contact lenses over 12 months

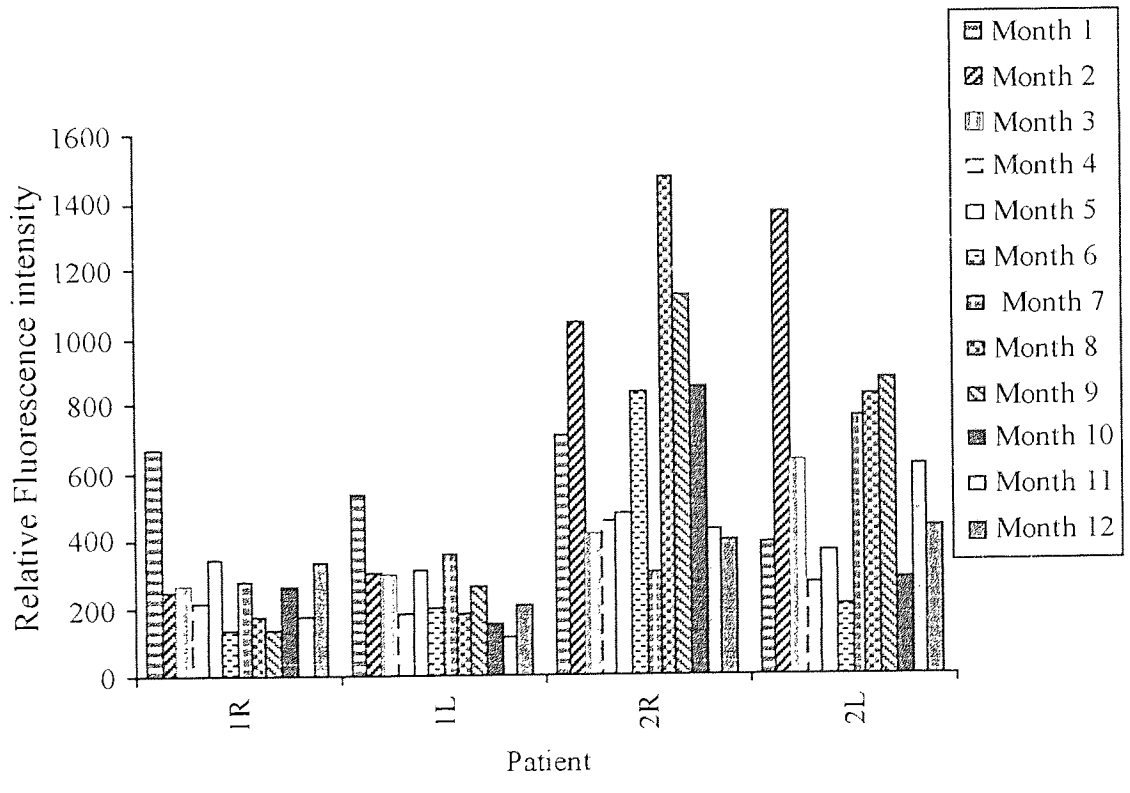

Figure 7.18 Lipid deposition for two patients wearing Medalist 66 contact lenses over 12 months

The average spoilation for each patient over the twelve months, in both eyes are given in figures 7.19 and 7.20.

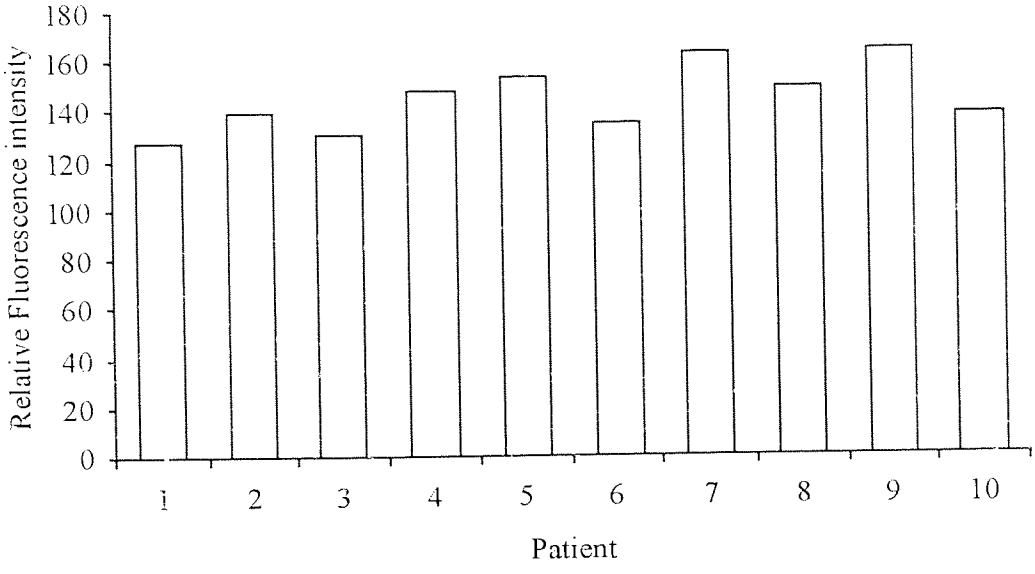

Figure 7.19 Average protein deposition for ten patients wearing Medalist 66 contact lenses for one month over a 12 month period

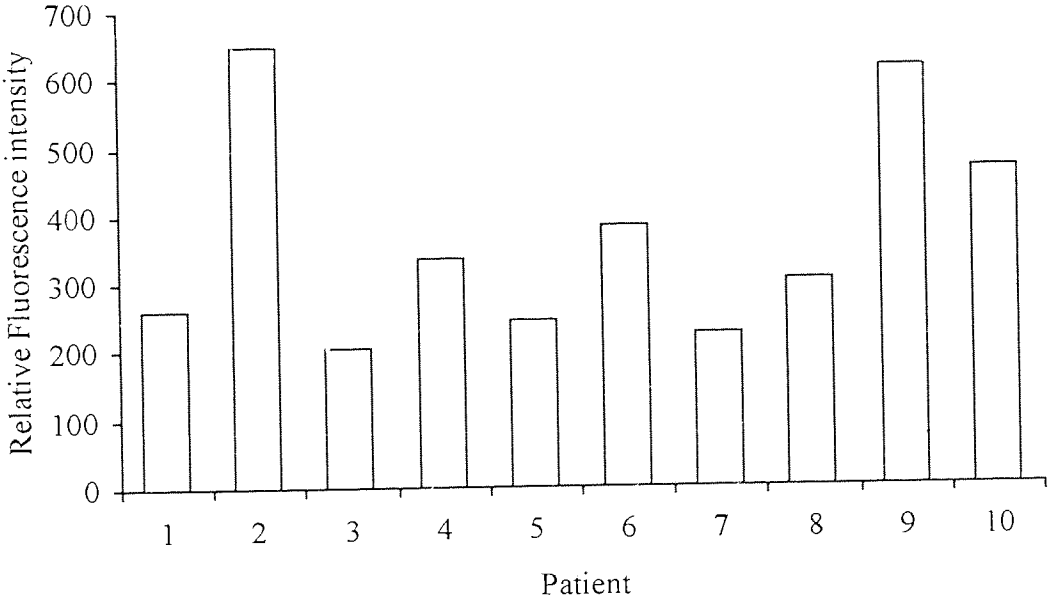

Figure 7.20 Average lipid deposition for ten patients wearing Medalist 66 contact lenses for one month over a 12 month period

Figure 7.21 plots the amount of surface protein, obtained by fluorescence, against the total protein within the lens, which is found by UV spectroscopy.

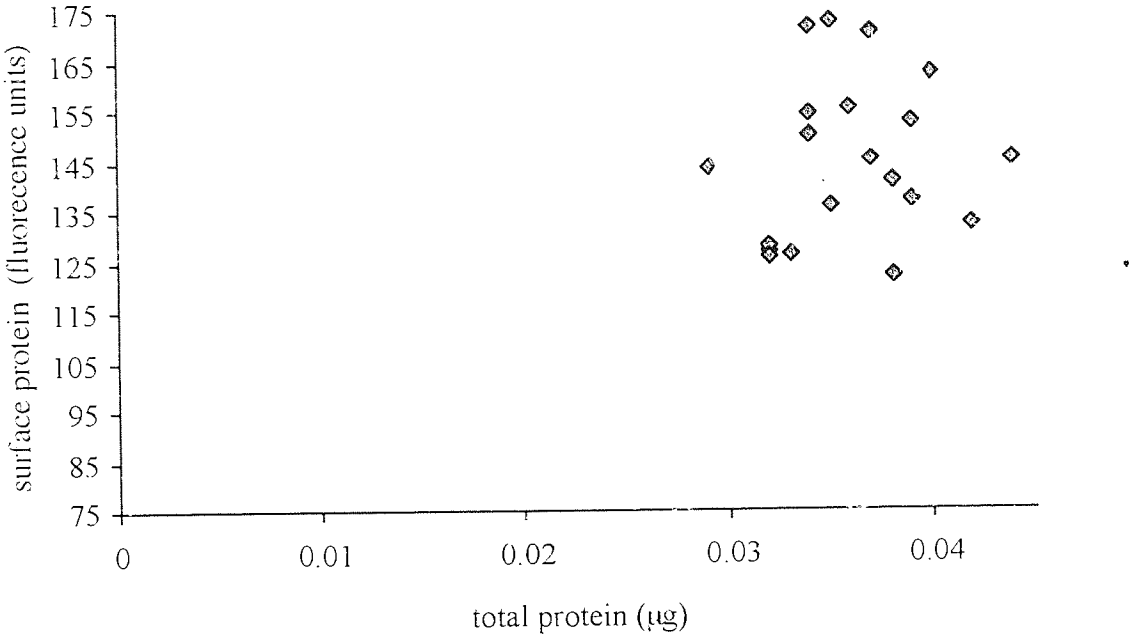

Figure 7.21 Surface versus bulk protein for Medalist 66 contact lenses measured using fluorescence and UV spectroscopy

Figure 7.21 indicates that the surface results obtained by fluorescence spectroscopy show a range of levels, whereas the results obtained by UV spectroscopy for the total amount of protein in the lens is only over a narrow range. This may suggest that the majority of protein present in these group II lenses is on the surface.

Figures 7.17 and 7.18 show again that there are intra patient differences as well as inter patient variations. Figures 7.22 and 7.23 show the differences between the eyes for protein and lipid respectively.

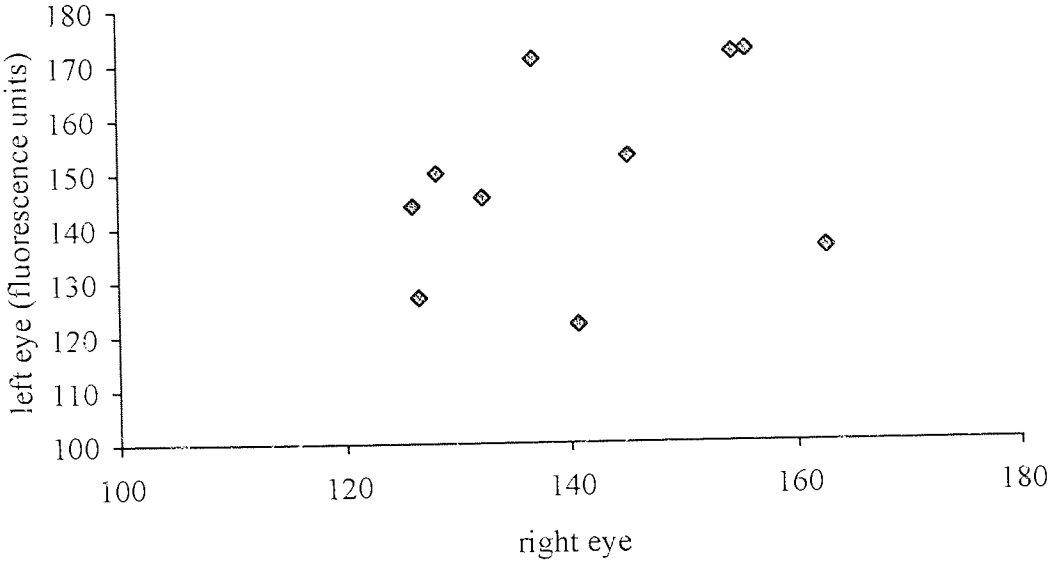

Figure 7.22 Right eye versus left eye protein deposition for Medalist 66 contact lenses in fluorescence units

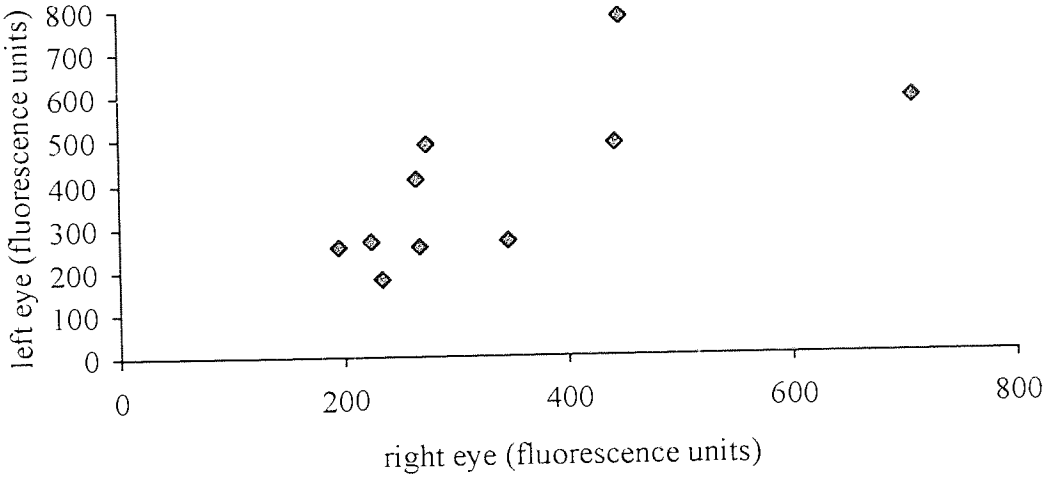

Figure 7.23 Right eye versus left eye lipid deposition for Medalist 66 contact lenses in fluorescence units

7.7.3 The repeatability of deposition effects over one years wear

Figures 7.17 and 7.18 indicate that even for the same patient, there are differences in the level of spoilation for the same lens worn for the same length of time. This is also demonstrated in figures 7.22 and 7.23, which show that the level of deposition on the right lens is not the same as that observed for the left eye. This indicates that there are a number of factors that influence deposition, not just the lens material. Tear quality and quantity varies from right eye to left eye, as does the composition of the tears. External factors can also have an effect on the level of spoilation including diet, air conditioning, alcohol consumption, medication and cosmetics[60].

The variation between patients is higher for lipids than proteins. Protein differences in the tear film of individual patients is less than that observed with lipids. Cleaning regime and extrinsic factors are patient dependent.

7.8 Reproducibility of Spoilation on Group II and Group IV lenses

Spoilation has been shown to be related to the water content and ionicity along with patient variations. Two high water content lenses were studied to investigate the effect ionicity had on the reproducibility of spoilation. This was done to asses whether a lens worn for a given period of time is a good guide to any other lens of the same type worn by the same patient for the same length of time.

7.8.1 Methodology

Twenty patients wore a Focus lens in one eye and a Precision UV lens in the other eye for three months on a daily wear basis. The lenses were replaced at the end of each month and replaced with the same type of lens in each eye every time. Information about the two lenses is given in table 7.6.

Lens	Focus Visitint	Precision UV
EWC	55 %	74 %
Monomers	HEMA + PVP + MAA	MMA + NVP
Manufacturer	CIBA-Vision	PBH
FDA Group	IV	II
USAN	Vifilcon A	Vasurfilcon A
Manufacture	Moulded	Moulded
ACLM	Filcon 4b	Filcon 4a
Centre thickness	0.1 mm	0.14 mm

Table 7.6 Characteristics of Focus and Precision UV contact lenses

Precision UV contains a UV blocker, so protein fluorescence was not recorded. The protein results were also obtained by an extraction procedure[218], and are not recorded here.

7.8.2 Results

The lipid fluorescence results obtained for three patients wearing each lens for one month are given in figure 7.24.

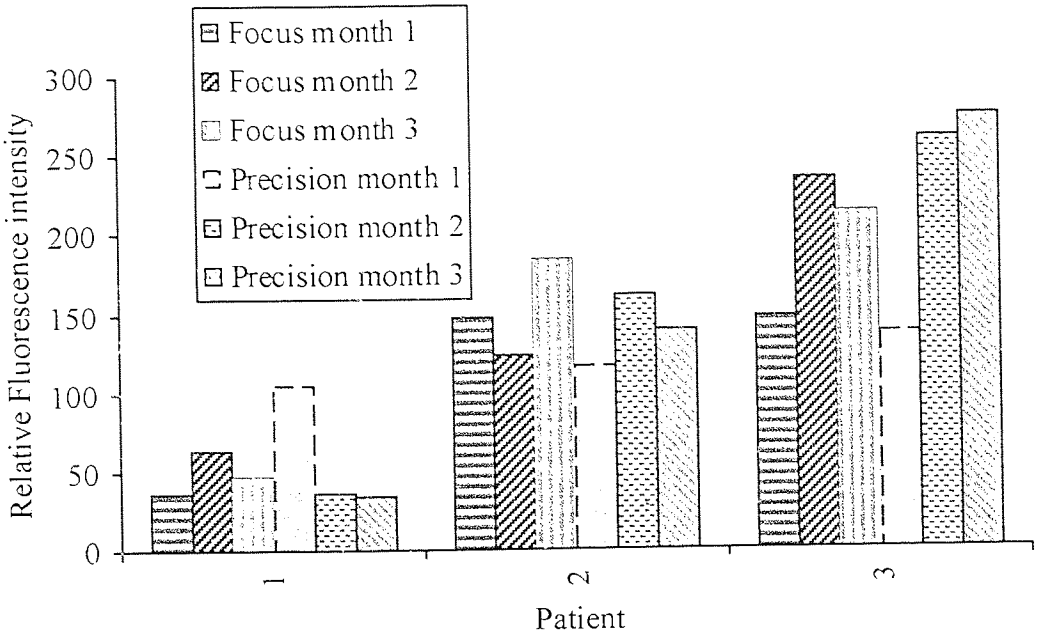

Figure 7.24 Lipid deposition for three patients wearing Focus and Precision UV contact lenses for three one month periods

The average lipid deposition for each lens type for each patient are given in figure 7.25.

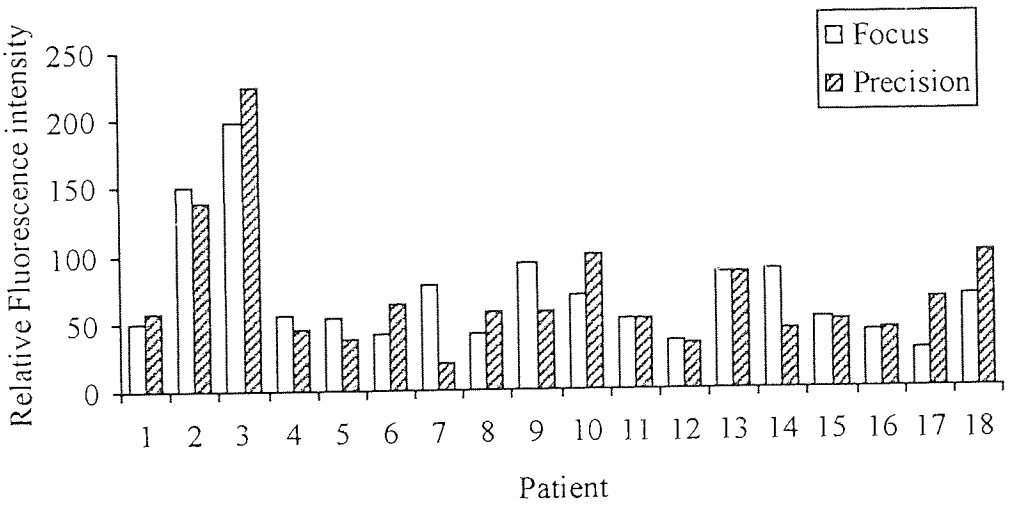

Figure 7.25 Average lipid deposition for three one month wear periods for Focus and Precision UV contact lenses

The results for the three patients from figure 7.24 are averaged for each lens type. The mean and standard deviation are shown in figure 7.26.

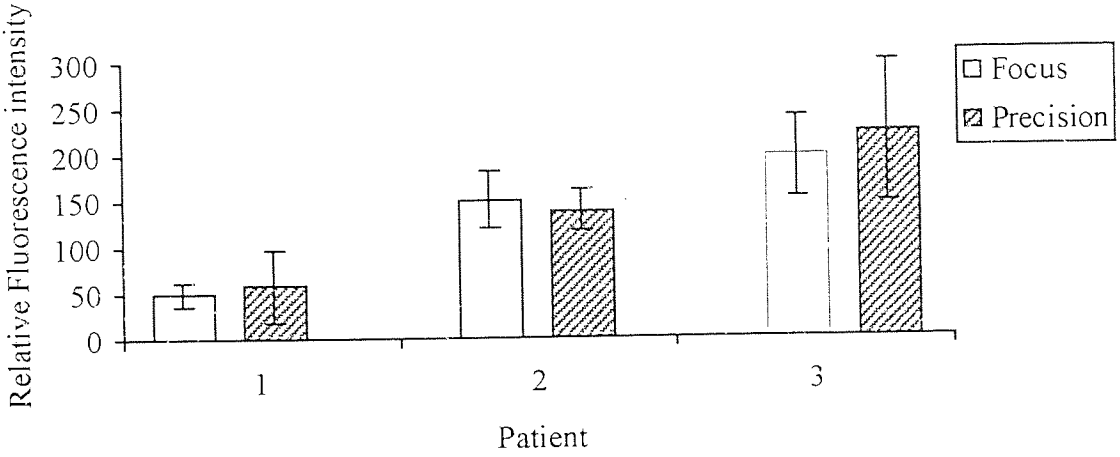

Figure 7.26 Mean and standard deviation lipid deposition for three patients wearing Focus and Precision UV contact lenses for three one month periods

7.8.3 The result of reproducibility of spoilation on Groups II and IV lenses

Figure 7.24 indicates how deposition is patient dependent, with less variation observed for lipid than protein. There are noticeable differences between the materials. There is more lipid deposited on the group II, and it was also found that there was more protein on the group IV lens[26,218].

Protein results were not obtained by fluorescence spectroscopy in this study due to the presence of a UV blocker in the Precision lens. Analysis of the protein levels was carried out following the lipid analysis, by an extraction method[218]. Protein deposition is influenced by the water content and ionicity of a material. Although the group II lens has a higher water content, the group IV lens is anionic, due to the presence of MAA. The thermodynamic driving force will attract the positively charged proteins to the negative surface[218]. Protein deposition is principally controlled by the water content

and ionicity of a material, generally displaying only a small amount of inter patient differences in comparison to lipid deposition.

A component of both lenses is N-vinyl pyrrolidone. As has been shown previously, this can lead to an increase in the amount of lipid deposition. The group II lens displayed approximately twice the amount of lipid than the group IV lens. However, the level of NVP present in Precision UV is about four times the level found in the Focus lens, which may account for the increased level of lipid deposition in the group II lens. The Focus lens will have an anionic surface, due to the presence of carboxyl groups, which may to a small degree repel the lipids some of which are also anionic[219].

7.9 Cleaning regime

All daily wear lenses require cleaning in order to optimise the length of time that the lens can be comfortably worn. Five cleaning solutions were used in conjunction with two different types of lenses tc investigate the effect the solution has on the levels of deposition. The details about the lenses are given in table 7.7, and the solution information in table 7.8.

Lens	Surevue	Rythmic
EWC	58 %	73 %
Monomers	HEMA + MAA	MMA + VP
Manufacturer	Vistakon	Lunelle
FDA Group	IV	II
USAN	Etafilcon A	-
Manufacture	Moulded	Moulded
ACLM	Filcon 1b	Filcon 4a
Centre thickness	0.105 mm	0.15 mm

Table 7.7 Characteristics of Surevue and Rythmic contact lenses

Solution	Manufacturer	Additional Cleaning
Oxysept I-Step	Allergan	rub-&-rinse with 3% hydrogen peroxide
Oxysept II-Step	Allergan	rub-&-rinse with 3% hydrogen peroxide
ReNu	Bausch & Lomb	rub-&-rinse with ReNu
Optifree	Alcon	prior surfactant cleaning with Alcon Opticlean
Softab	Alcon	prior surfactant cleaning with Alcon Pliagel

Table 7.8 Manufacturers and additional cleaning required with five cleaning solutions under investigation

7.9.1 Methodology

Ten male patients wore a group II lens in one eye and a group IV lens in the other eye on a daily wear basis for one month. At the end of each month, the lenses were changed, with the same lens type being worn in each eye as the previous month. The study was carried out for five consecutive months, with a different care regime used each month. At the end of each month, the lenses are collected, stored in saline and refrigerated prior to laboratory based analysis.

7.9.2 Results

Figures 7.27 and 7.28 show the protein and lipid deposition of the two lens types with the five solutions for three patients.

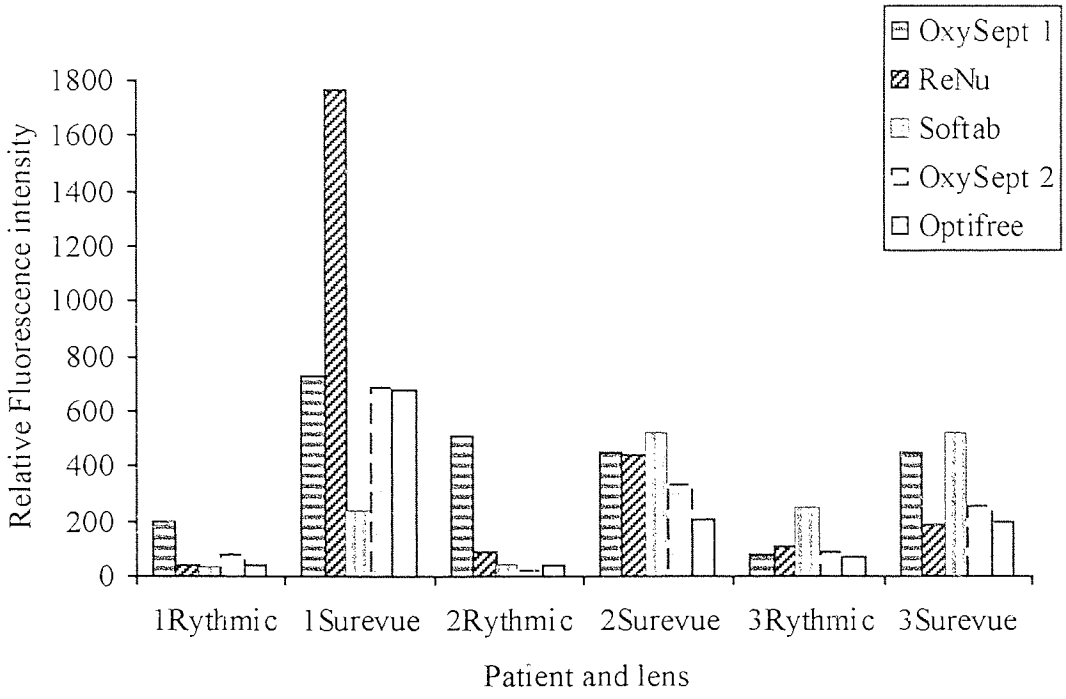

Figure 7.27 Protein deposition of three patients wearing two lens types and using five cleaning solutions

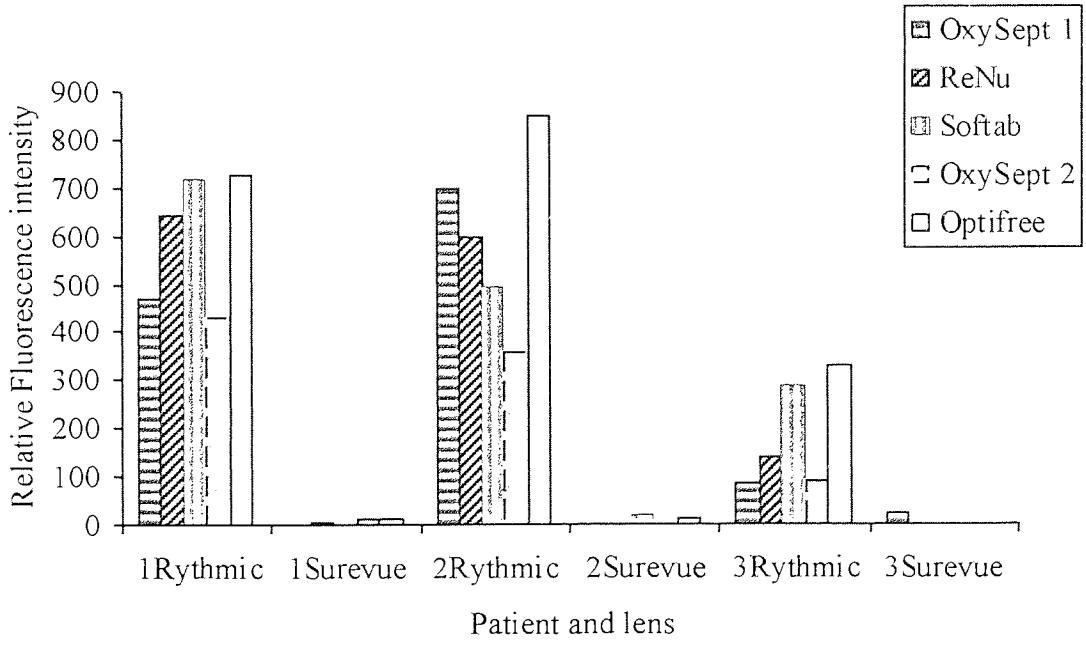

Figure 7.28 Lipid deposition of three patients wearing two lens types and using five cleaning solutions

Figures 7.29 and 7.30 show the average deposition for each lens type for each solution.

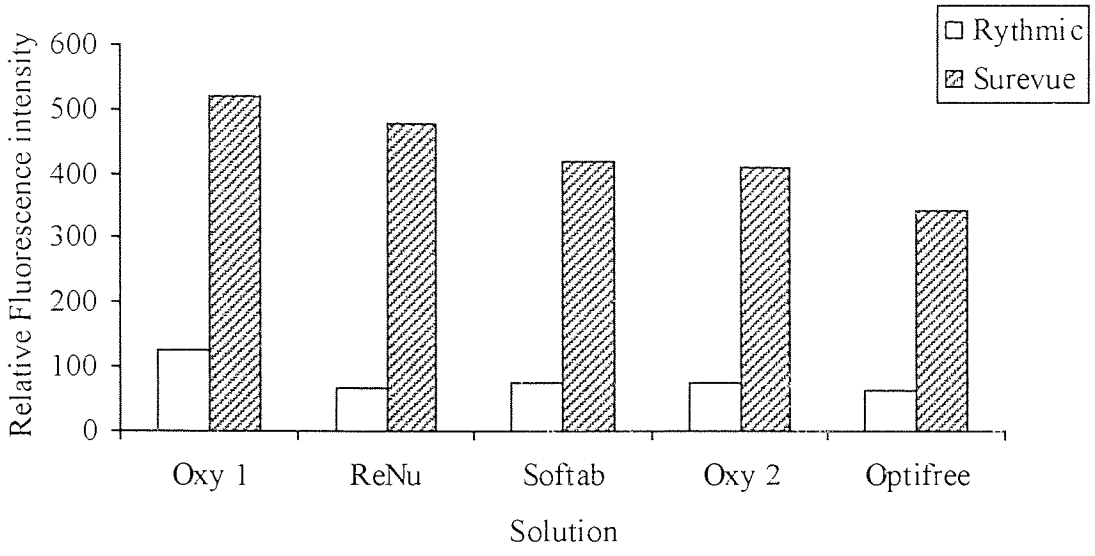

Figure 7.29 Average protein deposition for each lens type for each cleaning solution

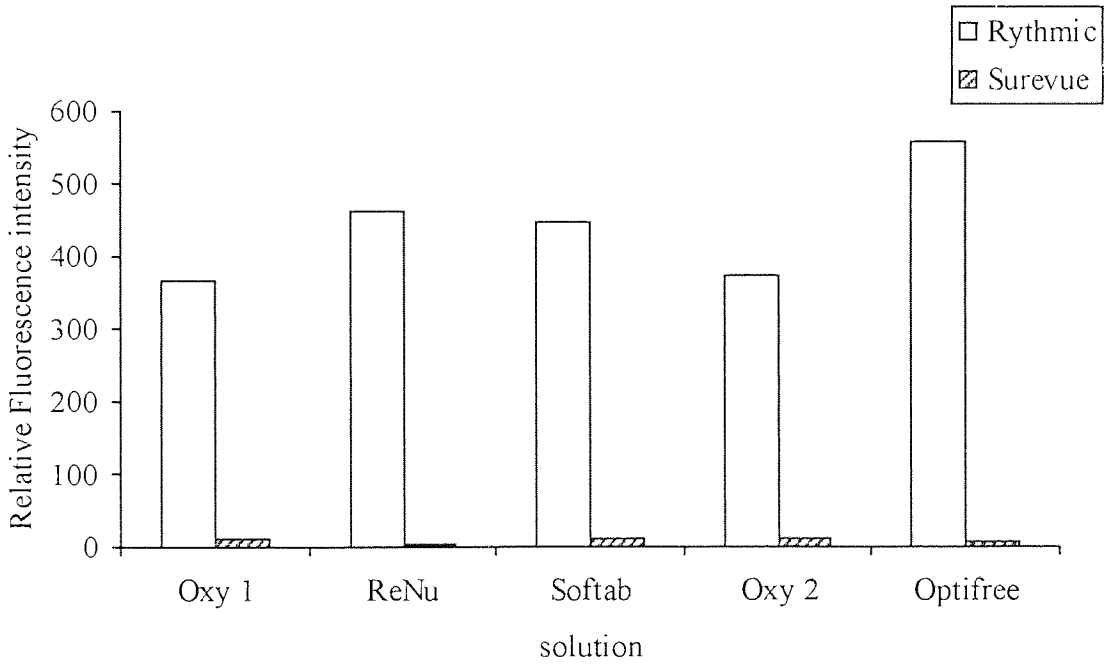

Figure 7.30 Average lipid deposition for each lens type for each cleaning solution

7.9.3 The effect of the cleaning regime on the levels of deposition

Figures 7.27 to 7.30 indicate that the same patient will exhibit differences in spoilation that depends upon both the lens and cleaning regime. Care systems have evolved from a many step procedure, to all-in-one cleaning solutions. The ease of cleaning is much improved with the one-step systems, but this must not compromise the efficacy of cleaning[220].

ReNu is classified as a multi-purpose cleaning solution. It is designed to clean, disinfect and rewet the contact lens surface, and contains an antimicrobial agent, biguanide[17].

It can be seen in figures 7.29 and 7.30 that there are differences between the two lens types, for each solution. The group II lens deposits more lipid but less protein than the group IV lens[26].

It is not possible to remove all of the deposited species. With a group IV lens, lysozyme penetrates into the polymer matrix, making it extremely difficult to remove. The group II lens contains NVP, which has been previously seen to increase the amount of lipid deposited. Lipid levels within the lens build up, becoming irreversibly bound to the polymer matrix Lipids interact with the surface of lenses. The formed lipid layer partitions with and penetrates into the lens matrix. Unsaturated lipids undergo autooxidation and oligomerisation. Once the lipid is located within the lens matrix, it is not removable[221]. The cleaning solutions are then unable to cleave the chemical bonds holding the lipid in the matrix.

The lenses were examined following removal from the eye, with no final cleaning. In order to determine the cleaning efficacy of the lenses, they should be cleaned with the appropriate cleaning solution and refluoresced. The difference in fluorescence intensity for both proteins and lipids would give an indication of the amount of deposition that could be removed by cleaning.

7.10 Length of wear time

Deposition of proteins has been shown to occur within minutes[26] of a lens being placed in the eye. Comfort may be affected with a highly spoilt lens, and can also contribute to inflammatory reactions such as Acute Red Eye Syndrome and Giant Papillary Conjunctivitis. One way to overcome the problem of deposition is to replace the lenses frequently. This study was carried out to investigate whether the currently used replacement schedule does result in reduced deposition.

7.10.1 Methodology

Twelve patients wore Precision UV (see table 7.9) lenses in both eyes, using ReNu as the cleaning and disinfection scheme. The lenses were worn for three months and then for three one month periods.

Lens	Precision UV
EWC	74 %
Monomers	MMA + NVP
Manufacturer	PBH
FDA Group	II
USAN	Vasurfilcon A
Manufacture	Moulded
ACLM	Filcon 4a
Centre thickness	0.14 mm

Table 7.9 Characteristics of Precision UV contact lenses

Precision UV contains a UV blocker, so protein fluorescence was observed using UV spectroscopy on protein extracted from the lenses. UV spectroscopy was carried out by Lyndon Jones.

7.10.2 Results

Figure 7.31 shows the lipid deposition for three patients, analysed using fluorescence spectrophotometry.

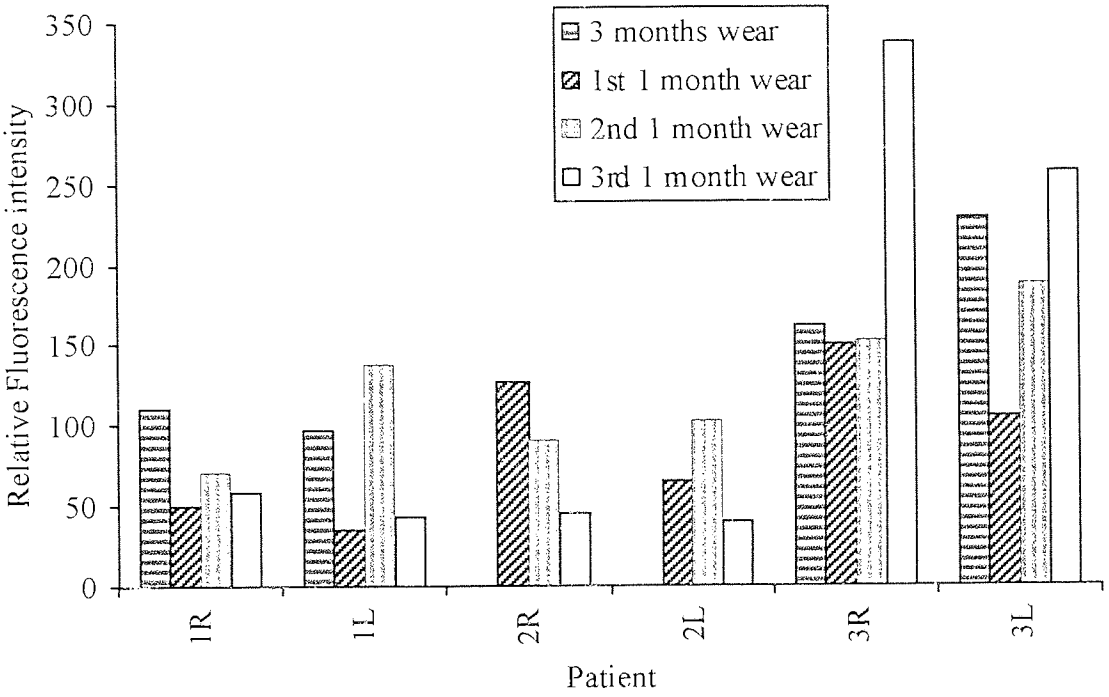

Figure 7.31 Lipid Deposition for three patients wearing Precision UV contact lenses for three months and one month by fluorescence spectrophotometry

As the lenses contained a UV blocker, protein was extracted from the lens and analysed by UV spectroscopy[26]. The results for the lenses worn for three month and the average of the three lenses worn for one month each are shown in figure 7.32.

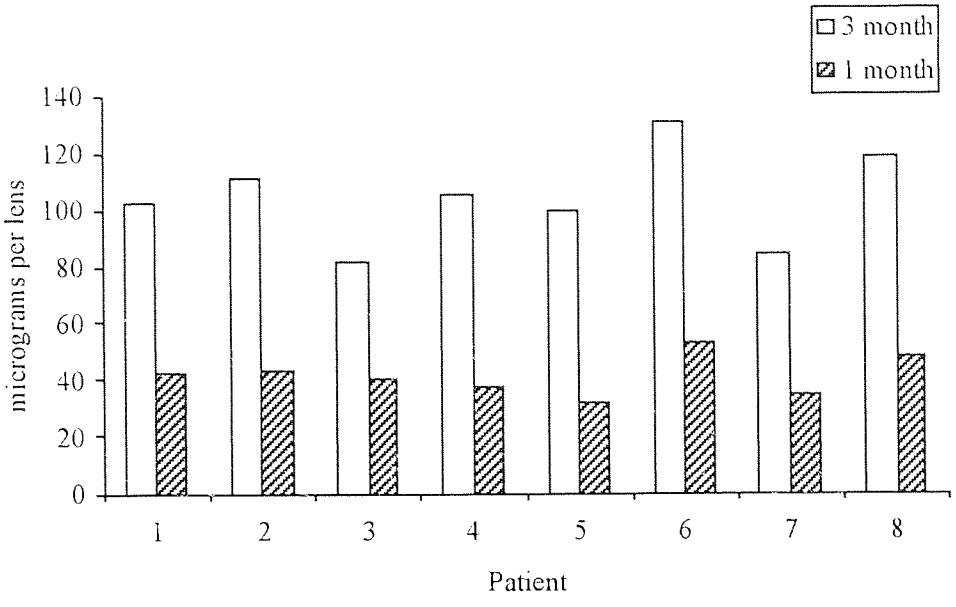

Figure 7.32 Protein extracted from lenses worn for three months and one month and assessed using UV spectroscopy

Figure 7.33 shows the average lipid deposition of the three lenses worn for one month compared to the lens worn for three months measured by fluorescence spectroscopy.

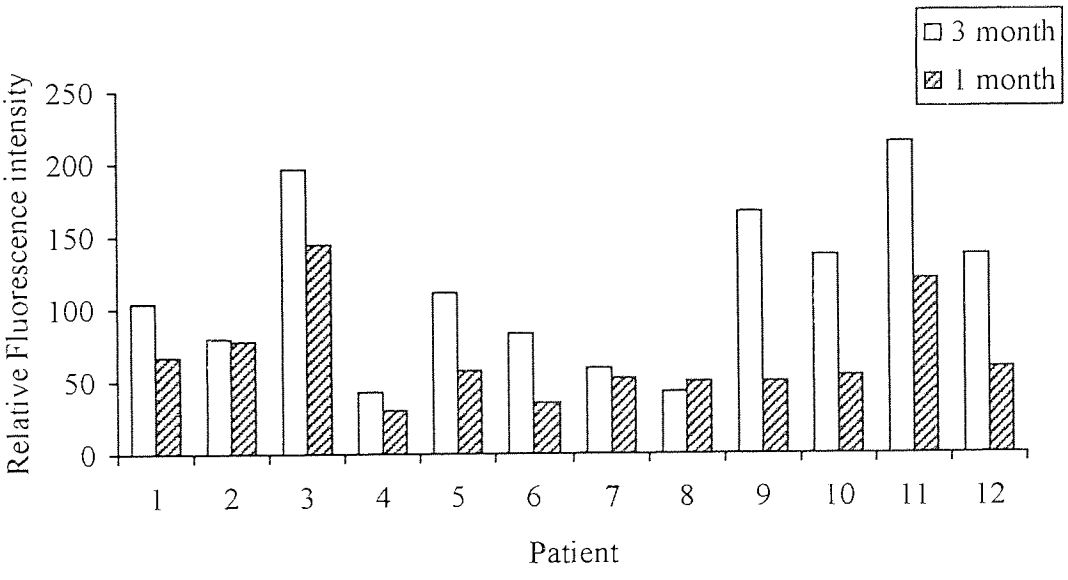

Figure 7.33 The average lipid deposition of three Precision UV lenses worn for one month compared to one worn for three months, analysed using fluorescence spectroscopy

7.10.3 The effect of wear time on the levels of deposition

It has been shown previously that lipid deposition varies both between eyes and between patients. Protein deposition is much more dependent upon water content and ionicity of the material, whereas lipid deposition is very subject dependent. Figure 7.33 shows that for some patients lipid deposition is lower on the lenses worn for one month than those worn for three months. However, some patients deposited similar amounts of lipid irrespective of the wear time. As expected the lipid results show much greater patient variation than the protein results.

Protein results show that the deposition is lower for the lenses worn for one month, than those worn for three months, with fewer differences between patients. This indicates that reducing the wear time will reduce the amount of deposition, as it appears to increase with wearing time[222]. The initial layer of deposition will act as a site for further deposition. Thus backing up the manufacturers recommendation of a one month wear schedule.

7.11 One Day wear study

The previous study showed how the length of time a lens is worn can effect the deposition. By reducing the wear period deposition, in particular protein, can be reduced. Therefore lenses can be replaced on a regular, planned basis before lenses become too heavily spoilt and uncomfortable to wear. The aim of this study is to examine the amount of deposition that can occur after only one days wear.

7.11.1 Methodology

Twenty patients wore one of two lens types in both eyes for 28 consecutive days, having a new pair every day. At the end of that period, the second lens type was worn in the same manner for 28 days. The two lenses investigated were Acuvue and Medalist 66, as shown in table 7.10.

Lens	Acuvue	Medalist 66
EWC	58 %	66 %
Monomers	HEMA + MAA	HEMA + VP
Manufacturer	Vistakon	Bausch & Lomb
FDA Group	IV	II
USAN	Etafilcon A	Alphafilcon A
Manufacture	Moulded	Moulded
ACLM	Filcon 1b	Filcon 4a
Centre thickness	0.07 mm	0.11 mm

Table 7.10 Characteristics of Acuvue and Medalist 66 contact lenses

Lenses were removed at the end of each day, after the patient had wiped their hands with an alcohol wipe to remove contamination of the lenses that may occur with the transfer of skin lipids. The removed lenses were placed in glass vials, refrigerated and left to dehydrate prior to analysis. Lenses were rehydrated using saline solution for at least two days before analysing them using fluorescence spectrophotometry, which was followed by other destructive techniques.

7.11.2 Results

Fluorescence was carried out on lenses worn on selected days only, due to the vast number of lenses worn during this study. All lenses worn on days 1, 7, 14, 21 and 28 were analysed. For a few patients, lenses worn every other day were also examined. The results for one patient wearing both lenses over the 28 days are shown in figures 7.34 and 7.35.

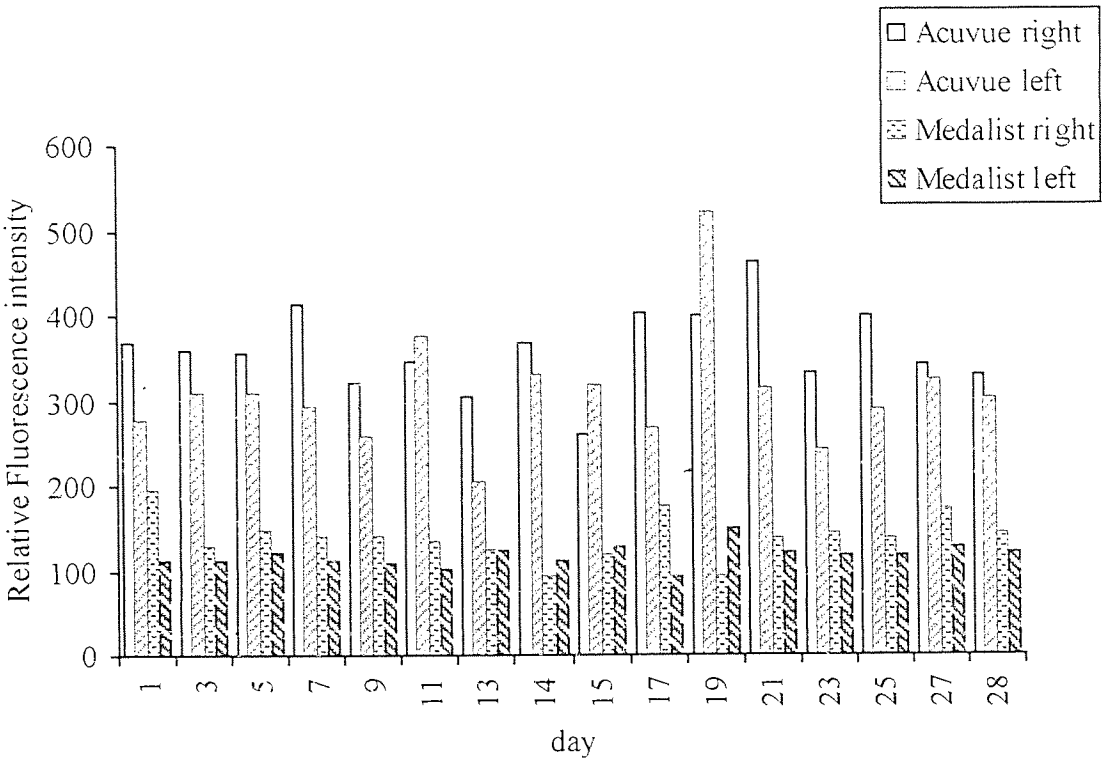

Figure 7.34 Protein deposition on Acuvue and Medalist 66 contact lenses that have each been worn for one day over a 28 day period

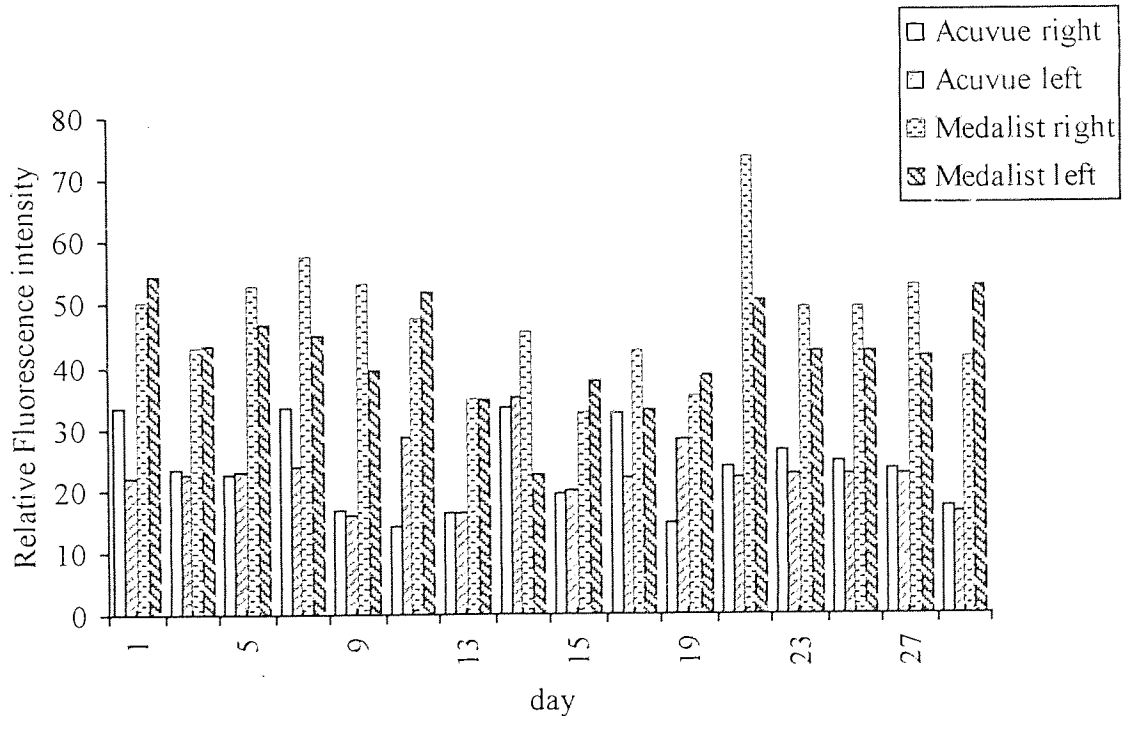

Figure 7.35 Lipid deposition on Acuvue and Medalist 66 contact lenses that have each been worn for one day over a 28 day period

Figures 7.36 and 7.37 show the mean values for both lenses for four patients.

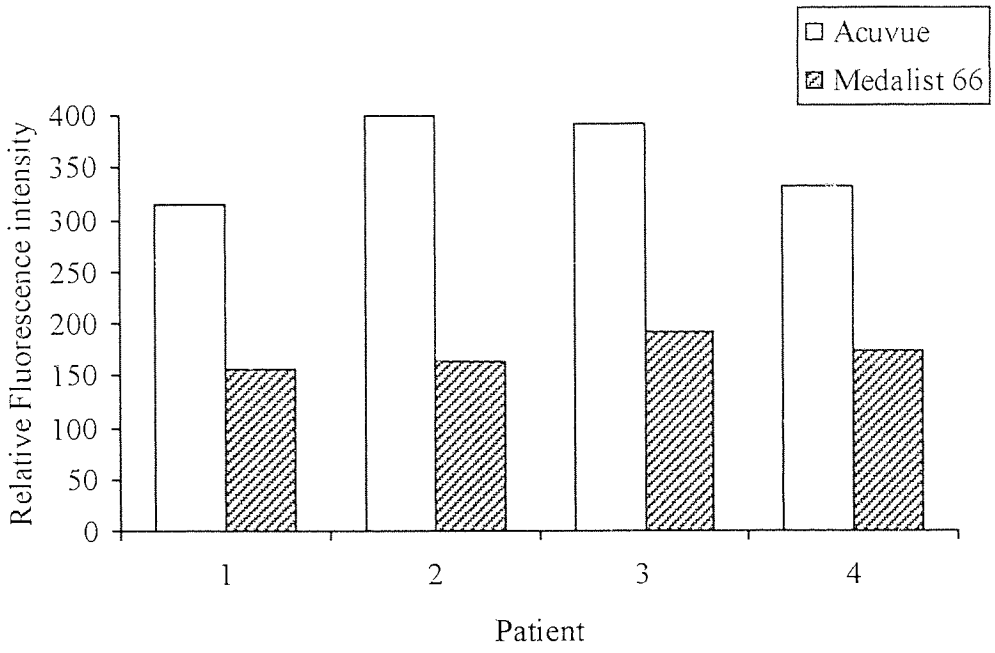

Figure 7.36 Average protein deposition of lenses that have been worn for one day from a 28 day period

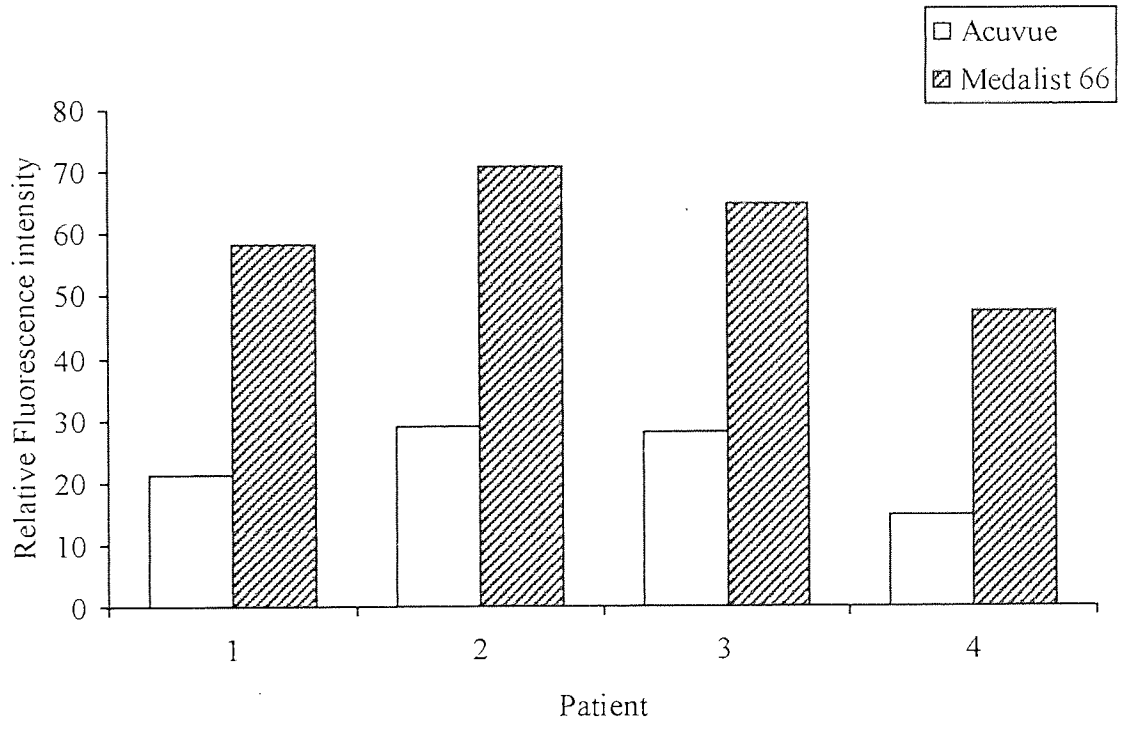

Figure 7.37 Average lipid deposition of lenses that have been worn for one day from a 28 day period

Figures 7.38 and 7.39 show the average protein and lipid deposition for all of the right Acuvue and Medalist lenses worn by each patient.

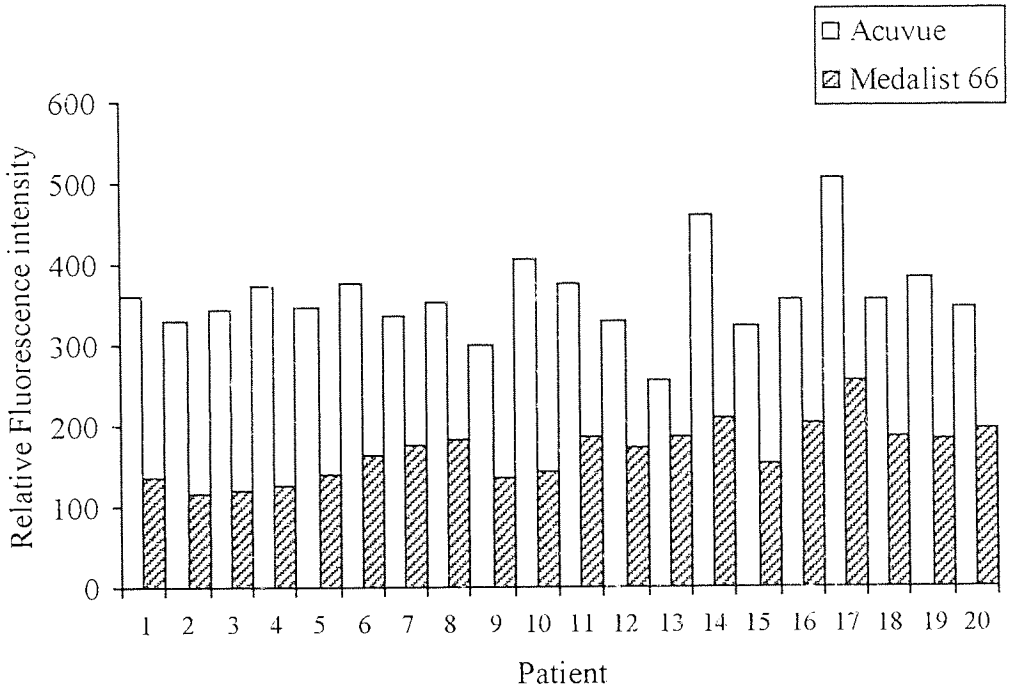

Figure 7.38 Graph comparing the average protein deposition on Acuvue and Medalist 66 contact lenses that have been worn for one day

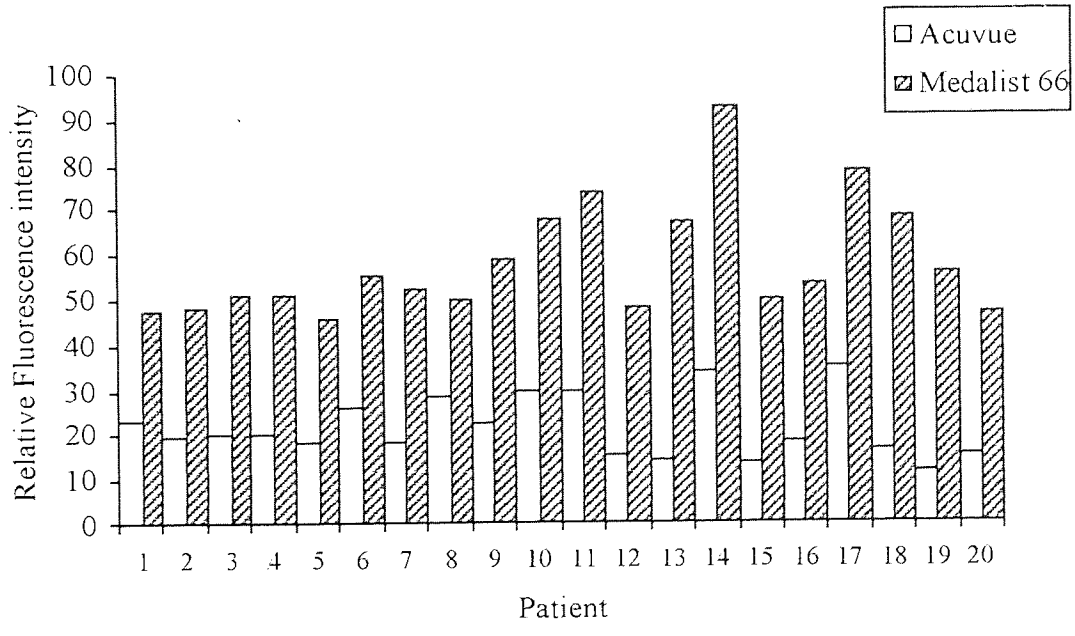

Figure 7.39 Graph comparing the average lipid deposition on Acuvue and Medalist 66 contact lenses that have been worn for one day

Figure 7.40 shows the bulk versus the surface protein obtained for each lens type. The total or bulk protein values are obtained using UV spectroscopy, and the surface values by fluorescence spectrophotometry.

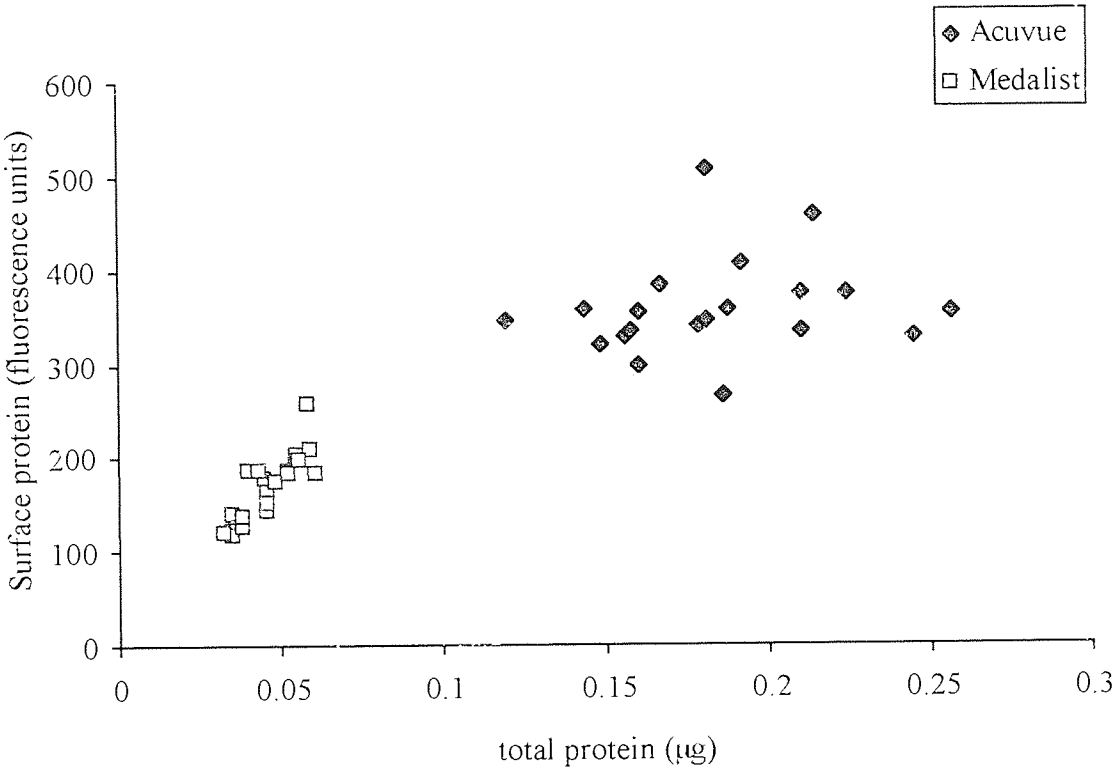

Figure 7.40 Surface versus total protein deposition for Acuvue and Medalist 66 contact lenses that have been worn for one day

7.11.3 The effect of One Day Wear

It can be seen in figures 7.34 and 7.35, that there are differences between deposition on the same lens type in the right and left eyes, which are detected using fluorescence even after only one days wear. There is considerable variation over the 28 days of wear by the same patient for both the group II and group IV lenses, suggesting that extrinsic factors play an important role in the level of deposition, not just the tear chemistry of the individual.

Deposition has been observed within minutes of the lens being inserted in the eye[26] and significant levels can be observed following just one days wear, which is typically 8 hours wear. The differences that may occur due to the level of patient compliance with cleaning regimes are removed, though it has been observed that finger lipids can be transferred to the lens upon insertion and removal[60], so the level transferred will differ among patients depending upon the method and care taken when this is undertaken. It is felt that the initial layer of deposition, forming a biofilm, may not be entirely detrimental, but will aid in making the surface more wettable, as initially the contact lens will be hydrophobic, so the biofilm will aid in making the lens more biotolerant[223].

Even after one days wear differences can be seen which are attributable to the material. The lipid deposition is greater for the group II lens which would be expected due to the presence of NVP, and protein levels were higher for the group IV lens. A potential problem that may occur with the one day lenses containing NVP is the toxicity of any unreacted monomer that is not removed from the storage solution. Each day the eye would be exposed to a relatively high level of the toxic component, which could cause problems with long term wear of these lenses[213].

Figure 7.40, indicates that for the group II lens, the amount of protein on the surface and the total protein shows a good correlation, whereas for the group IV lens the results are more broadly scattered. This suggests that for a group II lens the protein is located at the surface, whereas in a group IV lens, the protein is also located within the matrix. Lysozyme was found to penetrate into the matrix of the group IV lens, but this protein is mobile and would also leach back into any storage solution, or the tear film. Therefore, the storage solution for the group IV lenses should also be investigated, to establish the amount of protein that leaches out into solution.

7.12 Conclusions

The eye is an excellent site for studying the interaction of a synthetic material with a complex biological fluid. Spoilation of contact lenses is not a unique phenomenon, but the same underlying principle is also responsible for blood clotting on foreign surfaces and dental plaque formation. The eye therefore presents an ideal opportunity for *in vivo* studies which can be carefully controlled and do not require complicated or invasive surgery.

Fluorescence spectrophotometry is a very good technique for examining the surface of contact lenses. This non-destructive, sensitive technique allows differences to be seen on individual lenses, even after a few minutes wear. The sensitivity of the technique allows many variables that affect spoilation to be examined. It has been observed that spoilation is dependent on many factors. There are significant differences between right and left eyes for the same patient, which means that when a study involves wearing different lenses in each eye, this must be taken into account. The differences are due to the tear chemistry in each eye being independent of each other. Material characteristics also play an important role in determining the level of deposition on the lens, along with the length of time that it is worn for, and the care regime that is employed. Many extrinsic factors can also affect the type and level of spoilation encountered.

It is very clear that spoilation is dependent upon the individual. Tear chemistry varies from person to person, particularly in lipid composition. There are also observable differences between the right and left eyes of the same patient. Nobody will deposit exactly the same level of protein and lipid for the same lens worn for the same period of time. It is not just the tear chemistry that determines the level of spoilation. The composition of the tear film can be affected by many extrinsic factors, including diet, alcohol consumption and cosmetics. This may include air conditioning which will cause the lens to dry out. Another important consideration is patient compliance with the cleaning protocol. There will be differences in the amount of time taken over lens care

and wear, and with rub-&-rinse systems the length of time rubbing will vary from day to day and patient to patient.

Whilst there are many patient dependent factors influencing the degree of spoilation, it is also apparent that the material plays an important role. Generalisations can be made by considering the chemical composition of the lenses.

Protein deposition is largely influenced by the water content and ionicity of the material, whereas lipid is much more patient dependent, though in both cases extrinsic factors will also influence the degree and type of spoilation.

One of the major components of commercially available soft contact lenses is polyHEMA. HEMA dissociates forming methacrylic acid, which has a negative charge. This causes a negative charge on the contact lens surface, making it more susceptible to spoilation especially from positively charged proteins like lysozyme.

Group II lenses, which are high water content, and non-ionic, have shown the highest level of lipid deposition. This was even more pronounced in those lenses containing N-vinyl pyrrolidone. This is due to the increased lipid solubility and the blockiness of NVP when it is polymerised with HEMA. NVP has been used as a transdermal penetration enhancer[216]. Group IV lenses deposit high levels of protein, in particular lysozyme, which can penetrate into the polymer matrix due to the anionic nature of the lens surface attracting the positively charged protein.

A layer of deposition is not necessarily a disadvantage to the wearer. The lens may want some coating to act as a biofilm, to make the naturally hydrophobic lens surface hydrophilic and therefore more wettable and so comfortable to wear. In time, surfactant cleaning or disinfection may produce conformational and chemical changes to the deposits which may cause tear film disruption.

Deposition builds up over time, which may reduce comfort, acuity and invoke an inflammatory response such as acute red eye syndrome or giant papillary conjunctivitis.

The results given here are mainly from fluorescence spectrophotometry. To gain a full understanding of the exact species deposited and the sequence of events which lead to it, other analytical techniques must be used in conjunction with fluorescence. The details of which are beyond the scope of this thesis. High performance liquid chromatography (HPLC) and electrophoresis are examples of destructive techniques that can be used to identify individual components of spoilation.

There are several sources of error for fluorescence spectrophotometry. Care must be taken to ensure that the lens is positioned in the analysing cuvette in the same way, and that the cuvette is clean. It must also be noted which surface is being investigated. Fluorescence is a surface technique, so the surface closest to the excitation beam source is the one analysed. Differences were found in the levels of deposition of the anterior and posterior surfaces of the contact lens. Protein will leach into the storage solution, so over time the anterior and posterior surfaces will show similar degrees of deposition. Lipid is less mobile, and becomes bound to the lens matrix. Deposition levels were found to be higher on the anterior contact lens surface, that is the surface not resting against the eye. This surface will be constantly refreshed with new tear fluid during the blink cycle, increasing the potential levels available for deposition. The effect of any UV blocker or visual tint on the recorded fluorescence must be fully investigated, and the power of the lens must be taken into account.

It is evident that the degree of spoilation is dependent upon many factors. Various methods have been utilised to reduce the amount and type of spoilation present on contact lenses, including frequent replacement wear schedules and the biomimetic approach to the manufacture of contact lenses. The complete eradication of spoilation

is not possible. Deposition is very much dependent upon both the individual and the chemical composition of the material used.

CHAPTER 8

Conclusions and Suggestions for Future Work

8.1 Conclusions

The aim of this thesis was to investigate the use of synthetic hydrogels in three specific applications in the eye, namely, keratoprosthesis, a temporary mask for laser ablation, and soft contact lenses. Each application requires particular characteristics, which can be controlled by the choice of the constituent monomers in the hydrogel. The interaction between a synthetic material and a complex biological fluid is relatively easy to study in the eye as there is no need for complex or invasive surgery, and the material is retrievable allowing analysis to be undertaken. The spoilation of contact lenses has been studied to investigate this reaction, which is comparable to the interaction when any other material is placed into a biological environment, for example, blood clotting or plaque formation.

There have been significant improvements in the field of corneal transplantation's, which restores sight for many people. However, this is not always a viable option. Repeated graft failures, certain diseases and a shortage of corneal donors means that for some patients the only hope of any visual improvement lies in the use of an artificial cornea, or keratoprosthesis, KPro.

A series of hydrogel polymers were synthesised to investigate their use as potential materials for use as an artificial cornea. For a truly synthetic cornea the material would need to display epithelial downgrowth over the anterior surface, though non on the posterior surface, as this would lead to the extrusion of the device. It will be optically clear and mechanically strong enough to withstand the surgical procedure and *in situ* stresses of the eye. Keratoprostheses were first suggested in the eighteenth century, with many designs and materials considered since then to form an artificial cornea. One of the major advances occurred when the need for a porous periphery around a clear optical core was recognised. This allows for cellular ingrowth from the host cornea, forming a water-tight junction between the prosthesis and the eye. The literature survey in chapter 2, showed the vast number of materials that have been utilised as the skirt

material, which surround a PMMA optical core. In recent years, hydrogels have been studied as possible materials for an artificial cornea. One of the advantages this would bring, is that a contact lens like prosthesis could be used as opposed to the more bulky one with a PMMA cylinder that extends beyond the periphery.

A series of homogenous hydrogel copolymers were synthesised which had compositions similar to that of commercially available contact lenses, and those that had been investigated in the search for a synthetic articular cartilage. These materials were characterised, and their spoilation and cellular response investigated. Acryloyl morpholine was used as an alternative to NVP, as the polymers produced are not as 'blocky' due to the increased reactivity of AMO to radical polymerisation. The properties of the NVP and AMO polymers are very similar. HEMA was replaced by a series of heterocyclic monomers. Cell adhesion to HEMA is poor, and the heterocyclics had been investigated as alternative materials for PMMA in dental applications, so toxicity had already been considered.

The preliminary cytotoxicity and spoilation investigations of these materials showed that there was no adverse response, and that the spoilation was comparable to several commercially available contact lenses. However, the mechanical properties were not sufficient to withstand the surgery or *in situ* stresses. A series of semi interpenetrating polymer networks were synthesised, based on the copolymer compositions. The technology was based upon that previously used to investigate the use of a hydrogel as synthetic articular cartilage. Initial studies on the interpenetrant revealed that CAB would not be successful in this application as the polymers produced were opaque. Studies were therefore confined to using an ester polyurethane as the interpenetrant. Again these materials were fully characterised, and exhibited enhanced mechanical properties. The Cytotoxicitiy tests were favourable and the spoilation results showed no increase in the level of deposition.

One of the major problems encountered by previous devices was the lack of integration between the porous periphery and the optical core. To overcome this, the porous periphery was made from the same material as the core, with the addition of dextran and dextrin to form pores and channels respectively. The morphology required for the periphery was investigated, this considered the pore size needed and whether it was preferable to have just pores or pores and channels. This involved cytotoxicity testing with 3T3 Swiss mouse embryo cells, followed by subcutaneous implantation in rats. The initial results indicate where there were pores, infiltration of the cells did occur, and it was more pronounced when both pores and channels were present. Infiltration was not observed with pores smaller than 63 microns. No adverse inflammatory response was reported for the materials which were implanted for up to one month subcutaneously. The materials did not degrade during the course of implantation.

Several methods of manufacture of a prosthetic device were studied. These were based upon techniques used in the manufacture of contact lenses. The major difficulty was to get the porous periphery polymerised around the optically clear core, with integration between the two components to ensure a water-tight junction is formed. Three methods of manufacturing the device were studied, rotational, rod and button methods. The best results to date were found using the rod method.

Laser surgery is being used increasingly to correct refractive defects. However, if any irregular corneal surface is ablated, the cornea retains the irregularity following exposure to the laser. A review of the literature revealed that relatively little work has been carried out to try to find a mask for the cornea which would allow a smooth surface to be obtained following ablation. Initial studies had indicated that ablation rate was related to the water content of the mask, so a series of hydrogels were synthesised which had an equilibrium water content similar to that of the cornea, which is approximately 80%. A monomer mixture would be placed on the eye underneath a mould, which would be of a suitable viscosity to be able to fill in any irregularities on the corneal surface. The

As the hydrogel is polymerised on the eye, water must be present in the starting mixture, as leaving the xerogel to hydrate following polymerisation is not feasible in this case. Water soluble polymers, that had previously been utilised in various ophthalmic preparations, were used as the main polymer backbone, as the toxicity had already been studied. Initial attempts to modify the polymer backbone lead to problems in controlling the position and amount of modification, as well as lack of water solubility in the product and potential problems with toxicity. This lead to investigations based on aqueous solutions of two water soluble polymers, polyvinyl alcohol and hydroxypropyl methylcellulose, polymerised with polyethylene glycol, PEG, derivatives.

A series of high water content hydrogels were synthesised, for which a water soluble photoinitiator was required. Initial experiments with riboflavin proved unsuccessful, as even after exposure to the UV source for three hours, no membrane was formed. An alternative, Irgacure 184, was used in subsequent studies, which bought the polymerisation time down to minutes.

Various options were investigated, including the amount and length of PEG chain, the molecular weight and amount of the water soluble polymer used, and the resulting hydrogels were all characterised. Several ways of controlling the water content and mechanical properties were found, so that once all the factors that contribute to the ablation rate can be determined, the most suitable system can be used. Water, and a water-glycerol mixture were also considered as the diluent, as any factor that would restrict surface evaporation during the procedure would be an advantage.

Fluorescence spectrophotometry was developed as an analytical technique for studying the protein and lipid deposition on contact lenses. A new instrument was used, so initial studies were required to ascertain reproducible operating conditions and parameters, and calibrate the machine with one that had previously been used. Fluorescence is a sensitive technique, making it essential that the cuvette used in the machine was kept clean, and that the orientation of the contact lens relative to the excitation beam was kept constant. It is a useful technique for studying the surface of contact lenses as it is very sensitive,

water-glycerol mixture were also considered as the diluent, as any factor that would restrict surface evaporation during the procedure would be an advantage.

Fluorescence spectrophotometry was developed as an analytical technique for studying the protein and lipid deposition on contact lenses. A new instrument was used, so initial studies were required to ascertain reproducible operating conditions and parameters, and calibrate the machine with one that had previously been used. Fluorescence is a sensitive technique, making it essential that the cuvette used in the machine was kept clean, and that the orientation of the contact lens relative to the excitation beam was kept constant. It is a useful technique for studying the surface of contact lenses as it is very sensitive, non-destructive, quick and reproducible. The levels of protein and lipid deposition on the surface would be extremely difficult to monitor using any other technique. Differences are observable between the types of materials worn, patients and even right and left eyes of the same patients. The technique is sensitive enough to examine each lens individually, as opposed to other techniques which involve pooling many lenses together. However, it is not able to distinguish individual components.

Several clinically controlled studies were carried out on worn contact lenses, to determine the factors that influence the type and level of deposition. Each study revealed that there were significant inter patient differences observed in the level of spoilation. This is due to the variation in the tear chemistry of individuals. It was also seen that there were often considerable differences between the right and left eyes of the same patient. It is not possible to determine precisely how any particular patient will deposit on a specific lens, though generalisations can be made. The water content, degree of ionicity and chemical composition of contact lenses all play a part in governing the type and level of spoilation.

Lenses containing NVP display increased lipid deposition. NVP when copolymerised with HEMA will form 'blocky' polymers due to its low reactivity ratio. This leads to areas that promote lipid deposition. A biomimetic approach has been investigated in an attempt to reduce the level of spoilation.

Deposition occurs rapidly once a hydrogel is placed in the eye. The initial layer acts as a site for further deposition, so there is a build up over time. Several methods for controlling deposition have been tried. One day wear lenses remove the need for any cleaning, or potential for any significant build up of deposition, as they are worn for a very short period of time before being discarded. Frequent replacement wear schedules have been introduced, so that lenses are replaced on a regular basis. Daily wear lenses require cleaning following removal from the eye and prior to reinsertion the following day. Studies have shown that the cleaning solutions available are not able to remove all of the deposited layers.

The *ex-vivo* studies carried out using fluorescence spectrophotometry have shown that there are many factors that contribute to the spoilation of soft contact lenses. These include the method of manufacture of the lens, extrinsic factors (cosmetics, nicotine), chemical composition and water content of the lens, wear schedule, compliance to the cleaning regime and the tear chemistry of the individual.

8.2 Suggestions for future work

The success of any material placed in the body is ultimately determined by the biotolerance of that material.

A reproducible technique for producing a keratoprosthetic device needs to be further investigated. It is important to study the device as a whole, not just its component parts. It is imperative that the interface is well integrated, so that it will not fall apart under stress, and the hydrating does not compromise the integration due to the different

swelling characteristics that will be displayed as the core and skirt materials have slightly differing water contents. Therefore a reproducible manufacturing method needs to be ascertained, and the correct dimensions of the device determined.

Further implantation studies will show whether the material selection is correct and how it react when inserted into the body. Keratocyte work is essential to determine how it will interact with cells once placed in the eye. The implantation work should also indicate any modifications that may be required regarding the surgical procedure. The morphology of the periphery is important, and further implantation work is being undertaken to assess the optimum pore size, distribution, and depth into the material the pores and channels must exist to achieve good anchorage with the surrounding material.

Long term implantation studies must be undertaken. This will indicate the viability of the device, whether extrusion, retroprosthetic membrane formation or tissue melting occurs The device is essentially an extended wear contact lens, so the spoilation of the surface must also be taken into account, as there is no means of taking it out to clean. Ultimately the device needs to be implanted in eye, to determine whether any problems are encountered. Further studies may also involve surface treatment to promote or deter epithelial treatment, or looking at incorporation of a drug delivery system within the prosthesis.

For the laser ablation mask, a suitable mould and UV source must be investigated. The polymerisation time should be kept to a minimum, which may involve modification of the polymer backbone to introduce the necessary umber of double bonds. Toxicity of the material should also be considered, even though it will only be placed on the eye for a short period of time. Polymerisation may cause localised heating effects, which need to be carefully controlled so that no damage is caused to the cornea. A Tearscope is being investigated as the source to initiate polymerisation. This is used by

ophthalmologists to examine the eye, with a wavelength that does not cause any problems to the eye.

The surgical requirements of the hydrogel must be taken into account. The viscosity of the starting solution that is needed to fill in the irregularities on the corneal surface, the volume of monomer mixture required and over what area it will be placed need to be considered. Extensive laser ablation studies need to be carried out on the hydrogels to determine the factors that contribute to the ablation rate. Operating conditions for the laser should also be considered.

Many of the soft contact lenses becoming available recently contain a UV blocker, and many have a visual tint added. If fluorescence spectrophotometry is to be used to study the protein and lipid deposition on the lenses, the effects these components have on the observed fluorescence must be studied. It has been observed that the deposition varies on the anterior and posterior surfaces of the lenses, As fluorescence is such a sensitive technique, it could be utilised to study this further.

A unique feature of the fluorimeter used is its ability to perform three dimensional scans. These could be further studied to verify that the excitation wavelengths used are giving the maximum information, and whether the 3D image is characteristic of the polymer base of the deposited layers. If a fluorescence spectra of a lens and a patients tear film could be taken and used to predict how that patient would deposit on that lens, a lot of clinical time may be saved, as it would eliminate any material that the patient will be a high depositor on.

REFERENCES

1 Tighe, B.J., Hydrogels as contact lens materials, in Hydrogels in Medicine and Pharmacy, Vol. 3, Properties and Applications, Ed. Peppas, N.A., CRC Press, Boca-Raton, Florida, 1987, 53-82

2 Percival, S.P.B., and Jafree, A.J., Preliminary results with a new hydrogel intraocular lens, Eye, 1994, **8**, 672-675

3 Corkhill, P.H., Hamilton, C.J., and Tighe,B.J., Design of hydrogels for medical applications, Critical Reviews in Biocompatibility, 1990, **5**, 4, 363-436

4 Hicks, C., Artificial corneas - the search continues, Optician, 1995, Aug. 25, 15-17

5 Marshall, J., Excimer lasers in ophthalmology, Optician, 1987, Nov. 13, 15-24

6 Wichterle, O , and Lim, D., Hydrophilic gels for biological use, Nature, 1960, **185**, 117-118

7 Mackay T.G, Wheatley, D.J., Bernacca, G.M., Fisher, A.C., and Hindle, C.S., New polyurethane heart valve prostheses, Biomaterials, 1996, **17**, 19, 1857-1863

8 Ambrosio, L., Netti, P.A., Iannace, S, Huang, S.J., and Nicolais, L., Composite materials for invertebral disc prostheses, J. Mat. Sci., Mats. in Med., 1996, 7, 251-254

9 Netti, P.A., Shelton, J.C., Revell, P.A., Pirie, C., Smith, S., Ambrosio, L., Nicolais, L., and Bonfield, W., Hydrogels as an interface between bone and an implant, Biomaterials, 1993, **14**, 14, 1098-1104

10 Tighe, B.J., Towards the bionic man; Current trends in development of biomaterials, Int. Ind. Biotech., 1986/7, Dec./Jan., 204-210

11 Oxley, H.R., Corkhill, P.H., Fitton, J.H., and Tighe, B.J., Macroporous hydrogels for biomedical applications, Biomaterials, 1993, **14**, 14, 1064-1072

12 Packard, R.B.S., Garner, A., and Arnott, E.J., PolyHEMA as a material for IOL implantation : Preliminary report, Brit. J. Ophth, 1981, **65**, 585-587

13 Pedley, D.G., Skelly, P.J., Tighe, B.J., Hydrogels in biomedical applications, Brit. Pol. J., 1980, **12**, 99-110

14 Tighe, B.J., Hydrogel materials: Patents and products, parts I and II, Optician, 1989, June 2, 17-24, and July 7, 17-22

15 Corkhill, P.H., Novel hydrogel polymers, Ph.D. thesis, Aston University, 1988

16 Corkhill, P.H., Jolly, A.M., Ng, C.O., and Tighe, B.J., Synthetic hydrogels 1. Hydroxyalkyl acrylate and methacrylate copolymers - water binding studies, Polymer, 1987, **28**, 1758-1766

17 French, K.A., Novel cationic polymers for use at biological interfaces, Ph.D. thesis, Aston University, 1996

18 Ma, J.J., Novel hydrogel polymers, Ph.D. thesis, Aston University, 1996

19 Roodra, W.E., de Bleyser, J., Junginger, H.E., and Leyte, J.C., Nuclear magnetic resonance relaxation of water in hydrogels, Biomaterials, 1990, **11**, 17-23

20 Tighe, B.J., and Trevett, A.S., Characterisation of mechanical properties of soft contact lenses, BCLA Annual Clinical Conference, Glasgow, May 1990, reprinted in BCLA Transactions 1990, **13**, 2, 57-61

21 Hamilton, W.C., A technique for thew characterization of hydophilic solid surfaces, J. Coll. Interface. Sci., 1972, **40**, 2, 219-222

22 Domingue, J., Probing the chemistry of the solid/liquid interface, Am. Lab. 1990, **22**, 18, 50-53

23 Olson, A.P., Contact lens properties: Wettability and adsorption, Optometric Monthly, 1982, July, 376-380

24 Tretinnikov, D.H., Dynamic wetting and contact lens hystersis of polymer surfaces studied with the modified Wilhelmy balance method, Langmuir, 1994, 10, 1606-1614

25 Franklin, V.J., Lipoidal species in ocular spoilation processess, Ph.D. thesis, Aston University, 1990

26 Sariri, R., Tear protein interaction with hydrogel contact lenses, Ph.D. thesis, Aston University, 1995

27 Baker, D.A., Corkhill, P.H., Ng, C.O., Skelly, P.J., and Tighe, B.J., Synthetic hydrogels 2: Copolymers of carboxyl, lactam and amide containing monomers: Structure/property relationships, Polymer, 1988, **29**, 691-700

28 Barnes, A., Corkhill, P.H., and Tighe, B.J., Synthetic hydrogels 3: Hydroxylalkyl acrylate and methacrylate copolymers: Surface and mechanical properties, Polymer, 1988, **29**, 2191-2202

29 Lydon, F.J., Novel hydrogel copolymers and semi-interpenetrating polymer networks, Ph.D thesis, Aston University, 1996

30 Spering, L.H., Interpenetrating polymer networks and related materials, Plenum Press, New York, 1981

31 Barrett, L.W., and Sperling, L.H., Today's interpenetrating polymer networks, TRIP, 1993,**1**, 2, 45-49

32 Corkhill, P.H., Fitton, J.H., and Tighe, B.J., Towards a synthetic articular cartilage material, J. Biomat. Sci. Pol. Ed., 1993, **4**, 6, 615-630

33 Molyneux, P., Water soluble polymers: Properties and behaviour, CRC Press, Inc, Boca Raton, Florida, 1991

34 Water soluble polymers, in Encyclopaedia of Polymer Science, Vol 17,730-784 Wiley Interscience, New York. 1991

35 Cowie, J., Polymers: chemistry and physics of modern materials, 2nd Ed., Blackie Academic and Professional, London, 1991

36 Shaw, D.J., Introduction to colloid and surface chemistry, 4th Ed., Butterworth Heinemann, Oxford, 1992

37 Young, R.A., Rebiex, V., and Tighe, B.J., Tears, solutions and contact lens comfort: the role of biotribiology and surface chemistry, Poster presented at BCLA conference, Bournemouth, 1997

38 Baker, D. and Tighe, B.J., Polymers in contact lens applications (VIII): Problems of biocompatibility, Contact Lens J., 1981, **10**, 3, 3-14

39 Tighe, B.J., Blood, sweat and tears or some problems in design of biomaterials, Nissel Memorial lecture (invited), Royal Society of Medicine, London, Feb. 1989. Reprinted in B.C.L.A. Transactions, 1990, **13**, 1, 13-19

40 Franklin, V.J., Bright, A.M., and Tighe, B.J., Hydrogel polymers and ocular spoilation processes, TRIP, 1993, **1**, 1, 9-16

41 Hyon, S., Cha, W., Ikada, Y., Kita, M., Ogura, Y., and Honda, Y., Polyvinyl alcohol hydrogels as soft contact lens materials, J. Biomat. Sci. Pol. Ed., 1994, **5**, 5, 397-406

42 Bray, J.C., and Merril, E.W., PVA hydrogel for synthetic articular cartilage material, J. Biomed. Mater. Res., 1973, **7**, 431-443

43 Trevett, A.S., The mechanical properties of hydrogel polymers, Ph.D. thesis, Aston University, October 1991

44 Wang, H., Prendiville, P.L., McDonnell, P.J., and Chang, W.V., An ultrasonic technique for the measurement of the elastic moduli of the human cornea, J. Biomechanics, 1996, **29**, 12, 1633-1636

45 Wolffs anatomy of the eye and orbit, 7th Ed., Lewis & Co. London, 1976

46 Tighe, B.J., Eye contact, Chemistry in Britain, 1992, **28**, 3, 241-244

47 Bright, A.M., and Tighe, B.J., Composition and interfacial properties of tears, tear substitutes and tear models, J. BCLA, 1993, **16**, 2, 57-66

48 Bright, A.M., Towards an improved ocular drug delivery system, Ph.D. thesis, Aston University, 1992

49 Chirila, T.V., Modern artifical corneas: Use of porous polymers, TRIP, 1994, **2**, 9, 296-300

50 Larke, J.R., Ng, C.O., and Tighe, B.J., Hydrogel polymers in contact lens applications: Survey of existing literature, parts I and II, Optician, 1971, Dec. 3, 12-16, and Dec. 10, 12-16

51 Contact Lens Manual, Burnett-Hogg, N., Butterworth Heineman, 1989

52 Bowers, R.W.J., and Tighe, B.J. Studies of the ocular compatibilty of hydrogels. A review of the clinical manifestaions of spoilation, Biomaterials, 1987, **8**, 3, 83-88

53 Franklin, V.J., Bright, A.M., Pearce, E., and Tighe, B.J., Hydrogel lens spoilation 5: Tear proteins and proteinaceous films, Optician, 1992, Sept. 4, 16-26

54 Franklin, V.J., Pearce, E., and Tighe, B.J., Hydrogel lens spoilation 3: Deposit formation and the role of lipids, Optician, 1991, Nov. 1, 19-26

55 Hart, D.E., Ma, O., Lane, B.C., Josephson, J.E., Tisdale, R.R., Gzik, M, Leahy, R., and Dennis, R., Spoilation of hydrogel contact lenses by lipid deposits, Ophthalmology, 1987, 94, 1315-1321

56 Abbott, J.M., Bowers, R.W.J., Franklin, V.J., and Tighe, B.J., Studies in the ocular compatibility of hydrogels 4: Observations on the role of calcium in deposit formation, J. BCLA, 1991, **14**, 1, 21-28

57 Franklin, V.J., Bowers, R., and Tighe, B.J., Hydrogel lens spoilation 4: The structure and composition of surface films and plaques, Optician, 1992, Feb. 7, 30-34

58 Franklin, V.J., and Tighe, B.J., Hydrogel lens spoilation 1: Discolouration and staining processes within the lens matrix, Optician, 1991, **201**, 5299,16-22

59 Franklin, V.J., Bright, A.M., and Tighe, B.J., Hydrogel lens spoilation 6: Extrinsic contaminants and surfactant cleaners, Optician, 1993, July 2, 19-24

60 Tighe, B.J., Bright, A.M., and Franklin, V.J., Extrinsic factors in soft contact lens spoilation, J. BCLA, 1991, **14**, 4, 195-200

61 Gipson, I.K., and Surge, S.P., Corneal surfaces: Cell biology of corneal epithelium, chapter 1 in Principles and Practice of Ophthalmology, Eds. Albert, D.M., and Jakobiec, F.A., W.B. Saunders Co., Philadelphia, 1993

62 Bergmanson, J.P.G., An expert guide to contact lenses and the corneal epithelium, C.L. Spectrum, 1994, July, 34-39

63 Baron, N.A., Apparartus and process for recurving the cornea of an eye, US Patent, 4,461,294, 1984

64 Trokel, S.L., Srinivasan, R., and Braren, B., Excimer laser surgery of the cornea, Am. J. Ophth., 1983, **96**, 6, 710-715

65 Speidell, J.L., Pulaski, D.P., and Patel, R.S., Masks for laser ablation technology: new requirements and challenges, IBM J. Res. Dev., 1997, **41**, 1/2, 143-149

66 Snyder, R., and Klein, P., Laser vision correction 1: Understanding the tissue and beam interactions, C.L. Spectrum 1995, Nov., 34-40

67 Andrew J.E., Dyer, P.E., Forster, D., and Key, P.H., Direct etching of polymeric materials using a XeCl laser, App. Phys. Letts., 1983, **43**, 717-719

68 Pettit, G.H., Ediger, M.N., and Weiblinger, R.P., Excimer laser ablation of the cornea, Optical Engin., 1995, **34**, 3, 661-667

69 Bergmanson, J., and Sheldon, T.M., Current status of photrefractive keratectomy, Optician, 1994, Oct. 21, 20-24

70 Talamo, J.H., Steinert, R.F., and Puliafito, C.A., Update on laser corneal surgery, in Refractive Surgery, Int. Ophth, Clinics, 1991, **31**,. 1, Winter, 13-23

71 Puliafito, C.A., Steinert, R.F., Deutsch, T.F., Hillenkamp, F., Dehm, E.J., and Alder, C.M., Excimer laser ablation of the cornea and lens, Ophthalmology, 1985, **92**, 741-748

72 Ren, Q., Simon, G., and Parel, J-M., Ultraviolet solid -state laser (213nm) photorefractive keratectomy, Ophthalmology, 1993, **100**, 1828-1834

73 Marshall, J., Trokel, S., Rothery, S., and Schubert, H., An ultrastructural study of corneal incisions induced by an excimer laser at 193nm, Ophthalmology, 1985, **92**, 749-758

74 Dehm, E.J., Puliafito, C.A., Adler, C.M., and Steinert, R.F., Corneal endothelial injury in rabbits following excimer laser ablation at 193 and 248nm, Arch. Ophthal., 1986, 104, 1364-1368

75 DeVore, D.P., Scott, J.B., Nordquist, R.E., Hofman, R.S., Nguyen, H., and Eiferman, R.A., Rapidly poymerised collagen gel as a smoothing agent in excimer laser photoablation, J. Ref. Surg. 1995, **11**, Jan./Feb., 50-55

76 Krueger, R.R., and Trokel, S.L., Quantitation of cornal ablation by ultraviolet light, Arch. Ophthal., 1985, **103**, 1741-1742

77 Krauss, J., Puliafito, C.A., and Steinert, E.F., Laser interactions with the cornea, Surv. Ophth., 1986, **31**, 37-53

78 Marshall, J., Trokel, S., Rothery, S., and Krueger, R.R., A comparative study of corneal incisions induced by diamond and steel knives and two ultraviolet radiations from an excimer laser, Brit. J. Ophthal., 1986, **70**, 482-501

79 Hardten, D.R., and Lindstrom, R.L., Surgical correction of refractive errors after penetrating keratoplasty, in Current Concepts in Refractive Surgery, Int. Ophth. Clinics, Winter 1997, **37**, 1, 1-36

80 Campos, M., Wang, X.W., Hertzog, L., Lee, M., Clapham, T., Trokel, S.L., and McDonnell, P.J., Ablation rates and surface ultrastructure of 193nm excimer laser keratectomies, IOVS, 1993, **34**, 8, 2493-2500

81 Huebscher, H., Genth, U., and Seiler, T., Determination of excimer laser ablation rate of the human cornea using in vivo Scheimpflug videography, IOVS, 1996, **37**, 1, 42-46

82 Seiler, T., and McDonnell, P.J., Excimer laser photorefractive keratectomy, Surv. Ophth., 1995, **40**, 2, 89-117

83 Dougherty, P.J., Wellish, K.L., and Maloney, R.K., Excimer laser ablation rate and corneal hydration, Am. J., Ophth., 1994, **118**, 2, 169-176

84 Bor, Z., Hopp, B., Racz, B., Szabo, G., Marton, Z., Ratkay, I., Mohay, J., Suveges, I., and Fust, A., Physical problems of excimer laser cornea ablation, Optical Engin., 1993, **32**, 10, 2481-2486

85 Edmison, D.R., Complications of photorefractive keratectomy, in Current Concepts in Refractive Surgery, Int. Ophth. Clinics, Winter 1997, **37**, 83-94

86 Tuft, S.J., Zabel, R.W., and Marshall, J., Corneal repair following keratectomy, a comparison between conventional surgery and laser photoablation, IOVS, 1989, **30**, 8, 1769-1777

87 Marshall, J., Trokel, S.L., Rothery, S., and Krueger, R.R., Long-term healing of the central cornea after photorefractive keratectomy using an excimer laser, Ophthalmology, 1988, **95**, 1411-1421

88 Tuft, S.J., Gartry, D.S., Rawe, I.M., and Meek, K.M., Photorefractive keratectomy: implications of corneal wound healing, Brit. J. Optht., 1993, 77, 243-247

89 Taylor, D.M., L'Esperance, F.A., Del Pero, R.A., Roberts, A.D., Gigstad, J.E., Klintworth, G., Martin, C.A., and Warner, J., Human excimer laser keratectomy, Ophthalmology, 1989, **96**, 654-664

90 Marshall, J., Trokel, S., Rothery, S., and Krueger, R.R., Photoablative reprofiling of the cornea using an excimer laser: photorefractive keratectomy, Lasers in Ophth., 1986, **1**, 1, 21-48

91 Maloney, R.K., Friedman, M., Harmon, T., Hayward, M., Hagen, K., Gailitis, R.P., and Waring, G.O., A prototype erodible mask delivery system for the excimer laser, Ophthalmology, 1993, **100**, 542-549

92 Englanoff, J.S., Kolahdouz-Isfahani, A.H., Moreira, H., Cheung, D.T., Nimni, M.E., Trokel, S.L., and McDonnell, P.J., In situ collagen gel mold as an aid in excimer laser superficial keratectomy, Ophthalmology, 1992, **99**, 1201-1208

93 Wee, W.R., Nassaralla, B.A , Garbus, J., and McDonnell, P.J., Keratocyte-populated collagen gel as an in vitro model of excimer laser keratectomy, J. Ref. Surg., 1996, **12**, Jan./Feb., 98-102

94 Kornmehl, E.W., Steinert, R.F., and Puliafito, C.A., A comparative study of the masking fluids for excimer laser phototherapeutic keratectomy, Arch. Ophth., 1991, **109**, 860-863

95 Fasano, A.P., Moreira, H., McDonnel, P.J., and Sinbawy, A., Excimer laser smoothing of a reproducible model of anterior corneal surface irregularity, Ophthalmology, 1991, **98**, 1782-1785

96 Kubota, T., Seitz, B., Tetsumoto, K., and Naumann, G.O.H., Lamellar excimer laser keratoplasty: reproducible photoablation of corneal tissue, Doc. Ophth., 1992, **82**, 193-200

97 Spadaro, A., Battaglia, E., Mangiafico, S., and Vinciguerra, P., The potential use of sodium hyaluronate as a masking agent in excimer laser ablation and its comparison with hydroxypropyl methyl cellulose, IOVS, 1996 ,**36,** 4, 1245

98 Pallikaris, I.G., Margaritis, A.G., Lidataki, S., and Siganos, D.S., Potentialities of a new two component gel material as an aid in PRK and PTL remodeling on the rabbit cornea, IOVS, 1994, **35**, 4, 1298

99 Gallo, J.P., and Raizman, M.B., Phototherapeutic keratectomy for superficial corneal disorders, in Current Concepts in Refractive Surgery, Int. Ophth. Clinics, Winter 1997, **37**, 155-170

100 Fyodorov, S.N., Moroz, Z.I., and Zuev, V.K., Keratoprosthesis, Churchill, Livingstone, 1987

101 Trevor-Roper, P.D., The history of corneal grafting, in Advances in Prosthokeratoplasty, 1994

102 Barber, J.C., Keratoprostheses: Past and present, Int. Ophth. Clinics, 1988, **28**, 2, 103-109

103 Cardona, H., Keratoprosthesis, Am. J. Ophth., 1962, **54**, 284-294

104 Abel, R., Development of an artificial cornea 1: history and materials, in The Cornea: Transactions of the World Congress on the cornea III, Ed. D. Cavanagh, Raven Press, New York, 1988, 225-230

105 Mohan, M., and Panda, A., Artificial cornea, in The Cornea: Transactions of the World Congress on the cornea III, Ed. D. Cavanagh, Raven Press, New York, 1988, 383-385

106 Binder, H.F., and Binder, R.F., Experiments on plexiglass corneal implants, Am. J., Ophth., 1956, **41**, 793-797

107 Gasset, A.R., and Kaufman, H.E., Epikeratoprosthesis, replacement of superficial cornea by methyl methacrylate, Am. J. Ophth., 1968, **66**, 4, 641-645

108 Stone, W., Artificial corneal implants having a removable lens member, US Patent, 3,458,870, 1969

109 Stone, W., Artificial corneal implants, US Patent, 2,714,721, 1955

110 Evans, K.R., Lydon, F.J., Green, D.W., Tighe, B.J., and Liu, C.S.C., A brief history of artificial corneas, Poster presented at 8th Symposium Contact Lenses and Materials, New Orleans 1996

111 Cardona, H., Mushroom transcorneal keratoprosthesis, Am. J. Ophth., 1969, **68**, 4, 604-612

112 Cardona, H., Keratoprosthesis with a plastic fiber meshwork supporting plate, Am. J. Ophth., 1967, **64**, 228-233

113 Barber, J.C., Modifications of keratoprosthesis to improve retention, Ref. Corn. Surg., 1990, **9**, May/June, 200-201

114 Mortemousque, B., Dorot, N., Poirier, L., Williamson, W., Brousse, D., and Verin, P., Complication des keratoprostheses a fixation posterieure: les membranes retroprothetiques, J. Fr. Ophtalmol., 1995, **18**, 10, 608-613

115 Aquavella, J.V., Rao, G.N., Brown, A.C., and Harris, J.K., Keratoprosthesis, results, complications and management, Ophthalmology, 1982, **89**, 655-660

116 Dohlman, C.H., Biology of complications following keratoprosthesis, Cornea, 1983, **2**, 3, 175-176

117 Dohlman, C.H., and Doane, M.G., Some factors influencing outcome after keratoprosthesis surgery, Cornea, 1994, **13**, 3, 214-218

118 Heimke, G., and Polack, F.M., Ceramic keratoprostheses: Biomechanics of extrusion in through -lid implantation, Cornea, 1983, **2**, 3, 197-201

119 Bruns, R.R., and Gross, J., Collagen replacement prosthesis for the cornea, US Patent, 4,581,030, 1986

120 Kelman, C.D., Corneal implant and method of making the same, US Patent, 4,563,779. 1986

121 White, T.C., Corneal implant, US Patent, 4,612,012, 1986

122 White, T.C., Corneal implant, US Patent, 4,772,283, 1988

123 Fedorov, S.N., and Zuev, V.K., Through corneal prosthesis and method of installing the same, US Patent, 3,945,054, 1976

124 Peyman, G.A., Keratoprosthesis, US Patent, 4,470,159, 1984

125 Binder, P.S., Hydrogel keratoprosthesis, US Patent, 4,586,929, 1986

126 Legeais, J.M., Renard, G., and Anton, M., Implant corneen, French Patent, 2,649,605, 1991

127 Abel, R., Artificial cornea, US Patent, 4,693,715, 1987

128 White, T.C., Corneal implant, US Patent, 5,030,230, 1991

129 Chirila, T.V., Constable, I.J., Crawford, G.J., and Russo, A.V., Keratoprosthesis, US Patent, 5,300,116, 1994

130 Caldwell, D.R., and Jacob-LaBarre, J.T., Intraocular prosthesis, US Patent, 4,932,968, 1990

131 Franzblau, C., Farris, B.A., and Civerchia-Perez, L., Hydrogels capable of supporting cell growth, US Patent, 4,565,784, 1986

132 Carroll, D.M., Instrument for replacement temporary keratoprosthesis during pars plana vitrectomy, Am. J. Ophth., 1983, **95**, 5, 718-719

133 Harris, J.K., Rao, G.N., Aquavella, J.V., and Lohman, L.E., Keratoprosthesis: Technique and instrumentation, Annls. Ophth., 1984, **16**, 5, 481-484

134 Doane, M.G., Dohlman, C.H., and Bearse, G., Fabrication of a keratoprosthesis, Cornea, 1996, **15**, 2, 179-184

135 Cardona, H., The Cardona keratoprosthesis: 40 years experience, Ref. Corn. Surg., 1991, **7**, 6, 468-471

136 Dohlman, C.H., Postoperative regimen and repair of complications after keratoprosthesis surgery, Ref. Corn. Surg., 1993, **9**, 3, 198-199

137 Choyce, P., Treatment of bullous keratoplathy with acrylic inlays, experience with Choyce two piece acrylic keratoprosthesis, Corneo-plastic Surg., 1967, 399-403

138 Sletteberg, O., Hovding, G., and Bertlesen, T., Keratoprosthesis 2. Results obtained after implantation of 27 dismountable two-piece prostheses, Acta Ophth., 1990, **68**, 375-383

139 Cardona, H., Plastic keratoprosthese, Am. J Ophth., 1964, **58**, 2, 247-252

140 Polack, F.M., Clinical results with a ceramic keratoprosthesis, Cornea, 1983, **2**, 3, 185-196

141 Polack, F.M., Corneal optical prostheses, Brit. J. Ophth., 1971, **55**, 838-843

142 Polack, F.M., and Heimke, G., Ceramic keratoprostheses, Ophthalmology, 1980, **87**, 693-698

143 Girard, L.J., Keratoprostheses, Cornea, 1983, **2**, 3, 207-224

144 Girard, L.J., Girard keratoprosthesis with flexible skirt: 28 years experience, Ref. Corn. Surg., 1990, **9**, May/June, 194-195

145 Caiazza, S., Pintucci, S., and Donelli, G., Biointegrable keratoprostheses: performances and recent improvements, It. J. Ophth., 1993, **7**, 1, 13-20

146 Pintucci, S., Pintucci, F., Cecconi, M., and Caiazza, S., New Dacron tissue colonisable keratoprosthesis: clinical experience, Brit. J. Ophth., 1995, **79**, 825-829

147 Pintucci, S., Pintucci, F., and Caiazza, S., The dacron felt colonizable keratoprosthesis, Ref. Corn. Surg., 1990, **9**, May/June, 196-197

148 Legeais, J-M., Renard, G., Parel, J-M., Serdarevic, O., Mei-Mui, M., and Pouliquen, Y., Expanded fluorocarbon for keratoprothesis cellular ingrowth and transpaency, Exp. Eye Res., 1994, **58**, 1, 41-52

149 Legeais, J-M., Renard, G., Parel, J-M., Savoldelli, M., and Pouliquen, Y., Keratoprosthesis with biocolonizable microporous fluorocarbon haptic, Arch. Ophth., 1995, **113**, 757-763

150 Legeais, J.M., Les keratoprotheses, Rev. Prat. 1992, **42**, 9, 1125-1127

151 Renard, G., Cetinel, B., Legeais, J-M., Savoldelli, M., Durand, J., and Pouliquen, Y., Incorporation of a fluorocarbon polymer implanted at the posterior surface of the rabbit cornea, J. Biomed. Mat. Res., 1996, **31**, 193-199

152 Drubaix, I., Legeais, J-M., Malek-Chehire, N., Savoldelli, M., Menasche, M., Robert, L., Renard, G., and Pouliquen, Y., Collagen synthesized in fluorocarbon polymer implant in the rabbit cornea, Exp. Eye Res., 1996, **62**, 367-376

153 Kain, H.L., The development of the silicone-carbon keratoprosthesis, Ref. Corn. Surg., 1990, **9**, May/June, 209-210

154 Py, D., Keratoprosthesis, Ref. Corn. Surg., 1993, **9**, 206-208

155 Tu, A., Evaluation of hydroxyapatite as an integrated keratoprosthesis material, IOVS, 1992, **33**, 4, S315

156 Crawford, G.J., Chirila, T,V., Vijayasekaran, S., Dalton, P.D., and Constable, I.J., Preliminary evaluation of a hydrogel core-and-skirt keratoprosthesis in the rabbit cornea, J. Ref. Surg., 1996, **12**, 4,525-529

157 Hicks, C.R., Chirila, T.V., Dalton, P.D., Clayton, A.B., Vijayasekaran, S., Crawford, G.J., and Constable. I.J., Keratoprosthesis: preliminary results of an artificial corneal button as a full-thickness implant in the rabbit model, Aust. N. Z. J. Ophth., 1996, **24**, 3, 297-303

158 Trinkaus-Randall, V., Banwatt, R., Capecchi, J., Leibowitz, H.M., and Franzblau, C., In vivo fibroplasia of a porous polymer in the cornea, IOVS, 1991, **32**, 13, 3245-3251

159 Trinkaus-Randall V., Capecchi, J., Newton, A., Vadasz, A., Leibowitz, H.M., and Franzblau, C., Development of a biopolymeric keratoprosthetic material, IOVS, 1988, **29**, 3, 393-400

160 Yakimenko S., Results of a PMMA/titanium keratoprosthesis in 502 eyes, Ref. Corn. Surg., 1990, **9**, May/June,197-198

161 Linnola, R.J., Happonen, R.P., Andersson, O.H., Vedel, E., Yli-Urpo, A.U., Krause, U., and Laatikainen, L., Titanium and Bioactive glass-ceramic coated titanium as material for keratoprosthesis, Exp. Eye Res., 1996, **63**, 4, 471-478

162 Strampelli, B., Keratoprosthesis with osteo-odonto tissue, Am. J. Ophth., 1963, **89**, 1029-1039

163 Strampelli, B., Osteo-odonto cheratoprotesi, Anales di Ottalmologia, (Pavia), 1970, **96**, 1-57

164 Ricci, R., Percorella, I., Ciardi, A., Della Rocca, C., Di Tondo, U., and Marchi, V., Strampelli's osteo-odonto keratoprosthesis. Clinical and histological long-term features of three prostheses, Brit. J. Ophth., 1992, **76**, 232-234

165 Marchi, V., Ricci, R., Pecorella, I., Ciardi, A., and Di Tondo, U., OOKP - Description of surgical technique and results of 85 pateints, Cornea, 1994, **13**, 2 125-130

166 Caiazza, S., Falcinelli, G., and Pintucci, S., Exceptional case of bone resorption in an osteo-odonto keratoprosthesis, Cornea, 1990, **9**, 1, 23-27

167 Falcinelli, G., Barogi, G., Taloni, M, and Falcinelli, G., Osteo-odonto keratoprostheisis: present experience and future prospects, Ref. Corn. Surg., 1990, **9**, May/June, 193-194

168 Temprano, J., Keratoprosthesis with tibial autograft, Ref. Corn. Surg., 1990, **9**, May/June, 192-193

169 Bertlesen, T.I., and Syversen, K., Experience with keratoprosthesis, Acta Ophth., 1971, June, 45-51

170 Miller, D., and Dohlman, C.H., Optical properties of buried corneal silicone prostheses, Am. J. Ophth., 1968, **66**, 4, 633-640

171 Bradley, J.C., Insertion of an osteo-odonto keratoprosthesis into the human cornea, Brit. Dental J., 1966, 120, 1, 39-40

172 Evans, K.R., Lydon, F.J., Tighe, B.J., and Liu, C.S.C., Keratoprostheses: a summary of recent progres, Poster presented at BCLA Conference, Bournemouth, 1997

173 Crawford, G.J., Constable, I.J., Chirila, T.V., Vijayasekaran, S., and Thompson, D.E., Tissue interaction with hydrogel sponges implanted in rabbits, Cornea, 1993, 12, 4, 348-357

174 Tsuk, A.G., Trinkaus-Randall, V., and Leibowitz, H.M., Advances in polyvinyl alcohol hydrogel keratoprostheses: protection against ultraviolet light and fabrication by a moulding process, J. Biomed. Mat. Res., 1997, **34**, 299-304

175 Capecchi, J.T., Franzblau, C., Gibbons, D.F., Isaacson, W.B., Johnston, M.R., Knoll, R.L., Leibowitz, H.M., and Trinkaus-Randall, V., Corneal implants and the manufacture and use thereof, US Patent, 5,108,428, 1992

176 Aysta, J.E., Capecchi, J.T., Franzblau, C., Gibbons, Knoll, R.L., Leibowitz, H.M., and Trinkaus-Randall, V., Prosthesis holding device, US Patent, 5,032,131, 1991

177 Chirila, T.V., IPN as a permanent joint of new type of artificial cornea, J. Biomed. Mat. Res., 1994, **28**, 745-753

178 Chirila, T.V., Thompson-Wallis, D.E., Crawford, G.J., Constable, I.J., and Vijayasekaran, S., Production of neocollagen by cells invading hydrogel sponges in rabbit corneas, Graefe's Arch. Clin. Exp. Ophth., 1996, **234**, 193-198

179 Yocum, R.H., and Nyquist, E.B., Eds. Functional Monomers, Vols. 1 and 2, Marcel Dekker, NewYork, 1973

180 Tighe, B.J. and Franklin V.J., Lens Deposition and Spoilation, chapter 4, in The Eye in Contact Lens Wear, Ed. J. Larke, 2nd Edition, Butterworth Heinemann, London, 1997

181 Lydon, M.J., Minett, T.W., and Tighe, B.J., Cellular interactions with synthetic polymer surfaces in culture, Biomaterials, 1985, **6**, 11, 396-402

182 Patel, M.P., and Braden, M., Heterocyclic methacrylates for clinical applications 1. Mechanical properties, Biomaterials, 1991, **12**, 9, 645-648

183 Patel, M.P., and Braden, M., Heterocyclic methacrylates for clinical applications 2. Room temperature polymerizing systems for potential clinical use, Biomaterials, 1991, **12**, 9, 649-652

184 Patel, M.P., and Braden, M., Heterocyclic methacrylates for clinical applications 3. Water absorption characteristics, Biomaterials, 1991, **12**, 9, 653-657

185 Labella, R., Braden, M., Clarke, R.L., and Davy, K.W.M., THFMA in dental monomer systems, Biomaterials, 1996, **17**, 4, 431-436

186 Chirila, T.V., Constable, I.J., Crawford, G.J., Vijayasekaran, S., Thompson, D.E., Chen, Y., and Fletcher, W.A., Poly(HEMA) sponges as implant materials: in vivo and in vitro evaluation of cellular invasion, Biomaterials, 1993, **14**, 1, 26-38

187 Chen, Y., Chirila, T.V., and Russo, A.V., Hydrophilic sponges based on HEMA, Mat. Forum, 1993, **17**, 57-65

188 Thomas, K.D., Bilogical interactions with synthetic polymer, Ph.D. thesis, Aston University, 1988

189 Hamilton, C.J., and Tighe, B.J., Polymerisation in aqueous solutions, chapter 20 in Comprehensive Polymer Science, Vol. 3, Eds., Eastmond, G., Ledwith, A., Russo, A., and Sigwat, P., Pergamon, London 1989

190 Clinical Toxicology of Commercial Products

191 West, J.L., and Hubbell, J.A., Photopolymerised hydrogel matrices for drug delivery applications, Reactive Polymers, 1995, **25**, 139-147

192 Wang, T., Bruin, G.J., Kraak, J.C., and Poppe, H., Preparation of polyacrylamide gel-filled fused-silica capillaries by photopolymerisation with riboflavin as the initiator, Anal. Chem., 1991, **63**, 2207-2208

193 Guilbault, G.G., Practical fluroescence: theory, methods and techniques, Marcel Dekker, New York, 1973

194 Brown, S.B., An introduction to spectroscopy for biochemists, Academic Press, London, 1980

195 Lakowicz, J.R., Principles of fluroescence spectroscopy, Plenum Press, New York, 1984

196 Atkins. P.W., Physical Chemistry, 4th Ed., Oxford University Press, 1990

197 Standards in Fluorescence spectroscopy, Ed. J.N. Miller, Chapman and Hall, London, 1981

198 White, C.E., and Argauer, R.J., Fluorescence analysis: a practical approach, Marcel Dekker Inc., New York, 1970

199 Spectrophotometry and spectrofluorimetry; a practical approach, Ed. C.L. Bashford and Harris, D.A., IRL Press, Oxford, 1987

200 Bright, F.V., Modern molecular fluorescence spectroscopy, App. Spect., 1995, **49**, 1, 14A-19A

201 Kusba., J., Bogdanov, V., Gryczynski, I. and Lakowicz, J.R., Theory of light quenching - effects on fluorescence polarization, intensity and anisotropy decays, Biophys. J., 1994, **67**, 2024-2040

202 Somogyi, B., and Lakos, Z., Protein dynamics and fluorescence quenching, J. Photochem. Photobiol., 1993, **18**, 3-16

203 Gratton, E., Jameson, D.M., and Weber, G., A model of dynamic quenching of fluorescence in globular proteins, J. Biophys. Soc., 1984, **45**, 4, 789-794

204 Horne, A.M., Development of a non-destructive fluorescence technique for analysis of contact lens deposition levels, Ph.D. thesis, Aston University, 1993

205 Rangarajan, B., Coons, L.S., and Scranton, A.B., Characterisation of hydrogels using luminescence spectroscopy, Biomaterials, 1996, **17**, 7, 649-661

206 Griffiths, H.R., and Lunec, J., Protein fluorescence: its generation and measurement, Anal. Proc., 1990, **27**, Aug., 222-223

207 Gryczynski, I., Razynska, A. and Lakowicz, J.R., 2-photon induced fluorescence of linear alkanes - a possible intrinsic lipid probe, Biophys. Chem., 1996, **57**, 291-295

208 Lunec, J., and Dormandy, T.L., Fluorescent lipid-peroxidation products in synovial fluid, Clin. Sci., 1979, **56**, 53-59

209 Walton, A.G., and Maenpa, F.C., Application of fluorescence spectroscopy to the study of proteins at interfaces, J. Coll. Interface Sci., 1979, **72**, 2, 265-278

210 Ho, C., and Hlady, V., Fluorescence assay for measuring lipid deposits on contact lens surfaces, Biomaterials, 1995, **16**, 6, 479-482

211 Sariri, R., Evans, K.R., and Tighe, B.J., Protein mobility and activity on hydrogel contact lenses, Poster presented at BCLA conference, London 1995

212 Jones, L.W.J., Evans, K.R., Sariri, R., Franklin, V.J., and Tighe, B.J., An *in vivo* comparison of the deposition performance of high water content hydrogel contact lenses based on NVP and PVA hydrophiles, Biomaterials, in press

213 Sariri, R., Mann, A.M., Franklin, V.J., and Tighe, B.J., Acidic and basic impurities in soft contact lenses, Poster presented at BCLA, London, 1995

214 Bontempo, Lipid deposits on hydrophilic and rigid gas permeable contact lenses, CLAO J., 1994, **20**, 4, 242-245

215 Ma, J.J., Franklin, V.J., Tonge, S.R., and Tighe, B.J., Ocular compatibility of biomimetic hydrogels, Poster presented at BCLA conference, Torquay, 1994

216 Jones, L..W.J., Ma, J.J., Evans, K.R., Franklin, V.J., and Tighe, B.J., The *in vitro* and *in vivo* performance of a new biomimetic contact lens material, in press

217 Sasaki, H., Kojima, M., Mori, Y., Nakamura, J., and Shibasaki, J., Enhancing effect of pyrrolidone derivatives on transdermal penetration of 5-fluoruracil, triamcinolone acetonide, indomethacin and flurbiprofen, J. Pharm. Sci., 1991, **80**, 533-538

218 Jones, L.W.J., Evans, K.R., Sariri, R., Franklin, V.J., and Tighe, B.J., Lipid and protein deposition of N-vinyl pyrrolidone containing group II and group IV frequent replacement contact lenses, CLAO J., 1997, **23**, 2, 122-126

219 Tighe, B.J., Jones, L.W.J., Evans, K.R., and Franklin, V.J., Patient dependent and material dependent factors in contact lens deposition processes, Paper presented at Bermuda, 1997

220 Jones, L.W.J., Evans, K.R., Franklin, V.J., and Tighe, B.J., A multisolution comparison of group II and group IV disposable contact lenses, Paper presented at BCLA conference, London, 1995

221 Franklin, V.J., Evans, K.R., Jones, L.W.J., Sariri, R., and Tighe, B.J., Interaction of tear lipids with soft contact lenses, Poster presented at BCLA conference, London, 1995

222 Jones, L.W.J., Franklin, V.J., Evans, K.R., Sariri, R., and Tighe, B.J., Spoilation and clinical performance of monthly vs. three monthly group II disposable contact lenses, Optom. Vis. Sci., 1996, **73**, 1, 16-21

223 Guillon, M., McCrogan, L., Guillon, J-P., Styles, E., and Maissa, C., Effect of material ionicity on the performance of daily disposable contact lenses, Contact Lens and Anterior Eye, 1997, **20**, 1, 3-8

APPENDICES

APPENDIX 1

Equlibrium water contents and mechanical properties for keratoprosthesis device

Monomers	Composition	EWC %
HEMA:AMO	90:10	39.1
HEMA:AMO	80:20	43.5
HEMA:AMO	70:30	48.1
HEMA:AMO	60:40	54.7
HEMA:AMO	50:50	61.4
HEMA:AMO	40:60	66.6
HEMA:NVP	90:10	41.5
HEMA:NVP	80:20	44.5
HEMA:NVP	70:30	49.9
HEMA:NVP	60:40	54.9
HEMA:NVP	50:50	62.3
HEMA:NVP	40:60	69.2
HEMA:MAA	90:10	36.6
HEMA:MAA	80:20	35.8
HEMA:MAA	70:30	35.4
HEMA:MAA	60:40	33.7
HEMA:MAA	50:50	30.9
HEMA:MAA	40:60	28.4
HEMA:MMA	90:10	34.6
HEMA:MMA	80:20	30.6
HEMA:MMA	70:30	27.5
HEMA:MMA	60:40	22.5
HEMA:MMA	50:50	19.6
HEMA:MMA	40:60	15.7

Monomers	Composition	EWC %	Elastic modulus MPa	Tensile strength MPa	Elongation at break %
AMO:THPMA	90:10	81.5	0.13	0.13	77
AMO:THPMA	80:20	85.1	0.15	0.14	88
AMO:THPMA	70:30	84.5	0.15	0.14	89
AMO:THPMA	60:40	73.1	0.14	0.13	101
AMO:THPMA	50:50	63.9	0.14	0.18	141
AMO:THFMA	90:10	75.5	0.13	0.13	86
AMO:THFMA	80:20	73.7	0.13	0.17	94
AMO:THFMA	70:30	65.5	0.16	0.19	97
AMO:THFMA	60:40	54.6	0.17	0.21	109
AMO:THFMA	50:50	39.8	0.21	0.22	119
AMO:GMA	90:10	72.7	0.2	0.14	71
AMO:GMA	80:20	70.2	0.2	0.15	78
AMO:GMA	70:30	63	0.23	0.16	77
AMO:GMA	60:40	50.6	0.27	0.21	91
AMO:GMA	50:50	36.3	0.3	0.26	99

Monomers	Composition	EWC %	Elastic modulus MPa	Tensile strength MPa	Elongation at break %
THFMA:AMO:PU	41.6: 41.6: 16.8	29.9	12.6	4.2	168
THFMA:AMO:PU	36.6: 41.6: 21.8	47.9	24.4	5.6	106
THFMA:AMO:PU	30: 50: 20	41.4	8.4	1.4	139
THFMA:AMO:PU	25: 60: 15	53.7	7.3	1.6	121
THFMA:AMO:PU:DEX	43.75:43.75:12.5:20	34.8			
THFMA:AMO:PU:DEX	25:60:15:15	50			
THFMA:AMO:PU:DEX	37.5:43.75:18.7 5:20	33			
THFMA:AMO:PU:DEX:dextran	37:42:21:10:4	50			
THFMA:AMO:PU:DEX	30:50:20:20	41.6			
THFMA:AMO:PU:DEX:dextran	30:50:20:10:4	43			

APPENDIX 2

Water binding results for temporary laser ablation mask

Monomers	Composition	EWC %	Freezing water content %	Non-freezing water content %
HPMC(10000) 1%:PEG1000DMA	75:25	74.6	47.4	27.2
HPMC(10000) 2%:PEG1000DMA	75:25	73	50.2	22.8
HPMC(10000) 5%:PEG1000DMA	75:25	77.5	56.4	21.1
HPMC(12000) 1%:PEG1000DMA	75:25	73	47	26
HPMC(12000) 2%:PEG1000DMA	75:25	74.2	50.2	24
HPMC(12000) 5%:PEG1000DMA	75:25	75	53.6	21.4
HPMC(90000) 1%:PEG1000DMA	75:25	74.7	47.6	27.1
HPMC(90000) 2%:PEG1000DMA	75:25	74.9	55.6	19.3
HPMC(90000) 5%:PEG1000DMA	75:25	80.8		
PVA (14000) 1%:PEG1000DMA	75:25	72.4	46.6	25.8
PVA (14000) 2%:PEG1000DMA	75:25	70.3	43.9	26.4
PVA (14000) 5%:PEG1000DMA	75:25	65.9		
PVA (30000) 1%:PEG1000DMA	75:25	69.6	42.9	26.7
PVA (30000) 2%:PEG1000DMA	75:25	69.9	41.3	28.6
PVA (30000) 5%:PEG1000DMA	75:25	69.1		
PVA (50-85000) 1%:PEG1000DMA	75:25	70.8	47.9	22.9
PVA (50-85000) 2%:PEG1000DMA	75:25	70.9	30	40.9
PVA (50-85000) 5%:PEG1000DMA	75:25	70.7	48.7	22
HPMC(10000) 1%:PEG600DMA	75:25	70.9	47.5	23.4
PVA (14000) 1%:PEG600DMA	75:25	70.6	42	28.6
HPMC(10000) 1%:PEG400DMA	75:25	70	55.2	14.8
PVA (14000) 1%:PEG400DMA	75:25	71.6	54.5	17.1
HPMC(10000) 1%:PEG200DMA	75:25	9.4		
PVA (14000) 1%:PEG200DMA	75:25	8.1		

Monomers	Composition	EWC %	Freezing water content %	Non-freezing water content %
HPMC(10000) 1%:PEG1000DMA:EGDM	75:25:1	70.1	46.7	23.4
PVA (14000) 1%:PEG1000DMA:EGDM	75:25:1	72.4	50.5	21.9
HPMC(10000) 1%:PEG1000DMA	50:50	59.7	27.8	31.9
PVA (14000) 1%:PEG1000DMA	50:50	59.6	28.9	30.7
HPMC(10000) 1%:PEG1000DMA	90:10	83.3	68.7	14.6
PVA (14000) 1%:PEG1000DMA	90:10	85.3	65	20.3
HPMC(10000) 1% :PEG1000DMA:EGDM	90:10:1	86.2		
PVA (14000) 1% :PEG1000DMA:EGDM	90:10:1	87.4		
HPMC(10000) 1% :PEG1000DMA:EGDM	90:10:2	83.5		
PVA (14000) 1% :PEG1000DMA:EGDM	90:10:2	85.2		
HPMC(10000) 1%:PPG	75:25	4.3		
PVA (14000) 1%:PPG	75:25	3.3		
HPMC(10000) 1%:PEG200MA	75:25	85.8		
PVA (14000) 1%:PEG200MA	75:25	84.1		
HPMC(10000) 1% :PEG200MA:PEG1000DMA	75:6.25:18.75	75.7	51	24.7
PVA (14000) 1%: PEG200MA:PEG1000DMA	75:6.25:18.75	76	52	24
HPMC(10000) 1%: PEG200MA:PEG1000DMA	75:10:15	76.4	53.5	22.9
PVA (14000) 1%: PEG200MA:PEG1000DMA	75:10:15	75.5	50	25.5
HPMC(10000) 1% (glycerol/water):PEG1000DMA	75(10:90):25	75.4	48.7	26.7
HPMC(10000) 1% (glycerol/water):PEG1000DMA	75(50:50):25	70.5	45.2	25.3
HPMC(10000) 1% (glycerol/water):PEG1000DMA	75(60:40):25	76.7	55.4	21.3
PVA(14000) 1% (glycerol/water):PEG1000DMA	75(10:90):25	75.6	48	27.6
PVA(14000) 1% (glycerol/water):PEG1000DMA	75(50:50):25	72.5	49.3	23.2
PVA(14000) 1% (glycerol/water):PEG1000DMA	75(60:40):25	77.3	54.8	22.5

APPENDIX 3

Mechanical properties for temporary laser ablation mask

Monomers	Composition	EWC %	Elastic modulus MPa	Tensile strength MPa	Elongation at break %
HPMC(10000) 1%:PEG1000DMA	75:25	74.6	0.96	0.5	49
HPMC(10000) 2%:PEG1000DMA	75:25	73	0.96	0.2	32
HPMC(10000) 5%:PEG1000DMA	75:25	77.5	0.74	0.19	31
HPMC(12000) 1%:PEG1000DMA	75:25	73	1.2	0.47	40
HPMC(12000) 2%:PEG1000DMA	75:25	74.2	0.92	0.39	45
HPMC(12000) 5%:PEG1000DMA	75:25	75	0.9	0.32	41
HPMC(90000) 1%:PEG1000DMA	75:25	74.7	0.94	0.48	47
HPMC(90000) 2%:PEG1000DMA	75:25	74.9			
HPMC(90000) 5%:PEG1000DMA	75:25	80.8			
PVA (14000) 1%:PEG1000DMA	75:25	72.4	1.1	0.34	34
PVA (14000) 2%:PEG1000DMA	75:25	70.3	1.2	0.41	32
PVA (14000) 5%:PEG1000DMA	75:25	65.9			
PVA (30000) 1%:PEG1000DMA	75:25	69.6	1.8	0.5	31
PVA (30000) 2%:PEG1000DMA	75:25	69.8	1.4	0.54	36
PVA (30000) 5%:PEG1000DMA	75:25	69.1	1.8	0.3	17
PVA (50-85000) 1%:PEG1000DMA	75:25	70.8	1.6	0.4	31
PVA (50-85000) 2%:PEG1000DMA	75:25	70.9	1.3	0.3	24
PVA (50-85000) 5%:PEG1000DMA	75:25	70.7	1.4	0.3	24
HPMC(10000) 1%:PEG600DMA	75:25	70.9	0.9	0.3	32
PVA (14000) 1%:PEG600DMA	75:25	70.6	0.96	0.29	26
HPMC(10000) 1%:PEG400DMA	75:25	70	0.84	0.25	22
PVA (14000) 1%:PEG400DMA	75:25	71.6	0.89	0.5	12
HPMC(10000) 1%:PEG200DMA	75:25	9.3			
PVA (14000) 1%:PEG200DMA	75:25	8			

Monomers	Composition	EWC %	Elastic modulus MPa	Tensile strength MPa	Elongation at break %
HPMC(10000) 1%: PEG1000DMA:EGDM	75:25:1	70.1	1.5	0.2	15
PVA (14000) 1%: PEG1000DMA:EGDM	75:25:1	72.4	1	0.3	31
HPMC(10000) 1%:PEG1000DMA	50:50	59.7	4.5	0.9	22
PVA (14000) 1%:PEG1000DMA	50:50	59.6	4.6	0.8	18
HPMC(10000) 1%:PEG1000DMA	90:10	83.3	0.1	0.05	43
PVA (14000) 1%:PEG1000DMA	90:10	85.3	0.13	0.04	39
HPMC(10000) 1% :PEG1000DMA:EGDM	90:10:1	86.2	0.56	0.09	41
PVA (14000) 1% :PEG1000DMA:EGDM	90:10:1	87.4	0.5	0.1	36
HPMC(10000) 1% :PEG1000DMA:EGDM	90:10:2	83.5	0.05	0.04	69
PVA (14000) 1% :PEG1000DMA:EGDM	90:10:2	85.2	0.28	0.07	30
HPMC(10000) 1%:PEG200MA	75:25	85.8			
PVA (14000) 1%:PEG200MA	75:25	84.1			
HPMC(10000) 1% :PEG200MA:PEG1000DMA	75:6.25:18.75	75.7	0.6	0.2	38
PVA (14000) 1%: PEG200MA:PEG1000DMA	75:6.25:18.75	76	0.74	0.17	23
HPMC(10000) 1%: PEG200MA:PEG1000DMA	75:10:15	76.4	0.52	0.2	37
PVA (14000) 1%: PEG200MA:PEG1000DMA	75:10:15	75.5	0.5	0.1	18
HPMC(10000) 1% (glycerol/water):PEG1000DMA	75(10:90):25	75.4	0.7	0.2	31
HPMC(10000) 1% (glycerol/water):PEG1000DMA	75(50:50):25	70.5	0.8	0.4	30
HPMC(10000) 1% (glycerol/water):PEG1000DMA	75(60:40):25	76.7	0.34	0.14	31
PVA(14000) 1% (glycerol/water):PEG1000DMA	75(10:90):25	75.6	0.7	0.2	29
PVA(14000) 1% (glycerol/water):PEG1000DMA	75(50:50):25	72.5	0.9	0.3	29
PVA(14000) 1% (glycerol/water):PEG1000DMA	75(60:40):25	77.3	0.4	0.16	34